ORIGINS AND SOURCES OF ATMOSPHERIC PRECIPITATION FROM AUSTRALIA: CHLORINE-36 AND MAJOR-ELEMENT CHEMISTRY

By

Melita Keywood

A thesis submitted for the

degree of Doctor of Philosophy

of the

Australian National University

October 1995

CHAPTER 5 MAJOR ELEMENTS

The aims of investigating the major-element chemistry of precipitation from the present study are two-fold. In a general sense, the data from remote localities will provide information on baseline levels of constituents in unpolluted atmospheres, and will add to the sparse data base of precipitation chemistry from Australia. Of particular relevance to the present investigation however, is that an understanding of the major-element chemistry and the processes that affect it at different times and locations around Australia, will provide a basis upon which ^{36}Cl data can be interpreted.

Since the initiation of the sampling program in March of 1991, a total of 148 samples have been collected. Each sample was analysed for Cl, SO_4, NO_3, HPO_4, Br, Na, K, NH_4, Ca, Mg and pH, and the data split into two groups, those from the WE array (80 samples) and those from the SN array (68 samples). Following data quality checks outlined below, the data for 7 samples have been removed from the WE data set leaving 73 samples for detailed analysis, and 11 samples have been removed from the SN data set, leaving 57 samples for detailed analysis. The complete data set is listed in Appendix D.

5.1 DATA QUALITY

The data are subject to scrutiny with respect to their representativeness of precipitation in the collection area over the collection period. The following discussion applies the ion imbalance, regression and outlier analysis techniques described in Section 3.3 to each data set. Samples were only removed from the data set if they failed all the data quality checks. Thus, for example, while the dry samples from the northern section of the SN array had ion imbalances of greater than 100%, they satisfied the outlier analysis check, and were retained in the data set.

Ion Imbalance

Tables 5.1 and 5.2 display the ion imbalances for each sample collected from the WE and SN arrays respectively. Samples from the WE array with imbalances of greater than 100% are removed from the data set and are listed in Table 5.3. In each case, the imbalance can be attributed to contamination during sampling, eg. infestation of ants or the presence of algal matter, and are reflected by excessive amounts of cations, in particular NH_4.

TABLE 5.1 Ion imbalances for the WE array. Bold values highlight imbalances greater than 100%.

Site	Collection Period							
	A91	W91	Sp91	S91	A92	W92	Sp92	S92
16 Cliff Head	0	5	-1	41	14	24	11	-2
17 West Morawa	-17	-15	-20	6	32	11	79	-1
18 Badja	-3	-0.6	-37	26	59	12	31	15
19 Iowna	-48	13	-32	**122**	26	15	45	-14
20 Barrambie	-28	-42	-20	-23	**124**	90	45	-10
21 Yeelirrie	-17	-49	-9	-42	34	6	43	64
22 Lake Violet	-22	-64	-26	-17	37	25	25	29
23 Carnegie	-16	-74	-5	-6	30	35	12	81
24 Gunbarrel	-75	-88	-42	**146**	20	10	**124**	83
25 Everard Junction	-50	-91	-65	**127**	31	-10	**139**	**123**

TABLE 5.2 Ion imbalances for the SN array. Bold values highlight imbalances greater than 100%.

Site	Collection Period							
	W92	Sp92	S92	A93	W93	Sp93	S93	A94
26 Port Lincoln	3	58	7	-58	11	16	28	14
27a Gawler Ranges	13	61	30	40	25	31	5	88
27b Gawler Ranges					24	29	10	84
28 Wintinna	-9	40	20	58	-16	23	38	67
29 Alice Springs	14	32	**131**	-12	17	11	24	26
30 Tennant Creek	70	22	**197**	**104**	19	33	86	93
31 Dunmarra	**112**	35	75	**105**	91	37	**100**	57
32 Katherine	**132**	**104**	64	61	**125**	**117**	40	92
33 Kapalga	91	70	82	24	**126**	**148**	90	**169**

An apparent high ionic imbalance may also occur for samples where ionic strengths are at or near to analytical detection limits, where poorer precision can exaggerate differences. This is illustrated for the WE array in Table 5.4. Low total ionic strength for each season gives higher occurrences of imbalances greater than 50%. In comparison, the site at Cliff Head (site 16) exhibits a high ionic strength and nil

imbalances greater than 50%. This has been noted elsewhere (Ayers and Manton 1991).

TABLE 5.3 Samples removed from the WE data set, ion imbalances and reasons for removal.

Sample	Ion Imbalance %	Reasons for Removal
19-S91 Iowna	122	growth of algae
24-S91 Gunbarrel	146	insect infestation
25-S91 Everard Junction	127	insects and algae
20-A92 Barrambie	124	insects
24-Sp92 Gunbarrel	124	ant infestation
25-Sp92 Everard Junction	139	ant infestation
25-S92 Everard Junction	123	ant infestation

TABLE 5.4 Relationship between total ionic concentration and ionic imbalance for samples from the WE array.

Site	Mean total ions µeq/L	Imbalance				
		<10%	10 to <20%	20 to <50%	50 to <100%	>100%
16 Cliff Head	975	4	2	2	0	0
17 Morawa	220	2	3	2	1	0
18 Badja	176	2	1	3	2	0
19 Iowna	170	0	3	4	1	1
20 Barrambie	231	0	1	5	1	1
21 Yeelirrie	87	2	1	4	1	0
22 Lake Violet	175	0	1	6	1	0
23 Carnegie	93	2	2	2	2	0
24 Gunbarrel	69	1	1	2	2	2
25 Everard Junction	85	0	1	2	2	3

Table 5.5 displays the samples that have been removed from the SN data set. As in the WE data set, each of these samples can be directly attributed to contamination during the sampling program. Sample 26-A93 displays a very high concentration of SO_4 which acts to produce a high negative imbalance. While no obvious source of contamination was observed in the sample, the outlier analysis that follows justifies

the removal of this sample from the data set. It should be noted that dry samples with imbalances of greater than 100% have not been removed, and the reasons for this are shown in the following section.

Several features noted in the ion balances for the SN data set are shown in Table 5.6. Firstly there is a predominance of positive imbalances (i.e. indicating higher cation concentrations than anion concentrations). Secondly, the more northerly sampling localities in the array (sites 30 to 33) show a higher occurrence of imbalances of greater than 100%. These two features may reflect the absence of the measurement of all anions in the analytical program. The most likely missing anions are organic acids. Organic acids have been measured in rainfall from tropical regions (Noller et al 1990) where they have been found to be a major anion. However, organic acids were not measured in the present investigation as steps taken to preserve the organic acids in the sample during field collection were unsuccessful (Section 3.1) and the facility to measure organic acids as part of the analytical program did not exist at the Research School of Earth Sciences, Australian National University. The absence of rainfall during the non-monsoonal period in the northern half of the array is another feature that can be correlated with the higher occurrence of ion imbalances in the more northern section of the array. Finally, as seen in the WE array, low ionic strengths in some samples are correlated with increased ionic imbalances (Table 5.6).

TABLE 5.5 Samples removed from the SN data set, ion imbalances and reasons for removal. Cases marked with an * are removed because a reliable record of the volume of rain for the sampling period was not recorded due to the inappropriate design of the collector for that particular season.

Sample	Ion Imbalance %	Reasons for Removal
26-A93 Port Lincoln	-58	elevated SO_4 (?)
29-S92 Alice Springs	131	ants nest
30-S92 Tennant Creek	197	field site disrupted
30-A93 Tennant Creek	104	algae
31-S92 Dunmarra	75	field site disrupted
31-A93 Dunmarra	105	algae
32-S92 Katherine	64	unknown volume*
32-Sp93 Katherine	117	field site disrupted
33-S92 Kapalga	82	unknown volume*
33-Sp93 Kapalga	148	ash/algae
33-A94 Kapalga	169	ash

TABLE 5.6 Relationship between total ionic concentration and ion imbalances for samples from the SN array.

Site	mean total ions µeq/L	Imbalance				
		<10%	10 to <20%	20 to <50%	50 to <100%	>100%
26 Port Lincoln	1137	2	3	1	2	0
27a Gawler Ranges	383	1	1	4	2	0
27b Gawler Ranges	383	1	0	2	1	0
28 Wintinna	242	1	2	3	2	0
29 Alice Springs	202	0	4	3	0	1
30 Tennant Creek	549	0	1	2	3	2
31 Dunmarra	131	0	0	2	3	3
32 Katherine	578	0	0	1	3	4
33 Kapalga	147	0	0	1	4	3

Regression

Figure 5.1 shows the plots of total cations versus total anions for the WE and SN arrays. All samples are shown on the plots, including those removed from the data which failed to meet the ion balance criteria above. Also shown on the plots is the regression line derived using the reduced major axis technique. The results of the reduced major axis regression are also shown in Table 5.7. The data set used in these regressions does not include data with ionic imbalances of greater than 100%. In an ideal situation, where all ions are accounted for and analytical error does not exist, a regression slope of unity and intercept of zero will be attained. The results listed in Table 5.7 show a very high correlation coefficient between anions and cations for the WE data set, and a calculated slope and intercept close to the ideal situation at the 68% confidence interval (within twice the standard error). The coefficient of correlation for the SN data set is lower than for the WE data set, reflecting the high imbalances introduced by the dry samples. However, the slope and intercept of the regression fall within the bounds of an ideal situation at the 68% confidence interval (within two times the standard error), as is shown in Figure 5.1 where the data fall in the area bounded by the upper and lower 2σ limits rather than on the reduced major axis regression line.

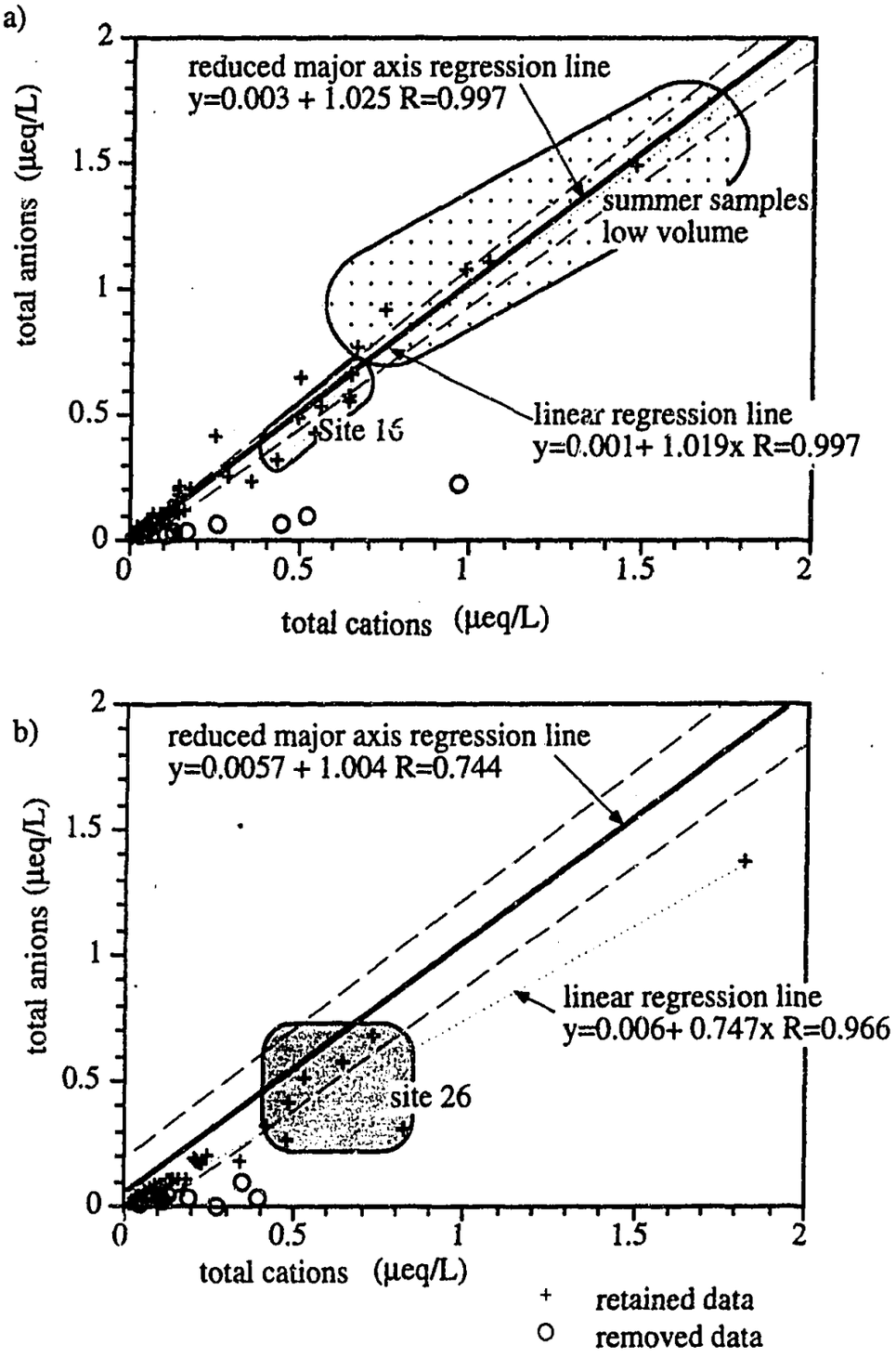

FIGURE 5.1 Total anions versus total cations (μeq/L) for a) WE Array and b) the SN Array. The reduced major axis regression lines are shown as solid thick lines, and the 2σ errors as thin short-dashed lines. For comparison, the linear regression line is also shown, as the thin dotted line. For the SN data set, the reduced major axis line passes through the data points within the bounds of the 2σ error for the line, and there is poor agreement between the reduced major axis and linear regression lines. This lack of agreement most likely reflects the low correlation coefficient for the reduced major axis regression (R=0.74) which occurs because of the high ionic imbalances introduced by the dry samples from the NS array.

TABLE 5.7 Statistics for reduced major axis regression on WE and SN data sets.

Statistic	WE Array	SN Array
number of data points	73	58
slope (std error)	1.025 (0.026)	1.004 (0.033)
intercept (std error)	0.003 (0.008)	0.057 (0.071)
correlation coefficient	0.99	0.74

Outlier Analysis

The geometric means used in the outlier analysis do not use the data removed during the ionic imbalance calculation. Samples with individual ionic concentrations that differ from the geometric mean by greater than 2σ for the WE array are listed in Table 5.8. As expected, these include all the samples with imbalances of greater than 100%. The remaining samples 21-Sp91 and 23-Sp91 represent samples of very low rainfall amount and hence have elevated concentrations of ionic species. However, because of the good balance between anions and cations in these samples, as shown in Table 5.1, these samples are not removed from the data set. Samples with individual ionic concentrations that differ from the geometric mean by greater than 2σ for the SN array coincide with those listed in Table 5.5, that have already been removed from the data set. Dry samples fell within 2σ of the geometric mean, justifying their inclusion in the SN data set.

TABLE 5.8 Samples that lie outside 2σ of the geometric mean for each site.

sample	ion imbalance %	rainfall mm
19-A92 Iowna	122	30
24-A92 Gunbarrel	146	38
25-A92 Everard Junction	127	98
20-W92 Barrambie	124	268
24-Sp92 Gunbarrel	124	23
25-Sp92 Everard Junction	139	35
25-S92 Everard Junction	123	34
18-S92 Badja	15	3
21-Sp91 Yeelirrie	-9	0
23-Sp9 Carnegie	-5	0

5.2 GENERAL RELATIONSHIPS

A summary of the minimum, maximum and means for each site on the WE and SN arrays, expressed in units of total deposition ($\mu eq/m^2/day$) is given in Appendix E. A typical frequency distribution of ionic species for each array is shown in Figure 5.2 for Cl which reveals a skewed distribution towards lower concentrations. Figure 5.3 confirms that the distribution displayed by the ions is approximately log-normal, a feature that has previously been noted by other workers (eg. Saylor et al 1992). The relative magnitude of ionic species over the entire WE array is Cl > Na > SO_4 > Ca > NO_3 > Mg > H > NH_4 > HPO_4 > Br. The general relative magnitude of ionic species for the SN data set is Cl, Na > SO_4, Ca, Mg > K, HPO_4, NO_3, NH_4 > Br. NH_4 displays locally high concentrations eg. at sites 30 (Tennant Creek) and 32 (Katherine). Ionic pair correlations and rainfall amount for each array are listed in Table 5.9 and 5.10. High affinities (greater than 0.5) are displayed between most species for the WE data set except H, HPO_4 and NH_4. The low affinities of these latter ions may be due to the influence of biodegradation on the concentration of these species. Good correlations are displayed between Cl, SO_4, Na, Ca and Mg in the SN data set. K displays good correlations with Ca, Mg, and HPO_4, and NO_3 correlates well with Ca, SO_4 and H (inversely). Both H and rainfall amount show negative correlations with all species.

TABLE 5.9 Table of ionic pair correlation coefficients for the WE array. Bold values highlight correlations of greater than 0.4.

	rain	H	Cl	SO_4	NO_3	HPO_4	Br	Na	K	NH_4	Ca	Mg
rain	1											
H	-.17	1										
Cl	-.02	-.38	1									
SO_4	-.30	-.16	**.79**	1								
NO_3	-.37	.07	.28	**.72**	1							
HPO_4	-.18	-.27	.35	**.42**	.31	1						
Br	-.08	-.11	.57	**.56**	.31	.29	1					
Na	-.11	-.37	**.98**	**.84**	.38	.39	**.59**	1				
K	-.27	-.40	**.59**	**.75**	**.48**	.40	.30	**.66**	1			
NH_4	-.05	-.27	-.01	.00	.02	.03	-.16	-.04	.31	1		
Ca	-.3	-.39	**.77**	**.86**	**.58**	**.42**	**.52**	**.82**	**.77**	.18	1	
Mg	-.17	-.40	**.95**	**.85**	.40	.37	**.54**	**.97**	**.72**	.01	**.88**	1

TABLE 5.10 Table of ionic pair correlation coefficients for the SN data set. Bold values highlight correlations of greater than 0.4.

	rain	H	Cl	SO_4	NO_3	HPO_4	Br	Na	K	NH_4	Ca	Mg
rain	1											
H	.14	1										
Cl	-.34	-.25										
SO_4	**-.59**	-.24	**.75**	1								
NO_3	**-.68**	-.13	.31	**.59**	1							
HPO_4	-.20	-.38	.25	.28	.22	1						
Br	.01	.19	**.57**	.44	.17	.25	1					
Na	-.35	-.27	**.97**	**.82**	.38	.22	**.56**	1				
K	**-.48**	-.31	**.45**	.50	.37	**.67**	.33	**.44**	1			
NH_4	-.03	-.33	-.04	.11	-.03	**.42**	-.24	-.08	.37	1	.	
Ca	**-.53**	**-.47**	**.87**	**.75**	**.51**	.39	.33	**.84**	**.57**	.09	1	
Mg	-.37	-.37	**.93**	**.78**	.37	.31	.53	**.95**	**.60**	.01	**.88**	1

The correlations give a general idea of the sources of ionic constituents to precipitation. For example, correlations between Cl, Na, Mg, Ca, K and SO4 suggest a seawater origin, while a continental source of material would be indicated by similar correlations, but with elevated concentrations of K and Ca. The inverse correlation of rainfall volume with all species is a commonly noted feature of rainfall chemistry (Lindberg 1982, Khwaja and Husain 1990, Saylor et al 1992). One possible explanation involves a 'washout' effect of the rain cloud during initial stages of the rain period. This initially concentrated rainfall is then diluted if deposition continues. Saylor et al (1992) invoked in-cloud and below-cloud removal of aerosols during brief showers that occur after periods of dryness as a mechanism for concentrating ions in low rainfall amounts. As discussed in Chapter 4 other workers have recognised the significance of precipitation type, i.e. frontal or convective. For example, Likens et al (1984) suggest that evaporation below the cloud at the leading edge of a frontal storm may lead to increased concentrations of ions during the initial stages of a period of rainfall.

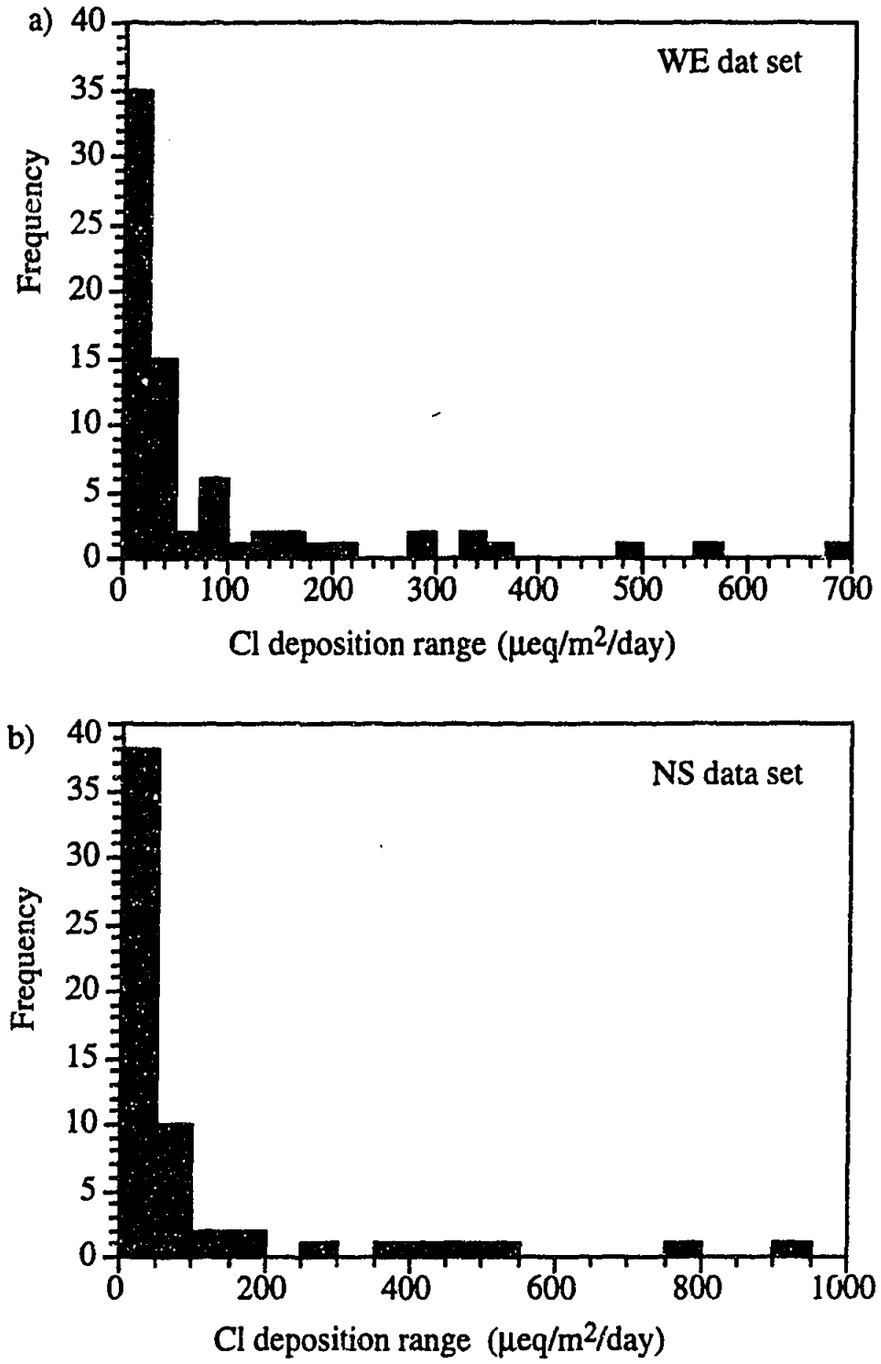

FIGURE 5.2 The frequency distribution of Cl deposition for a) all samples in the WE data set (n=73) and b) for all samples in the SN data set (n=57), remaining after data quality tests. The distribution is skewed towards lower concentrations. A similar pattern of distribution is displayed by the other major elements.

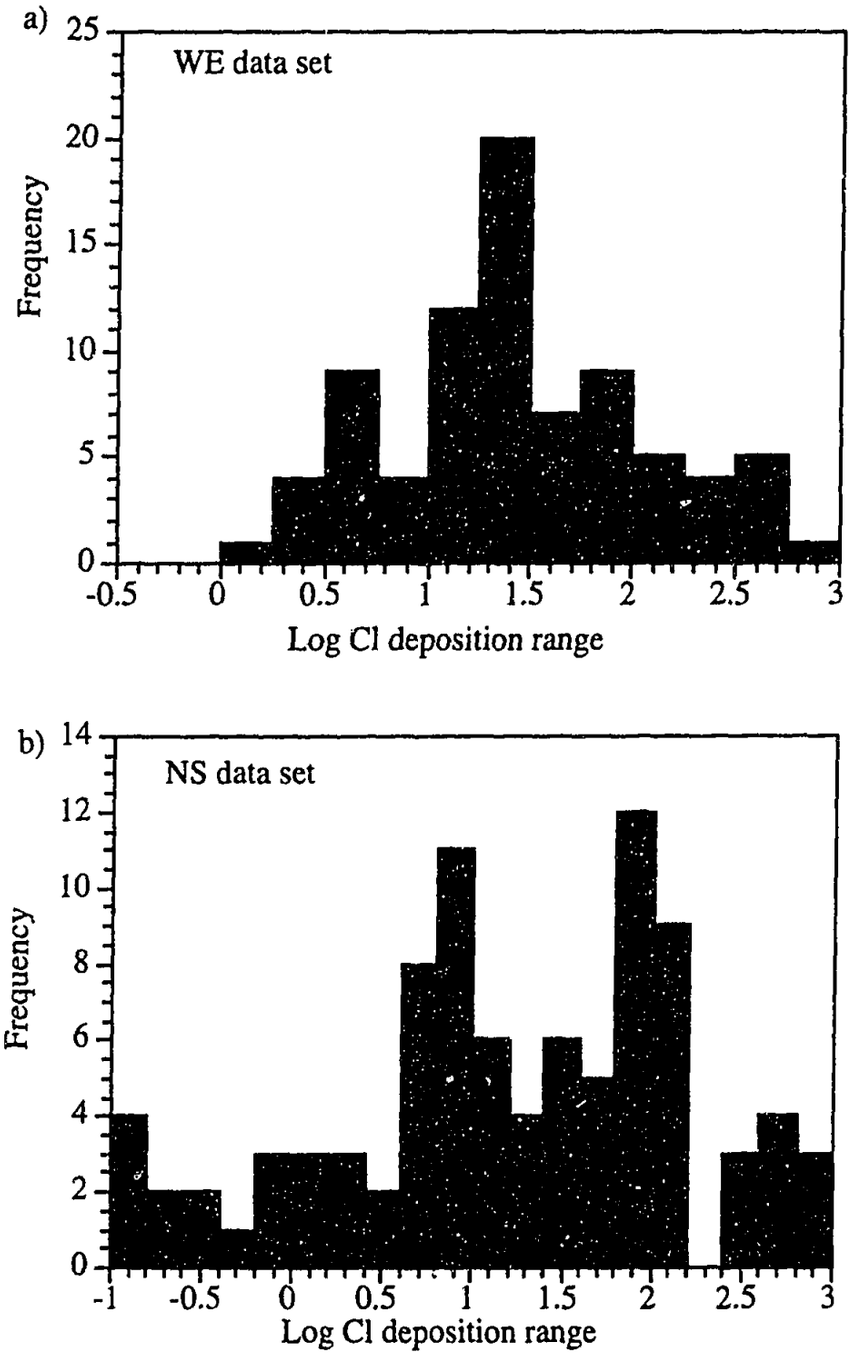

FIGURE 5.3 The logarithmic transformed frequency distribution of Cl deposition for a) the WE Array data set (n=73) b) the SN data set (n=57).

Spatial and Seasonal Variations

WE Array

Ionic fluxes generally decrease with increasing distance from the coast (Figure 5.4).

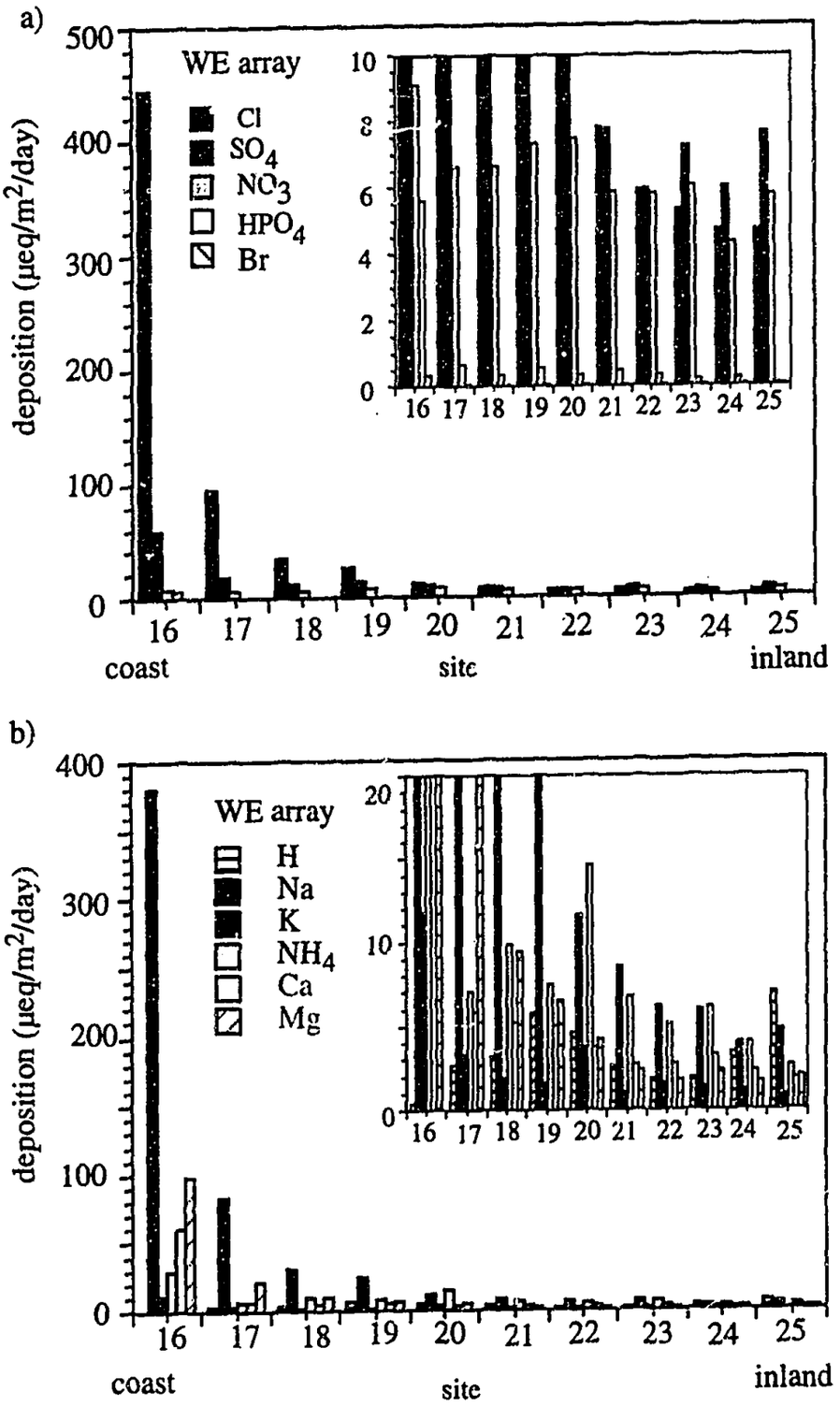

FIGURE 5.4 Mean deposition of a) anions and b) cations for the WE Array. Insets show spatial variations of ionic species with low deposition rates. Coastal localities have higher deposition rates than inland localites. See Figure 3.1 for site number localities.

This trend most likely reflects the decreasing influence of seawater on rainfall composition at continental sites. The general seasonal distribution of ionic fluxes over time is summarised in Figure 5.5. Maximum values occur in winter of each year, and minimum values in summer and autumn, reflecting the influence of rainfall volume on deposition. When individual ions are investigated (Figure 5.6) it can be seen that the above variation pattern is predominantly followed by Na, Mg, and Cl, ions characteristic of seawater. This may suggest there is a change in the influence of seawater on rainfall composition with time. The influence of seawater as a source of material to the chemistry of rainfall across the WE array is discussed in more detail later in this chapter.

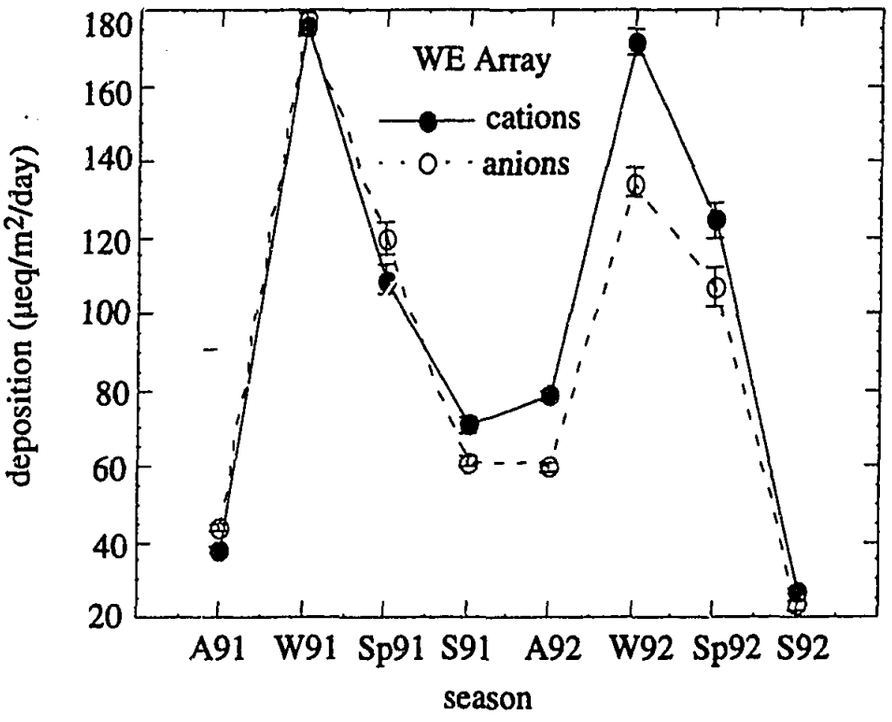

FIGURE 5.5 Seasonal variations in the deposition of total cations and anions for the WE array. A91=autumn 91, W91=winter 91, Sp91=spring 91, S91=summer 91 etc.

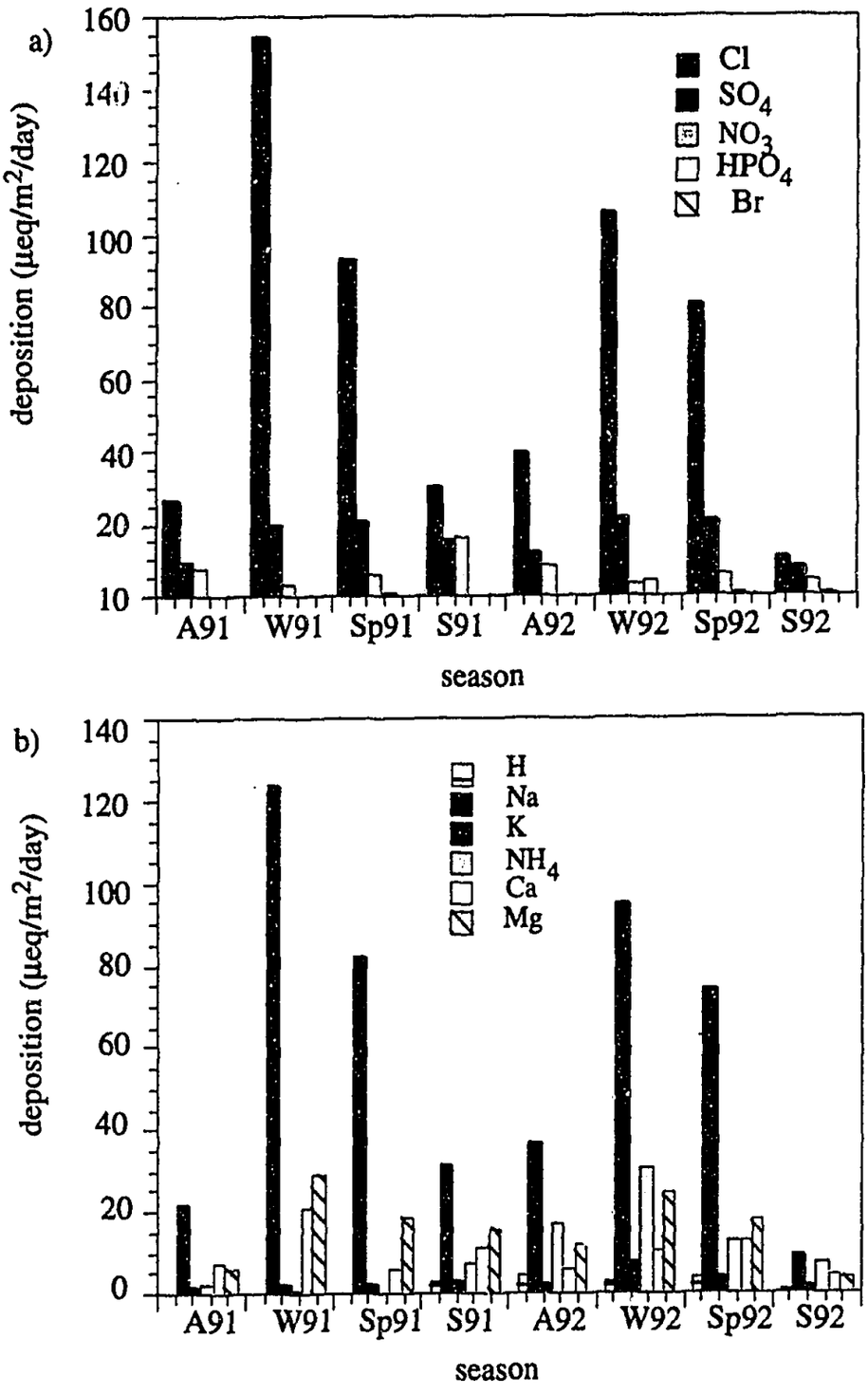

FIGURE 5.6 Mean seasonal deposition of a) anions and b) cations for the WE Array. A91= Autumn 91, W91=Winter 91, Sp91=Spring 91, S91=Summer 91 etc.

SN Array

Figure 5.7 show spatial variation of ionic deposition for the SN array.

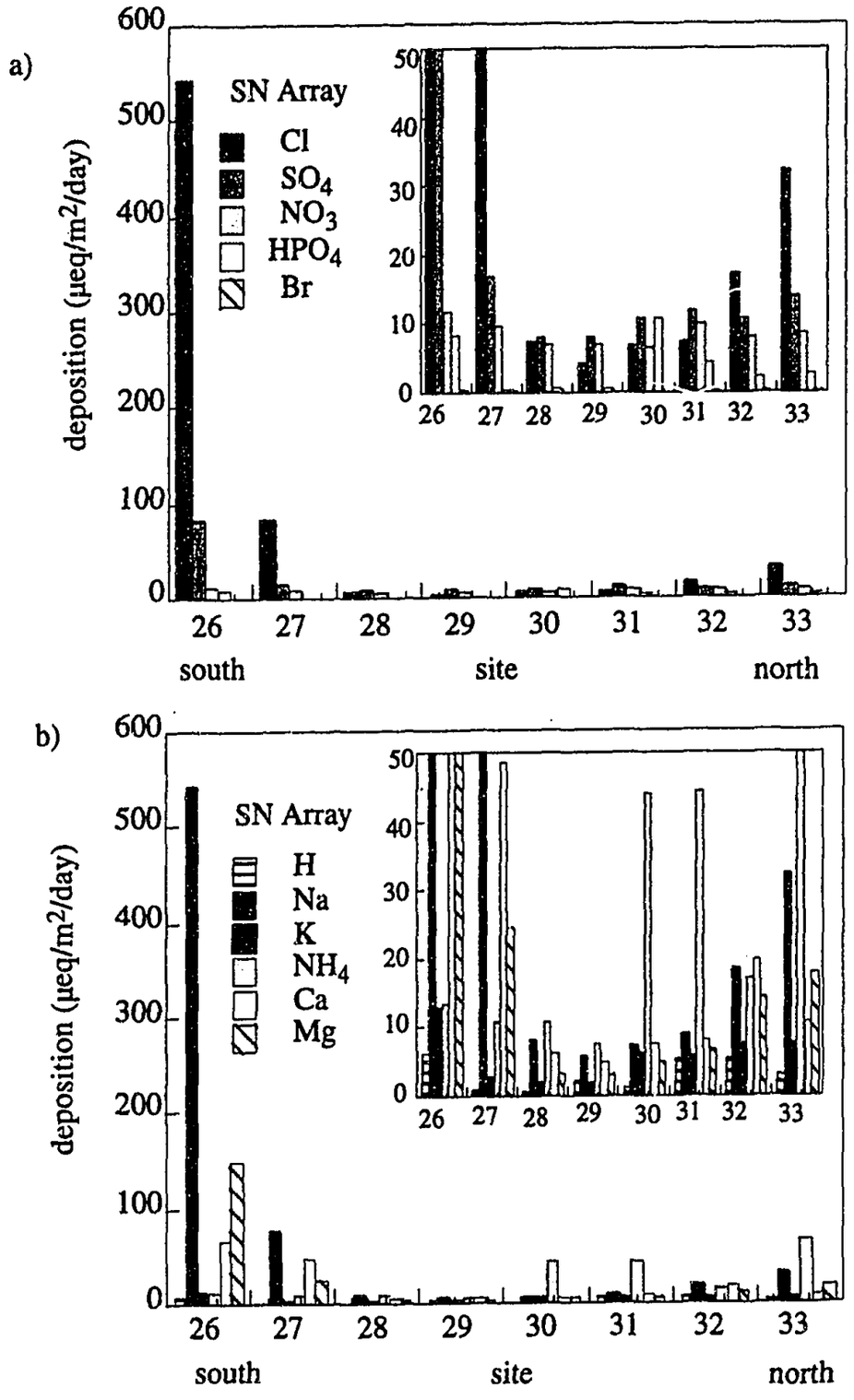

FIGURE 5.7 Mean deposition of a) anions and b) cations for the SN Array. Insets show spatial variations of ionic species with low deposition rates. See Figure 3.1 for site number locations.

The most obvious pattern displayed by both cations and anions is for very high deposition rates at the southern coastal site, (26 Port Lincoln), decreasing inland, and increasing at the most northern site 33 (Kapalga). This pattern again most likely reflects the influence of seawater at the coastal margins of the continent. When the inland sites are examined in more detail (Figure 5.7) a change in the significance of major chemical species is noted at sites 28 (Wintinna), 29 (Alice Springs), 31 (Dunmarra) and 32 (Katherine). At these sites anions, SO_4 and NO_3 become as, or more, significant as Cl, and cations NH_4, Ca and Mg become comparable to Na. This again reflects the limited influence of seawater to deposition at these inland sites, where if it were significant, Na and Cl would be the most important species as at site 26 (Port Lincoln). The high flux of NH_4 at sites 30, 31 and 33 most likely reflects the high level of biological activity as expected in tropical regions.

The mean total ion deposition for each season is shown in Figure 5.8 for the southern and northern section of the SN array. Deposition in the south of the array is greater than in the north. Maximum deposition occurs in the south during spring 92, and the relatively high deposition that occurs during winter of each year, represent the importance of winter rainfall in the south of the array. Maximum deposition rates occur during the summer seasons in the north of the array, while minimum deposition occurs during winter of each year, reflecting the control of the monsoonal rainfall on deposition. When individual ions are investigated (Figure 5.9), it can be seen that the above seasonal variation patterns are predominantly followed by Na and Cl in the south of the array. In the north of the array the pattern is dominated by Cl, Na, SO_4, NO_3 and NH_4.

5.3 MULTIVARIATE RELATIONSHIPS

Multivariate analysis is performed on total and subsets of WE and SN data sets to isolate the sources of ionic constituents in precipitation, by grouping ionic species with similar variances. The background, theory and previous examples of the application of factor analysis (FA) and principal component analysis (PCA) are given in Section 3.3.

The application of FA to the data from both arrays reveals the influence of three major sources/processes that control the ionic composition of precipitation collected in the present investigation. These are termed a mixed seawater/continental source, acid-base balance factor and biodegradation.

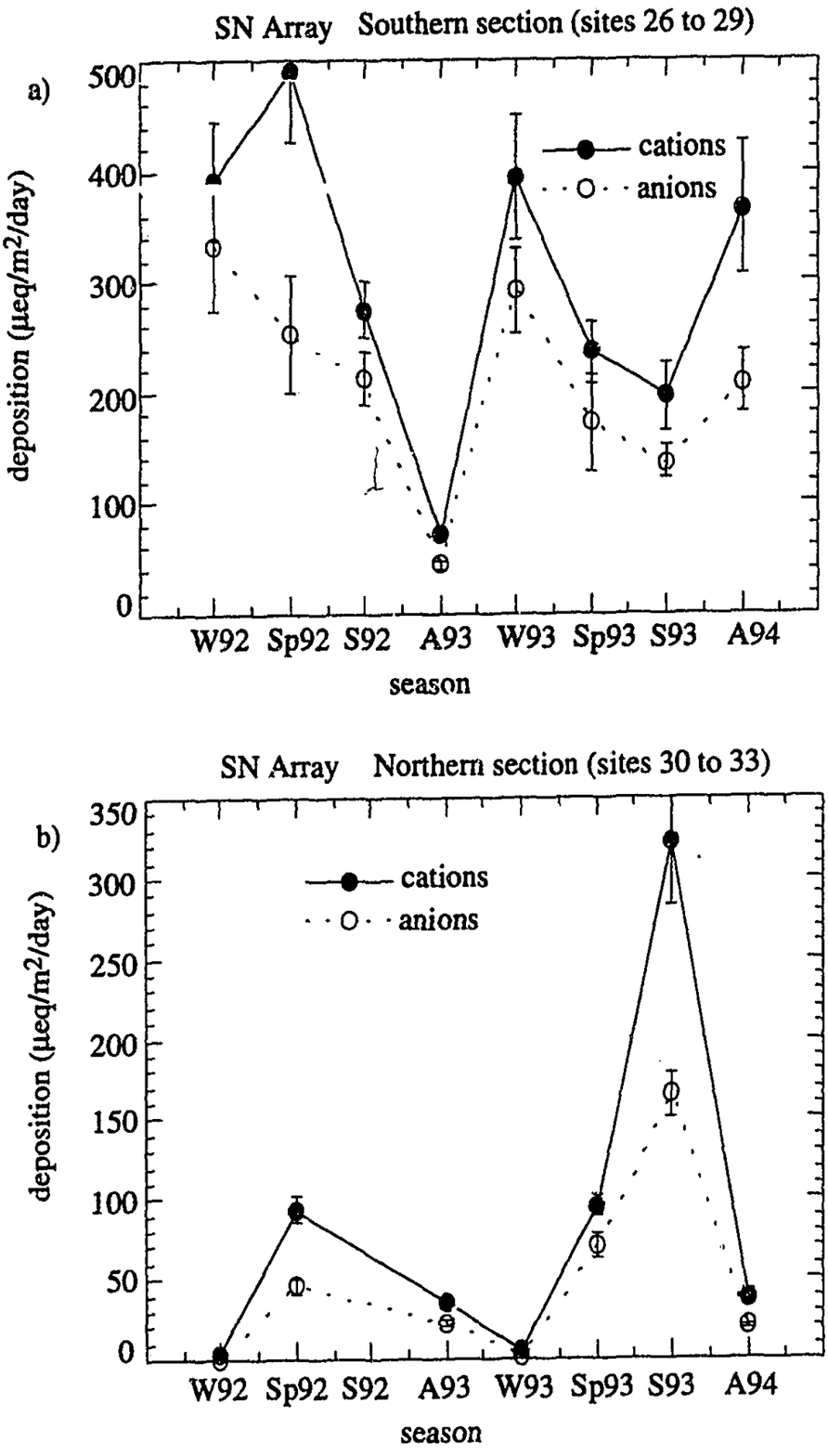

FIGURE 5.8 Seasonal variations in the deposition of total cations and anions for a) the southern section of the SN array and b) the northern section of the SN array. W93=winter 93, Sp93=spring 93, S93=summer 93, A93=autumn 93 etc.

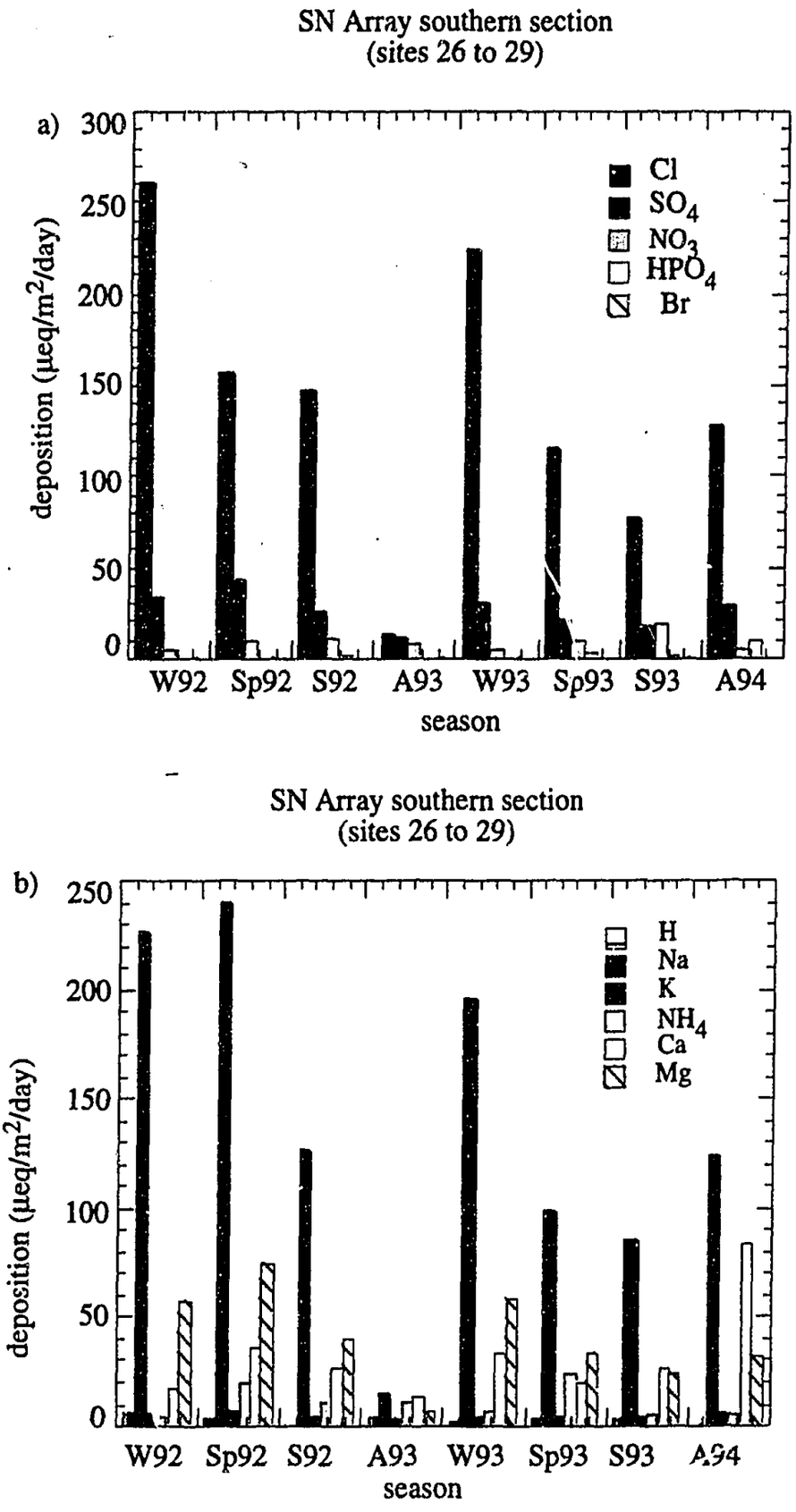

FIGURE 5.9 Mean seasonal deposition of a) anions and b) cations for the southern section of the SN array and c) anions and d) cations for the northern section of the SN array. A93= Autumn 93, W93=Winter 93, Sp93=Spring 93, S93=Summer 93 etc.

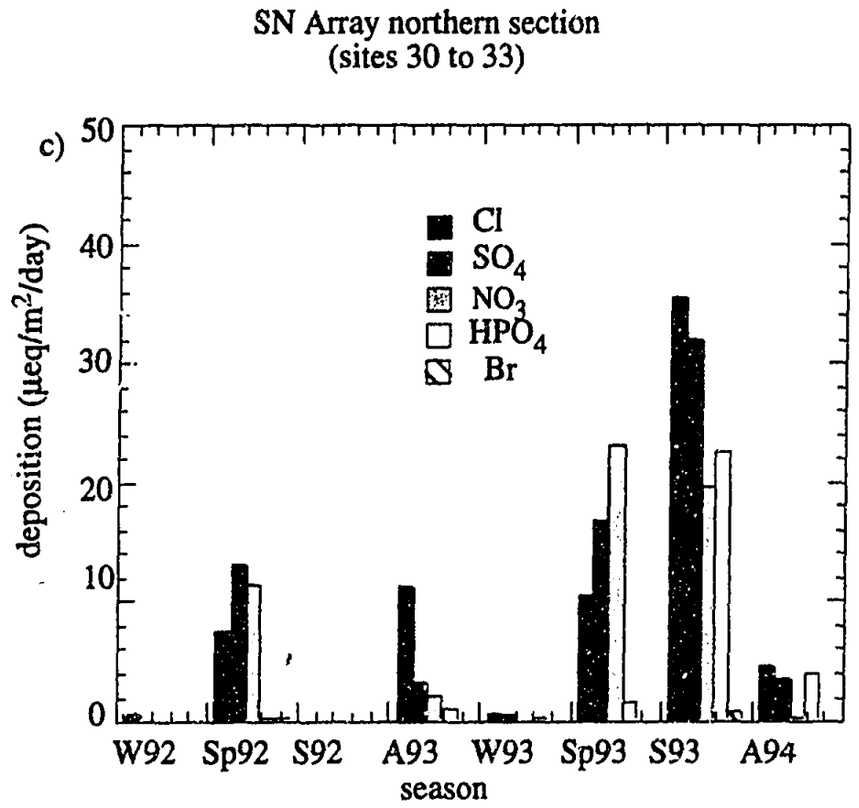

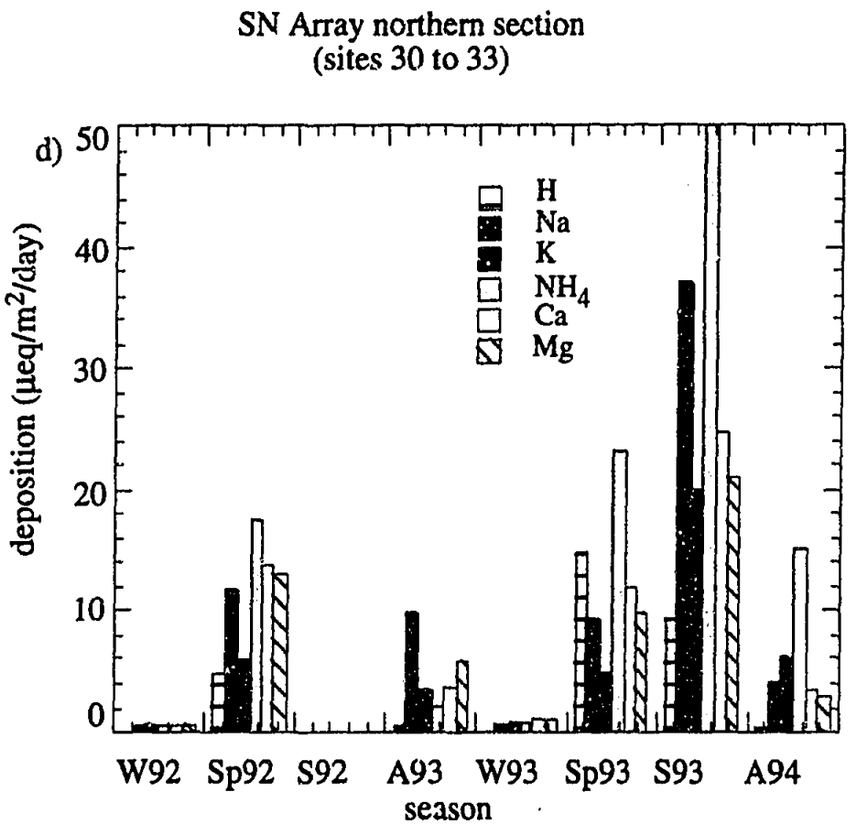

FIGURE continued

The seawater/continental source defines common variation between Cl, Na, Mg, SO_4, Br, Ca and K. FA is generally unable to distinguish between the two end-members of this source, although dividing the data into subsets (eg. coastal and non-coastal) shows higher loadings of seawater constituents (Cl, Na and Mg) with respect to continentally sourced ions (eg. Ca and K) in coastal subsets. The natural acid-base balance factor groups all or some of NO_3, SO_4 and H. Biodegradation groups NH_4, H, K and HPO_4. HPO_4 may also indicate agricultural input in the form of fertiliser, and may be particularly significant in the southern section of the SN array where agricultural activities are concentrated. Note that the assignment of sources based upon species groupings is a subjective process.

The significance of the influence of each of the three factors differs between data sets and subsets, and in some cases a factor may be described in terms of a combination of sources. For example, a mixed seawater/continental/biodegradation source may be invoked to explain the grouping of Cl, Na, Mg, SO_4, Ca, K, NH_4 and H.

Principal component analysis is applied to subsets made up of data for individual sites and isolates the same three sources/processes as FA performed on the larger data sets.

Within the framework provided by the three factors described above the following discussion describes details of the application of FA and PCA to the WE and SN data sets (and subsets of these). Because of the approximately log-normal distribution of the data described above, all multivariate analyses are performed on log-transformed data. Factor loadings of greater than 0.4 are considered to be significant, following the technique of Crawley and Sievering (1986).

Factor Analysis of the WE Data Set

The results of the FA of the total WE data set are shown in Table 5.11. The three factors described above explain 78% of the variance in the data set. High loading of seawater components (i.e. Na, Cl and Mg) in the mixed seawater/continental factor indicates the predominance of seawater in this mixed source. The presence of Br in the acid-base balance factor most likely reflects the low concentration of this ion (usually less than the level of detection) at all sites except the coastal site 16 (Cliff Head), and is therefore most likely an artifact of the measurement technique. The relationships between the factor loadings of each species can be more clearly seen in the factor loading diagrams of Figure 5.10. In these plots factor loadings are plotted as co-ordinates. Species that have high loadings on a single factor will cluster along the end of the axis of that factor, eg. Cl, Na and Mg for factor 1. Species that cluster

near the origin have small loadings on both factors, eg. Na, Cl and Mg for factor 2 and 3. Species that plot between two axes may be explained by two factors, eg. K for factors 1 and 3.

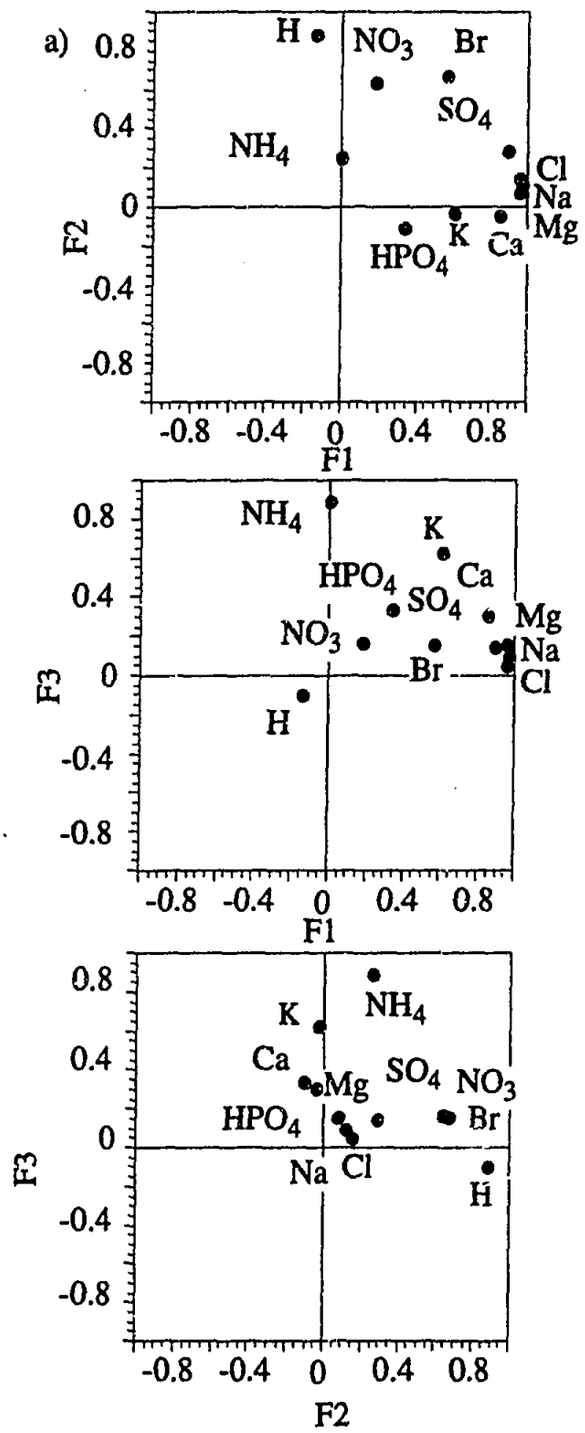

FIGURE 5.10 Factor loading plots for data from the WE array. F1, F2 and F3 represent factor 1, factor 2 and factor 3. Species that have high loadings on a single factor cluster along the end of the axis for that factor, eg. Na, Cl and Mg have high loadings on F1. Species that cluster near the origin, have small loadings on both factors in the plot, eg. Na, Cl and Mg for F2 and F3. Species that plot between two axes may be explained in terms of two factors, eg. K for F1 and F3.

TABLE 5.11 Factor loadings for the WE data set (n=73). Bold values highlight loadings of greater than 0.4.

Factor	Factor 1	Factor 2	Factor 3
% variance	52.9%	14.9%	9.9%
eigen value	5.8	1.6	1.1
H	-0.14	**0.89**	-0.10
Cl^-	**0.96**	0.15	0.06
SO_4	**0.90**	0.29	0.15
NO_3	0.18	**0.64**	0.17
HPO_4	0.34	-0.11	0.34
Br	**0.56**	**0.67**	0.16
Na	**0.97**	0.11	0.10
K	**0.61**	-0.03	**0.63**
NH_4	0.00	0.26	**0.90**
Ca	**0.86**	-0.04	0.31
Mg	**0.96**	0.08	0.16
source/process	seawater/continental	acid/base balance	biodegradation

The results of this FA suggest the major source of ionic constituents to WE precipitation is of mixed seawater/continental origin. The relationship between the continental and seawater source may be further investigated by dividing the data set into coastal and non-coastal data sets based on the proximity of the sample location to the Western Australian coast, and comparing factor loadings for each data subset. Coastal localities were chosen to lie within 200 km of the coast, (after Simpson and Herczeg 1994), so include sites 16 (Cliff Head) to 18 (Badja). Inland sites include the remaining sampling localities, i.e. 19 (Iowna) to 25 (Everard Junction). It should be noted here and for elsewhere in this section that dividing the larger data set into subsets (i.e. coastal and non-coastal) has the effect of increasing the uncertainties associated with FA, because the number of cases is reduced.

The results of FA performed on the coastal and non-coastal data subsets are summarised in Table 5.12 and detailed in Appendix F. The results are similar to the FA performed on the entire WE data set. However, the factor loadings of species in the mixed seawater/continental source are greater for the coastal data subset suggesting that at non-coastal sites the remaining two factors are also important to the variance of these species. The high loading of all species into F1 for the coastal data subset may be showing the predominance of seawater as a source at the coast, as is intuitively suggested by the coastal locality of these sampling sites.

TABLE 5.12 Summary of FA performed on coastal and non-coastal data subsets. Ionic species are listed in order of decreasing factor loadings.

	Factor 1	Factor 2	Factor 3
% variance	59%	13%	10%
Coastal	Mg, Cl, Na, SO_4, K,	H, NO_3, Br	NH_4
n=24	Ca, Br, HPO_4		
source/process	seawater/continental	acid-base balance	biodegradation
% variance	42%	16%	14%
Non-coastal	Na, Mg, Cl, SO_4,	NH_4, K, Ca, NO_3	H, NO_3
n=49	Ca, NO_3		
source/process	seawater/continental	biodegradation/continental	acid-base balance

Principal Component Analysis on the WE Data Set

The change in emphasis of each species in the three factors between the coastal and non-coastal data subsets can be further investigated by looking at principal component loadings that are calculated when the data set is divided into individual sites. PCA is used to calculate the principal component loadings as outlined in Section 3.3. The results of PCA on data sets of each site are shown in Figure 5.11 and summarised in Table 5.13. The sites display variance explainable by three or four components. The loading of species in the fourth component for sites 19 (Iowna) to 23 (Carnegie) represent duplications of one of the three sources/processes described by FA, thus Figure 5.11 shows only three components. Of note in Figure 5.11 are both negative and positive component loadings, which provide additional information with regards to the importance of each component to a particular species. For example, Site 20 (Barrambie) shows highly negative loadings for species in PC2 (H, SO_4, NO_3, NH_4 and Ca), suggesting the acid-base balance, biodegradation and possibly a gypsum (Ca and SO_4) input, while high positive loadings of Na and Cl may suggest halite input.

All sites are characterised by a high loading of most species into PC1. At sites 16 (Cliff Head) to 19 (Iowna), 23 (Carnegie) and 25 (Everard Junction) the loading of species in PC1 suggests a mixed seawater/continental origin. However, the high loadings of H and NO_3 in PC1 for sites 20 (Barrambie), 21 (Yeelirrie), 22 (Lake Violet) and 24 (Gunbarrel) suggest a mixed continental/acid-base balance. The

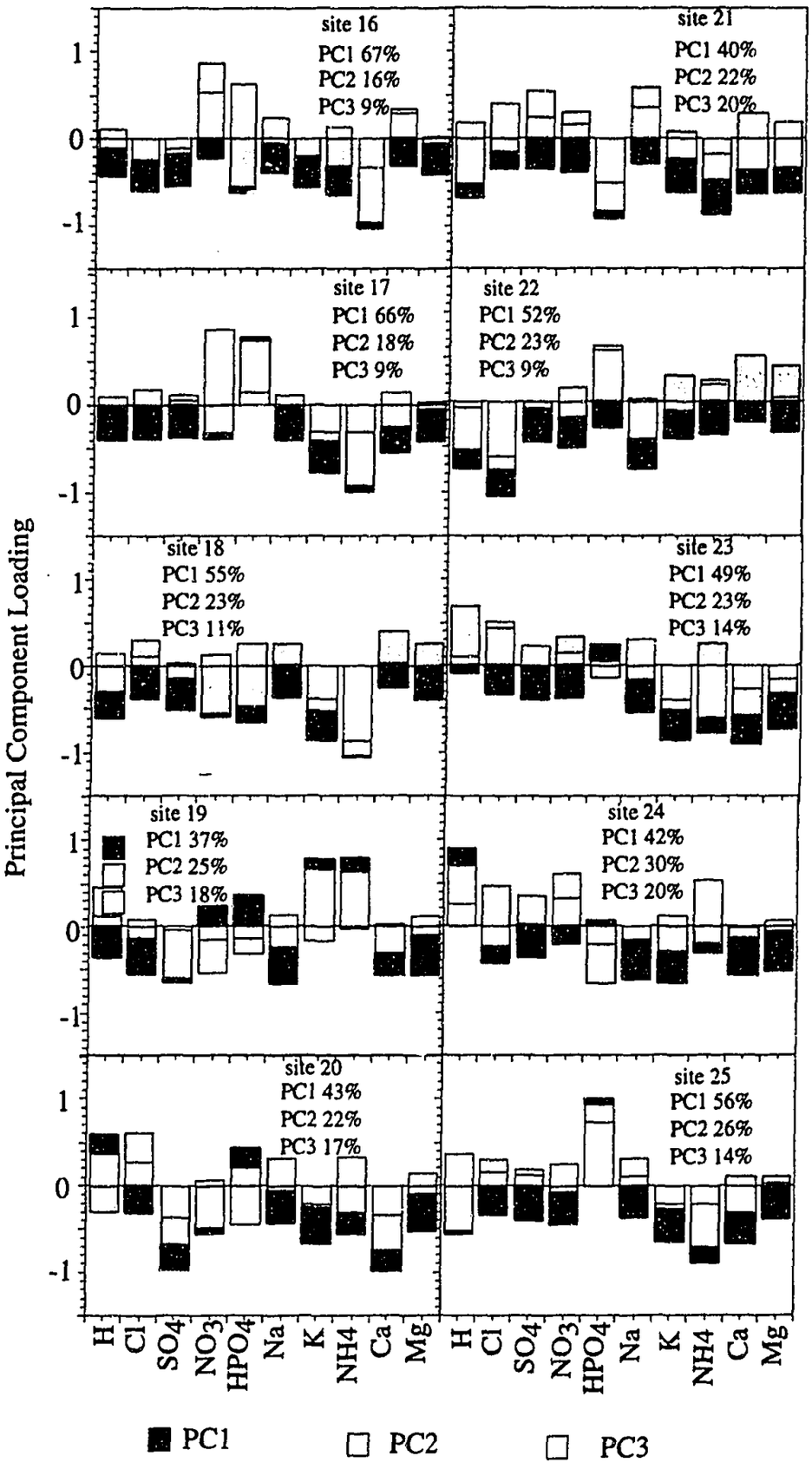

FIGURE 5.11 Principal component loadings for individual sites along the WE array. PC = principal component loading. See Figure 3.1 for site number localities

extent of this influence at each site differs however, as suggested by the differences in variation explained by PC1 at each site (Table 5.13). As distance from the coast increases, the amount of variance explained by this mixed continental seawater source decreases from 66% at the coastal site to 37% at site 19 (Iowna). Sites 23 (Carnegie) and 25 (Everad Junction) display the influence of a mixed seawater/continental source, explaining approximately 50% of variance at these sites.

The loading of species amongst the three PCs at inland sites, 20-25 (Barrambie to Everard Junction), may be interpreted as showing the stronger influence of continental sources of material to precipitation. For example, at site 20 (Barrambie), PC2 shows high negative loadings of Ca, SO_4, NO_3 and H, and high positive loadings of Na and Cl, suggesting a mixed acid/base and continental source. The continental source in this case appears to be supplying halite. Other sites where a salt-lake source of material may be inferred include site 21 (Yeelirrie) and 22 (Lake Violet) where PC2 has high loadings for Ca and SO_4, suggesting a gypsum source, and PC3 has high loadings for Na and Cl, suggesting a halite source. Site 23 (Carnegie) also shows high loadings of Na and Cl for PC3. The importance of salt lakes as sources of material to these inland sites is not surprising when the number of salt lakes in the proximity of the WE array is considered, and will be important in the discussions of ^{36}Cl compositions of Chapter 6.

TABLE 5.13 Summary of variances attributable to each PC for the WE data set.

site	% variation PC1	% variation PC2	% variation PC3	% variation PC4
16 Cliff Head	67	16	9	
17 Morawa	66	18	9	
18 Badja	55	23	11	6
19 Iowna	37	25	18	10
20 Barrambie	43	22	17	8
21 Yeelirrie	40	22	20	8
22 Lake Violet	52	23	9	9
23 Carnegie	49	23	14	7
24 Gunbarrel	42	30	20	
25 Everard Junction	56	26	14	

Acid-base balances and sample biodegradation are also significant at each site, being more so at inland sites than coastal localities.

Factor Analysis of the SN Data Set

Two factors explain 85% of the variance displayed by the SN data set (Table 5.14 and Figure 5.12). The first factor (74%) suggests mixed seawater/continental and biodegradation, and the second (11%), acid-base balances. Again, the high loading of Br in the second factor is most likely an artifact of the below-detection-level of Br at all sites except the coast, as described for the WE data set. The continental component of this mixed source may include an agricultural input, as suggested by the high loading of HPO_4 in factor 1.

TABLE 5.14 Factor loadings for SN data set (n=57). Bold values highlight loadings of greater than 0.4.

	factor 1	factor 2
% variation	73.5	10.6
eigen value	8.1	1.2
H	0.08	**0.94**
Cl	**0.85**	0.35
SO_4	**0.89**	0.33
NO_3	**0.74**	**0.50**
HPO_4	**0.85**	-0.23
Br	**0.76**	**0.60**
Na	**0.87**	0.37
K	**0.89**	0.15
NH_4	**0.76**	0.14
Ca	**0.90**	0.26
Mg	**0.89**	0.35
source/process	continental/seawater/ biodegradation	acid-base balance

The extreme differences in rainfall regimes experienced by the southern and northern sections of the SN array (i.e. the northern section experiences summer rainfall while the southern section experiences winter rainfall), suggests it may be useful to divide the SN data set into northern (30-33) and southern (26-29) sites. The northern data set is further subdivided into wet and dry sampling periods. The dry periods are

times when the prevailing wind direction is from the southeast (i.e. off the continent). The wet periods represent monsoonal and transitional monsoonal activity. The transitional monsoon periods are marked by the monsoonal trough existing north of the latitude of Jabiru (Gillett et al 1990) and therefore are also represented by southeasterly winds. However, as discussed in Chapter 2, the monsoonal period involves winds from the northeast. Thus dividing the northern data subset into wet and dry periods may provide some information about the effect of the monsoon on precipitation chemistry. The southern data subset is also further divided, into coastal (sites 26 and 27) and inland (sites 28 and 29) data subsets, to assess the effect of seawater input to these localities.

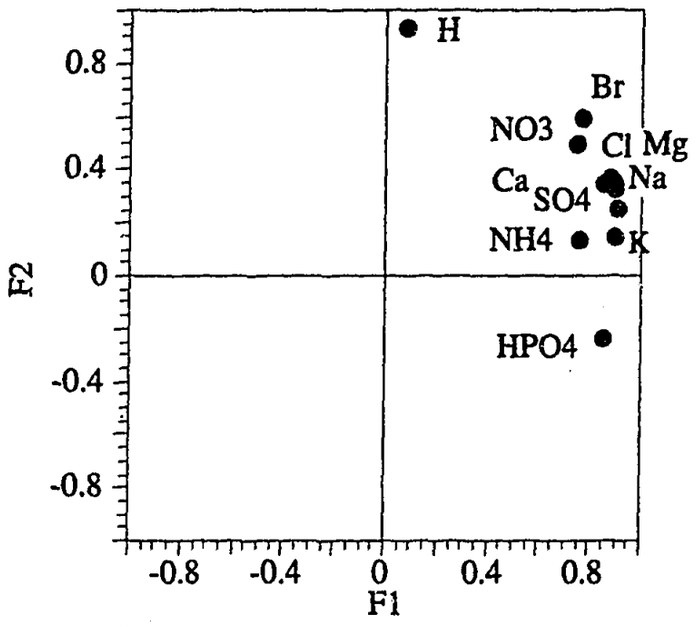

FIGURE 5.12 Factor loading plot for all data from the SN array.

Northern Subset

The results of the FA on the northern data subsets are summarised in Table 5.15 and detailed in Appendix F. A mixed seawater/continental and biodegradation source explains most of the variance for each data subset. Little effect on the overall variance explained by each factor is observed for the wet data set. The dry data set, however, has a lower amount of variance explained by the two-factor model (85%) than does the wet or complete northern data set (93%). The loading of individual species in each factor also differs between data subsets. High loadings of seawater species (i.e. Na, Cl and Mg) in the second factor for the wet data subset suggest an isolation of the seawater source associated with monsoonal and transitional monsoon deposition. This is not surprising since monsoonal precipitation moisture is derived from tropical marine air masses, as discussed in Chapter 2. It is also not surprising

that the distinct seawater source of wet deposition explains only a very small proportion of the variance in the wet data subset, and indicates the influence of southeasterly winds during transitional periods when wet deposition occurred.

TABLE 5.15 Summary of FA performed on northern, northern wet and northern dry data subsets. Ionic species listed in order of decreasing factor loadings.

	Factor 1	Factor 2
% variance northern subset (all seasons) n=24 source/process	82% K, Na, Mg, Cl, Ca, HPO_4, SO_4, NH_4, NO_3 seawater/continental and biodegradation	12% H, NO_3 acid-base balance
% variance wet samples (n= 14) source/process	81% HPO_4, K, NH_4, SO_4, Ca, Cl, Na, Mg, NO_3 biodegradation and mixed continental seawater	12% H, NO_3, Mg, Na, Ca, Cl SO_4 acid-base balance and seawater
% variance dry samples n=11 source/process	77% Na, Cl, Mg, Ca, K, HPO_4, NH_4, NO_3 seawater/continental and biodegradation	8% H, HPO_4, NO_3 acid-base balance

Southern Subset

The results of the FA performed on data subsets from the southern section of the SN array are summarised in Table 5.16 and detailed in Appendix F. Three factors explain the variance of the data sets, with the loadings of ionic species again suggesting the sources/processes discussed throughout this section. The high loading of HPO_4 in the third factor may represent an agricultural input.

Isolation of seawater from the mixed seawater/continental source is again noted when the southern data set is divided into coastal and non-coastal subsets. The negative loading of Ca in the second factor may represent the neutralising property of $CaCO_3$, evidenced by the presence of carbonate crusts on dunes in the vicinity of the coastal site 26 (Port Lincoln). The non-coastal data subset shows lower magnitude in loadings of species for factor 1 than for the coastal data subset,

indicating the importance of factors 2 and 3 on the variance of the species in the non-coastal data subset.

TABLE 5.16 Summary of FA performed on northern, northern wet and northern dry data subsets. Ionic species listed in order of decreasing factor loadings.

	Factor 1	Factor 2	Factor 3
% variance southern subset (all sites) n=34 source/process	61% Mg, Cl, Na, Ca, SO_4, K mixed seawater/continental	12% H, NO_3, Br, SO_4, K acid-base balance and continental?	10% HPO_4, NH_4 biodegradation
% variance Coastal n=19 source/process	57% Mg, Na, Cl, SO_4, K, Br, H, Ca seawater/continental	16% H, NO_3, HPO_4, -Ca acid-base balance	16% -NH_4, HPO_4, NO_3, Ca biodegradation
% variance Non-coastal n=15 source/process	60% Cl, Na, Mg, NO_3, Cl, NH_4, Ca seawater/continental	18% H, SO_4, Mg, K, NO_3 acid-base balance and continental	10% HPO_4, K, NH_4, Ca biodegradation

Principal Components in the SN data set

PCA performed on individual site data sets show very similar results to the FA for the various groups of data. Results of PCA on individual site data sets are shown in Figure 5.13 and summarised in Table 5.17.

Variance at the southern sites can be explained by three components. The coastal site (26 Port Lincoln) has a PC1 with high loadings of seawater species, while PC2 represents mixed acid/base continental source with the neutralising role of Ca as sourced from calcareous dunes inferred by the high loading of Ca in this component. The third PC has high loadings of acid-base and biodegradation species. Site 27 (Gawler Ranges) has similar loadings of species in the three components, although the seawater component is less significant in explaining the variance. At site 28 (Wintinna), most of the variance can be explained in terms of a continental source and acid-base balance. A mixed seawater/continental source makes up PC2 which is almost as significant as PC1, and PC3 represents a continental (possibly agricultural)

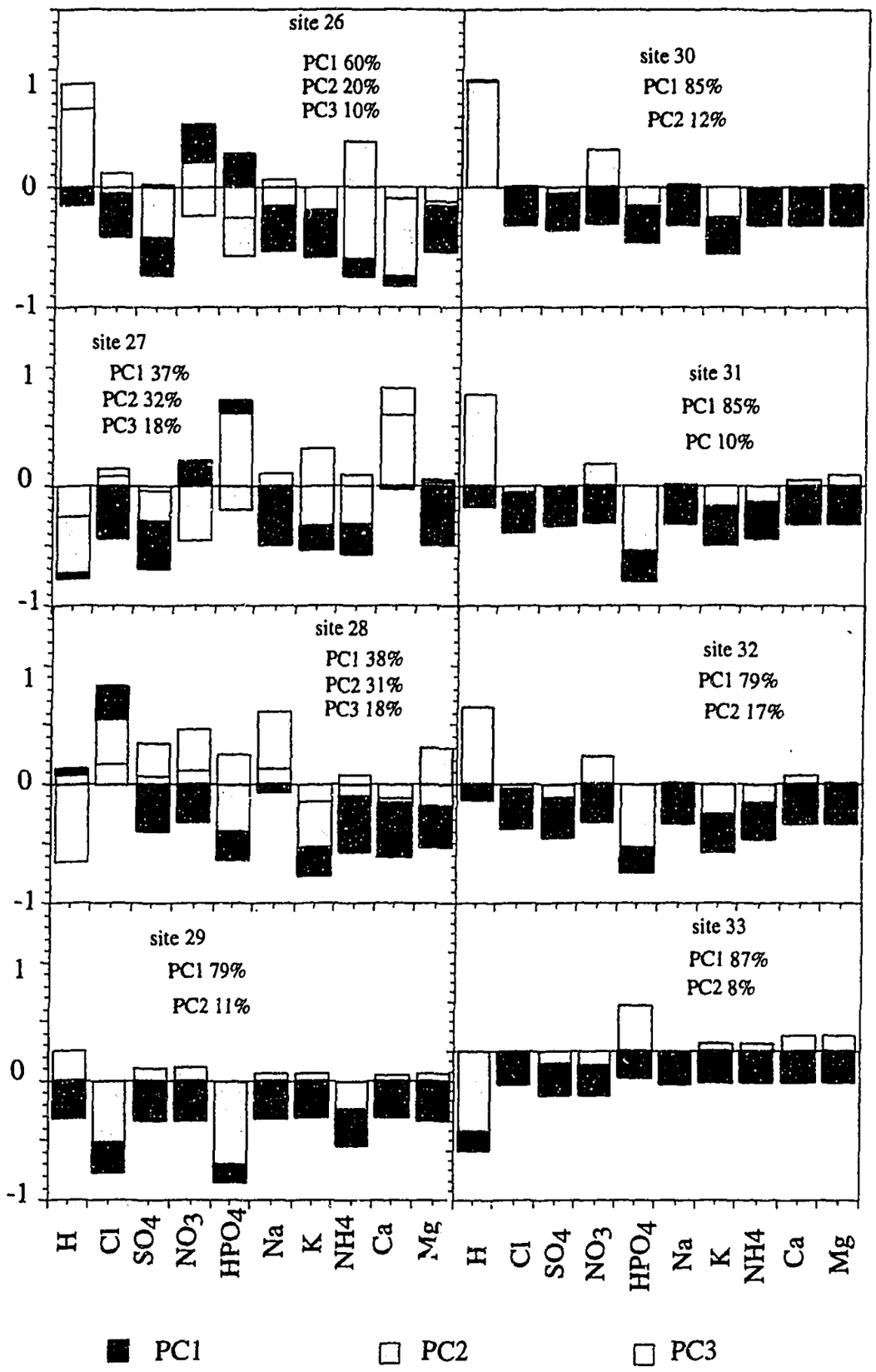

FIGURE 5.13 Principal component loadings for individual sites along the SN array. PC= principal component.

source. Sites 29-33 (Alice Springs to Kapalga) display two principal components, comprising a mixed continental/seawater/biodegradation origin and acid-base balances. The amount of variance explained by each component ranges between 79 and 87% for PC1, and 8 to 11% for PC2.

TABLE 5.17 Summary of variances attributable to each PC for the SN data set.

site	% variation PC1	% variation PC2	% variation PC3
26 Port Lincoln	60	20	10
27 Gawler Ranges	37	32	18
28 Wintinna	38	31	18
29 Alice Springs	79	11	
30 Tennant Creek	85	12	
31 Dunmarra	85	10	
32 Katherine	79	17	
33 Kapalga	87	8	

The results of multivariate analyses performed on the SN data set reveal that variations are primarily controlled by the variations that occur in the northern half of the array. This is suggested by the similarity between results of FA analysis on the entire data set and the results of PCA on the northern most individual sites 29-33 (Alice Springs to Kapalga). The northern sites of the array are influenced primarily by mixed continental/seawater/biodegradation sources. During periods of monsoonal and transitional precipitation, a seawater factor can be isolated in the variation displayed by the northern sites, but this factor is only responsible for a very small amount of variation during the wet season. The southern localities are influenced by three factors; a mixed seawater/continental source, acid-base balances and biodegradation. The coast proximal sites 26 (Port Lincoln) and 27 (Gawler Ranges) show the influence of a seawater source which contributes to a large proportion of variance (30-60%).

5.4 SPATIAL AND SEASONAL VARIATIONS

The results of multivariate analyses show that there are three major processes that affect the composition of rainfall across the arrays; the influx of a mixed seawater/continental source, natural acid/base balances in the atmosphere and decomposition of the sample between deposition and collection from the field. The following discussion assesses each of these processes in more detail.

Mixed Seawater/Continental Source

The most significant source of material to the rain collectors along the WE and SN arrays is of mixed seawater/continental origin. The results of dividing the WE data set and southern section of the SN data set into coastal, non-coastal and individual sites, suggests that the relative input of a seawater and continental source is dependent on sample locality. The mean seasonal patterns of depositional flux, described in Section 5.2, suggest that there is a seasonal dependency in the supply of most species to the collectors. The following discussion uses simple graphical techniques described in Section 3.3 to carry out a detailed investigation of the variations displayed by this mixed seawater/continental source over space and time.

Spatial Variations along the WE Array

The mean ratios of Cl, SO_4, K, Ca and Mg to Na at each site on the WE are shown in Figure 5.14. Also plotted are the ratios of these species in seawater. As expected, the coastal locality (site 16 Cliff Head) displays ratios found in seawater, suggesting the coastal rainwater samples represent diluted seawater. The Cl/Na ratio displays a decrease with increasing distance from the coast, while each of the ratios of the other ions to Na show an increase. The decreasing Cl/Na ratio with increasing distance from the coast may be attributable to the addition of continental soil or dust material that has a Cl/Na ratio lower than that of seawater, or to the liberation of Cl and H (to produce gaseous HCl) by H_2SO_4. This latter process has been used to explain depletions of Cl in marine aerosols of up to 12% (Warneck 1988). The inland sites of the WE array (site 20 Barrambie to site 25 Everard Junction) display depletions of up to 18%, suggesting that both processes are acting to decrease the Cl/Na ratio as distance from the coast increases. In addition, attributing the trend mostly to the input of non-seasalt aerosol material with low Cl/Na ratios agrees with the trend of increasing ratios displayed by SO_4, K, Ca and Mg ratios with Na with increasing distance from the coast. Thus, seawater may be the main source of Cl to the rain collectors, while the ions SO_4, K, Ca and Mg are influenced by an additional source at non-coastal localities. The very low concentrations (i.e. near the detection level of instrumentation) of Br in rainfall at non-coastal localities also suggests seawater to be the sole source of Br to the array. However, because of the low concentrations and therefore high errors, Br is excluded from the following discussion.

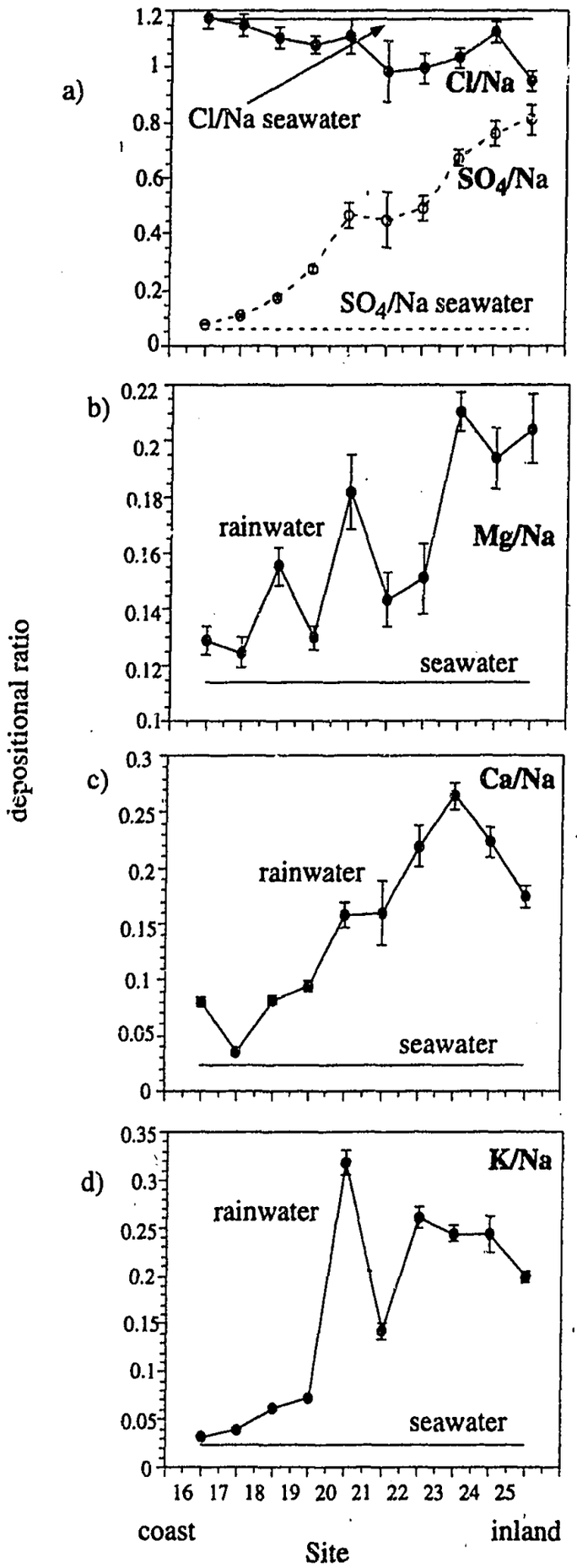

FIGURE 5.14 Mean Ratios of a) Cl and SO_4, b)Mg, c) Ca and d) K with Na for sites along the WE array compared with the ratios found in seawater. Seawater ratios calculated from Millero 1977. Ratios calculated from depositional units ($\mu eq/m^2/day$). See Figure 3.1 for site number names.

The non-seasalt source for SO_4, K, Ca and Mg to the rain collectors can be further investigated by looking at the "non-seasalt" (nss) fraction of these ions in rainfall (as defined in Section 3.3). Figure 5.15 displays the percentage of the nss ions as a function of distance from the coast for the WE array. In general, nss ions increase with increasing distance from the coast, with nss SO_4 and nss Ca reaching a steady state of between 40-50% at approximately 400 km from the coast. The percentage of nss K at inland sites reaches values of close to 90%, while nss Mg remains below 30% at inland sites. These patterns may suggest that the source of K to inland sites is almost exclusively from a source other than seawater, while seawater remains an important source of Mg at inland sites, and the ions SO_4 and Ca are influenced by a mixture of sources, one of which is seawater.

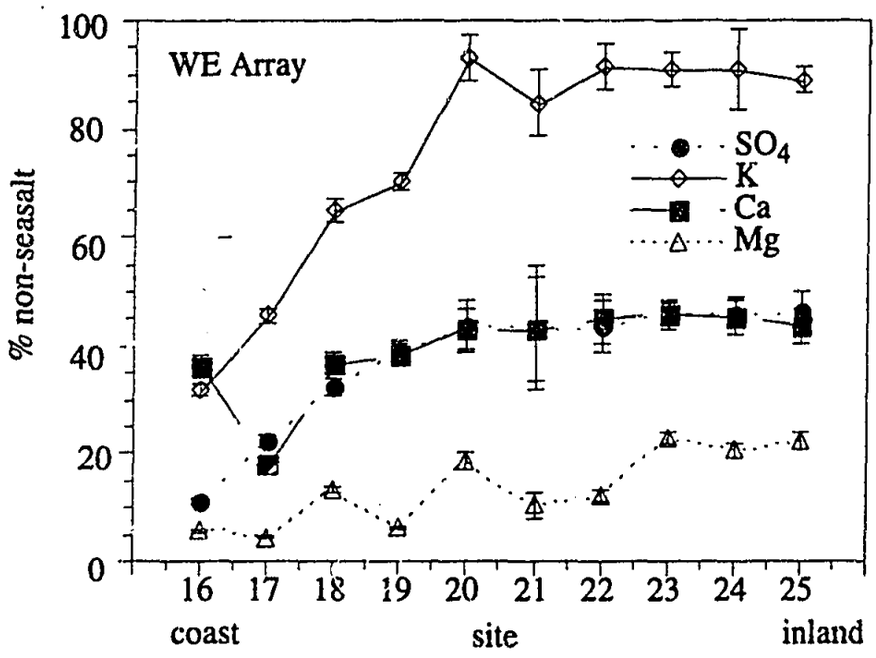

FIGURE 5.15 The mean non-seasalt proportions of SO_4, Ca, Mg and K for sites along the WE array. See Figure 3.1 for site locations.

Comparisons of mean ratios of Cl, SO_4, Na, K and Mg with Ca in rainfall and soil/dust samples collected from each site on the WE array are shown in Figure 5.16. Further evidence of the importance of seawater to the concentrations of Cl, Na and Mg can be seen with the decreasing of ratios of these elements to Ca as distance from the coast increases. The ratios generally move closer to those of the soil/dust compositions at inland sites, though SO_4/Ca in rainwater remains greater than in soil/dust compositions across the entire array, and no relationship can be discerned between rainfall and soil/dust K/Ca ratios.

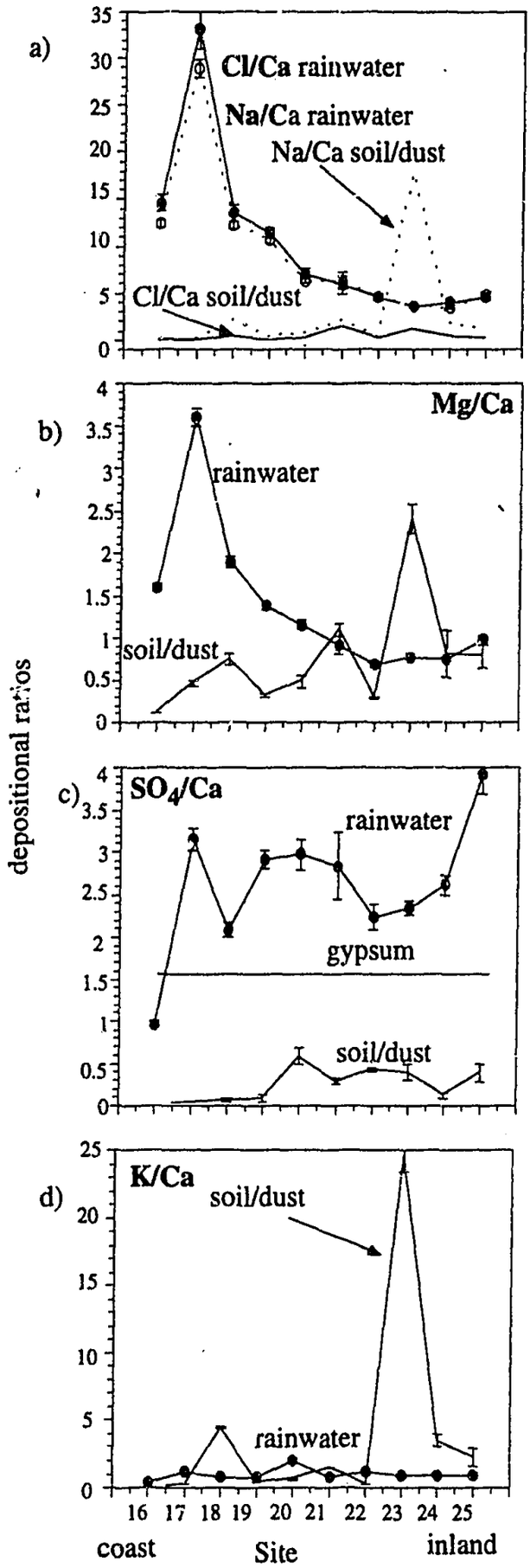

FIGURE 5.16 Mean ratios of a) Cl and Na, b) Mg, c) SO_4, and d) K with Ca for sites along the WE array compared with the ratios found in soil/dust collected at each site. Ratios calculated from depositional units ($\mu eq/m^2/day$). See Figure 3.1 for site localities.

Spatial Variations along the SN Array

The mean ratios of Cl, SO_4, K, Ca and Mg to Na at each site on the SN are shown in Figure 5.17. Site 26 (Port Lincoln), the southern coastal site, shows with ionic concentrations that approximate those found in seawater. The remaining sites show an increase in ratios (Cl shows a decrease) relative to seawater in a northward direction, suggesting the importance of a non-seawater source at these non-coastal sites. At the northern end of the array, ratios begin to fall closer to that of seawater, reflecting the influence of seawater at site 33 (Kapalga).

The non-seasalt fractions for sites along the SN array are shown in Figure 5.18. All nss concentrations show an increase from site 26 (Port Lincoln) to inland sites and a slight decrease at sites 32 (Katherine) and 33 (Kapalga). The relatively high nss fractions shown at site 33 suggest that seasalt is less important to the chemistry of precipitation than a non-seasalt source. This supports the work of Ayers and Gillett (1988a) who found high levels of non-seasalt Ca, Mg and SO_4 in rainfall at Jabiru. Despite site 33 (Kapalga) being within 100 km of the north coast of Australia, and the prevailing northwest winds during the monsoon, the high non-seasalt fractions represent the predominance of southeasterly winds during the non-monsoon periods. Thus, this locality may be considered continental rather than maritime.

The mean ratios of Cl, SO_4, K, Na and Mg to Ca, are compared with local soil/dust ratios for each site along the SN array in Figure 5.19. The importance of seawater to site 26 can be inferred from this plot by the high ratios of Cl, Na and Mg. An increase from the generally low ratios at inland sites to values seen at site 33 (Kapalga) also points to the importance of seawater at this site. The ratio of K with Ca increases from north to south, and SO_4 to Ca ratios approximate that of gypsum.

Simpson and Herczeg (1994) looked at the relative abundances of Ca and Na in rainfall from southeastern Australia in order to investigate the input of resuspended soil to precipitation. High Ca/Na ratios (greater than unity) were considered to represent a significant regional dust input, since Ca salts such as $CaCO_3$ and $CaSO_4.2H_20$, tend to be the first salts to precipitate out of soils. The WE data set all show Ca/Na ratios of less than 0.5 and sites along the SN array show mean Ca/Na ratios of less than 0.5. However several individual samples display ratios greater than 1, suggesting the influx of resuspended soil material. These samples include sites from both the north and south of the array, and represent some of the seasons of low to nil rainfall.

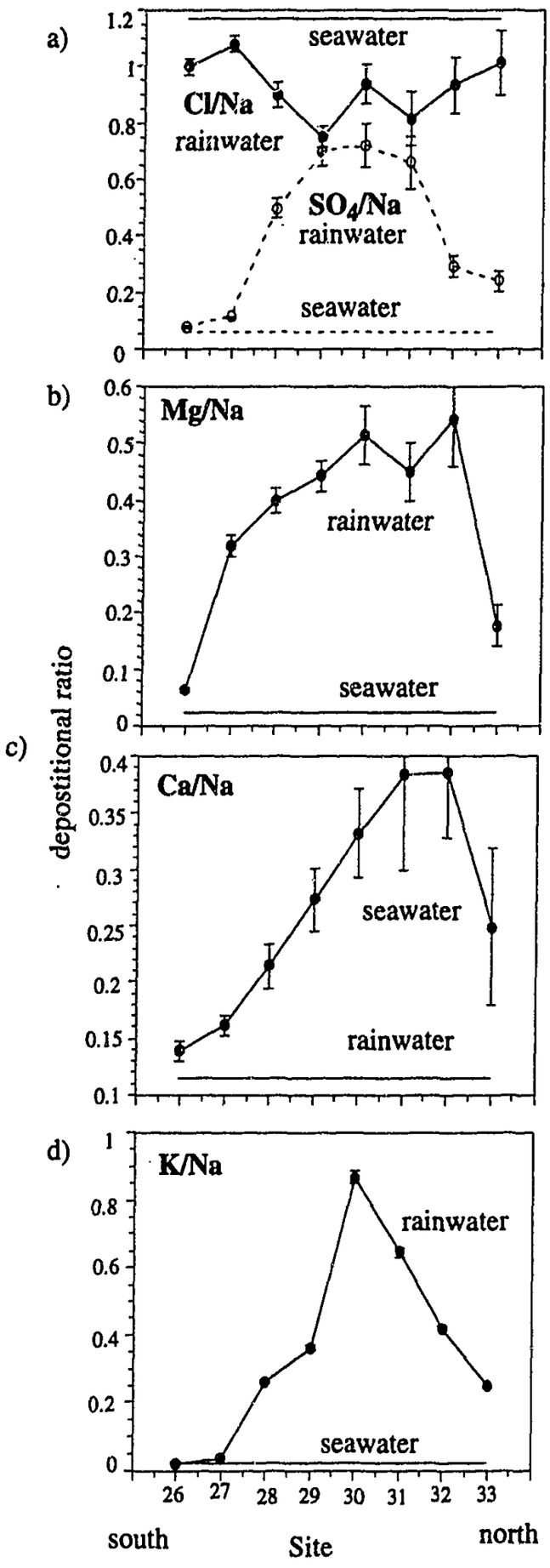

FIGURE 5.17 Mean Ratios of a) Cl and SO_4, b) Mg, c) Ca and d) K with Na for sites along the SN array compared with the ratios found in seawater. Seawater ratios calculated from Millero 1977. Ratios calculated from depositional units ($\mu eq/m^2/day$). See Figure 3.1 for site locations.

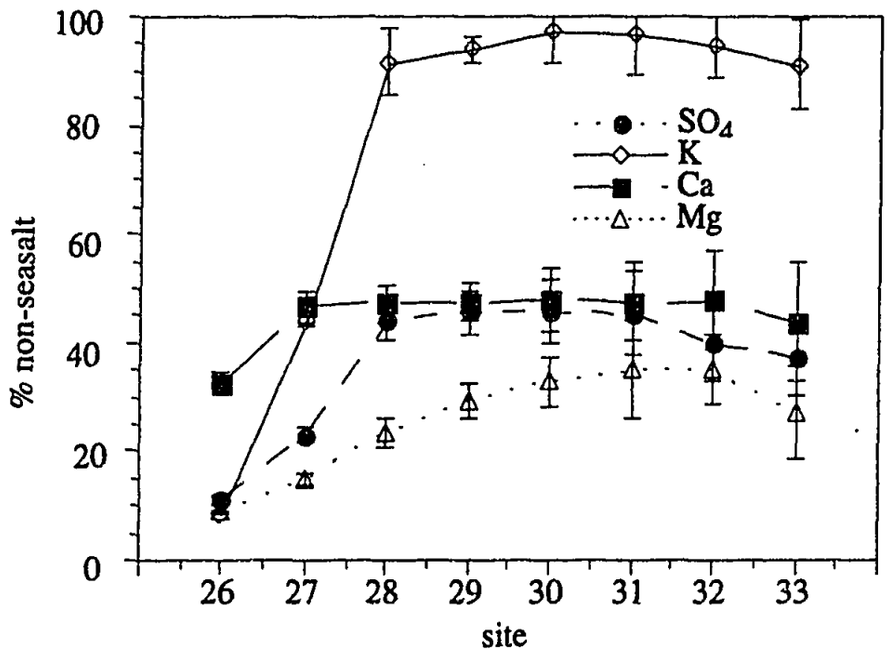

FIGURE 5.18 The mean non-seasalt proportions of SO_4, Ca, Mg and K for sites along the SN array. See Figure 3.1 for site localities.

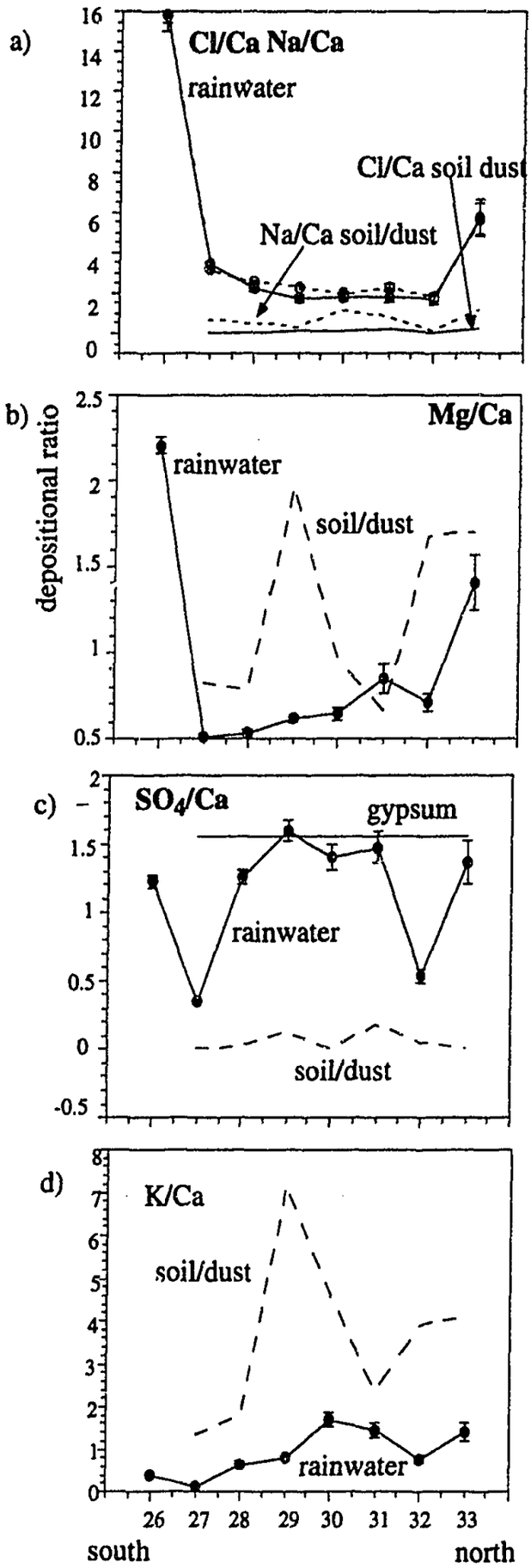

FIGURE 5.19 Mean ratios of a) Cl and Na, b) Mg, c) SO_4, and d) K with Ca for sites along the SN array compared with the ratios found in soil/dust collected at each site. Ratios calculated from depositional units ($\mu eq/m^2/day$). See Figure 3.1 for site localities.

Seasonal Variations

Seasonal changes in the influence of seawater as a source of material to rainfall at each site can be investigated by looking at the ratios of various species to Na and Ca at each site over time. The plots shown in Figure 5.20 show the ratios of Cl, SO_4, K, Mg, Ca and Na with Na and Ca for sites 16 (Cliff Head), 21(Yeelirrie) and 23 (Carnegie) along the WE array and Figure 5.21 shows the same ratios for sites 26 (Port Lincoln), 30 (Tennant Creek) and 33 (Kapalga) along the SN array. Also shown are the seawater ratios of these species, the local soil/dust ratios at each site, and the Cl/Na ratio of halite and SO_4/Ca ratio of gypsum.

Calcium is assumed to be of continental origin. Thus when a continental source is predominant at a site, increased supply of Ca leads to a decrease in the ratio of other species with respect to Ca. Hence low Ca ratios are generally interpreted as representing increased continental source influence. Low Ca ratios are often matched by Na ratios higher than that of seawater, suggesting an alternative source to seawater is adding all species except Na. The exception is when the Cl/Na ratio falls below that of seawater, indicating that the alternative source is then also adding Na. The local soil/dust ratios shown in the plots do not represent the end-member composition of the continental source, but rather, the composition of rainfall that would arise if soil/dust from the site in question were to enter the collector. The halite and gypsum ratios also do not represent the end-member composition of the continental source, but are shown on the plots as references for possible input of salt lake material to the rain collectors at each site. Because the concentration of seawater is well known, and we therefore have better constraints on the seawater source, the ratios are summarised in Figure 5.22 in terms of the dominance of a seawater source. During some collection periods, the behaviour of the different ratios is inconclusive or contradictory. Such cases are marked with a slash in Figure 5.22. For cases where analyses are missing, no results are shown.

As expected, site 16 (Cliff Head) is dominated by a seawater source throughout most of the sampling program, except for summer of each year and autumn of 91. An investigation of the synoptic patterns (Figure 5.23) reveals the dominance of cold front activity in association with rainfall at Dongara meteorological observation station (approximately 50 km north of site 16) throughout the sampling program. A similar trend is displayed by site 26 (Port Lincoln) on the SN array (Figure 5.24). Cold fronts affecting Western Australia and South Australia, involve air masses that are sourced from the south or southwest, i.e. of marine origin.

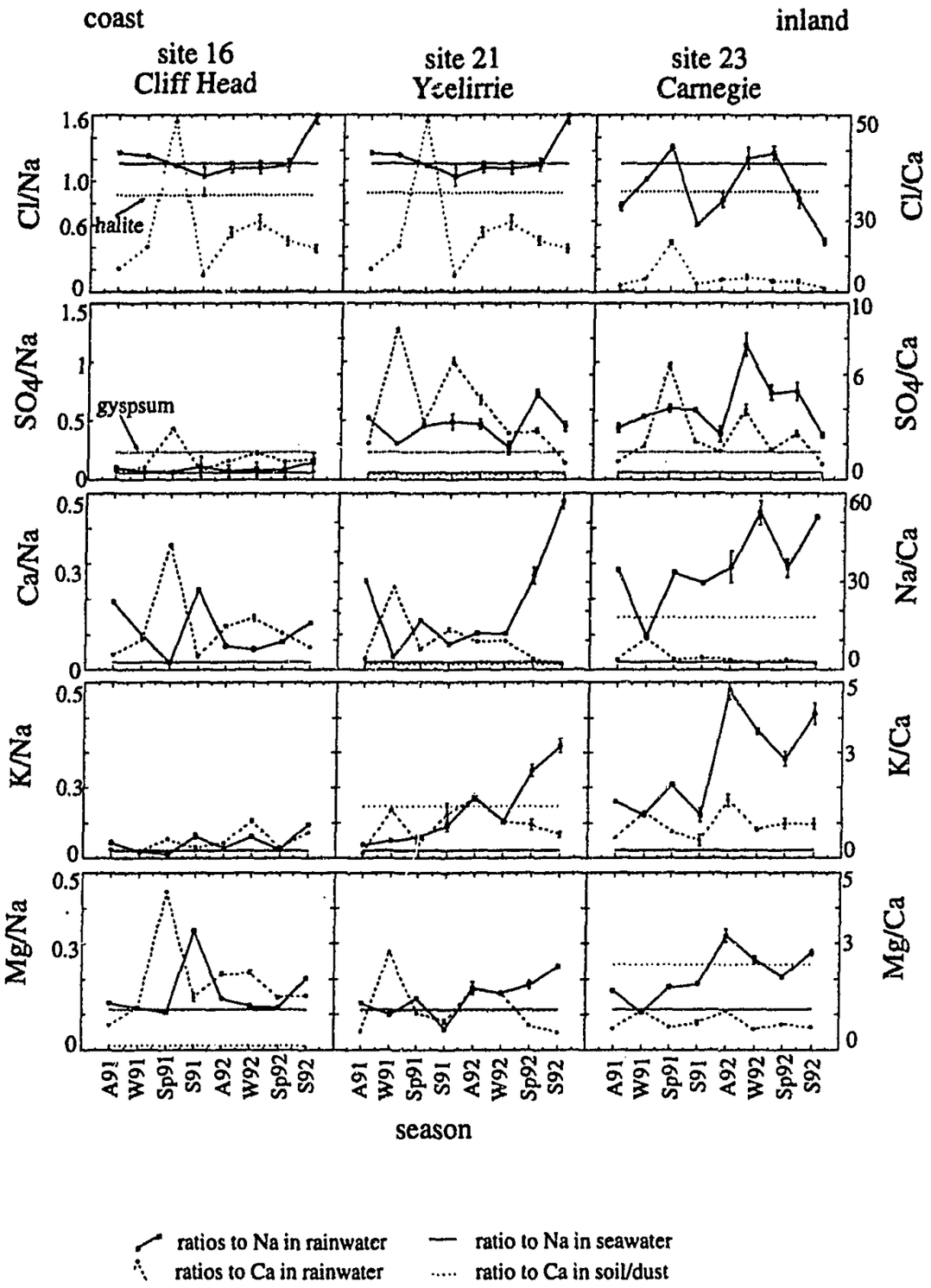

FIGURE 5.20. Seasonal variations in the ratios of Cl, SO_4, Ca, K and Mg to Na, and Cl, SO_4, Na, K and Mg to Ca for sites 16, 21 and 23 on the WE array. Circles with the solid line are ratios to Na in precipitation. Circles with the dashed line are ratios to Ca in precipitation. The solid horizontal line is the ratio to Na in seawater (from Millero 1974). The dashed horizontal line is the ratio to Ca in soil/dust at the site. The left vertical axes are scales for the Na ratios. The right axes are scales for the Ca ratios. In the SO_4/Na and SO_4/Ca plots the dotted line is ratio of SO4/Ca in gypsum. In the Cl/Na and Cl/Ca plots the dotted line is the ratio of Cl/Na in halite.

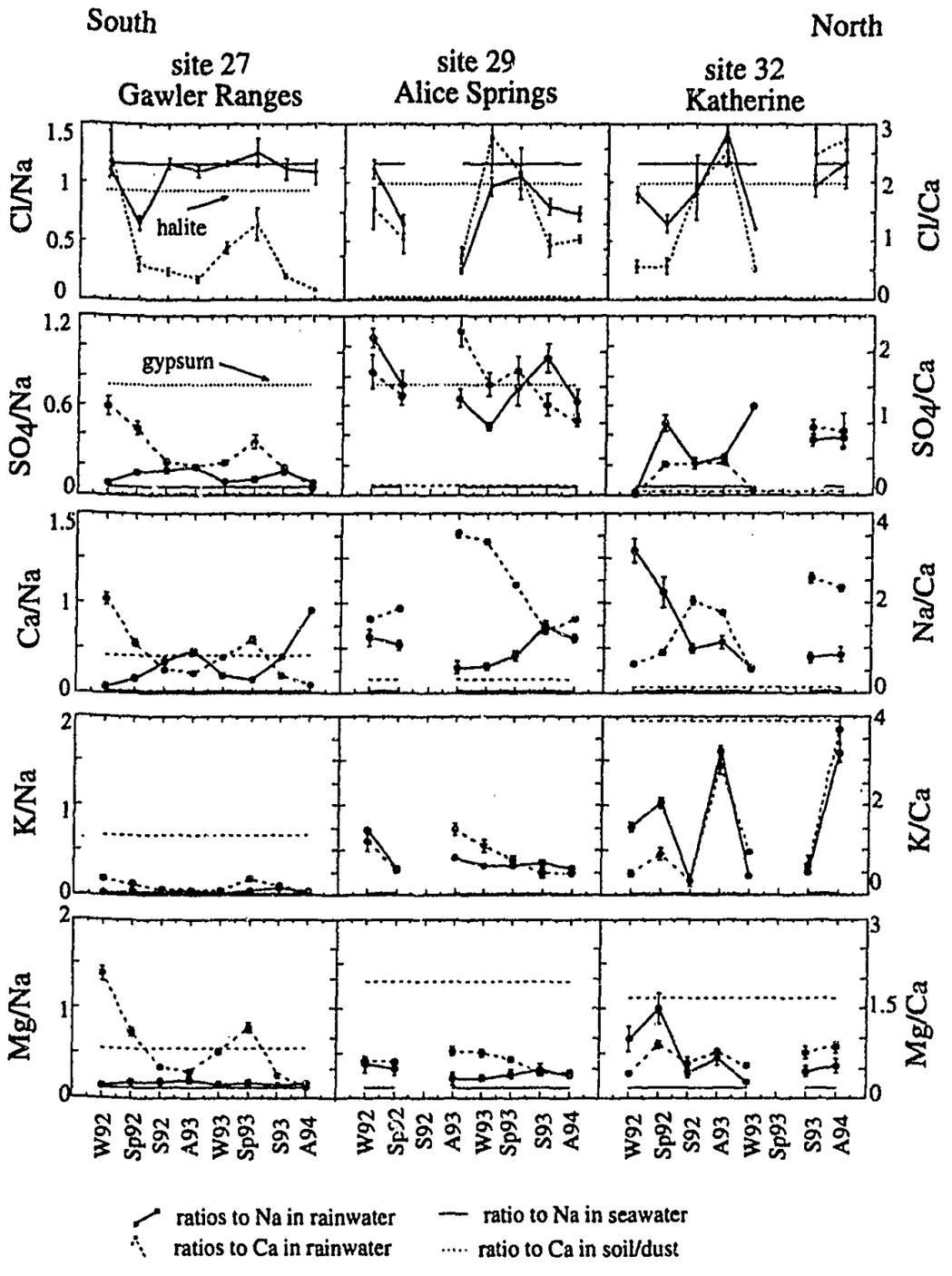

FIGURE 5.21. Seasonal variations in the ratios of Cl, SO_4, Ca, K and Mg to Na, and Cl, SO_4, Na, K and Mg to Ca for sites 27, 29 and 32 on the SN array. Circles with the solid line are ratios to Na in precipitation. Circles with the dashed line are ratios to Ca in precipitation. The solid horizontal line is the ratio to Na in seawater (from Millero 1974). The dashed horizontal line is ratio to Ca in soil/dust at the site. The left vertical axes are scales for the Na ratios. The right axes are scales for the Ca ratios. In the SO_4/Na and SO_4/Ca plots the dotted line is ratio of SO4/Ca in gypsum. In the Cl/Na and Cl/Ca plots the dotted line is the ratio of Cl/Na in halite.

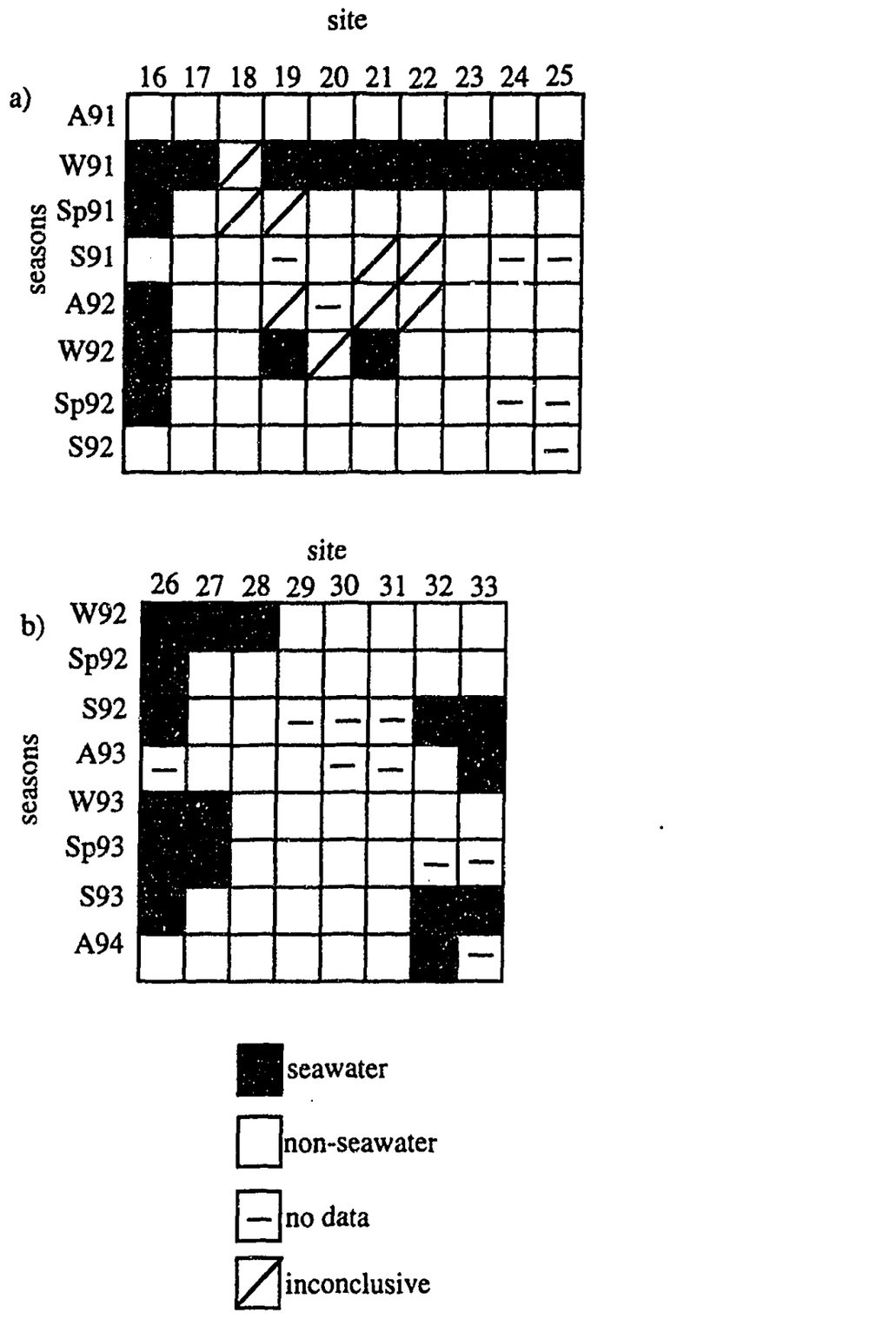

FIGURE 5.22 Summary of seasonal variations in terms of the dominance of a seawater source for a) the WE array and b) the SN array.

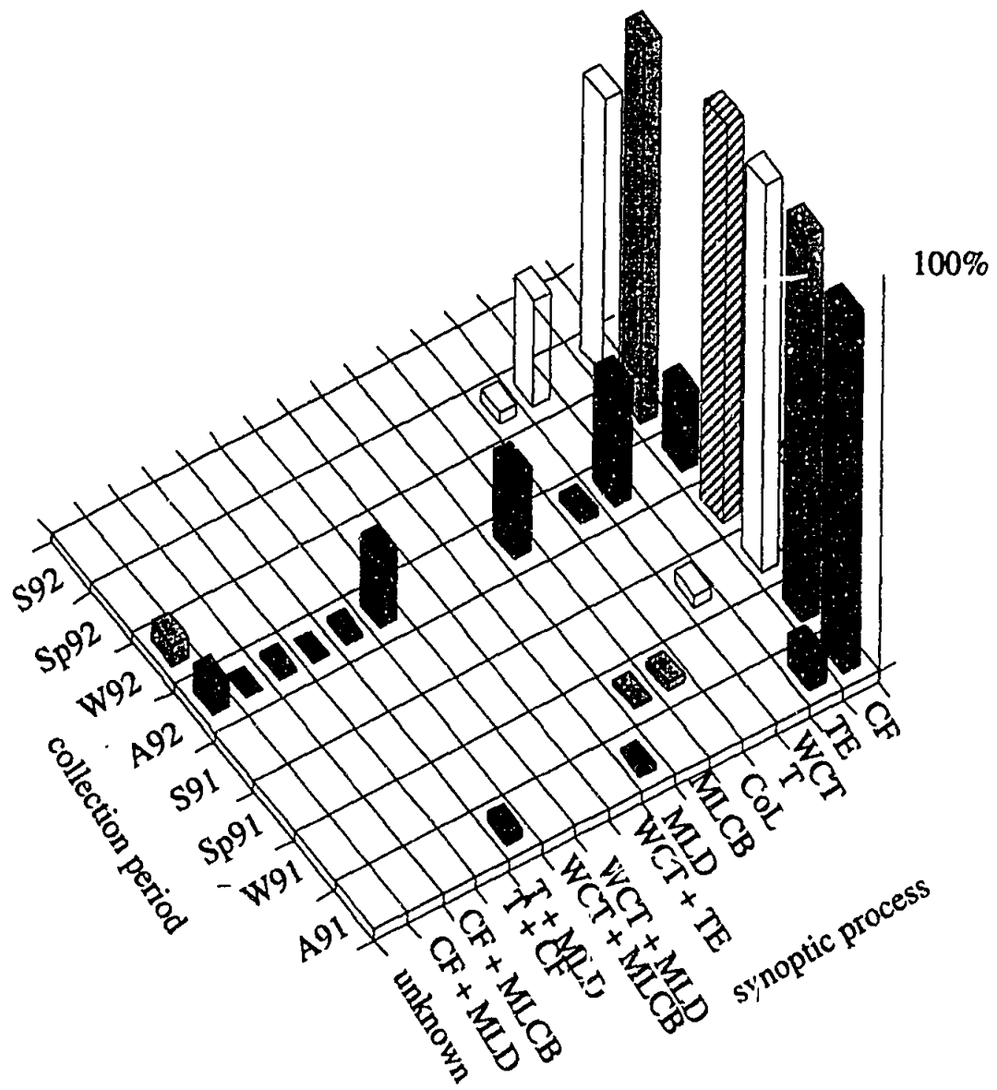

FIGURE 5.23 The percentage of rain attributable to different synoptic processes (defined in Chapter 2) during each collection period at Dongara (Met station closest to site 16, Cliff Head). CF = cold front, TE = tropical event, WCT = West Coast Trough, T = trough, CoL = cut-off low, MLCB = middle-level cloud band, MLD = middle-level disturbance. A91 = autumn 91, W91 = winter 91, Sp91 = spring 91, S = summer 91 etc. Note that throughout most of the sampling program rainfall at Dongara was associated with cold fronts.

The dominance of the seawater source at all sites along the WE array during winter 91, including the most inland site, Everard Junction (site 25), is unexpected. An investigation of the synoptic patterns for each meteorological observation station across the WE array (Figure 5.25), again reveals that a high proportion of rainfall for winter 91 is associated with cold front activity. The more coastal sites 17 (Morawa), 18 (Badja), 19 (Iowna) and 21(Yeelirrie) also display seawater source dominance during winter 92, again corresponding to periods of enhanced cold front activity. The remaining sites show dominance of a non-seawater source throughout the sampling program (except during winter 91 as described above).

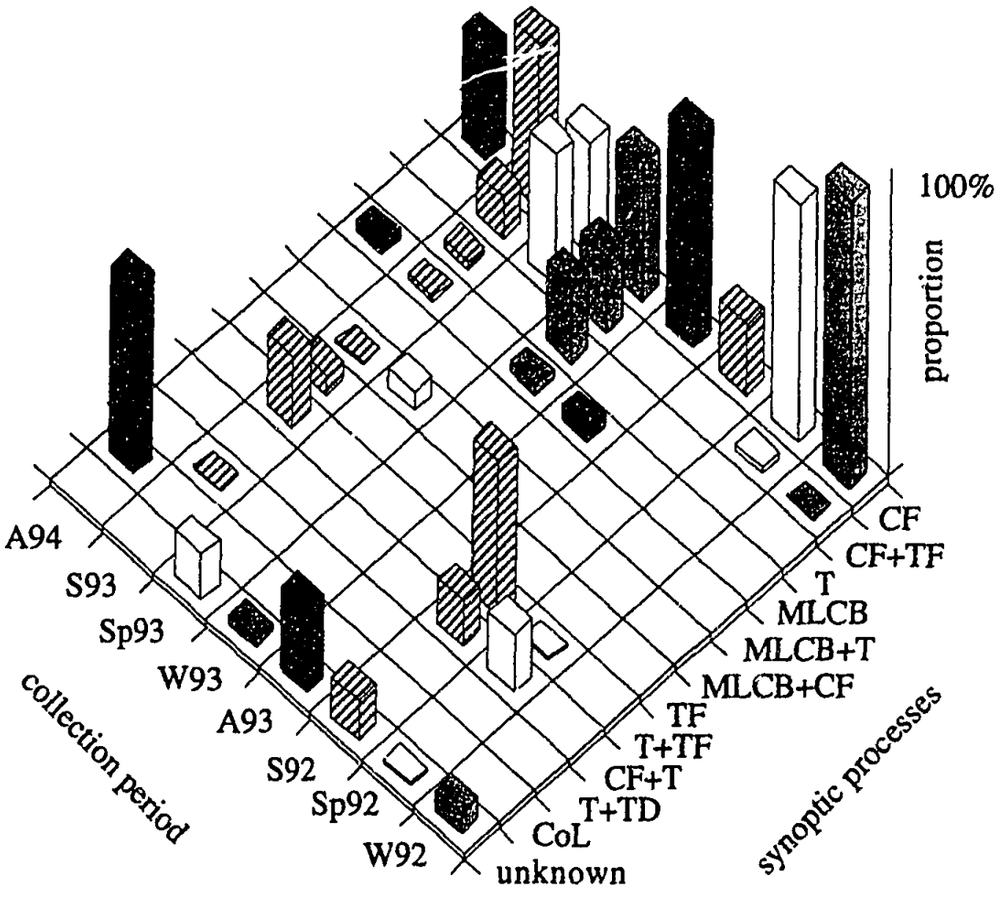

FIGURE 5.24 The percentage of rain attributable to different synoptic processes (defined in Chapter 2) during each collection period at Port Lincoln (Met station closest to site 26, Port Lincoln). CF = cold front, TF = tropical flow, WCT = West Coast Trough, T= trough, CoL = cut-off low, MLCB = middle level cloud band. A92 = autumn 92, W92 = winter 92, Sp92 = spring 92, S92 = summer 92 etc. Note that throughout most of the sampling program rainfall at Port Lincoln was associated with cold fronts.

Sites 27 (Gawler Ranges) and 28 (Wintinna) along the SN array display the dominance of a seawater source during winter of each year, and non-seawater dominance during autumn of each year. Between autumn and winter there is a gradation towards seawater dominance. The distinction between the influence of seawater and non-seawater sources is less obvious as distance from the coast increases. Sites 29 (Alice Springs), 30 (Tennant Creek) and 31 (Dunmarra) do not experience the dominance of a seawater source during any stage of the sampling program (Figure 5.22). The contradictory nature of many of the Na and Ca ratios may suggest something about the non-seawater source and possible changes in its composition. The SO_4/Ca ratio approximates that of gypsum at various times during the sampling program. Sites 32 (Katherine) and 33 (Kapalga) show a high ratios of Na during winter of each year, and minium Na ratios during summer. This represents the dominance of continental material bought to the collectors by the southeasterlies that characterise the dry season in the north of Australia. During the

summer, when northerlies associated with the monsoon become more important, the ratios move closer to those of seawater (Figure 5.26).

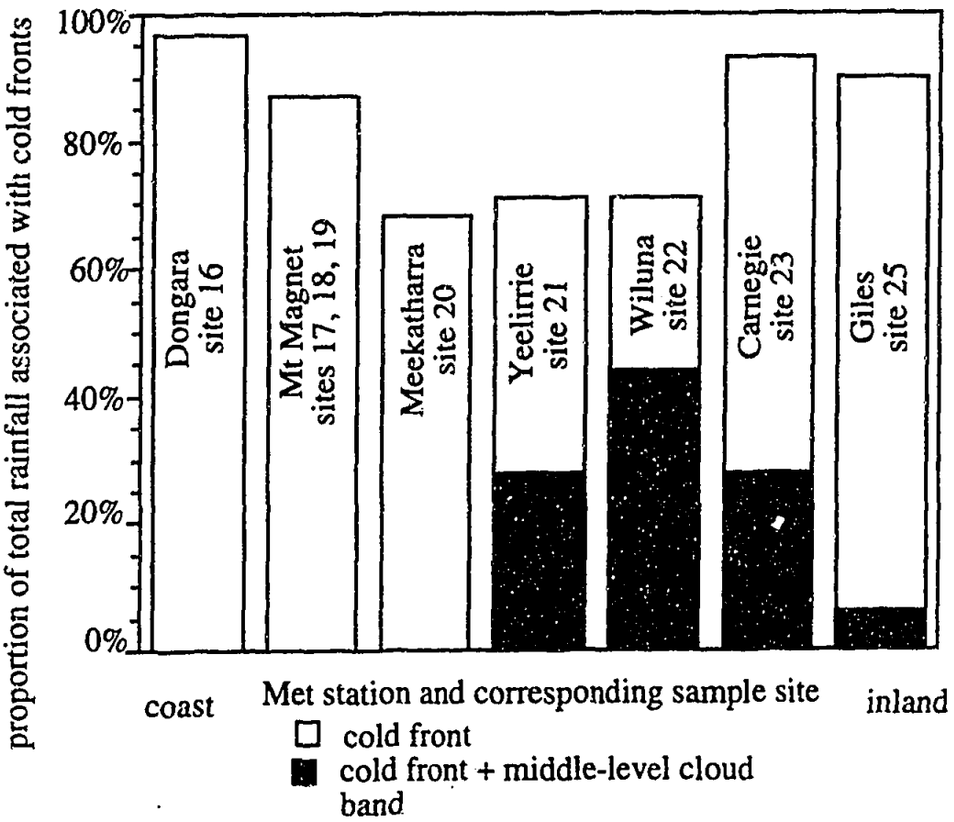

FIGURE 5.25 Proportion of total rainfall at Met stations along the WE array associated with cold fronts during winter 1991.

These results are not unexpected, i.e. seawater compositions in rainfall correspond to increased cold front activity. Thus rainfall during winter of 1991 is mainly of marine origin, even as far inland as Everard Junction (1800 km from the coast). However, it is surprising that the tropically sourced rainfall does not have a marine signature (we would expect to see seasons and sites dominated by tropical events or middle level cloud bands eg. Site 22 (Lake Violet) during summer 92, to display a seawater dominance). This may represent the extent of the land mass over which the airmass must pass, therefore adopting a continental signature, or may be an artefact of the three-month sampling period. The results from the SN array support these speculations. During the summer seasons, the north of Australia experiences both monsoonal (ie marine-sourced airmasses) and transitional monsoonal (i.e. continental airmass from the southeast of the continent). This is represented by the data from sites 33 (Kaplaga) and 32 (Katherine) displaying only weak seawater signatures.

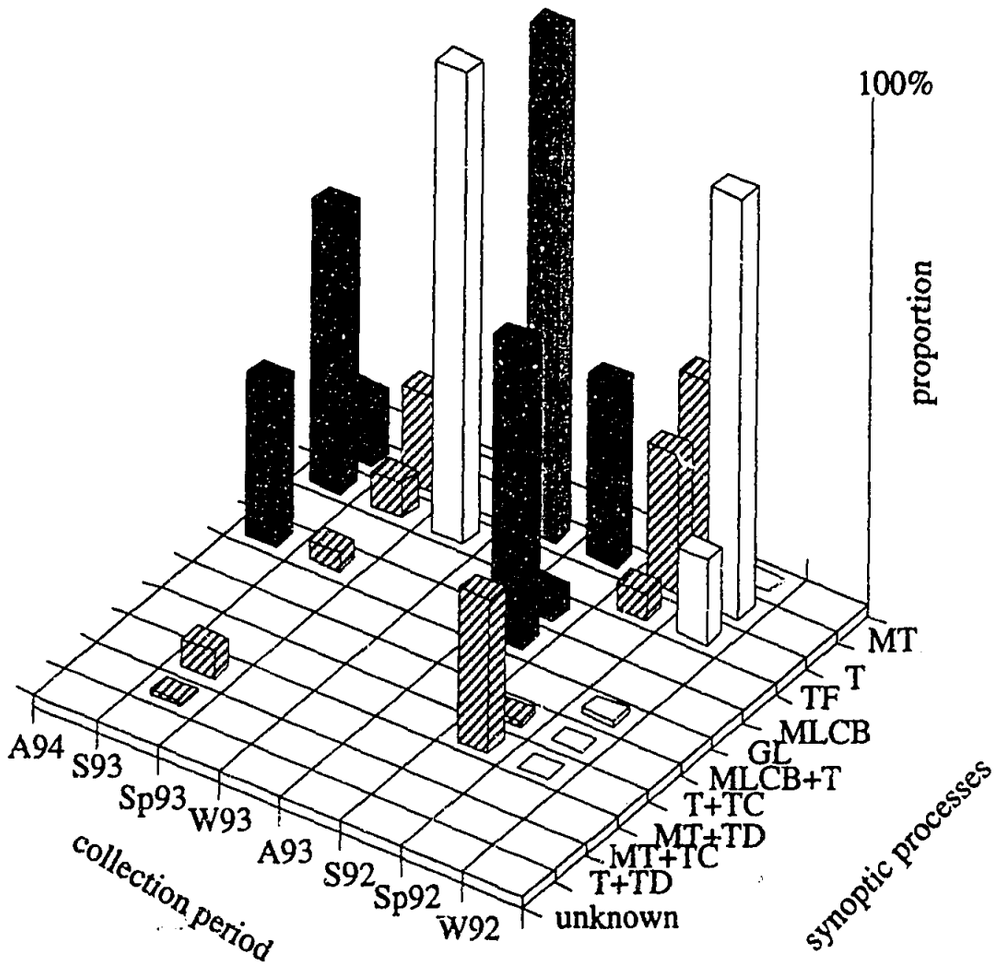

FIGURE 5.26 The percentage of rain attributable to different synoptic processes (defined in Chapter 2) during each collection period at Darwin (Met station closest to site 33, Kapalga). MT = monsoon trough, T = trough, TF = tropical flow, GL = Gulf Lines, MLCB = middle level cloud band, TC = tropical cyclone. A92 = autumn 92, W92 = winter 92, Sp92 = spring 92, S92 = summer 92 etc. Note that throughout most of the sampling program rainfall at Darwin is associated with synoptic processes sourced from the topical north of Australia.

Acid-Base Balance and Biodegradation

The results of multivariate analysis on the total WE data set show that 25% of variation in the data set may be explained in terms of the acidity of the sample, or a combination of acidic anions and biodegradation. Acid-base balances account for 10% of variance in the overall SN data set and northern subset of the SN data set, and 12-20% variance in the southern subset of the SN data set. Input of an agricultural source and biodegradation, are only found in the southern data subset and accounts for approximately 10% of variation. For the purpose of the following discussion, acid-base balance and biodegradation are grouped together as it will be seen that the effects of both processes produce the acidity measured in the samples.

Rainfall acidity has been shown to change within ten days of sample deposition in wet precipitation samples (Vesely 1990). We would expect changes in pH to occur even sooner in bulk depositional collectors used in the present investigation. Thus the pH values measured in this project may not reflect the true H concentrations of rainfall as deposited. Instead, the pH levels of the samples may represent processes that occur after deposition of the sample eg. biodegradation. The high positive ion imbalances for the SN data set suggest the presence of an unmeasured species in the precipitation samples, possibly organic acids. Herlihy (1987) showed formic and acetic acids to be very unstable, and readily utilised by microorganisms in precipitation for their growth. Both formate and acetate are also known to be intermediate metabolic products. Thus the presence of organic acids may influence the extent of biodegradation and thus the acid-base balances of precipitation. Unfortunately, organic acids were not measured in the present study for the reasons outlined in Chapter 3. Despite this however, we do see H showing variances with inorganic acid ion NO_3, and at particular sites with SO_4, NH_4 and HPO_4.

WE Array

There have been many previous investigations into acidic precipitation, especially in polluted areas, eg. Ayers and Gillett (1984). These investigations often directly link acid precipitation to sources of anthropogenic emissions of SO_2, NO_x and hydrocarbons. The remoteness of the sampling localities in the present investigation, however, minimises the effect of anthropogenic sources along the WE array.

As described in Chapter 4, the natural sources of NO_3 to rainfall may include biogenic emissions, biomass burning and lightning. The NOx emission rates for temperate grassland and agricultural land as taken from Galbally (1984) are listed in Table 5.18. While many of the localities along the WE array are situated on agricultural land predominantly used for grazing, the number of domestic grazing animals per acre is very low because of the poor suitability of the land in the arid regions of the array for grazing. Thus it seems more useful to compare emission rates from temperate grassland systems than from agricultural systems. It should be noted that there is a complete lack of information regarding the emission of NOx from desert areas. When agricultural emissions are ignored, the major contributors of NOx are soil emissions and lightning.

TABLE 5.18 Emission of NOx (g $N/m^2/a$) after Galbally 1984.

source	Emission
soil emissions temperate grassland	-0.006-0.08
soil emissions agricultural	0.04-0.26
biomass burning	0.003
lightning	0.05

The importance of lightning on the supply of NO_3 can be investigated by comparing the mean depositional flux of NO_3 for each season with the lightning. Figure 5.27 attempts to correlate between the total number of lightning flashes per day for Western Australia and the NO_3 fluxes for each sampling season. Maximum NO_3 deposition during summer 91 is matched by maximum number of lightning flashes, and there is a generally sympathetic trend between NO_3 deposition and lightning flash counts. Summer 92 does not fit into this general pattern however, with extremely high lightning counts being matched by average NO_3 deposition. This may be a function of the low rainfall amount during summer 92 (less than 0.5 mm/day), reflecting the dependence of flux on rainfall amount, or may be due to processes that occur after sample deposition that involve the consumption of NO_3.

Natural sources of SO_4 include seawater and gypsum from salt-lake material. Ayers and Gillett (1988a) suggest that SO_2 introduced by biogenic emissions or biomass burning may be significant precursors to acidification in tropical Australia. It is likely that these sources are much less significant in the semi-arid, and therefore less densely vegetated area of the WE array than is the seawater or gypsum source.

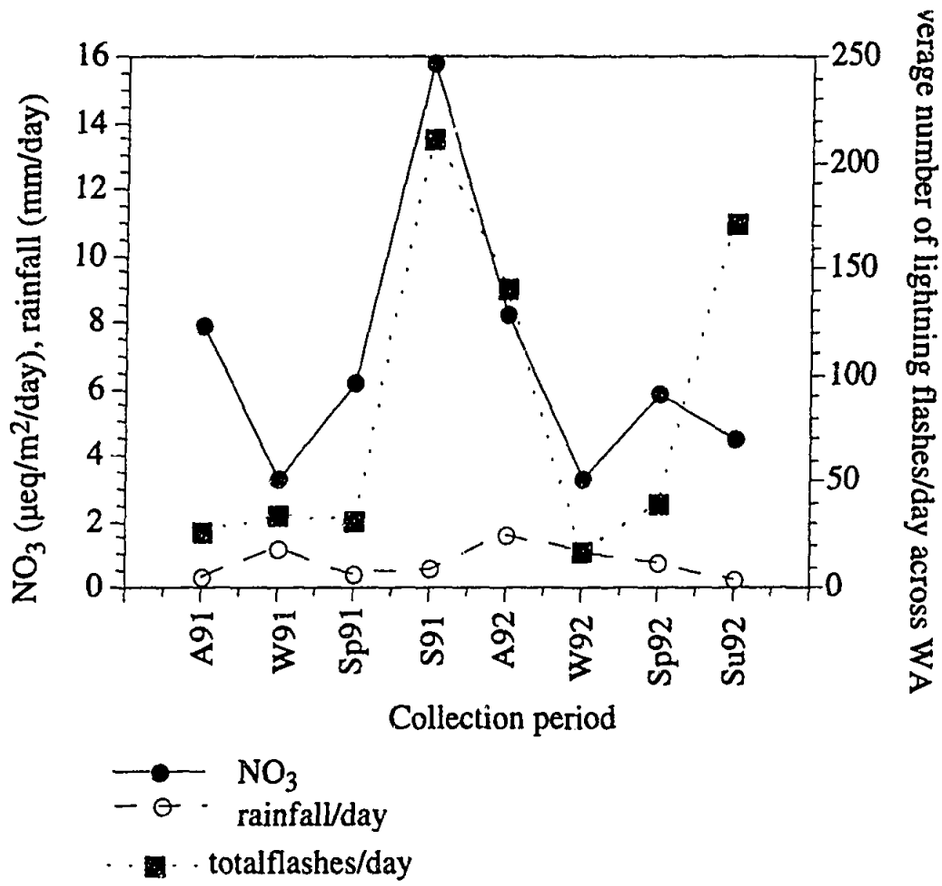

FIGURE 5.27 Deposition of NO_3 and rainfall per day for sites along the WE array and average number of lightning flashes for 10 lightning observation stations across Western Australia plotted as a function of seasons. There is a stronger relationship between rainfall per day and NO_3 deposition than between lightning flashes per day and NO_3 deposition. Monthly records of lightning flashes were obtained from the Bureau of Meteorology. The observation sites for WA include Albany, Geraldton, Kalgoorlie, Kununurra, Meekatharra, Moora, Perth Airport, Port Hedland and Three Springs. Observations are made using lightning flash counters. For the purpose of this work, total lightning flash counts per day is calculated by adding all lightning flashes recorded at all observation stations for each sampling period and dividing by the number of days in each sampling period.

Vesely (1990) investigated the change in H, NO_3 and NH_4 in rainwater samples over time, under various conditions of sample treatment and storage. He described bioconsumption as being caused by microbially induced oxidation of NH_4 (nitrification), which consumes NH_4 and produces NO_3 and H, or the assimilation of NH_4 into organic matter, which consumes NH_4 and produces H. Once all the NH_4 is consumed, or if initial NH_4 values were low, bioconsumption of NO_3 then proceeds, consuming NO_3 and H. These processes were found to occur at a greater rate under warmer conditions. An investigation of the depositional fluxes of NH_4 and H for each season for the WE data set, shows that H fluxes are constant throughout most of the sampling program, while NH_4 concentrations decrease during summer and

spring of each year (Figure 5.28). This suggests that NH_4 is being consumed during warm months, but other processes have a stronger effect on controlling the deposition of H. Because of the common association of NH_4 and K displayed in multivariate analyses, K deposition is also shown on Figure 5.28. High depositional fluxes of K are matched by high deposition of NH_4. The absence of a strong relationship between H, NH_4 and NO_3, as suggested by the work of Vesely (1990), indicates that either bioconsumption involves assimilation of NH_4 into organic matter, rather than the nitrification reaction, or that the supply of N_2O via lightning is far greater than that produced by bioconsumption, so that the bioconsumption of NO_3 is being swamped.

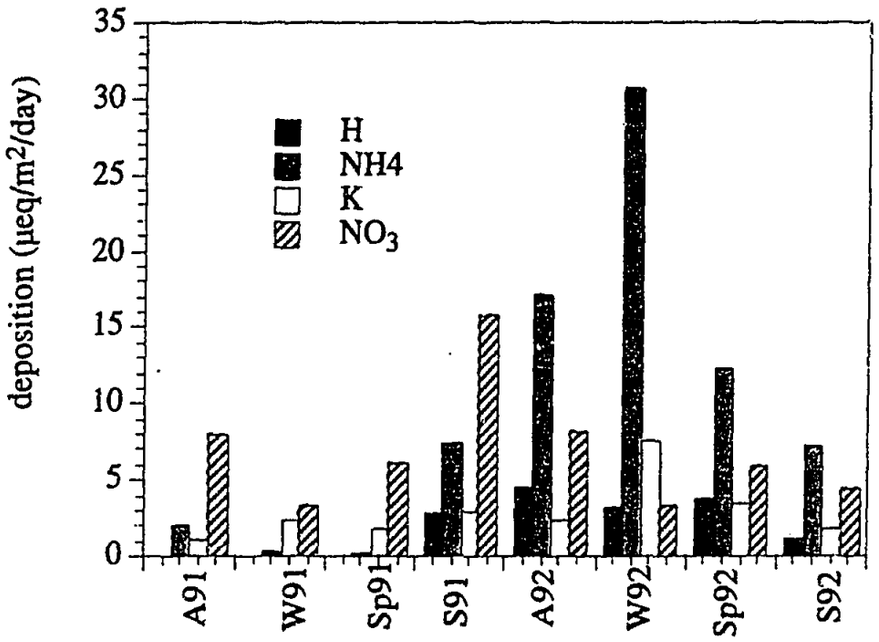

FIGURE 5.28 Seasonal variation in the deposition of H, NH_4, K and NO_3 for the WE array.

SN Array

As for the WE data set, the acid-base balance process in the SN data set is represented primarily by co-variance between H and NO_3. However, depending on the data subset used, SO_4, HPO_4, K, Ca and NH_4 may also vary in accordance with the more typical acid-base species. Anthropogenic sources of NO_3 and SO_4 to precipitation along the SN array cannot be completely discounted, because of the proximity of major areas of settlement to some of the collection sites; in particular Port Lincoln is 30 km north of site 26, Alice Springs is 100 km southwest of site 29,

and Katherine is 25 km south of site 32. As none of these settlements support industries that would emit large quantities of SO_2 or NO_x, the major anthropogenic emissions from these settlements would most likely be from motor vehicle use. However, the results of this work are insufficient to do more than acknowledge that anthropogenic sources of SO_4 and NO_x may play a small part in the acid-base balance of precipitation along the SN array.

Northern Subset

The northern data subset sees the covariance of H and NO_3 in the acid-base balance factor. Natural sources of NO_3 to tropical Australia have been summarised by Ayers and Gillett (1988a) and are listed in Table 5.19. The major input of nitrogen shown in Table 5.19 appears to be from biomass burning. This is because tropical Australia is prone to bushfires, both controlled burns and wildfires. It should be noted that site 33 is located at the CSIRO Kapalga research station where one of the major areas of research is the effect of burning on tropical ecosystems (Hurst et al 1994). While the collector was located in a natural fire compartment (i.e. no fires were deliberately lit), the adjacent compartments were burnt in late May-June (early burning), progressively (fires in late May-June followed by a series of fires as vegetation dries out downslope towards permanent water), and in September (late burning). The late burns were usually very hot, while the early burns were patchy and low temperature. Figure 5.29 shows the flux of NO_3 during all seasons at site 33 and the dates of burning in the adjacent compartments. While no relationship can be discerned between the dates of burning and NO_3 flux at site 33, the fact that burning occurs throughout most of the sampling program suggests that biomass burning should be an important source of nitrogen emissions in the north of the array.

TABLE 5.19 Summary of N inputs (tonnes/year) for northern Australia, after Ayers and Gillett (1988a).

source	input (tonnes/year)
biomass burning	388,000
soil emissions	33,000
lightning	23,000
anthropogenic (power stations, cars)	22,000

A comparison of NO_3 depositional fluxes and lightning flash rates at observation stations at Darwin and Tennant Creek are shown in Figure 5.30 There is a very strong correlation between deposition of NO_3 at site 33 (Kapalga) and lightning rate

at Darwin. The relationship between NO_3 deposition and lightning rate at Tennant Creek (site 30) is weaker but is still present. A direct relationship is also observed between lightning flash rate and rainfall amount. This has been observed by the Bureau of Meteorology (Ayers and Gillett 1988a). The absence of a strong relationship between lightning flash rate and NO_3 concentration (μeq/L) in rainfall, however suggests that the relationship between deposition of NO_3 and lightning flash rate displayed in Figure 5.30 primarily reflects the relationship between rainfall amount and lightning flash rate.

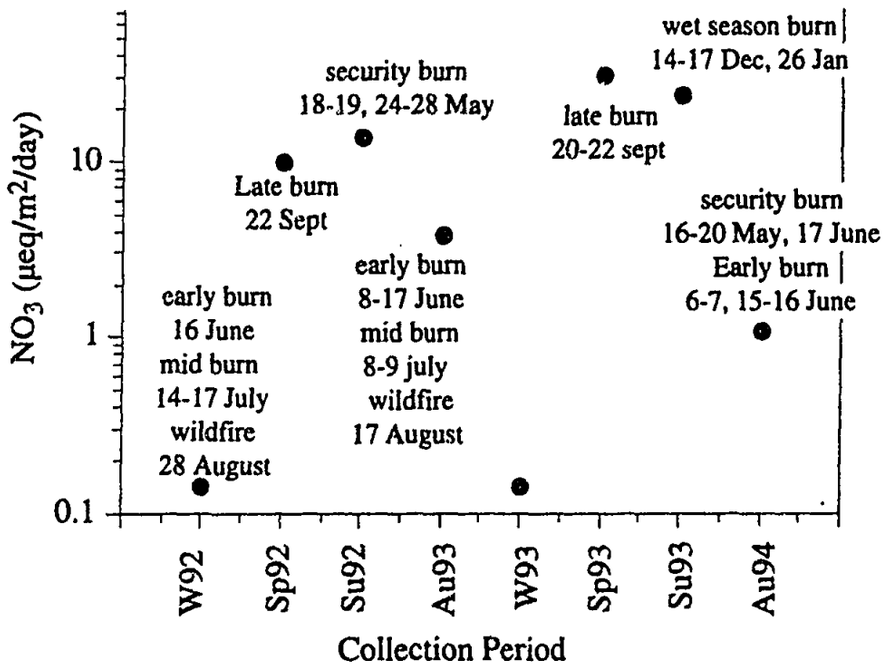

FIGURE 5.29 NO_3 deposition at Kapalga (site 33) and times and types of burns in adjacent compartments of the Kapalga Research Station. Burning occurred throughout the sampling program.

From the present study, the acid-base balances in the northern half of the SN array reflect the supply of NO_3 to the atmosphere by both biomass burning and lightning flash production of NO. While soil and vehicle emissions may also be important, there is insufficient evidence to discuss the extent of the importance of these sources. However, the clear relationships between lightning flash rates and NO_3 deposition, and the extent of burning throughout most of the sampling program suggest that lightning flashes and biomass burning are the most significant sources of NO_3 to the north of the SN array.

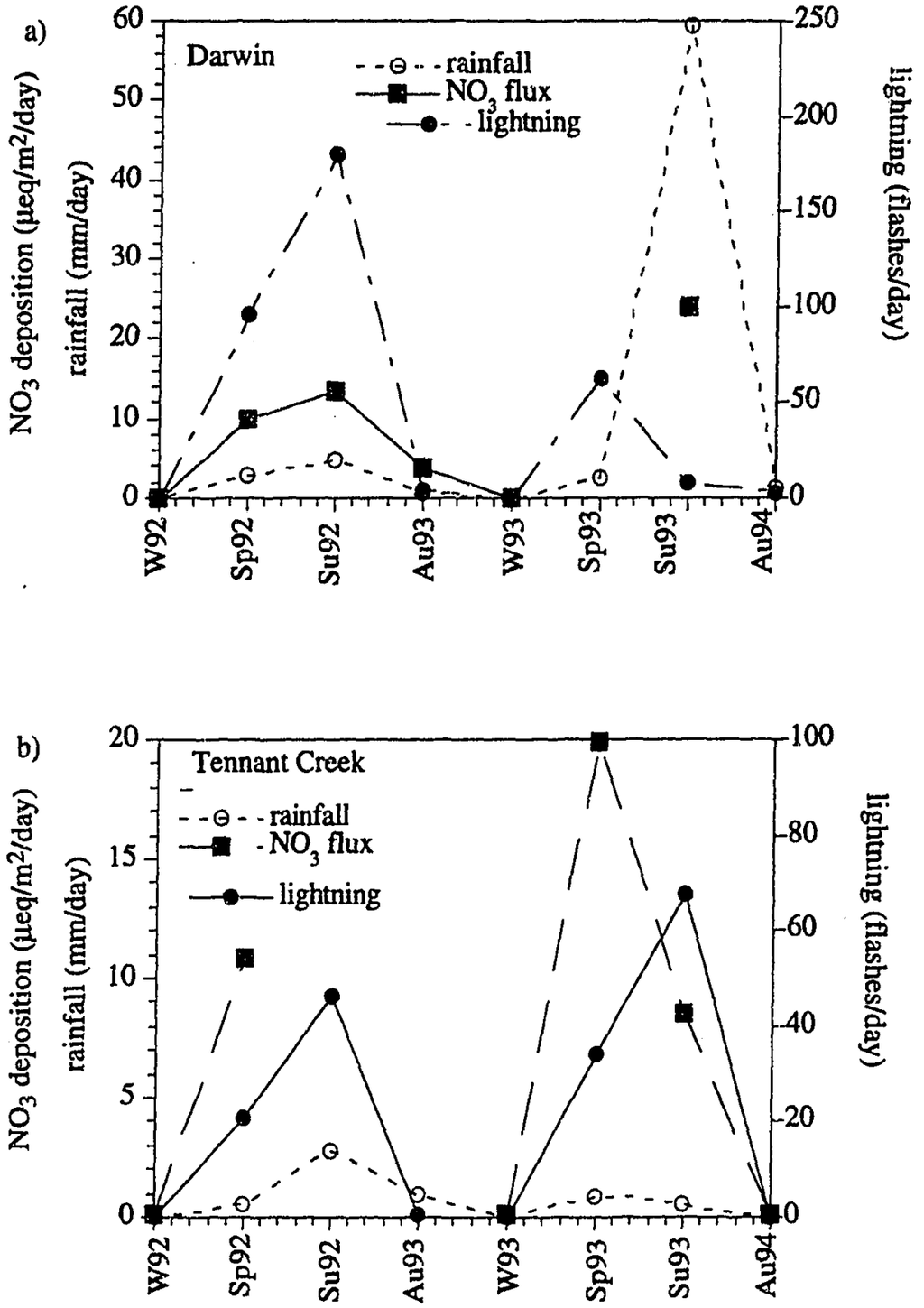

FIGURE 5.30 Mean NO_3 deposition, rainfall per day and lightning flashes per day for each season at a) Darwin and b) Tennant Creek. The postitive relationship between all three factors at each site suggests lightning to be a source of NO_3 in the north of Australia.

Southern Subset

The acid-base balance factor for the southern sites of the SN array explains variance primarily between NO_3 and H, with SO_4 and K also being significant. A comparison of lightning flash rates and NO_3 deposition for site 26 (Figure 5.31) reveals a very poor relationship, suggesting that lightning flash is not a major source of NO_3 to precipitation in the south of the SN array. Burning is also not as extensive in the south of the array as in the north. Thus, these two sources (burning and lightning) that are considered to be significant to the supply of NO_3 in the north of the array, do not appear to be significant in the south of the array, and the importance of soil, plant and anthropogenic emissions can only be suggested by default. SO_4 also has high loadings in this factor (except in the coastal data), and is most likely sourced from seasalt. Thus at coastal sites, the variance of SO_4 with other seawater-supplied species masks the variance of SO_4 with the acid-base balance species.

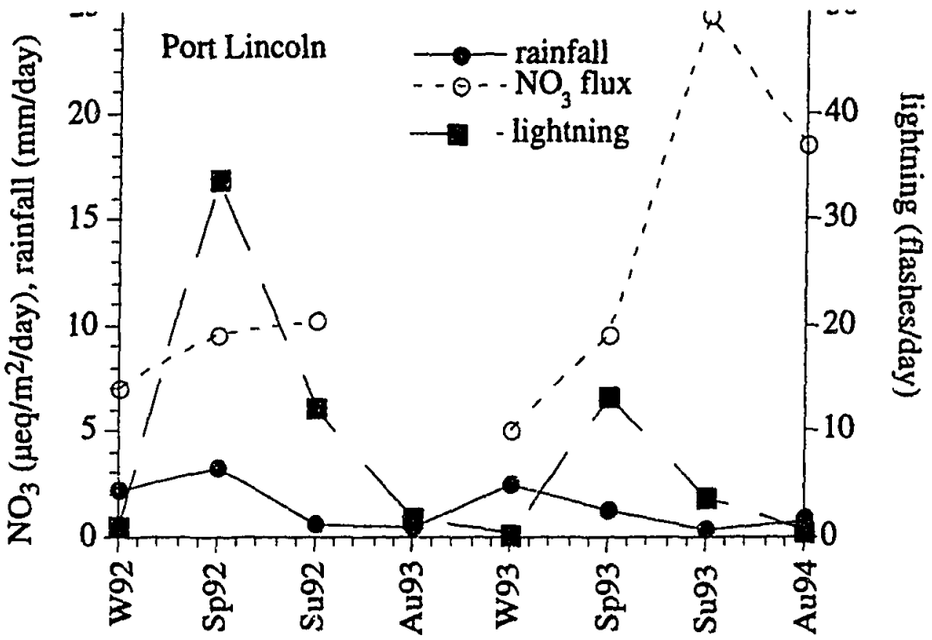

FIGURE 5.31 Mean NO_3 deposition, rainfall per day and lightning flashes per day during each season at Port Lincoln (site 26) in South Australia.

Biodegradation and a supply of agricultural material that group NH_4 and HPO_4 are suggested by the third factor of the multivariate analysis carried out on the southern subset of the SN data set. The agricultural source is not unexpected when it is considered that the southern sites of the SN array are located in areas of high density grazing. As discussed in Chapter 4, one of the largest sources of NH_3 to the atmosphere involves volatilization of animal urine. All sites in the southern section of the SN array are used for sheep and cattle grazing, with the highest density of domestic animals on the SN array, occurring on the property on which site 26 (Port

Lincoln) is located. The negative correlation of NH_4 with other species with high loadings in this factor may represent biodegradation of the sample. The source of HPO_4 is most probably fertiliser.

5.5 SUMMARY AND DISCUSSION

The major-element chemistry of precipitation from the WE and SN array shows the main influence on the composition of precipitation from remote areas of Australia is the mixing between a seawater and continental source. At most sites along the two arrays it is difficult to distinguish between the separate end-members of this source, except at coastal localities where seawater dominates the chemistry of precipitation. However, the influence of seawater can be discerned at non-coastal sites in association with favourable synoptic conditions, such as cold frontal activity in southern and western Australia during winter, and monsoonal activity in northern, Australia during summer. The continentally-derived end-member is most likely composed of re-suspended soil/dust material, including salt lake and calcareous dune components. In the south of the SN array where agriculture is intense this continental source may also include a fertiliser component. The chemistry of precipitation across Australia is also affected by an acid-base balance factor, the components of which are derived from natural sources such as biogenic emissions, biomass burning and lightning flash production. The nature of the collection program means that biodegradation is also a feature of rainfall chemistry.

Results from the major-element chemistry of precipitation provide information important for Chapter 6, in particular in the interpretation of $^{36}Cl/Cl$ ratio anomalies.

WE Array

Three processes affect the composition of rainfall along the WE array: the supply of a mixed seawater/continental source, acid-base balances and bioconsumption of the sample between deposition and sample collection. The extent of the influence of each of these factors is dependent on locality and/or season. Further, due to the well constrained composition of seawater, differences in the influence of the mixed continental/seawater source can be discussed in terms of the dominance of seawater and otherwise derived aerosols. The coastal site is dominated by a seawater source throughout most of the sampling program, while the effect of the seawater source at inland sites is dependent upon season. This seasonal dependence can be linked to weather patterns, eg. with increased cold front activity being conducive to the

transportation of seawater great distances inland, eg. as far as 1800 km to Everard Junction during winter 1991.

The acid-base balance describes the variations displayed in H and NO_3. Nitrate is supplied to the atmosphere by natural sources, including biogenic emissions of soils and via lightning strikes. The deposition of NO_3 is also dependent on season, and is associated with increased lightning occurring during summer of 1991. The third factor arises from biodegradation of the sample. This really represents modification of the rainfall after its deposition, rather than a possible source of influx of constituents to the sampling vessels. Biodegradation is also dependent on season, with maximum biodegradation occurring during warm seasons.

As discussed in Chapter 4, many of the previous investigations into the chemistry of precipitation of Western Australia have been concerned with the accession of salts to the landmass. The results from the present investigation can most usefully be directly compared with the results of Hingston and Gailitis (1976) who carried out a comprehensive investigation of 59 sites throughout WA, many of which coincide with sites in the present investigation. Figure 5.32 shows a figure from Hingston and Gailitis displaying the pattern of deposition of Cl (kg/ha) across Western Australia. Also shown on the diagram are the average deposition rates measured at each site in the present investigation. It can be seen that deposition measured in the present study falls within the ranges defined by the Cl isochrones calculated by Hingston and Gailitis dependent on locality. As in other investigations of rainfall chemistry from the southwest of the state (Farrington and Bartle 1988, Farrington et al 1993), deposition in the present investigation is lower than was measured in the southwest of Western Australia by Hingston and Gailitis. It has been suggested that Cl accession increases at inland sites when strong westerly onshore winds are able to transport oceanic seaspray inland (Farrington and Bartle 1988). This is supported in the present investigation by characteristically seawater compositions of precipitation up to 1800 km inland associated with enhanced cold frontal activity during winter months.

SN Array

Four processes affect the composition of rainfall along the SN array: supply of a seawater/continental source, acid-base balances, supply of an agricultural source material and biodegradation. The effect of these processes on the north and the south of the array is quite different. Sites in the north of the array have a large proportion of variance that can be explained in terms of a mixed

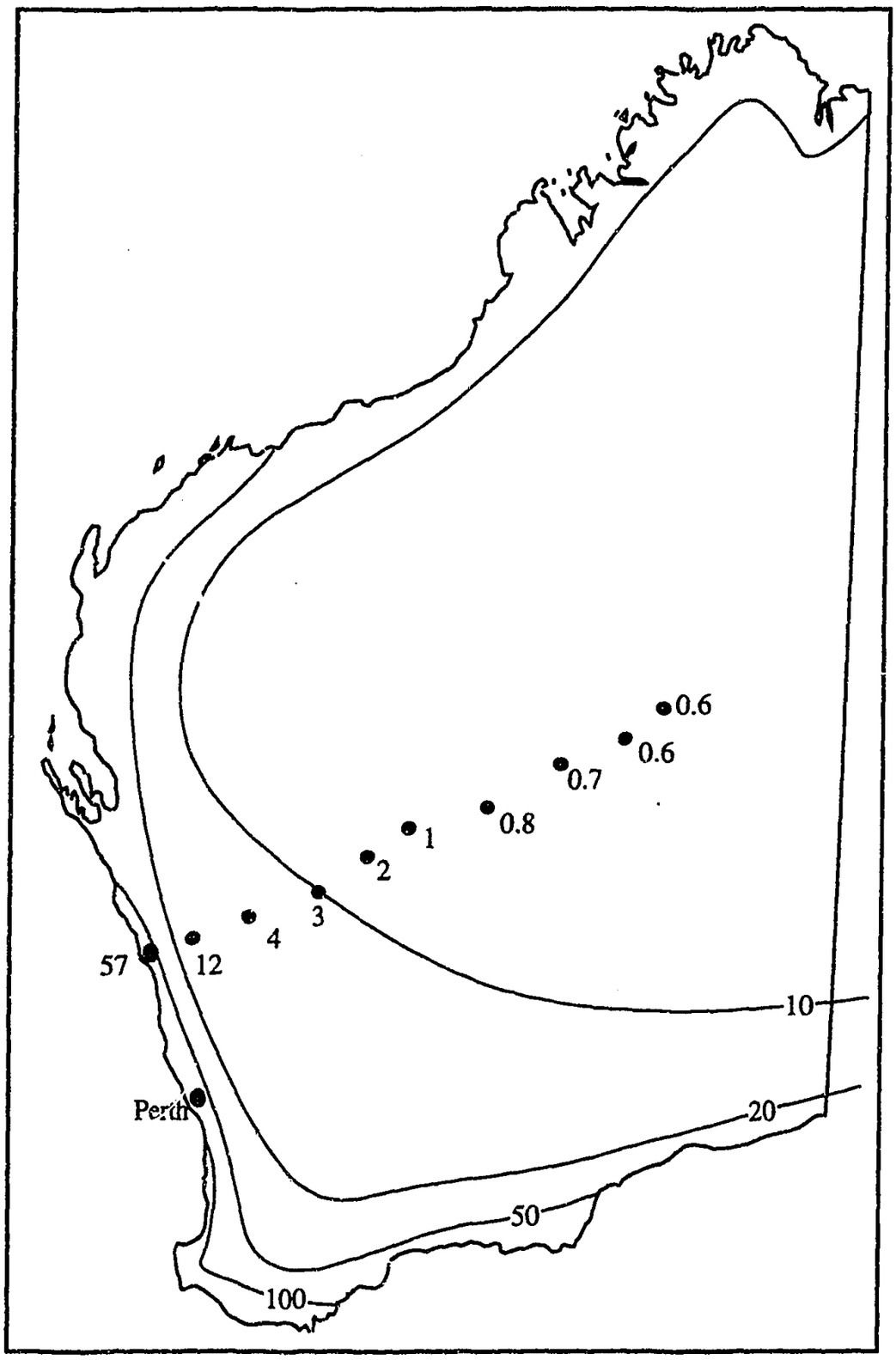

FIGURE 5.32 The mean Cl deposition rates for sites along the WE array (in kg Cl/ha) and the isochrons calculated from the investigation of Hingston and Gailitis 1976. The WE array shows broad agreement with the isochrons.

seawater/continental source. During the monsoonal period, seawater can be separated from the mixed seawater/continental source, but this only explains a small amount of variance. The extent of seawater influence from the north coast of Australia can only be seen as far inland as site 32 (~200 km), and only during the summer season when the monsoon occurs. Acid-base balances explain less than 20% of variance in the north of Australia, and are described by variation between H and NO_3. A seasonal variation in the supply of NO_3 to precipitation can be related to lightning flashes and rainfall amount in the north of Australia.

Sites in the south of the SN array are influenced by three factors, a mixed seawater/continental source, acid-base balances and a mixed agricultural input/biodegradation factor. The seawater source can be isolated for coastal sites 26 (Port Lincoln) and 27 (Gawler Ranges), and seawater can be seen to influence the composition of precipitation as far inland as site 28 (Wintinna) during winter of each year, in accordance with the strong influence of cold frontal precipitation from the south coast of Australia at this time of year. The acid-base factor is defined by covariance between H, NO_3, SO_4 and Ca, representing the supply of SO_4 by seasalt and the neutralising effect of $CaCO_3$ at the coastal locality. A mixed agricultural/biodegradation factor is suggested by covariance of HPO_4, NH_3, Ca and K.

It is difficult to make direct comparisons between previous investigations and the present investigation despite the extensive number of investigations into precipitation in the north of Australia (Table 4.1), due to of the difference in sample collection techniques. The present investigation uses bulk-depositional collectors and therefore incorporates both wet and dry deposition, while previous investigations in the Alligator Rivers Region (eg. Noller et al 1990, Gillett et al 1990) and Katherine (Galloway et al 1982, Likens et al 1987) looked at wet-only deposition. This means that comparisons of the rate of deposition of material between the different studies is unrealistic. However, some general comparisons can be seen between the various investigations: i) the large cation excesses over anions in the present study may be interpreted to suggest the presence of large amounts of organic acid anions as seen in previous studies (eg. Galloway et al 1982). ii) the importance of seawater as a source of material to monsoonal rain as suggested by Likens et al (1987) and Noller et al (1990), is supported in the present investigation, although, the tropical airmasses are modified of their marine character after movement 300 km inland. iii) contrary to previous investigations, is the correlation between lightning flash rates and NO_3 depositional flux shown strongly in the north of the SN array. This good correlation

most likely reflects the strong relationship displayed between lightning flash rate and rainfall amount (Ayers and Gillett 1988a).

Results from the Alice Springs collector (site 29) can be compared with those of Hutton (1983) for a site 100 km north of Alice Springs. Table 5.21 shows that concentrations measured in the present investigation are much lower than the volume weighted mean for 1958 to 1962 measured by Hutton. Also of note is the higher average amount of rainfall recorded during the present investigation. An individual rainstorm measured on 13/11/58 has a similar rainfall volume to the present investigation, and it can be seen from Table 5.21 that the concentrations measured in the present investigation are much more comparable to the high rainfall sample collected in 1958. This suggests that the difference displayed between the mean concentrations is a artifact of the rainfall volume.

TABLE 5.21 Comparison of a previous precipitation investigation at Alice Springs with the present investigation.

Investigation Alice Springs	rainfall mm	Cl µeq/L	SO_4 µeq/L	Na µeq/L	K µeq/L	Ca µeq/L	Mg µeq/L
13/11/58 (Hutton 1983)	30	4	20	8	2	20	10
*vwm 1957-1962 (Hutton 1983)	14	25	<30	28	9	32	23
1992-1994 (Present investigation)	55	6.3	12.2	8.6	3.1	9.6	4.8

* vwm=volume weighted mean

CHAPTER 6 CHLORINE-36

This chapter describes ^{36}Cl in precipitation from remote areas of Australia. It begins with a review of the production and fallout mechanisms of ^{36}Cl from the atmosphere (both natural and anthropogenic), followed by a description of observations. The chapter is concluded with a discussion of the observations and implications of this work for atmospheric and hydrologic investigations.

6.1 CHLORINE-36 PRODUCTION AND FALLOUT

Chlorine-36 is produced in the atmosphere and lithosphere by various reactions. In the atmosphere, it is formed by the cosmic ray spallation of ^{40}Ar. During the detonation of a thermonuclear device in a marine environment, neutron capture of ^{35}Cl may also inject large quantities of ^{36}Cl into the atmosphere as a single pulse (Schaeffer et al 1960). Within the top 2 m of the Earth's surface, cosmic ray spallation of ^{39}K and ^{40}Ca produces ^{36}Cl. Below 2 m, negative muon induced reactions become an important source of ^{36}Cl. At greater depths in the crust (>50 m), neutrons produced by U and Th decay and subsequently captured by ^{35}Cl are the dominant source of ^{36}Cl. Cosmic ray spallation in the upper few metres of the ocean produces large amounts of ^{36}Cl (30 atoms/m^2/s). However the $^{36}Cl/Cl$ ratio of oceanic water is low ($<1x10^{-15}$) due to dilution during oceanic circulation (Andrews and Fontes 1992).

This project is concerned with atmospherically produced ^{36}Cl, but production in the lithosphere may also contribute to groundwater systems. In general however, this contribution is very small compared to atmospheric production.

Natural Production and Fallout

Most of the production of ^{36}Cl by cosmic ray spallation occurs in the stratosphere with less than 40% occurring in the troposphere (Lal and Peters 1967). Stratospherically produced ^{36}Cl mixes with stable Cl (sometimes termed dead Cl), usually of marine and terrestrial origin in the troposphere, and it s beli ed that this mixed aerosol, containing ^{36}Cl and stable Cl, is quickly washed out as wet or dry precipitation. The residence time of aerosols in the troposphere has been calculated to be about one week (Turekian et al 1977).

The latitudinal dependence of ^{36}Cl fallout has been calculated by Lal and Peters (1967). Their values, which were based on production from ^{40}Ar alone, ranged from 5 atoms/m^2/s near the equator to a maximum of 28 atoms /m^2/s at 40°N, with a mean of 11 atoms/m^2/s. Onufriev (1968) suggested that neutron activation of ^{36}Ar should produce an additional fallout of 5 atoms/m^2/s. Accordingly, Bentley et al (1986a) reproduced the shape of the fallout curve of Lal and Peters (1967), but adopted a mean fallout of 16 atoms/m^2/s. More recently however, the cross sections for the neutron activation reaction of ^{36}Ar have been measured (Jiang et al 1990) and shown to result in negligible ^{36}Cl production. Best modern estimates (Andrews and Fontes 1992) use a mean fallout of 11 atoms/m^2/s. The most recent fallout curve dependent on geographic latitude is shown in Figure 6.1 and is taken from Andrews and Fontes (1992). This shows a reduction in the values reported in Bentley et al (1986a) by a factor or 11/16 and reproduces the curve of Lal and Peters (1967).

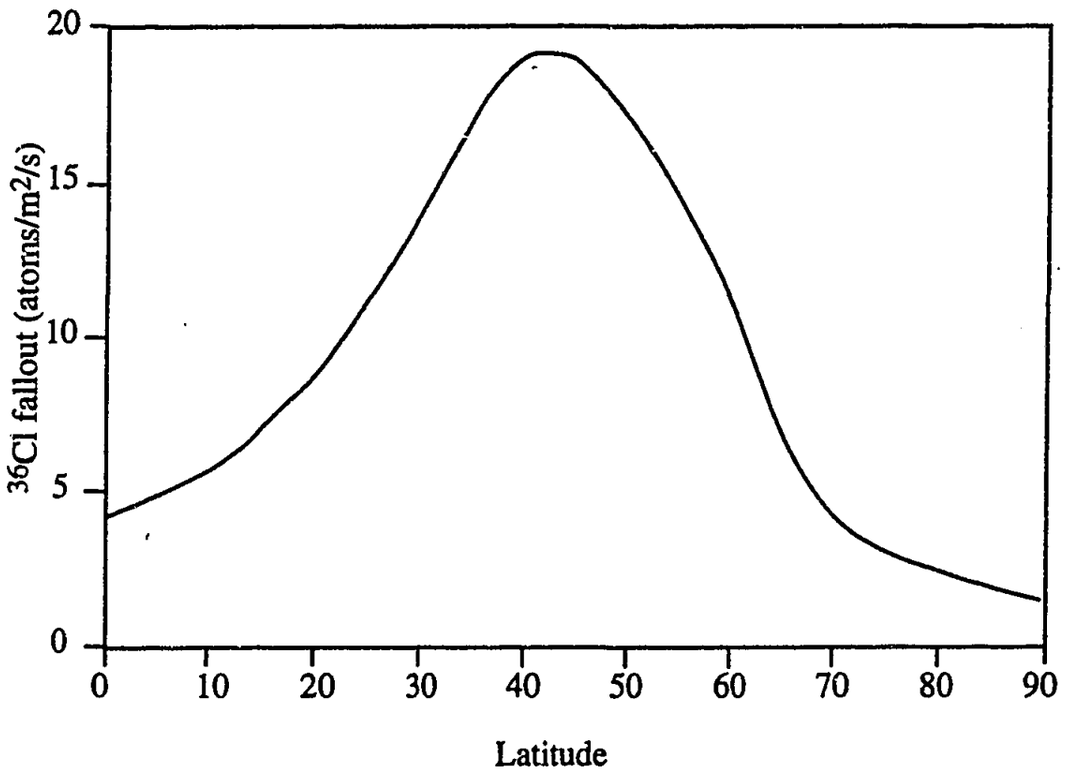

FIGURE 6.1 The pattern of fallout of ^{36}Cl as a function of latitude. From Andrews and Fontes 1992.

The latitudinal dependence of ^{36}Cl fallout has two components: i) variation due to the effect of the Earth's dipole and ii) variation due to the atmospheric transfer between the stratosphere and troposphere.

Geomagnetic Dependence

Cosmic ray fluxes to the Earth's surface are affected by the Earth's magnetic field. The geomagnetic dipole field of the Earth prevents charged particles below a certain rigidity (the ratio of the particle's momentum and charge) from penetrating into the atmosphere. The shielding effect is greatest at the equator, and decreases towards the magnetic poles. At geomagnetic latitude λ the minimum rigidity $R(\lambda)$ which can penetrate the atmosphere is given by

$$R(\lambda) = R_0 \cos^4\lambda \qquad (6.1)$$

where R_0 is the magnetic rigidity at the equator. Thus when a particle's rigidity at a certain latitude λ is less than $R(\lambda)$, it is unable to reach the atmosphere.

Variations in the flux of cosmic rays to the Earth's surface have been noted in association with the 11-year sun spot cycle (Lal and Peters 1962). It is well established that cosmic ray intensity decreases with increasing solar activity (Figure 6.2). Lal and Peters (1962) suggest that the average eleven-year cycle produces a fluctuation of about ±5% around mean global production of cosmogenic isotopes, and that the emission of high energy particles in solar flares may offset reduced isotopic production during periods of strong solar activity (i.e. during the sunspot maxima). Solar flares may also be responsible for major changes in the flux of cosmic rays to the Earth's surface (Lal and Peters 1962). Solar flares involve the emissions of high-energy particles from the sun and are rare even at the height of sun spot activity.

Transfer Between Atmospheric Domains

While the production of ^{36}Cl in the stratosphere is dependent upon geomagnetic latitude (Lal and Peters 1967), geographic latitude controls the transfer of stratospheric ^{36}Cl to the troposphere and the dispersion of the mixed aerosol in the troposphere. The most effective processes of transfer between the stratosphere and the troposphere involve mean meridional circulation dominated by Hadley circulation and large-scale eddy transports associated with the jet streams (Reiter 1975). Hadley cell circulation carries tropospheric air into the stratosphere at tropical latitudes and stratospheric air into the troposphere at middle and high latitudes (see Figures 2.1 and 2.2).

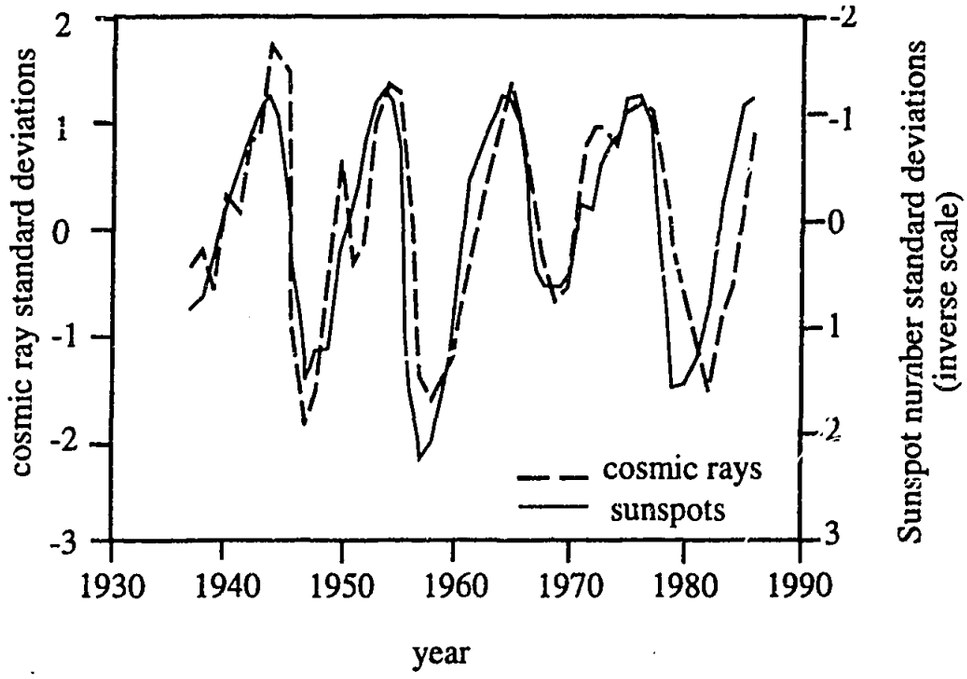

FIGURE 6.2 Comparison of groundlevel cosmic ray flux secondary-particle fluxes with sunspot number over the past 150 years. Cosmic ray fluxes are recorded by ionisation chambers and neutron monitors. The amplitudes are given in units of standard deviations (i.e. the number of standard deviations the value is from the normalised mean). All data points represent annual mean values. The correlation factor is -0.8. From Beer et al 1991.

Air circulation in the vicinity of the jet streams promotes air mass transfer from the stratosphere to the troposphere. Figure 6.3 shows a schematic north-south cross section through a jet stream. The tropopause is defined by the thick line. At the jet stream core, the tropopause cannot be defined and a gap appears. A frontal zone extends from the tropopause section on the right of the diagram into the lower troposphere. Circulation relative to the position of the jet stream causes air from the stratosphere to extrude into the frontal zone (as shown by the curved arrow). This process is also known as tropospheric folding (Danielsen 1968, Reiter 1975). Jet streams occur in the 30-50° latitude belt (subtropical jet stream) and more regularly in the 50-60° latitude belt (the stronger subpolar jet stream) where they are associated with cyclones (See chapter 2).

The combination of mean meridional circulation and large-scale eddy transports result in the transfer of 73% of the mass of the stratosphere, i.e. 38% by mean meridional flow, 15% from the northern hemisphere to the southern hemisphere, and 20% by large-scale eddy transport (Reiter 1975). Thus, maximum transfer of air from the stratosphere to the troposphere occurs in the middle latitudes (35-40°).

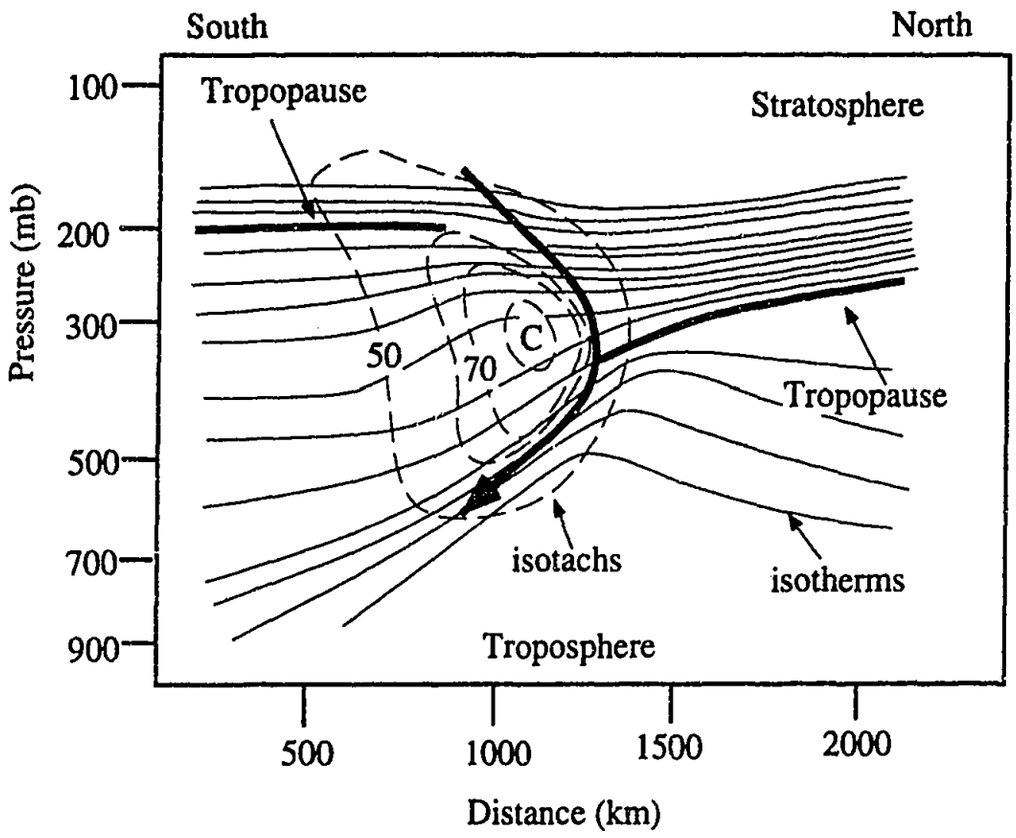

FIGURE 6.3 South-north cross section through a jet stream. Isotachs (lines of constant wind speed m/s) are shown as dashed lines, isotherms of potential temperature (temperature an air parcel would assume if compressed adiabatically to 1 bar) are solid lines. Tropopause is the solid thick line. The flow of air through the jet stream is the thick curved arrow. C is the core of the jet stream. After Warneck 1988.

Another significant mechanism of transfer of stratospheric air mass involves seasonal adjustments in the height of the mean tropopause level. This leads to changes in the mass of air contained in the stratosphere (Staley 1962), and is seen as a net flux (upwards or downward) of stratospheric air. Increased tropopause heights in the warmer seasons, promote inclusion of stratospheric air into the troposphere, where trace species such as ^{36}Cl can be scavenged. In addition for ^{36}Cl, more cosmic rays can penetrate the troposphere, enhancing the production of tropospheric ^{36}Cl. Based upon seasonal measurements of tropopause heights made at four different latitudes in the northern hemisphere, it was suggested that seasonal variations in the height of the tropopause results in transfer of 10% of the mass of the stratosphere (Reiter 1975). Small-scale eddy transport across the tropopause eg. penetration of thunderstorm cells into the lower stratosphere, result in transfer of less than 10% of material between the stratosphere and troposphere.

Air is also transferred across the interhemispheric tropical convergence zone (ITCZ) between the northern and southern hemispheres. Exchange between the two hemispheres occurs by eddy diffusion in the equatorial troposphere. However, most exchange occurs by seasonal shifts in the ITCZ, which lies to the north of the equator in July and may lie to the south of the equator in January, in the vicinity of Australia. The displacement is greatest over the Indian Ocean, highlighting the importance of the monsoon for interhemispheric exchange (Figure 2.2).

Warneck (1988) summarises movement of airmasses through the different atmospheric domains in terms of a four-box model, where the stratosphere and troposphere of each hemisphere belong to a separate box. The exchange rates shown in Figure 6.4 are summarised by Warneck from various tracer observations (including CO_2, $^{14}CO_2$, ^{185}W, ^{144}Co, ^{137}Cs, ^{54}Mn, ^{85}Kr, ^{90}Sr and meteorological data). This model treats the northern and southern hemispheres the same, i.e. assumes that the rate of stratospheric/tropospheric exchange is the same in both hemispheres.

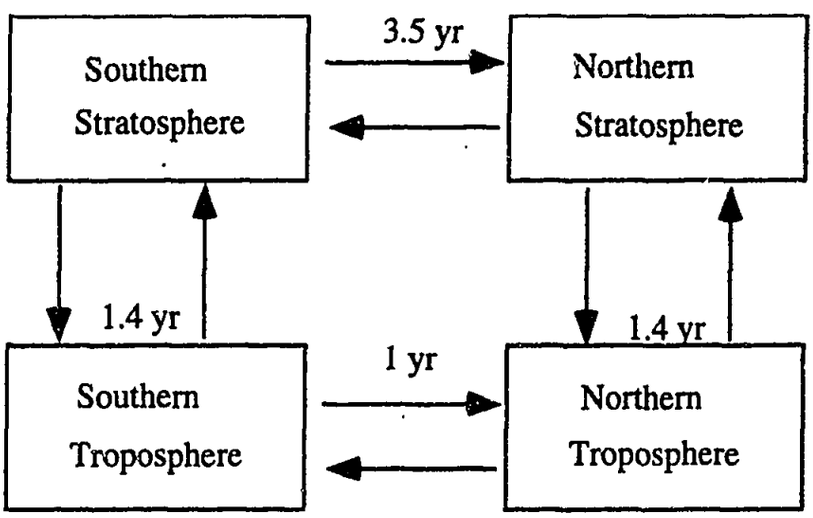

FIGURE 6.4 Standard four-box model of the atmospheric reservoirs and the rate of exchange between reservoirs. After Warneck 1988.

However, asymmetry in the exchange of material between the stratosphere and troposphere in the northern and southern hemispheres has been noted in several studies involving a variety of tracers. For example, the fallout of ^{90}Sr in the southern hemisphere was lower than in the northern hemisphere after atmospheric bomb tests (Lal and Peters 1962, Figure 6.5). Measurements of ^{10}Be in northern hemisphere precipitation also appear to be greater than in southern hemisphere precipitation. Raisbeck et al (1979) measured a deposition rate of 4.2 $x10^{-2}$ atoms $^{10}Be/cm^2/s$ at 39°N, and more recent measurements have been in agreement with

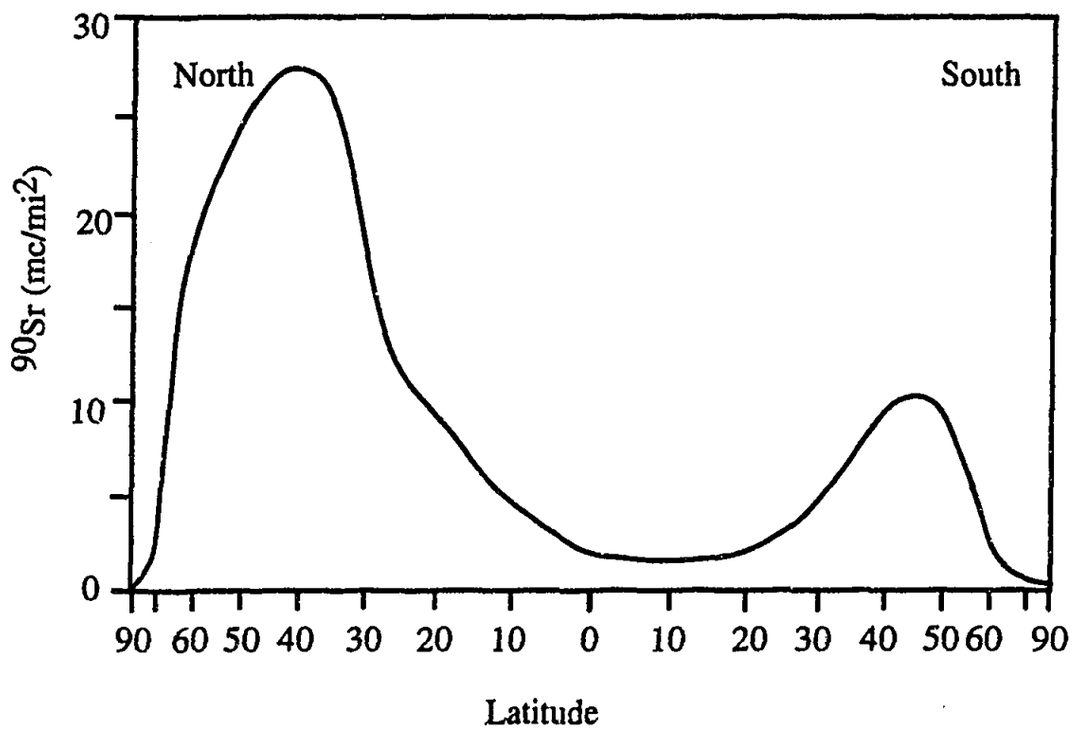

FIGURE 6.5 The fallout pattern of ^{90}Sr from the stratosphere in the northern and southern hemisphere. From Lal and Peters 1962.

this value (eg. 6.9 x10^{-2} ^{10}Be atoms/cm^2/s measured in precipitation at 40°N by Knies 1994 and 4.4 x10^{-2} ^{10}Be atoms/cm^2/s for continental sites in the US measured by Monaghan 1985/1986). A surface snow sample from Antarctica (Raisbeck et al 1978), however, gives a lower rate of deposition (3.1 x10^{-3} ^{10}Be atoms/cm^2/s), ten times lower than measured in Greenland ice. This extremely low value was attributed to the low rate of precipitation at the Antarctic site.

Investigations into the meridional distribution of ozone in the troposphere also highlighted this asymmetry between the hemispheres (Fabian and Pruchniewicz 1973). Peaks in ozone mixing were observed for northern hemisphere subtropical and high latitudes, while only occasional peaks were observed in the southern hemisphere subtropical latitudes. These peaks trace the latitudinal ranges where enhanced stratospheric/tropospheric exchange occurs in association with tropopause folding events. Figure 6.6 shows the mean ozone injection from the stratosphere as a function of latitude, based upon flight data (Fabian and Pruchniewicz 1973). Pruchniewicz (1973) attributed the asymmetry observed between northern and southern hemisphere ozone levels to the lower efficiency of the southern

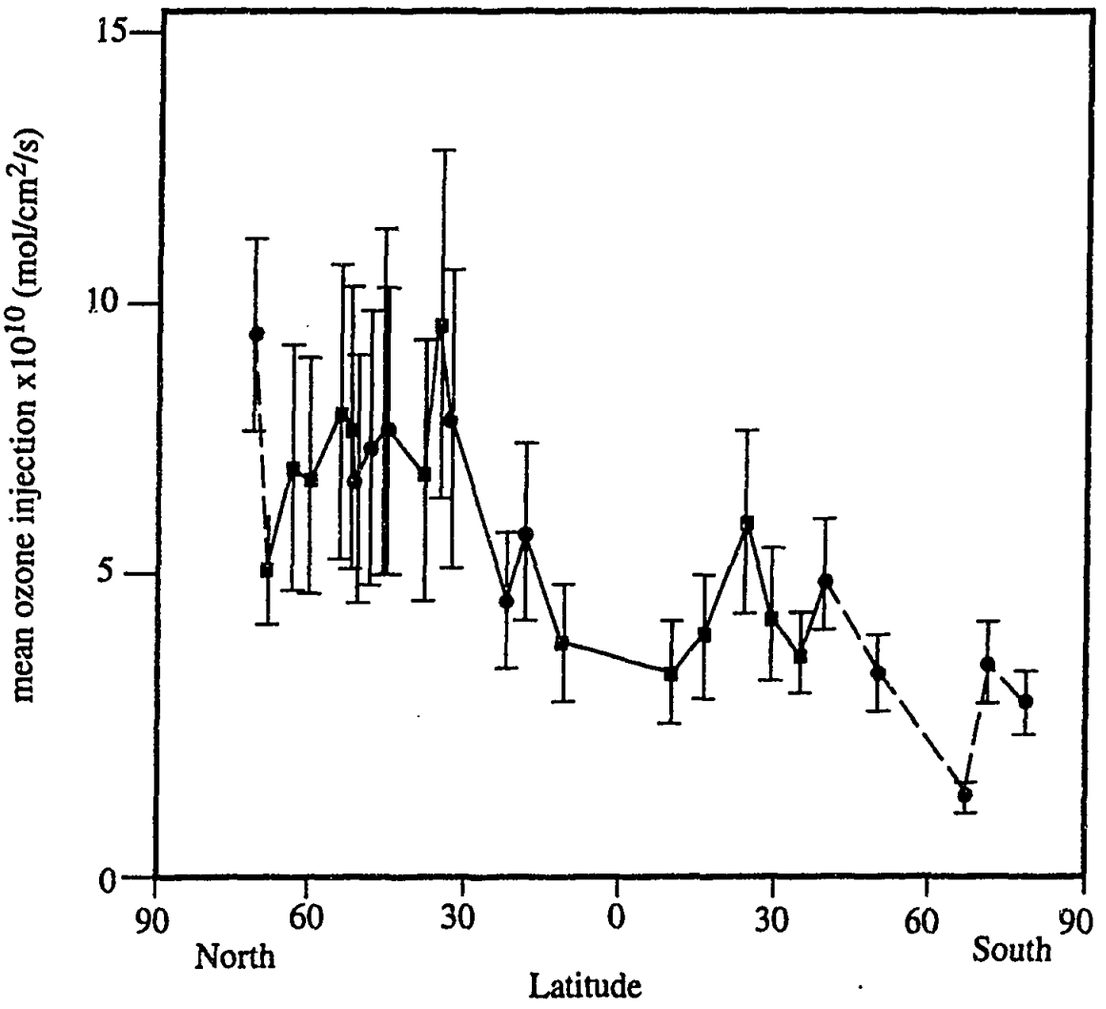

FIGURE 6.6 Mean ozone injection from the stratosphere as a function of latitude. From Faiben and Pruchniewicz (1977).

hemisphere gap region in transferring ozone from the stratosphere to the troposphere.

Holton (1990) used climate data to model the rate of flux of material between atmospheric domains and found transfer in the northern hemisphere to be 50% greater than in the southern hemisphere. In extratropical regions, poleward and downward transport of aerosols was found to be most robust during winter, and stronger in the northern hemisphere than in the southern hemisphere (Hitchman et al 1994). Robinson (1980), Holton (1990), Follows (1992) and Yulaeva et al (1994) attributed the enhanced poleward and downward transport of air during winter in the northern hemisphere to a more pronounced driving lower stratospheric wave. Lower stratospheric stationary waves are generated by orographic and thermal forcing in the troposphere, the effects of each process being equally important (Gill 1982, Smith 1979).

Orographic Forcing

Figure 6.7 shows a schematic representation of the role of mountains in producing stationary waves. Mountain waves have been observed, eg. in the Rocky Mountains and the Tibetan Plateau (Lilly et al 1974) and modelled (see Smith 1979 for a review of planetary-scale mountain wave models). Manabe and Terpstra 1974, used a complex three layer model to show that the disturbance to zonal air flow is stronger in the presence of mountains. Smith and Davies (1977) used a simpler two-layer model to show that in the absence of mountains recurring transient disturbances in the middle latitude wind flow occurred. In the presence of mountains large amplitude standing waves were produced, and the amplitudes of the transient waves decreased.

The smaller area of land mass and therefore lesser amount of topography in the southern hemisphere mean that less orographic production of stationary waves occurs in the southern hemisphere. This factor contributes to the reduced amount of lower stratospheric wave driving in the southern hemisphere.

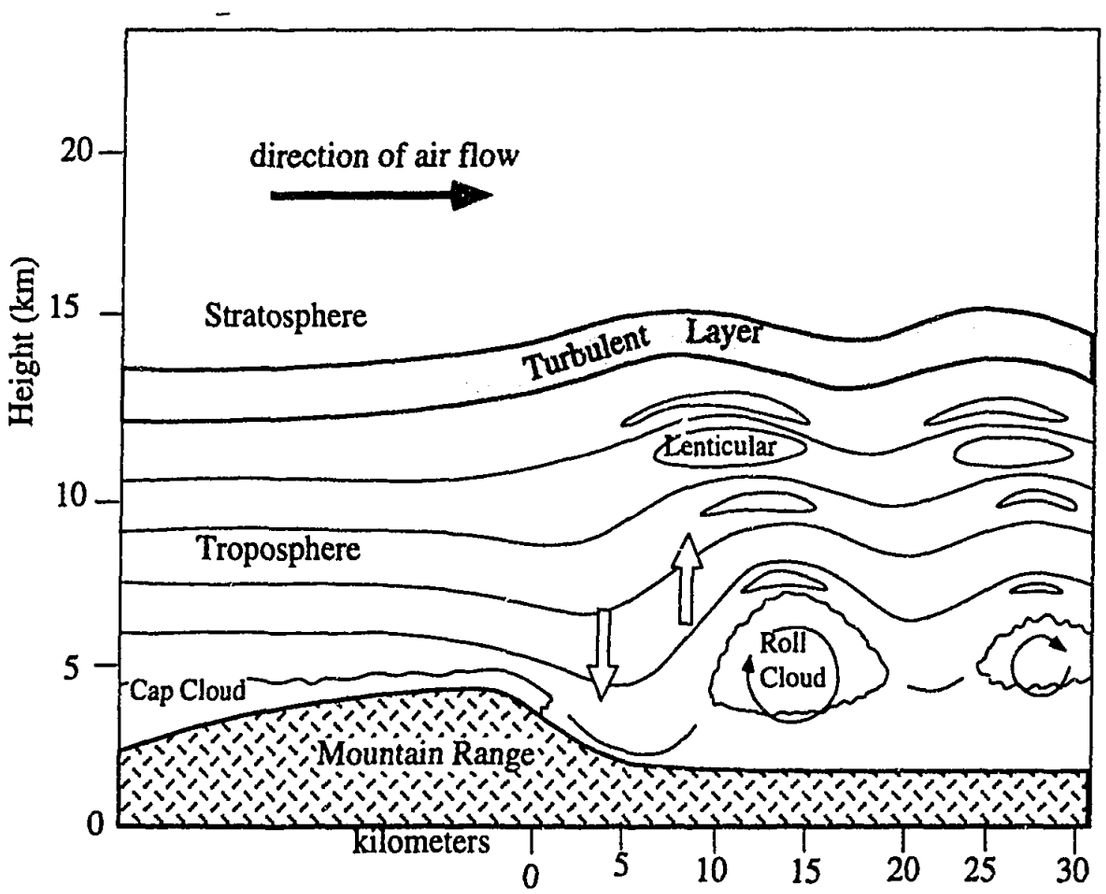

FIGURE 6.7 Schematic representation showing the formation of turbulence in the lower stratosphere by air flowing over mountains to produce mountain waves. After Gossard and Hooke 1975.

Thermal Forcing

Waves are able to propagate vertically if a uniform mean wind (U) is below a critical velocity (Uc), where Uc is dependent on the zonal and meridional components of the wave, the Coriolis effect, buoyancy and height. Arising from this transmission criteria, upward propagation of waves is forbidden in easterly and strong westerly winds (Plumb 1989).

Stationary waves have high amplitudes in the northern hemisphere during winter and are absent during summer. During the southern hemisphere winter, stationary waves have high amplitudes at the beginning and end of winter, but collapse in mid-winter. The behaviour of the southern hemisphere stationary waves is therefore not simply a reflection of tropospheric forcing, but can be explained in terms of the transmission criteria described above. During the southern hemisphere mid-winter westerly winds are too strong to permit vertical propagation of stationary waves. A feedback mechanism seems to exist in which the difference in the mid-winter wind regimes of the two hemispheres arises from the difference in thermal structure of the two hemispheres. The temperature of the southern hemisphere polar night is lower than that of the northern hemisphere polar night (Figure 6.8a). Departures from radiative equilibrium arise from differences in wave transport (Andrews 1989). Therefore the differences in geopotential heights between the two hemispheres in winter (Figure 6.8b) arise from the difference in wave transport, with the southern hemisphere waves being weaker.

Summary

In conclusion, the enhanced lower stratospheric wave driving in the northern hemisphere arises from the greater amount of orographic forcing, a consequence of the greater amount of land mass in the northern hemisphere. Differences in the thermal structure of the two hemispheres are also significant, giving rise to differences in mean zonal winds between the two hemispheres during winter. In the southern hemisphere, the mid-winter westerlies are stronger and therefore inhibit vertical propagation of the stationary waves. In the northern hemisphere, wave propagation in mid-winter is enabled as a result of the reduction to the mean westerlies by the waves themselves (Plumb 1989).

The ^{36}Cl prediction curve of Lal and Peters (1967) is constructed on the basis of the southern hemisphere representing a mirror image of the northern hemisphere in a similar way to the atmospheric box models discussed above. However, for the transfer of many species from the stratosphere to the troposphere (eg. ozone, ^{90}Sr)

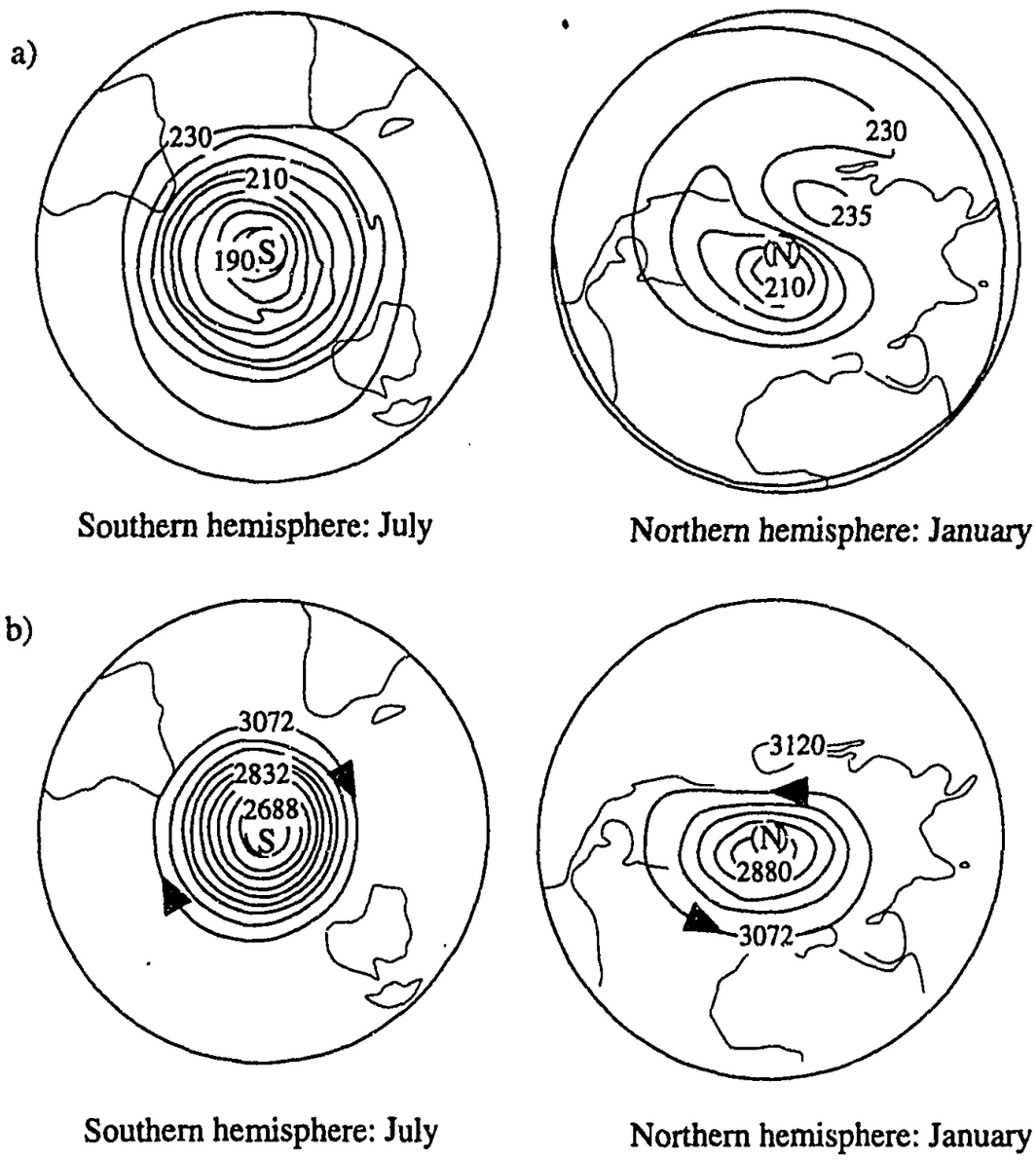

FIGURE 6.8 Polar stereographic maps of a) monthly averaged temperature (K) at 10 mb and b) monthly averaged geopotential height fields at 10 mb during winter in both hemispheres (i.e. July in the southern hemisphere and January in the northern hemisphere). Geopotential height field is calculated from the geopotential/9.8 m/s^2. Geopotential at a certain height in the atmosphere is the amount of work required to move a unit mass from sea-level to that height. Note the zonal symmetries displayed by both parameters for the southern hemisphere winter. Arrows in b) represent direction of geostrophic flow.

this is not the case, and up to 50% less transfer appears to occur in the southern hemisphere. This difference may be reflected in the fallout of ^{36}Cl, with lower values being observed in the present investigation than those measured for the northern hemisphere.

Anthropogenic Production and Fallout

During the 1950s large amounts of ^{36}Cl were injected into the stratosphere by thermonuclear weapons tests in marine environments. Chlorine-36 was produced by the neutron capture of ^{35}Cl in seawater. This injection of ^{36}Cl has become known as the 'bomb pulse'. The bomb pulse was characterised by fallout levels that peaked at 1,000 times the background levels in middle latitudes and occurred between 1953 and 1964 (Schaeffer et al 1960, Bentley et al 1982). The elevated ^{36}Cl levels associated with the bomb pulse are recorded in the Dye-3 Greenland ice core (Elmore et al 1982, Suter et al 1987, Synal et al 1990), the Camp Century ice core (Elmore et al 1987), soils from New Mexico (Phillips et al 1988) and Australia (Fifield et al 1987), and groundwaters from Ontario (Bentley et al 1986a). At Maralinga in South Australia, the site of British nuclear weapons tests during the 1950s, localised $^{36}Cl/Cl$ ratios of up to 10^{-11} occur (Bird et al 1991).

In the Dye-3 Greenland ice core, ^{36}Cl levels in 1957 corresponded to 500 times the background level (Elmore et al 1982, Suter et al 1987). Synal et al (1990) used the data from the Greenland ice core to develop a model of atmospheric bomb-produced ^{36}Cl, and calculated a residence time of 2±0.3 years for bomb-produced ^{36}Cl in the stratosphere. Bentley et al (1982) modelled ^{36}Cl fallout from nuclear tests by using estimates of ^{36}Cl injection into the stratosphere from individual explosions as input for an atmospheric box model. The model was calibrated using the ^{36}Cl concentrations in rainfall reported by Schaeffer et al (1960). In general, good agreement was found between the model and the ^{36}Cl levels found in the Dye-3 Greenland ice core.

As the levels of ^{36}Cl associated with the bomb pulse are so much greater than background levels, the bomb pulse is a useful environmental tracer, eg. in the study of hydraulic flow and dispersive mixing in groundwater investigations. The long half-life of ^{36}Cl eliminates ambiguities that result from decay and dispersive mixing when other radionuclides, such as tritium are used.

Results obtained from the Dye-3 Greenland ice core showed that ^{36}Cl produced during the weapons tests of the 1950s was influencing precipitation until as late as 1985 (Suter et al 1987). While the present-day ^{36}Cl fallout levels have again reached pre-nuclear weapons testing levels, neutron capture of ^{35}Cl associated with nuclear technology may occur on a local scale, eg. nuclear reactor or processing operations. For example, operation of the HIFAR reactor at Lucas Heights, Sydney

Australia has produced ratios up to 10^{-11} on the reactor site (Bird et al 1991). These levels are not considered an environmental hazard. Much more significantly, nuclear reactor accidents such as Chernobyl, have released considerable amounts of ^{36}Cl into the environment (Andrews and Fontes 1992).

6.2 PREVIOUS ^{36}Cl PRECIPITATION INVESTIGATIONS

The first measurements of ^{36}Cl in rainfall were from Long Island, USA, during the period of nuclear weapons testing in the 1950s (Schaeffer et al 1960). As discussed above, levels of ^{36}Cl were several orders of magnitude above background levels. These large values were measured in a screen-wall counter, a technique whose detection limit is too high to measure background levels of ^{36}Cl. With the refinement of AMS, it has become possible to measure much lower levels of ^{36}Cl. For example, Elmore et al (1979) measured ^{36}Cl concentrations in seawater and surface waters from North America with a background level of $3x10^{-15}$ $^{36}Cl/Cl$. Finkel et al (1980) measured ^{36}Cl in ice, rain and upper seawater levels in Antarctica. Variations of up to three orders of magnitude were observed in snow and firn and were attributed to the effects of atmospheric mixing and scavenging, or to radioactive decay of ^{36}Cl in the very old ice. A rainfall sample measured by Finkel et al (1980) showed ^{36}Cl levels lower than rainfall collected during the early 1960s, showing the decrease in atmospheric ^{36}Cl derived from nuclear weapons tests.

Investigations of anthropogenic levels of ^{36}Cl in ice-cores were discussed in the previous section. Pre-bomb ^{36}Cl concentrations of ice from the Dye-3 Greenland ice core were also measured and found to be 3 to 5 times greater than predicted from production rate calculations (Suter et al 1987). In contrast, the global fallout rate of ^{36}Cl estimated from measurements of Antarctic ice (Nishiizumi et al 1979, Finkel et al 1980 and Nishiizumi et al 1983) were close to the predicted calculations. (Table 6.1). Reliable ^{36}Cl fallouts of between 10 and 14 atoms/m^2/s can be deduced from the ^{36}Cl concentrations measured in the surface ice samples when snow deposition rate and latitude are taken into account.

Chlorine-36 has been used as a tool to model evapotranspirative loss from the upper Jordan River catchment (Magaritz et al 1990). Stable Cl concentrations and $^{36}Cl/Cl$ ratios of several water bodies were compared with those of precipitation, and were found to experience between 40 to 90% evapotranspirative loss. The representative precipitation sample was Mt Hermon snow (latitude 32.5°N), which had a ratio of 1589 ± 12 $^{36}Cl/Cl$ and was calculated to be made up of less than 1% of bomb-produced ^{36}Cl.

TABLE 6.1 Concentration of ^{36}Cl in ice from Antarctica and the estimated ^{36}Cl fallout calculated from A=fc/s (from Nishiizumi et al 1979), where A is ^{36}Cl concentration (atoms/kg of ice), f is fallout, c is latitude scaling factor (0.4 at 70°) and s is snow deposition rate (5 cm/y) .

sample	^{36}Cl atoms/kg of ice ($x10^6$)	^{36}Cl fallout (atoms/m^2/s)	Reference
Yamato Mountains	2.5	9.9	Nishiizumi 1979
Allan Hills	2.6±0.1	10.3	Finkel 1980
	7.5±0.3*	30	
	2.8±0.2	11.1	
	3.6±0.2	14.2	
Siple Firn	8.7±0.8**	34	
Allan Hills (0-12 cm)	3.38±0.2	13.4	Nishiizumi 1983
Yamato Mountains c-8	3.17±0.22	12.6	

*higher snow accumulation rate

** remelting of old ice near the surface of the ice sheet (based on field evidence) may have allowed incorporation of bomb ^{36}Cl in the modern ice

Herut et al (1992) investigated the ^{36}Cl composition of Cl-rich rainwater (defined as having greater than 2.9 meq/L Cl) from Israel. A positive strong correlation between $^{36}Cl/Cl$ ratio and Cl concentration was interpreted as a solute relationship defined by mixing between two endmembers, sea-spray with a low $^{36}Cl/Cl$ ratio and Cl-rich marine-dust aerosol with a high $^{36}Cl/Cl$ ratio.

Hainsworth (1994) measured the ^{36}Cl levels in monthly rainfall from Maryland, USA. Seasonal changes in the flux of ^{36}Cl were observed, with a maximum in the northern hemisphere spring reflecting the seasonal changes in stratospheric-tropospheric mixing. Wet-only collectors were compared with bulk depositional collectors, and dry deposition was estimated to account for 25% of flux to the site, being significant during periods of low rainfall. The mean depositional flux at the Maryland site was 59±8 ^{36}Cl atoms/m^2/s, three times greater than that predicted for latitude 38°N, but in accordance with the fallouts measured in the pre-bomb Dye-3 Greenland ice cores (Suter et al 1987).

Ratios of $^{36}Cl/Cl$ ratios in surface waters from the Susquehanna River basin (Pennsylvania) and groundwaters from the Aquia Aquifer (Maryland) were found to be 3 to 5 times higher than predicted by Bentley et al (1986a). Hainsworth (1994)

recalculated the depositional pattern of $^{36}Cl/Cl$ for the USA based upon the deposition pattern of ^{90}Sr. The model included latitudinal and longitudinal variations in ^{36}Cl deposition. The longitudinal variations arise due to the effect of topography on stratospheric/tropospheric mixing. The recalculated $^{36}Cl/Cl$ deposition pattern agreed with that of Bentley but values were two times greater than Bentley's. Bulk-deposition samples were collected from six sites in eastern USA and one site in central northern USA. The measured $^{36}Cl/Cl$ ratios agreed with the predictions of Hainsworth for the eastern sites, but were anomalously high for the central site (i.e. measured at 4220 $x10^{-15}$, when predicted to be between 1200 $x10^{-15}$ and 1600 $x10^{-15}$ by Hainsworth). Measured fluxes were two times greater than Hainsworth's predictions and stable Cl was two times greater than measurements from the National Atmospheric Deposition Program. These discrepancies were attributed to a combination of oversampling, recycling of crustal material and dry deposition. A global production of 40 atoms/m^2/s was suggested, almost four times greater than that predicted by Lal and Peters (1967).

Knies (1994) measured ^{36}Cl, ^{10}Be and ^{7}Be from wet deposition in Illinios, USA. Fluxes of each isotope correlated with precipitation amount. The mean flux of ^{36}Cl was measured to be 67±5 ^{36}Cl atoms/in^2/s, approximately four times that predicted even when dry deposition of 15% was taken into account.

In summary, measurements of ^{36}Cl in precipitation from the northern hemisphere suggest a ^{36}Cl fallout that is 3-5 times greater than predicted by Lal and Peters (1967). The few published values of ^{36}Cl in the southern hemisphere (i.e. Antarctic ice measured by Nishiizumi et al 1979, Finkel et al 1980 and Nishiizumi et al 1983) suggests a fallout that is only slightly higher than the predictions of Lal and Peters (1967), i.e. a factor 3 less than in the northern hemisphere. Data from the present investigation allows a detailed examination of the discrepancy between northern and southern hemisphere fallout estimates.

6.3 CHLORINE-36 INVESTIGATIONS IN AUSTRALIA

There have been many $^{36}Cl/Cl$ measurements made on samples from various parts of the Australian environment. These have all been measured by the AMS group in the Research School of Physical Sciences and Engineering at the Australian National University with the exception of early measurements on the Great Artesian Basin (Bentley et al 1986b). Some early results are reported in Fifield et al 1987, Davie et al (1989) and Bird et al (1991), although a substantial body of data is awaiting

publication. The following discussion will focus on those studies for which the atmospheric deposition results from the present investigation may be of particular relevance.

The present study has relevance to groundwater investigations, as precipitation provides the means of input of ^{36}Cl to groundwater systems. The Great Artesian Basin showed the application of ^{36}Cl to date groundwater greater than 1 Ma (Bentley et al 1986b). The Great Artesian Basin occupies one fifth of the area of Australia, and is located in central and northeastern Australia. Recharge to the basin occurs along the coastal ranges of northeast Australia, and outflow emerges near Lake Eyre in central Australia. Ages of the groundwater ranged between less than 100,000 years and greater than 1 Ma, and were in agreement with age estimates from hydraulic models. The $^{36}Cl/Cl$ ratio was found to be constant in the recharge area and decreased smoothly away from the recharge zone. The $^{36}Cl/Cl$ ratio at the recharge zone was used as an estimate of the initial $^{36}Cl/Cl$ ratio required in the age calculation.

Davie et al (1989) used $^{36}Cl/Cl$ ratios to identify chlorides of different origins in groundwater from the Mallee region of the Murray-Darling Basin, southeastern Australia. Isotope ratios were found to increase in the direction of flow. This trend was opposite to that expected based upon probable relative ages since recharge, and was interpreted as the influx of saline groundwater along the flow path. The generally low $^{36}Cl/Cl$ ratios and the associated increases in Cl along the flow lines were interpreted as the percolation of rainwater downwards at several places within the aquifer.

A major increase in stable Cl concentration and falling $^{36}Cl/Cl$ ratios was noted in the downflow (from east to west) direction of the Lachlan Fan area of the Murray-Darling Basin (Bird et al 1989). The young age of the groundwater (<<300,000 years) ruled out decay as being an explanation of this increase. Instead, evaporation and dissolution of a constant ratio chloride was invoked as a cause.

Simpson and Herczeg (1994) reinterpreted data on the stable Cl concentration of rainfall from eastern Australia and concluded that it consisted of up to 50% recycled Cl. It was recognised that this has implications for the calculated $^{36}Cl/Cl$ ratios as a function of distance from the coast for the Murray-Darling basin. If marine Cl accounts for only half of the Cl in rain, the $^{36}Cl/Cl$ ratio would be twice that calculated for Cl that is 100% marine in origin if the $^{36}Cl/Cl$ composition of the

recycled component is comparable with recent precipitation rather than the low ratios typical of seawater. The present investigation may tell us something about the recycled Cl component by comparing the measured ratio with a recalculated ratio based upon latitude and distance from the coast.

Salt lakes provide a source of recycled Cl to precipitation. Relatively low ratios (30-60x10^{-15}) are found in salt lakes mainly from Western Australia (Fifield et al 1987). The lack of variation in the ratios as a function of location, and the similarity of the average ratio to granites, was interpreted as weathering of surface rocks as being the main source of ^{36}Cl to the salt lakes. However, further investigations of the ^{36}Cl content of halite from Western Australian salt lakes found that ^{36}Cl/Cl ratios in halites from salt lakes in Western Australia showed increasing ratios with increasing distance from the coast (Chivas et al 1994). The present investigation, by measuring precipitation of ^{36}Cl in the vicinity of the Western Australian salt lakes, may provide further insight to this suggestion of the source of ^{36}Cl to salt lakes.

The results of previous investigations of ^{36}Cl in the Australian landscape highlight several areas in which basic measurements of ^{36}Cl are necessary in order to fully interpret existing ^{36}Cl data. For example, although good agreement was found between predicted ^{36}Cl/Cl ratios of precipitation and measured values of ^{36}Cl/Cl in recharge waters in the Mallee area of the Murray-Darling Basin (Davie et al 1989), recharge ratios in the Lachlan River region were higher than the calculated values (Bird et al 1989). This was also the case for the Great Artesian Basin (Bentley et al 1986b). Thus there is a need for more information on the Cl and ^{36}Cl precipitation rates as a function of latitude and distance from the coast. Bird et al (1991) also speculated that the ^{36}Cl/Cl ratios in tropical rainfall would be low because of the very high rainfall carrying marine Cl. Recycled solids in rainfall from inland Australia would be expected to contribute to high ^{36}Cl/Cl ratios in meteoric fallout at inland sites.

The investigation of the ^{36}Cl in precipitation from the two arrays established in this research project provides some of the basic information required to fully interpret existing ^{36}Cl data. The WE array allows an investigation of the change in ^{36}Cl/Cl ratios with changing distance from the coast. The SN array allows an assessment of the latitudinal dependence of ^{36}Cl fallout. Both arrays provide information on the seasonal variations of the ^{36}Cl in precipitation.

6.4 THE DATA SET

The ^{36}Cl data set is made up of 115 (of a possible 144) values spread over the 18 sites that make up the WE and SN arrays. Samples excluded from the data set include those removed during the major-element data quality checks (Chapter 5) and those which experienced problems during collection and subsequent manipulation, eg. northern sites along the SN array during summer 1992 are excluded because an accurate rainfall record was not measured due to a fault in the rain-collector design. The data set is listed in Appendix G.

6.5 OBSERVATIONS

In the following discussion, fallout of ^{36}Cl is in atoms/m^2/s. Stable Cl concentration is in μeq/L (unless stated otherwise) and ^{36}Cl concentration is in units of atoms/L.

Spatial variations

Mean $^{36}Cl/Cl$ Ratios

The mean ratios of $^{36}Cl/Cl$ as a function of distance from the coast, are shown in Figure 6.9 for both the WE and SN arrays. The mean stable Cl concentrations at each site are also shown on the plots. The WE array shows an increase in the $^{36}Cl/Cl$ ratio with increasing distance from the coast. A similar trend is observed for the SN array from the southern and northern coasts. It should be noted that the mean north coastal ratios (eg. at sites 32 and 33) greatly exceed those measured at an equivalent distance from the western coast of the WE array (eg. sites 16, 17 and 18) and from the southern coast of the SN array (sites 26 and 27). The increase in $^{36}Cl/Cl$ ratio with increasing distance from the coast is matched by a decrease in stable Cl. This trend reflects the influence of marine chloride at coastal localities and the decreasing influence with increasing distance from the coast.

Mean Stable Cl Concentrations

The relationship between $^{36}Cl/Cl$ and distance from the coast reflects the decreasing influence of stable Cl of marine origin with increasing distance inland. Figure 6.10 shows the rapid decrease of Cl concentration in rainfall with increasing distance from the coast for the WE and SN arrays. The relationship between Cl concentration of precipitation and distance from the coast has been discussed, both world wide (Junge 1963) and for Australia (Hutton 1976). Junge (1963) showed that wet and dry removal of salt by in-cloud and below-cloud scavenging (calculated from salt residence times in the atmosphere and wind directions) were insufficient to explain

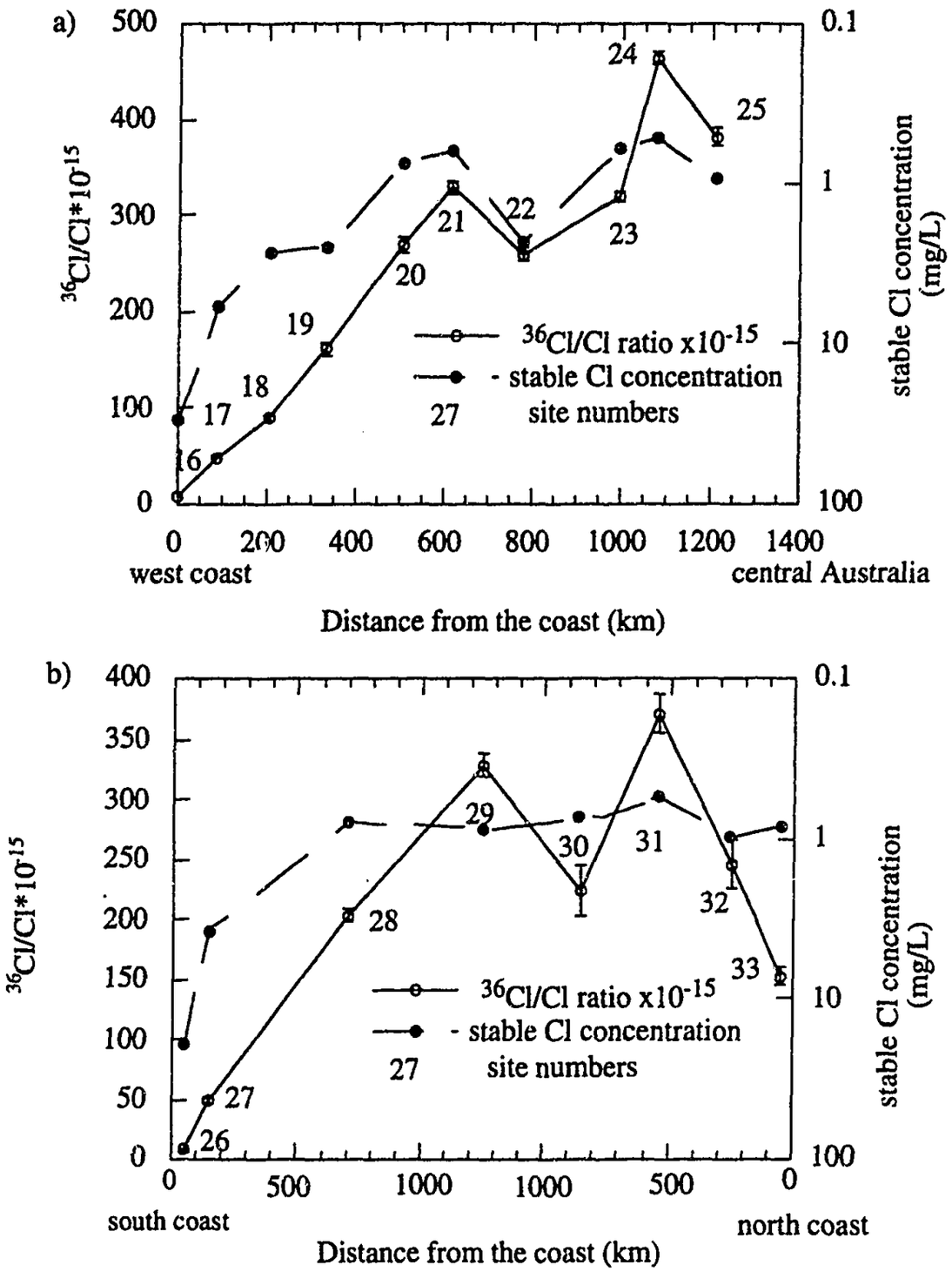

FIGURE 6.9 Mean ^{36}Cl/Cl ratios and stable Cl concentrations as a function of distance from the coast for a) the WE array and b) the SN array. Coast for a) is Leeman, WA b) is Port Lincoln SA for the southern section of the SN array and Finke Bay, NT for the northern section of the SN array. Note that the stable Cl axis is reversed. Mean ratios and stable Cl concentrations are calculated from seasonal means (see text).

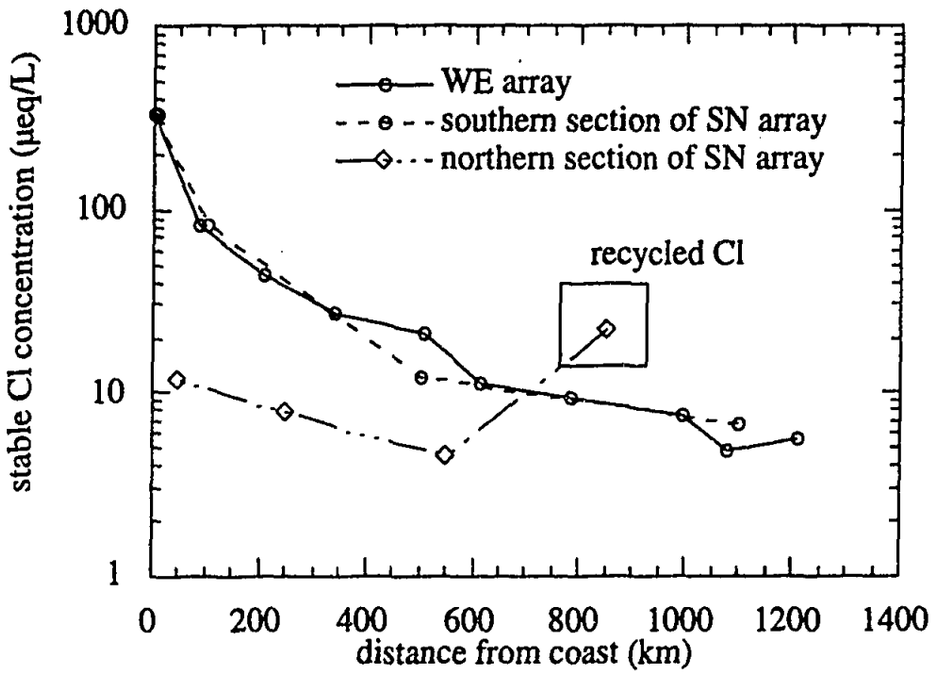

FIGURE 6.10 Mean stable Cl concentrations as a function of distance from the coast. Coast for the WE array is Leeman, WA, coast for the southern section of the SN array is Port Lincoln, coast for the northern section of the SN array is Finke Bay, NT. Mean stable Cl concentrations are calculated from the seasonal means.

the dramatic decrease in rainfall Cl concentration with increasing distance from the coast for Europe, USA and Australia. Instead this dependence was explained in terms of increased convective mixing of marine air masses moving inland. Mixing results in a decrease of salt concentration in subcloud layers, and therefore a decrease in salt concentrations in rainfall. At coastal sites, where convective mixing has not begun, the airmass is not well mixed so that Cl is available for easy removal by in-cloud and below-cloud deposition. As the airmass moves inland, convective mixing occurs and salts are distributed vertically through the airmass. Thus, less Cl is available in the in-cloud and below-cloud regions, so that concentrations in rainfall decrease. The distance from the coast where vertical distribution becomes uniform is marked by a plateau of Cl concentrations, and this distance is dependent upon the original vertical salt profile, which varies with geographical location.

Previous Models

The rate of decrease of Cl concentration in rainfall with distance from the coast has been shown for Australia to follow the form (Hutton 1976)

$$y = 0.99d^{-1/4} - 0.23 \qquad (6.2)$$

where y is volume weighted mean concentration of Cl in μeq/L and d is distance from the coast in km. For data from Victoria (Hutton and Leslie 1958) this gave a good fit with r^2= 0.992, n=24. Restrictions necessary for the application of this equation include the removal of sites influenced to a large extent by terrestrial sources, exclusion of sites with annual rainfall less than 500 mm, sampling over at least 12 months and removal of sites greater than 300 km from the coast. The regression form of Hutton's equation was applied to the data from Western Australia of Hingston and Gailitis (1976) in Isbell et al (1983), and gave different constants i.e.

$$\text{southwest WA: } y = 0.724d^{-1/4}-0.09 \quad r^2 = 0.855 \qquad (6.3)$$

$$\text{northwest WA: } y = 0.14d^{-1/4}-0.02 \quad r^2 = 0.687 \qquad (6.4)$$

Mean annual Cl concentration in rainfall for southwest Western Australia (Farrington et al 1993) was shown to follow the following relationship

$$Cx = Cmin + (Cmax-Cmin)e^{-\lambda x} \qquad r^2 = 0.975 \qquad (6.5)$$

where Cx is the concentration of Cl at distance x km (mg/L), Cmax is the concentration of Cl at coast, Cmin is the concentration of Cl at the most inland site, x is the distance from coast (km) and λ is the spatial decay constant. This exponential decay function was then used to predict the amount of Cl accession in southwestern Western Australia.

The regression equations described by Hutton (1976) and Farrington et al (1993) are applied to data for the WE and SN arrays in Figure 6.11. Also shown in Figure 6.11 are the equations for data from north-west and south-west of Western Australia from Hingston and Gailitis (1976) reported in Isbell et al (1983). Figure 6.11 shows that neither regression form adequately fits the data for the WE and SN arrays. However, the WE data set, falls between the curves defined for the south-west (curve A) and northwest (curve B) of Western Australia. This reflects the location of sampling sites on the WE array which are between those of the northwest and southwest of Western Australia as sampled by Hingston and Gailitis (Figure 6.12). A trend of decreasing Cl concentration in rainfall from the south to the north of the State is suggested. The sites along the northern section of the SN array display lower concentrations than those observed for the north-west of Western Australia by Hingston and Gailitis (1976). The northern sample locations of the SN array are further north than those of Hingston and Gailitis (Figure 6.12), supporting the

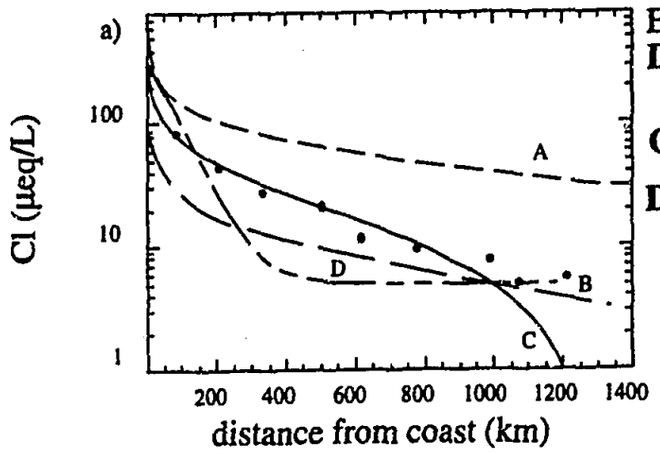

Equations of best fit C Hutton's form, D Farrington's form

C y= $489d^{-1/4}$ -82 r=0.979

D y= 4.9 +$333.1e^{-0.015d}$ r=0.718

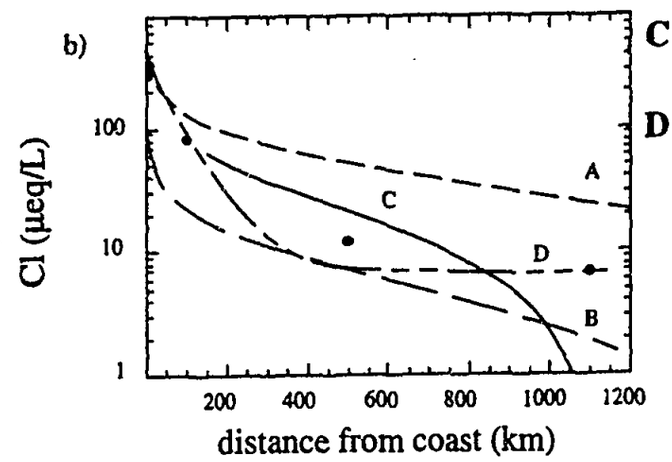

C y= $559d^{-1/4}$ -97 r=0.981

D y= 6.7 +$326.3e^{-0.0136d}$ r=0.974

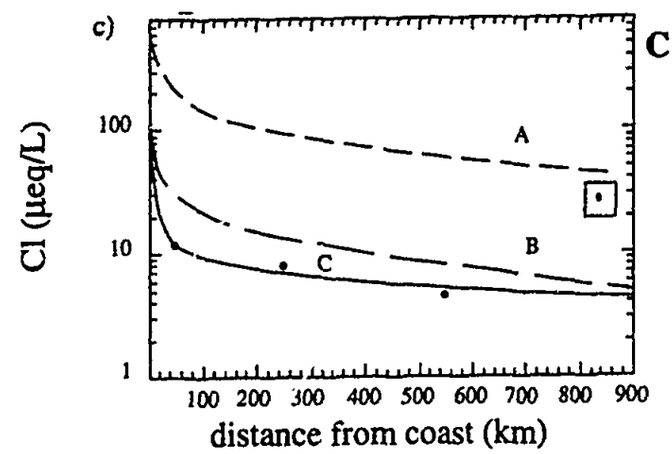

C y= $39d^{-1/4}$ -3 r=0.936

Hutton (1976) form

A y = 724 $d^{-1/4}$ - 90 South-west WA (Hingston and Gailitis 1976)

B y = 140 $d^{-1/4}$ -20 North-west WA (Hingston and Gailitis 1976)

C y= $ad^{-1/4}$ -b

Farrington et al (1993) form

D y= Cmin + (Cmax-Cmin) $e^{-\lambda d}$

FIGURE 6.11 Mean stable Cl concentrations versus distance from the coast for a)WE array, b) southern section of SN array and c) northern section of SN array. Cl concentrations are fitted to equations of Hutton (1976) and Farrington et al (1993). Coast for a) is Leeman, WA, b) is Port Lincoln, SA and c) is Finke Bay, NT.

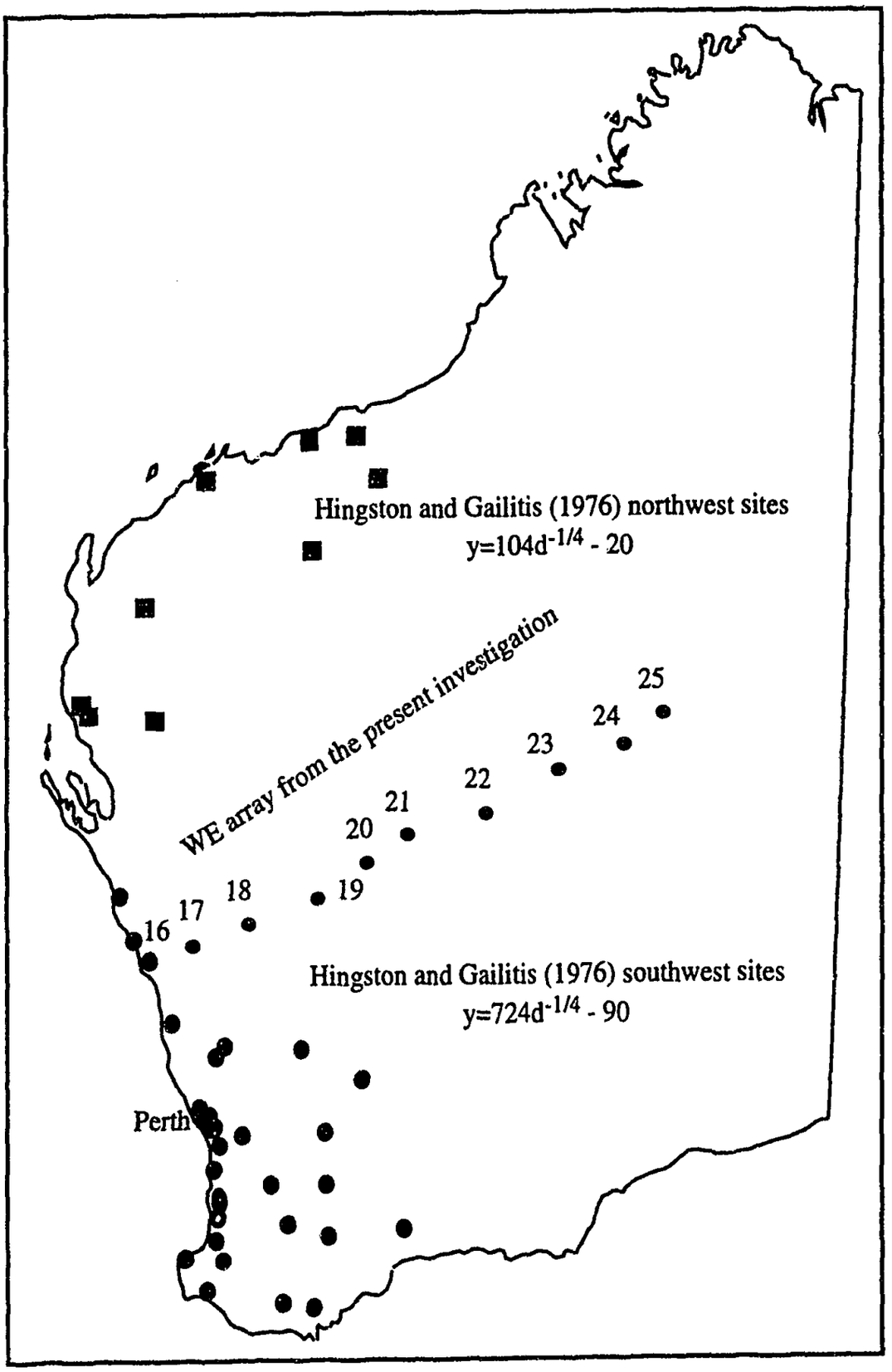

FIGURE 6.12 Map showing the location of the WE array with respect to the northwest (squares) and southwest (circles) sampling sites of Hingston and Gailitis (1976).

suggestion of decreasing Cl concentration of rainfall from the south to the north of Australia. The site at 850 km inland in Figure 6.11c, which is displaced from the regression curve is most likely influenced by recycled Cl.

The data is more adequately explained in terms of a two-exponential equation of the form

$$y = A_1 e^{-d/\lambda 1} + A_2 e^{-d/\lambda 2} \qquad (6.6)$$

where A_1 and A_2 are fitting parameters, $\lambda 1$ and $\lambda 2$ are decay constants and d is distance from the coast. Figure 6.13 shows the WE and southern section of the SN array fitted to this equation.

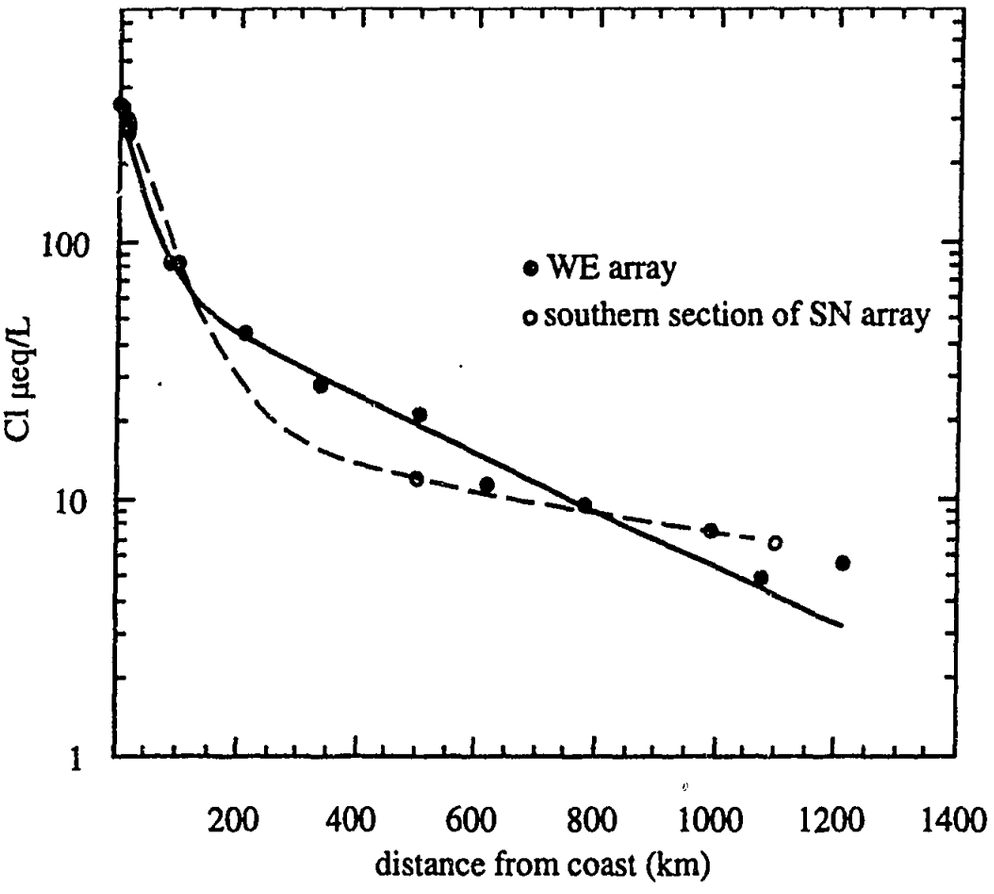

FIGURE 6.13 Stable Cl concentration versus distance from the coast for the WE array (filled circles) and southern section of the SN array (unfilled circles) with a double exponential fit applied to the data. The fit to the WE data (solid line) follows the equation

$$y = 69.4 \exp^{(-d/394.9)} + 284.0 \exp^{(-d/37.1)} \quad \chi^2=16$$

The fit to the southern section of the SN array data (dashed line) follows the equation

$$y = 19.4 \exp^{(-d/1036.9)} + 357.7 \exp^{(-d/58.4)}$$

(Note that a $\chi 2$ could not be calculated because of the lack of degrees of freedom that arises from having only four data points for the southern section of the SN array).

The good fit between the data and the equation suggests that there are two processes influencing the Cl concentration of rainfall as a function of distance from the coast, one that causes rapid decay of Cl concentrations, and the other a slow decay. There are two possible combinations of processes that may cause this two-fold decay of Cl concentrations with distance from the coast: i) the enhanced mixing of airmasses moving inland as discussed above and ii) differences in the rate of removal of Cl aerosols and Cl gas from marine and continental airmasses. The rapid decay of Cl concentrations at the coastal regions represent the removal of Cl in aerosols, introduced to the atmosphere by bubble-bursting at the ocean surface. The second, slower decay process represents the removal of Cl introduced to the atmosphere by volatilisation of Cl from aerosols by strong acids (this process is discussed in Section 6.6). It seems likely that the decreasing Cl concentrations with distance from the coast is influenced by both of the above situations.

Mean ^{36}Cl Fallout

The mean fallouts of ^{36}Cl at each site as a function of latitude are shown in Figure 6.14. Also shown on Figure 6.14 is the predicted fallout curve for the latitudes sampled in this project (Lal and Peters 1967, Andrews and Fontes 1992). In order to minimise the influence of missing values on the mean calculations, mean ^{36}Cl fallouts are calculated from the mean of fallouts for each season (winter, summer, spring and autumn).

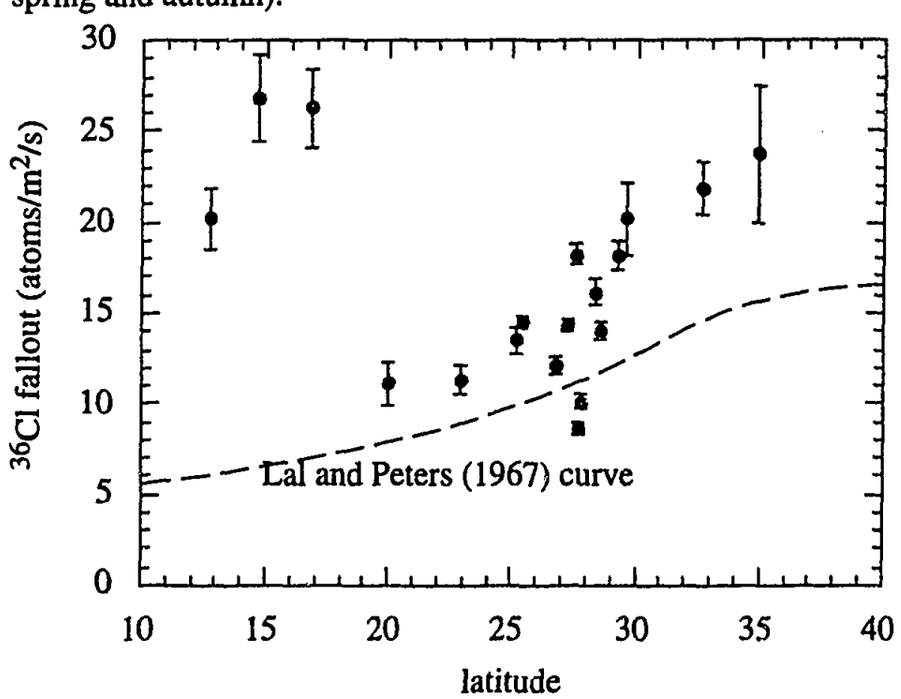

FIGURE 6.14 Mean ^{36}Cl fallout as a function of latitude. Also shown is the predicted fallout curve of Lal and Peters (1967). Error bars represent propagation of standard errors. Mean ^{36}Cl fallouts are calculated from seasonal mean fallouts (see text).

With the exception of the three northernmost points, the data appear to agree with the general shape of the predicted curve, although the predicted curve appears to underestimate the fallout by about 40%. The anomalously large values for sites from the north of the SN array (latitude 12°-18°) reflect the large fallouts during summer (monsoonal period) for these sites, and will be discussed in detail in the following section. A more detailed comparison between predicted and measured fallout values is given in the Discussion (Section 6.6).

Seasonal Variations

The seasonal variations of $^{36}Cl/Cl$ ratios, ^{36}Cl fallout and ^{36}Cl concentration, rainfall amount and stable Cl concentration for each site on the WE and SN arrays are displayed in Figure 6.15. Each value represents the mean value for each season over two years. Where there are missing values (as discussed in Section 6.4), the value in the plot represents single measurements. At site 25 during summer and site 33 during spring, there are no measurements available.

Investigating the trends displayed by $^{36}Cl/Cl$ ratios, ^{36}Cl fallout, ^{36}Cl concentration, rainfall amount and stable Cl concentration over time provide information concerning the processes that effect the ^{36}Cl composition of precipitation. While exceptions exist, the following discussion describes the general trends displayed by the different variables and attempts to explain the processes that may produce these correlations. From the data, a positive correlation is observed between rainfall amount and ^{36}Cl fallout and a negative correlation between rainfall amount and ^{36}Cl concentrations. $^{36}Cl/Cl$ ratios exhibit both positive and negative correlations with ^{36}Cl and stable Cl concentration, reflecting the site dependent input of ^{36}Cl and stable Cl. This is corroborated by a lack of correlation between ^{36}Cl concentration, stable Cl concentration or $^{36}Cl/Cl$ ratio with ^{36}Cl fallout.

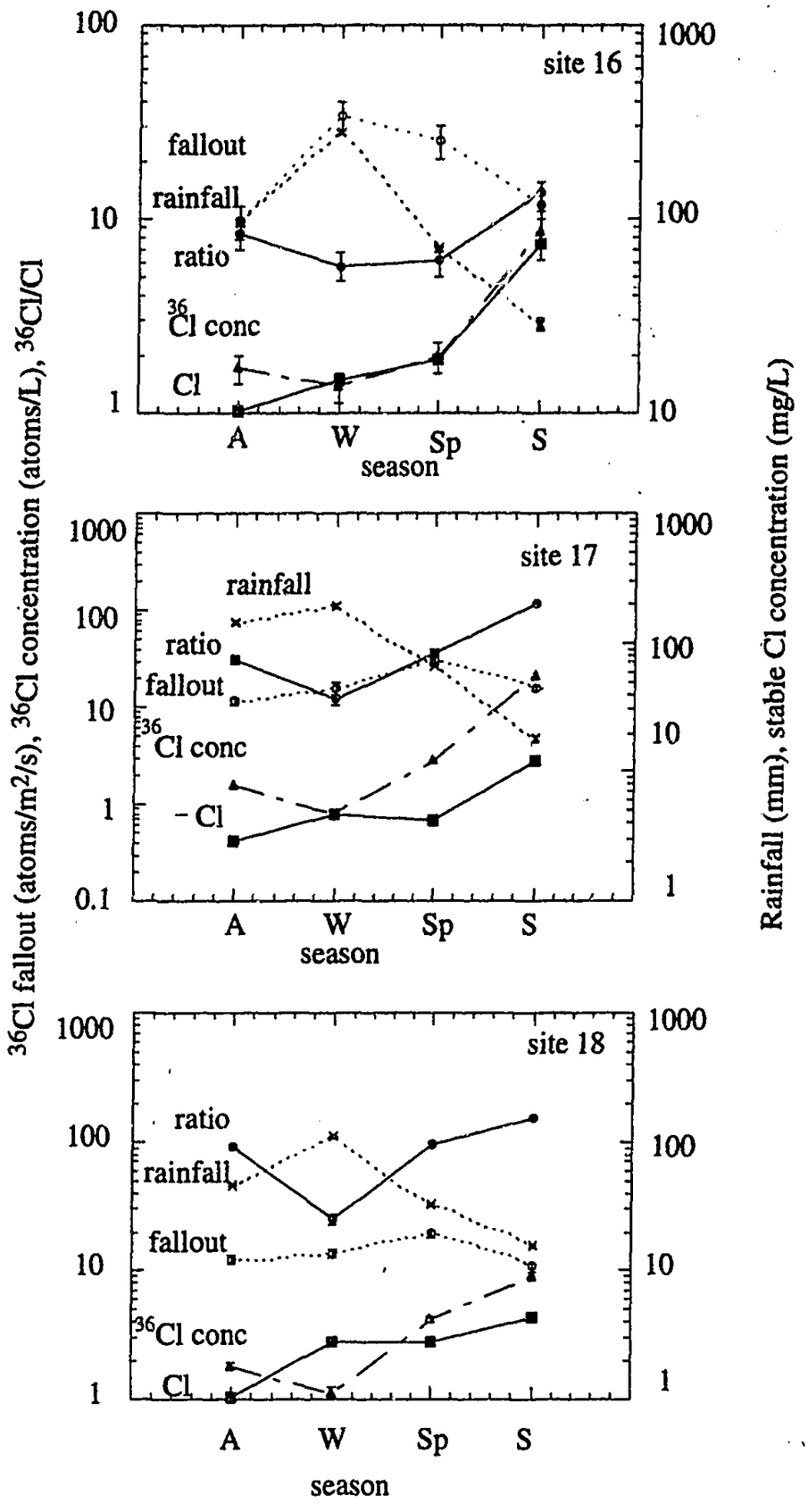

FIGURE 6.15 Seasonal variations displayed by ^{36}Cl fallout, ^{36}Cl concentration, $^{36}Cl/Cl$ ratio, stable Cl concentration and rainfall amount at each sampling site. A=autumn, W=winter, Sp=spring, S=summer. Values represent the mean for each season over the sampling program.

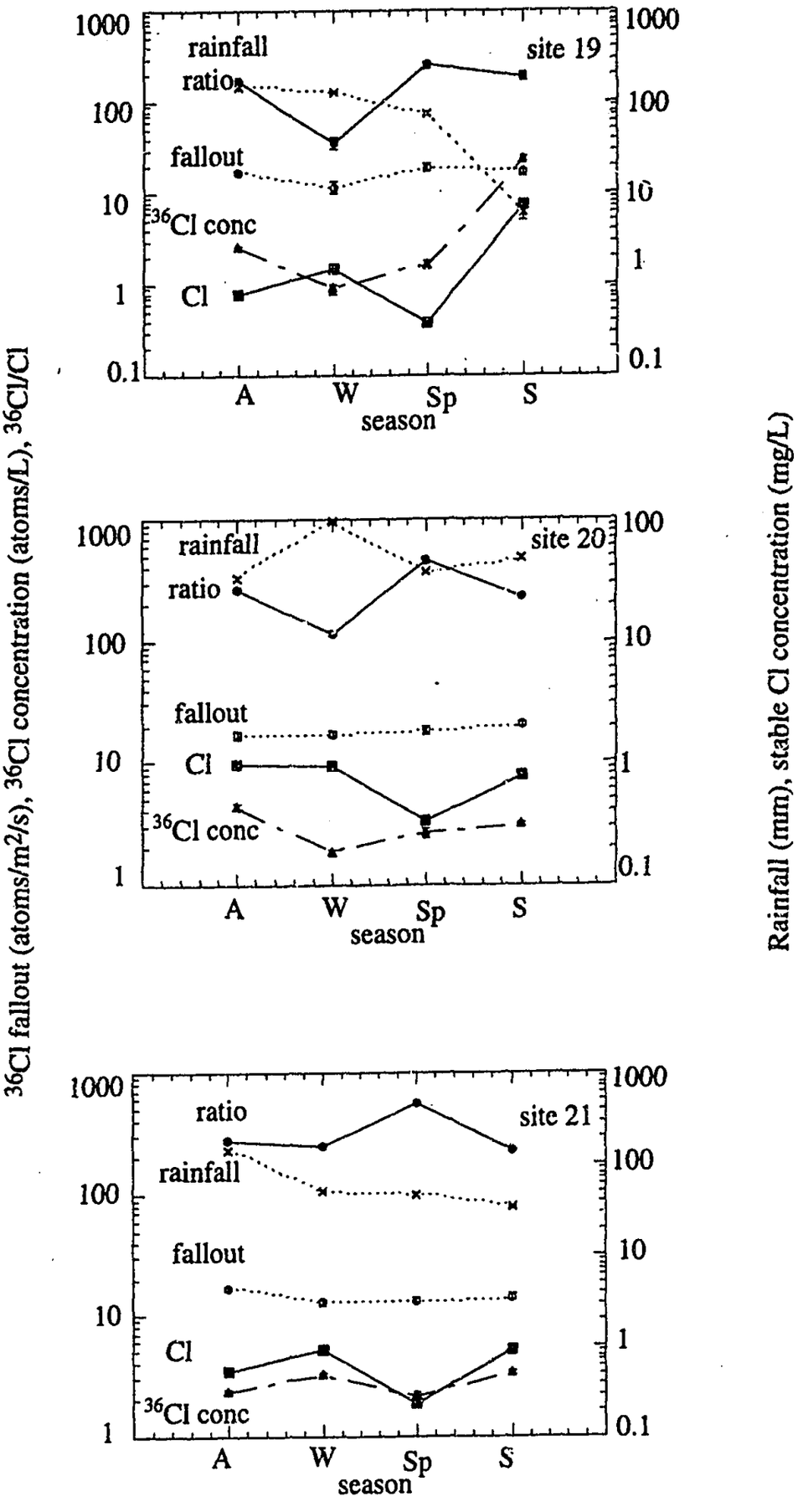

FIGURE 6.15 continued

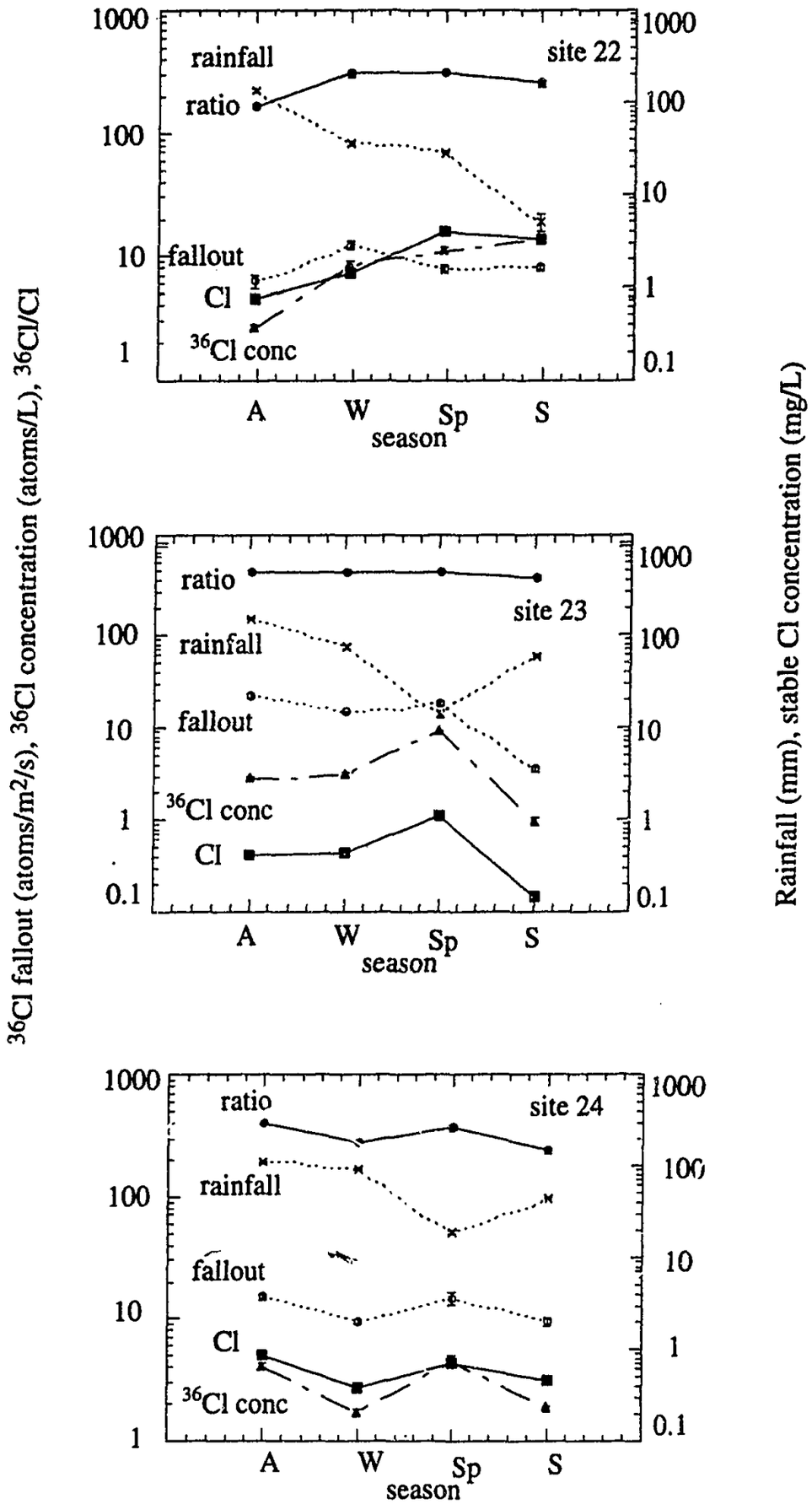

FIGURE 6.15 continued

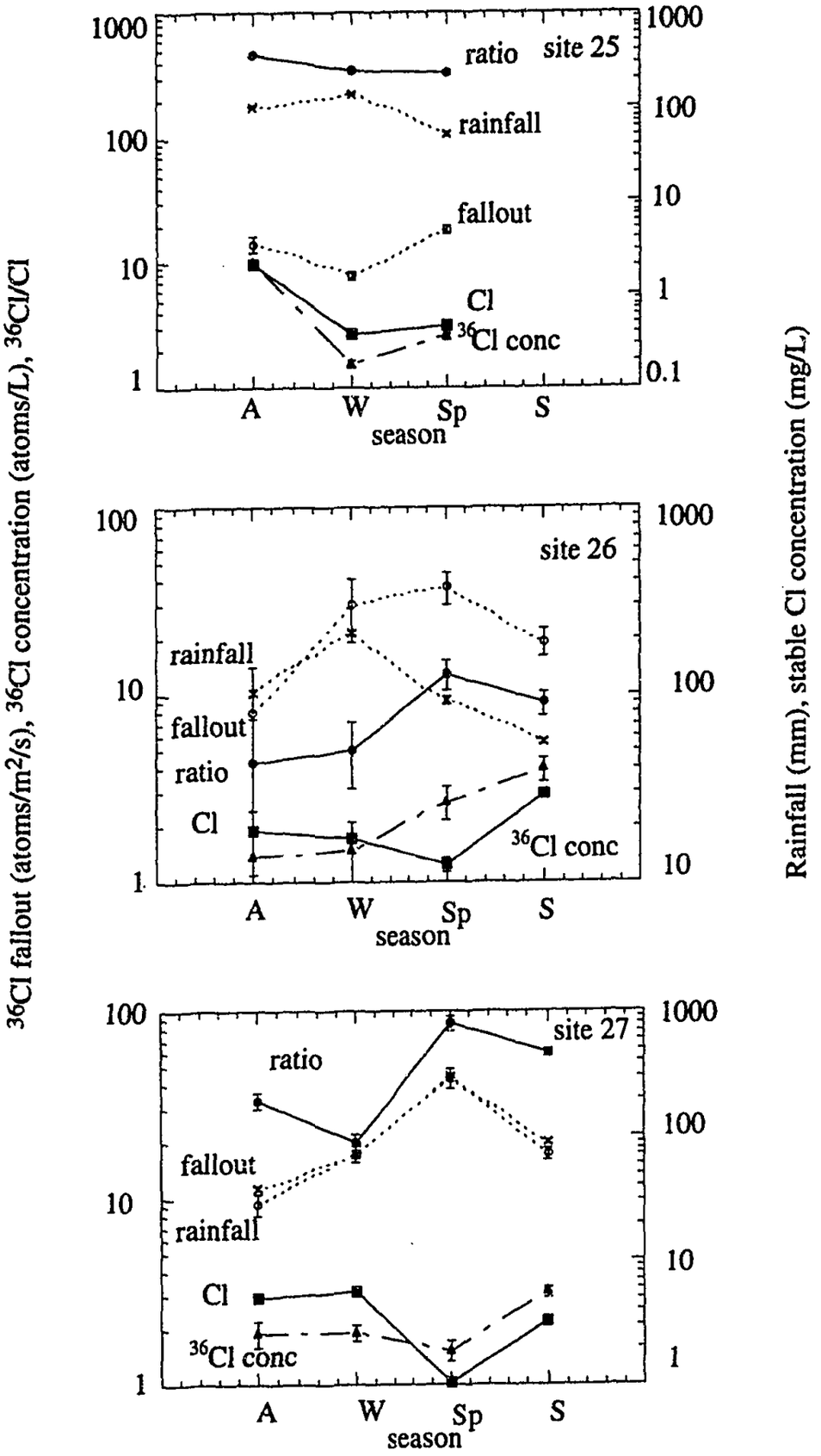

FIGURE 6.15 continued

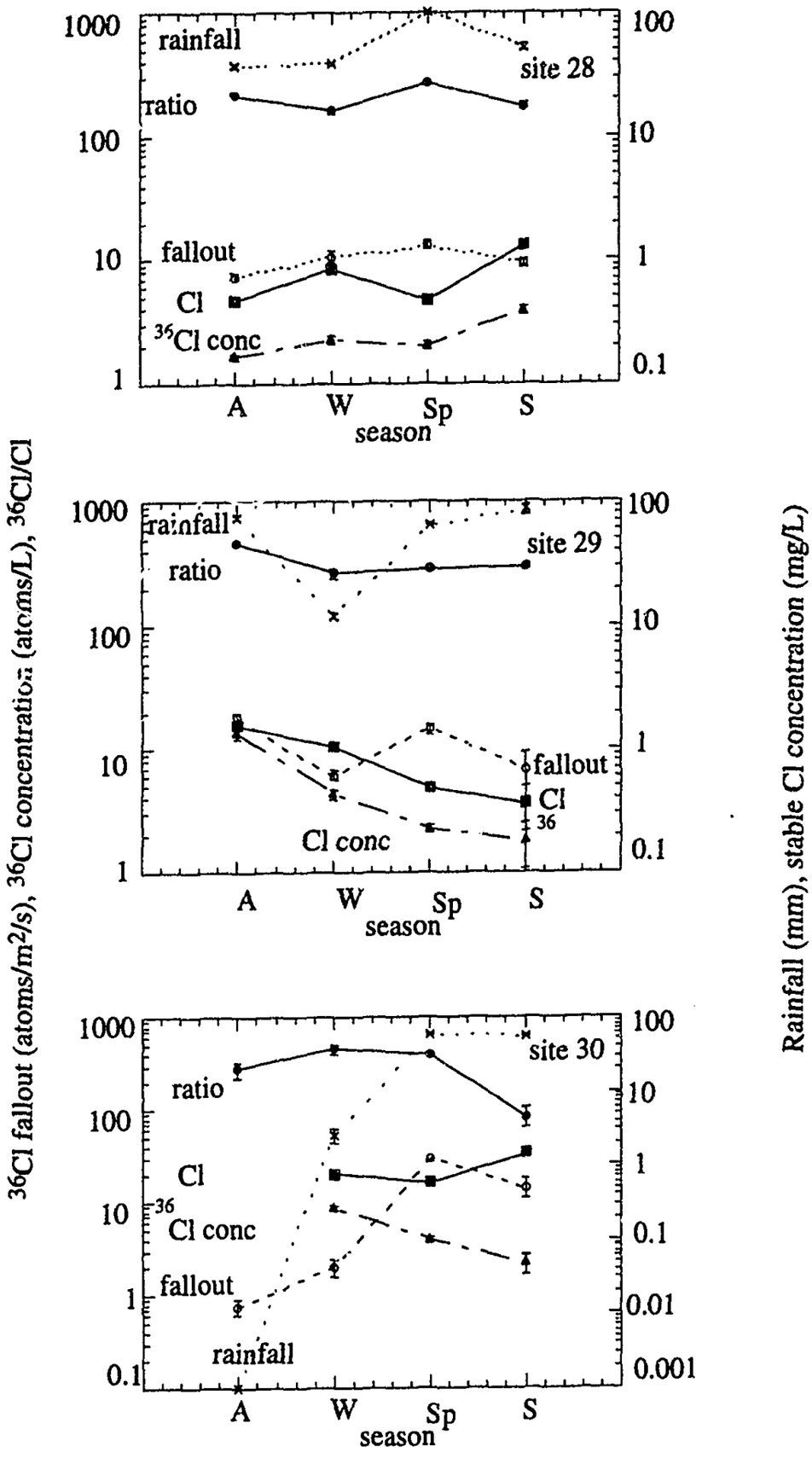

FIGURE 6.15 continued

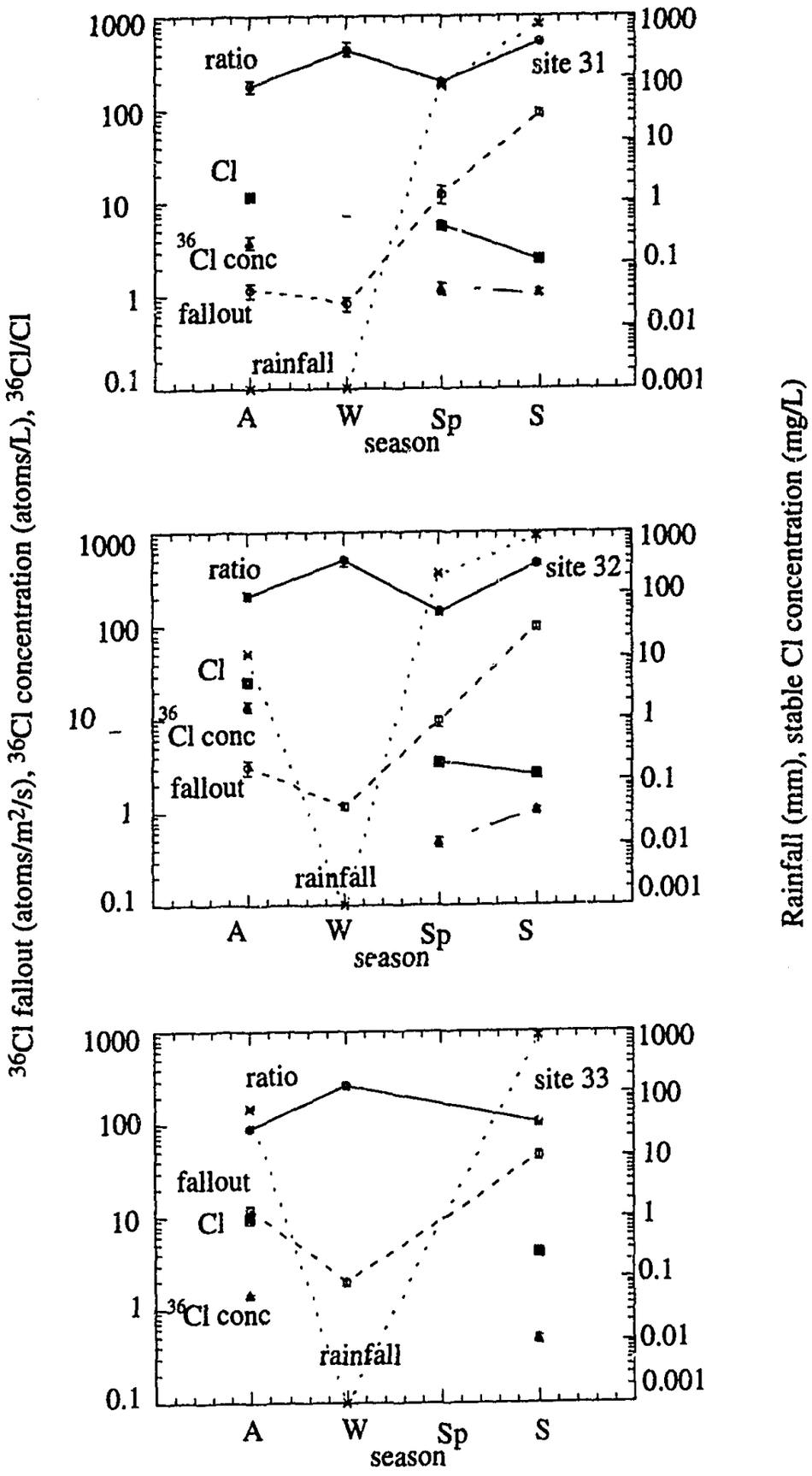

FIGURE 6.15 continued

Chlorine-36 Fallout

The general seasonal trends displayed by ^{36}Cl fallout can be seen in Figure 6.16 which shows the mean ^{36}Cl fallout for each season for sites along the WE array, and northern and southern sections of the SN array. The WE and southern section of the SN array display maximum fallout during spring. High spring fallouts are in accordance with the findings of Hainsworth et al (1994) for rainfall in Maryland, USA (latitude 38°N). It was suggested that this enhanced fallout may be due to an increase in transfer of stratospheric air to the troposphere that occurs as the tropopause rises during spring to its maximum height during mid-summer (Reiter 1975). The elevated tropopause allows transfer of stratospheric ^{36}Cl as well as the penetration of cosmic rays into the troposphere, increasing the production of tropospheric ^{36}Cl. If this mechanism were the sole cause of enhanced $^{36}Cl/Cl$ ratios, it is expected that summer ratios would also be high, which is not observed. The same behaviour for summer fallouts was observed by Hainsworth et al (1994) who were equally puzzled by this inconsistency.

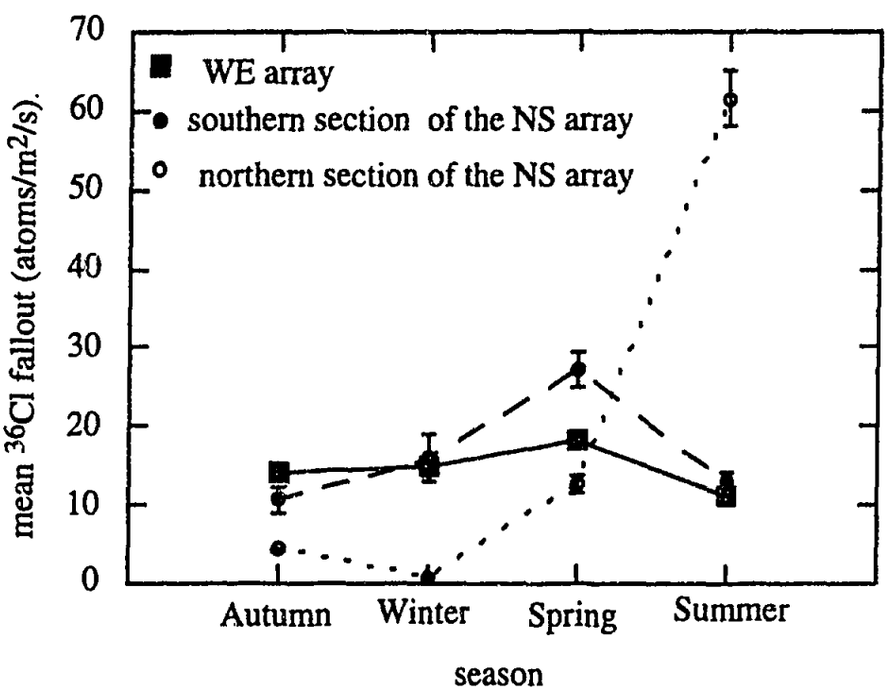

FIGURE 6.16 Mean ^{36}Cl fallout for each season along the WE array, northern section of the SN array and southern section of the SN array. Maximum fallout occurs during spring on the WE and southern section of the SN array, reflecting the change in tropopause height during spring. Maximum fallout occurs during summer on the northern section of the SN array, reflecting direct entrainment of stratospheric ^{36}Cl during convective cumulus activity associated with the monsoon.

The northern section of the SN array displays maximum fallout during summer. However, the fact that high fallouts during summer are restricted to the northern

section of the SN array where the monsoon dominates, suggests that raising of the tropopause during summer is not the main cause of enhanced summer fallout. Instead, entrainment of stratospheric air during convection may be invoked (Reiter 1975). Equatorial Indonesia is known as a fountain region where troposheric air is injected into the stratosphere (Newel and Gould-Stewart 1981), so that tall cumulus clouds exclusively generated near Indonesia sometimes penetrate above the tropopause allowing exchange between the troposphere and the stratosphere (Danielsen 1982, Kley et al 1982).

Rainfall Amount Versus Fallout

In many instances, rainfall amount and fallout variations with season follow similar trends, eg. sites 16-19 (Cliff Head to Iowna) on the WE array, and all sites along the SN array (Figures 6.15).

The positive correlation between rainfall and fallout can be seen in a plot of the two variables for the complete data set (Figure 6.17a). The linear correlation coefficient is 0.47. The dependence of the relationship on array is shown by the difference in correlation when data from the two arrays are separately analysed. Data for the SN array shows a higher correlation coefficient (Figure 6.17b) than data from the WE array (Figure 6.17c).

The more distinct positive relationship between rainfall and fallout displayed by the sites from the SN array most likely reflects the extreme rainfall regimes that sites along this array experience (i.e. nil rainfall in the northern half of the array during winter, and up to 800 mm during summer). Rainfall along the WE array is less variable over time so that the influence of rainfall on fallout appears to be less dramatic. The mechanism for the high fallout along the northern section of the SN array during summer has been discussed above in terms of high-reaching cumulus convective activity.

Sites 20 -25 (Barrambie to Everard Junction) along the WE array do not display a sympathetic trend between rainfall and fallout with season (Figure 6.15). The similarity in trends displayed by fallout, Cl concentration and/or ratio suggest that at these sites rainfall does not control fallout of ^{36}Cl. Instead the supply of ^{36}Cl and Cl (where the sympathetic trends between ratio and Cl suggest the two are sourced from a similar process) is more dominant.

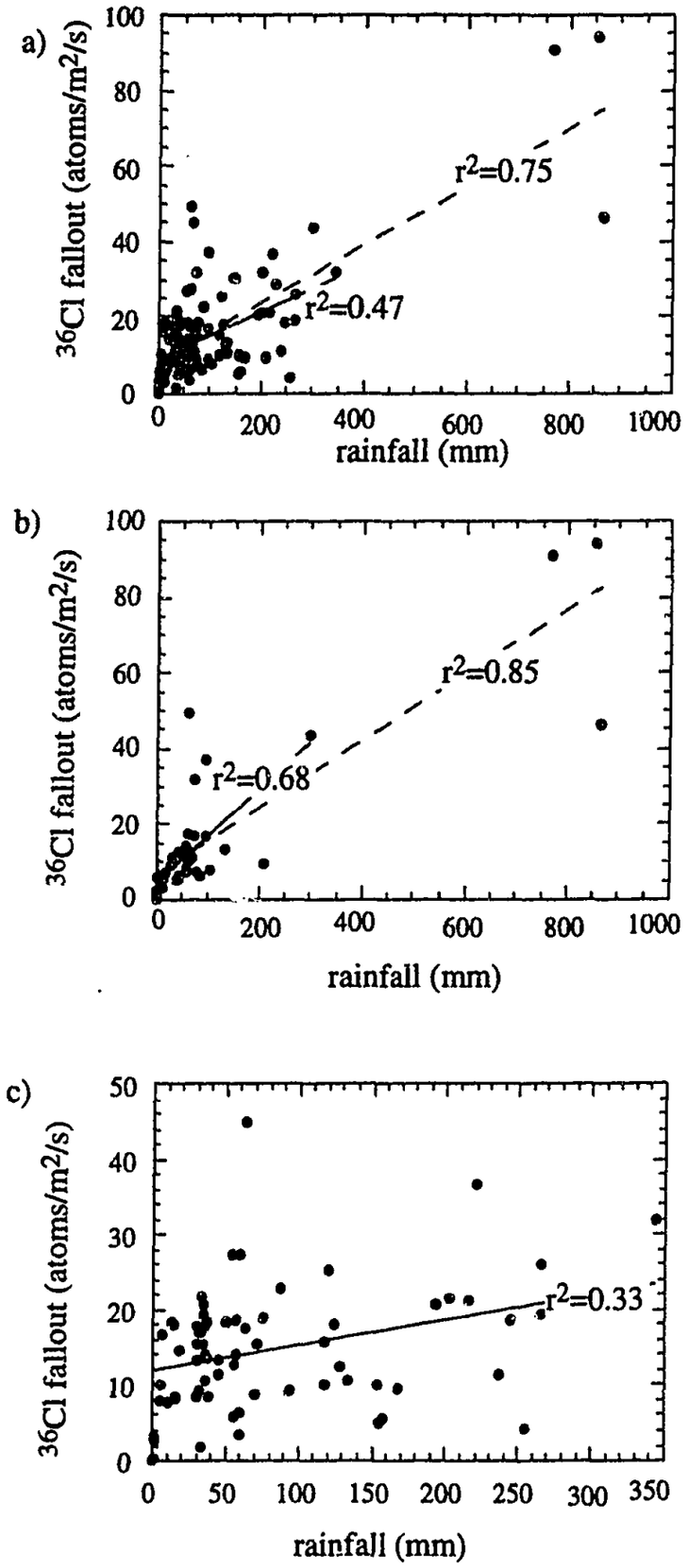

FIGURE 6.17 Fallout of ^{36}Cl versus rainfall amount. a) WE and SN data sets, b) SN dataset, c) WE data set. For figures a and b, full line is the correlation for data with rainfall greater than 700 mm removed and the dashed line is the correlation for all data.

Rainfall Amount Versus ^{36}Cl Concentration

Figure 6.18 shows an inverse relationship between rainfall amount and ^{36}Cl concentration of precipitation. This is in agreement with the behaviour displayed by the major-element concentrations and rainfall amount described in Chapter 5. At coastal localities, ^{36}Cl concentration and stable Cl concentrations show similar trends, but this disappears at non-coastal localities. The relationship between ^{36}Cl and rainfall amount will be discussed further in the Discussion (Section 6.6).

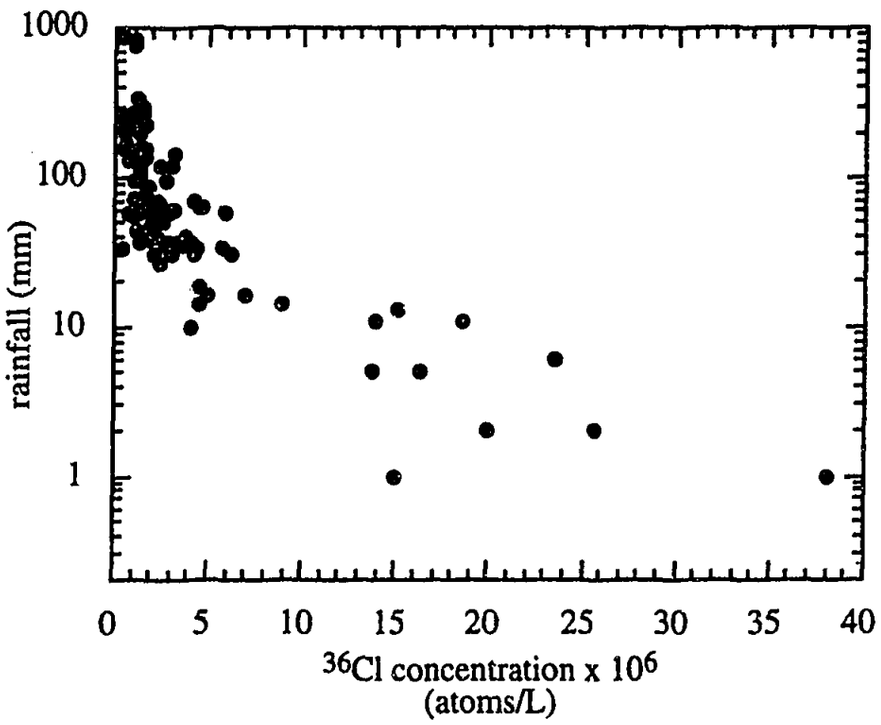

FIGURE 6.18 Rainfall versus ^{36}Cl concentration for all data. The negative correlation displayed between rainfall and ^{36}Cl concentration is in agreement with the behaviour displayed between the major-element concentrations and rainfall amount in Chapter 5.

$^{36}Cl/Cl$ Variations

The seasonal trends displayed by the $^{36}Cl/Cl$ ratio and the stable Cl concentrations of precipitation in Figure 6.15 show variable patterns: sympathetic (eg. high ratios and high Cl, or low ratios and low Cl) and antipathetic (eg. low ratios and high Cl or high ratios and low Cl). The sympathetic trends represent changes in the supply of ^{36}Cl and Cl which have the same magnitude of effect on both species. Conversely, the antipathetic relationships represent independent changes in the supply of ^{36}Cl and Cl. Low ratios and high Cl compositions suggest a supply of stable Cl that has a low ^{36}Cl composition. High ratios and low Cl suggest a supply of Cl that has a high ^{36}Cl composition. Figure 6.19 displays a schematic representation of the processes

that may affect the $^{36}Cl/Cl$ ratio. The following discussion suggests possible explanations for the seasonal variations in $^{36}Cl/Cl$ ratios.

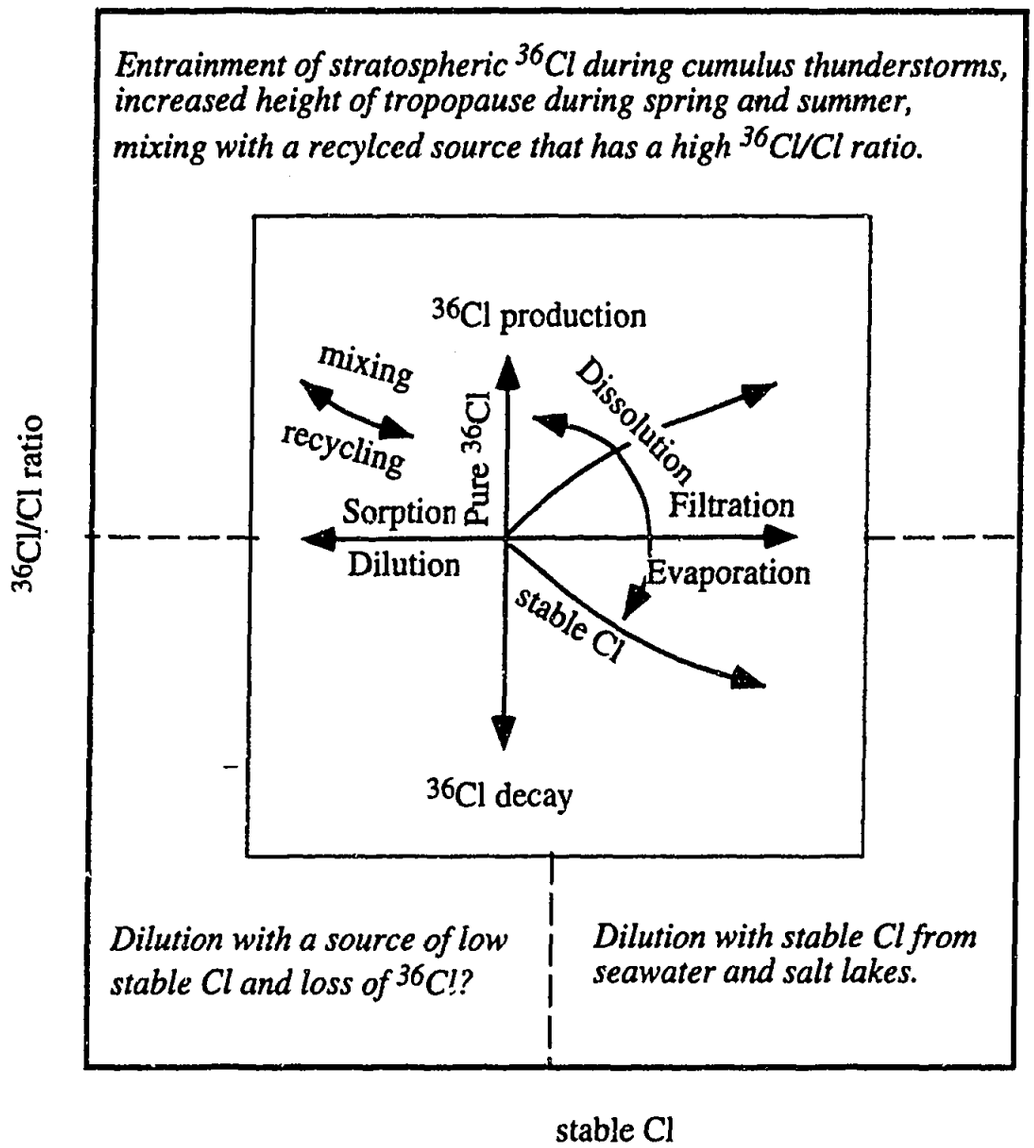

FIGURE 6.19 Schematic diagram of the processes that control the distribution of ^{36}Cl in the environment. Italics describe processes relevant to ^{36}Cl in precipitation.

Low ratios

Low $^{36}Cl/Cl$ ratios that occur in association with high Cl concentrations represent precipitation that has been diluted with Cl with negligible or significantly lower ^{36}Cl composition. The two major sources of this Cl for the present sampling program are seawater and salt-lake material.

a) Seawater

Chapter 5 showed that sites along the WE and SN arrays displayed major ion ratios (eg. Cl/Na, SO_4/Na, Mg/Na) characteristic of seawater during certain seasons.

These seasons of influx of seawater could be tied into the prevailing rain producing synoptic processes described in Chapter 2. The coastal sites 16 (Cliff Head) and 26 (Port Lincoln) displayed seawater ratios throughout most of the year; all sites along the WE array displayed seawater ratios during winter 91 and sites 16 to 21 (Yeelirrie) during winter of 1992.

Low $^{36}Cl/Cl$ ratios and high Cl concentrations are exhibited by the coastal sites 16 and 26 throughout the year, by sites 17 (Morawa) to 20 (Barrambie) along the WE array during winter, and by sites 27 (Gawler Ranges) and 28 (Wintinna) along the SN array during winter. Thus seawater Cl is acting to decrease the $^{36}Cl/Cl$ composition of precipitation at these sites during these times.

b)Salt Lakes

An additional source of Cl that acts to dilute $^{36}Cl/Cl$ ratios at non-coastal localities may be Cl of salt lake origin. Salt lakes are especially common on the WE array and there are a number of salt lakes that may influence the $^{36}Cl/Cl$ ratio of precipitation at inland sites of the WE array (Figure 6.20). There are a number of instances where low ratios and high stable Cl compositions of rainfall can be correlated with surface wind directions that support influx of Cl from a salt lake to a collection site. These are summarised in Table 6.2 and include :

1) Site 20 (Barrambie) during summer; the predominant frequency of surface wind directions at Meekatharra for each summer season are from the southeast (Appendix H) and Lake Mason is situated 30 km towards the east-southeast of the collector site.

2) Site 21 (Yeelirrie) during summer; the predominant frequency of surface wind directions at Yeelirrie are northeast-east-southeast and Lake Way lies 50 km to the northeast of collector 21.

3) Site 24 (Gunbarrel) and 25 (Everard Junction) during winter of 92; the prevailing wind directions at Giles are southeast-south and north and Lake Gillen is located 100 km to the southeast of collector 24 and Lake Breaden is located 100 km to the southeast of site 25.

It should be noted that there are numerous small unmapped salt lakes throughout Western Australia which may also supply stable Cl to the collectors. In addition, the presence of recycled salt in soils may also be a source.

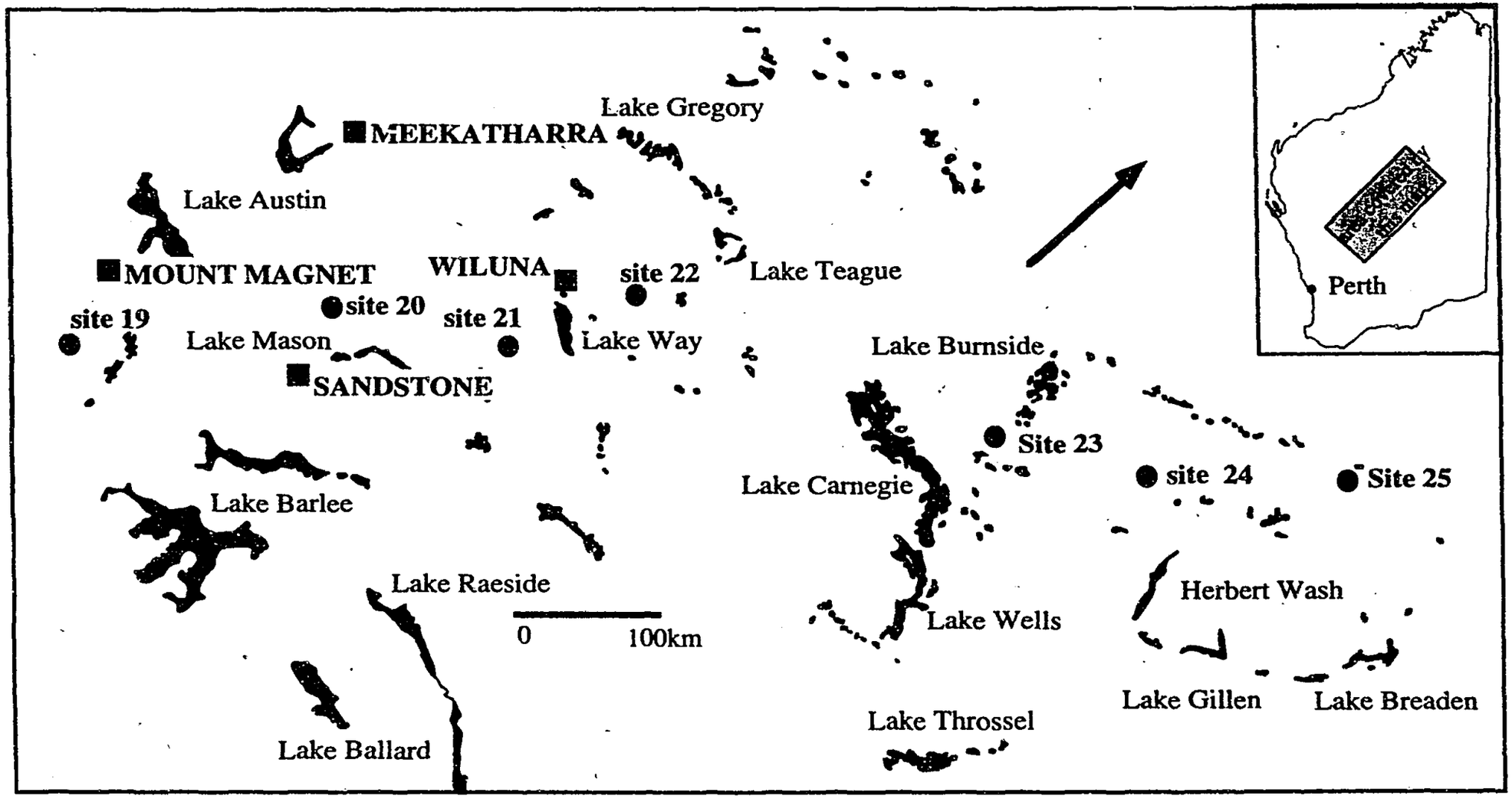

FIGURE5.20 Salt Lakes on the WE array. Circles are sample sites. Squares are Met stations. Location of the area is shown in the inset.

TABLE 6.2 Mean wind direction at sites along the WE array displaying low $^{36}Cl/Cl$ ratios and high stable Cl concentrations, and the salt lakes that may be a source of stable Cl.

Site	Met Station	Season	Wind direction	Lake
20	Meekatharra	summer 91	E-SE	Lake Mason
20	Meekatharra	summer 92	E-SE	Lake Mason
21	Yeelirrie	summer 91	NE-E-SE	Lake Way
21	Yeelirrie	summer 92	NE-E-SE	Lake Way
24	Giles	winter 92	SE-S	Lake Gillen
25	Giles	winter 92	SE-S	Lake Breaden

The $^{36}Cl/Cl$ ratios and stable Cl concentrations at site 23 (Carnegie) do not suggest that Lake Carnegie, a major salt lake located 100 km to the southwest of site 23, influences the $^{36}Cl/Cl$ ratio. This makes sense when the surface wind directions at Carnegie are considered. The predominant surface wind direction is never from the southwest at Carnegie (Appendix H).

Chivas et al (1994) reported increasing $^{36}Cl/Cl$ ratios, in halite, from modern salt lakes in Western Australia with increasing distance from the coast. This reflects the trend shown by the $^{36}Cl/Cl$ ratios of precipitation and increasing distance from the coast (although at lower levels). The relationship between precipitation and salt lake $^{36}Cl/Cl$ ratios suggests that the main source of stable Cl to the Western Australia landscape is meteoric. Chivas et al (1994) used this to calculate a residence time of ~1 Ma for Cl in the Australian landscape.

High ratios

High ratios of $^{36}Cl/Cl$ are observed at most sites during spring. For coastal sites on the WE array (sites 16 to 18) this is associated with high stable Cl concentrations. At inland sites on the WE array, high $^{36}Cl/Cl$ ratios are observed with low stable Cl concentrations. All sites along the SN array exhibit high $^{36}Cl/Cl$ ratios during spring in association with low stable Cl concentrations. High ratios and/or high fallouts are observed during summer in some instance, in particular along the northern section of the SN array.

The mechanisms for producing high spring and summer ratios have been discussed earlier in terms of the high ^{36}Cl fallouts during these seasons. During spring high

ratios occur because of the enhanced transfer of stratospheric ^{36}Cl that occurs with tropopause rising during this time. High summer ratios in the north of Australia arise from direct entrainment of stratospheric ^{36}Cl during cumulus convective activity associated with the monsoon. The expected, but unobserved widespread occurrence of high ratios during summer suggests that other localised processes, (such as the supply of stable Cl from local salt lakes) can significantly effect the ratios, as has been shown for sites 20 (Barrambie) and 21 (Yeelirrie) on the WE array.

The supposition by Bird et al (1991) that $^{36}Cl/Cl$ ratios in tropical rainfall should be low because of the anticipated high stable Cl fallout due to very high monsoonal rainfall deriving moisture from oceanic areas to the north of Australia, is not true for the northern section of the array. Ratios of approximately 400 x 10^{-15} are measured at sites 30 (Tennant Creek) to 32 (Katherine) for summer 1993. Even for the near-coastal locality 33 (Kapalga) the measured ratio of ~100 x 10^{-15} is significantly greater than ratios observed at a similar distance (50 km) from the southern and western coasts.

The Relationship Between ^{36}Cl and Major-Element Concentrations

The generally accepted process of incorporation of ^{36}Cl into rainfall involves production of ^{36}Cl in the stratosphere, movement into the troposphere, mixing with stable Cl of marine origin within the troposphere and deposition as rain within one week of entry to the troposphere. It has been shown here that an inverse relationship exists between rainfall amount and ^{36}Cl concentration (Figure 6.18). In addition, there is a lack of correlation between ^{36}Cl and stable Cl concentrations (Figure 6.15). For the above process to control the movement of ^{36}Cl from the stratosphere to the troposphere and removal from the troposphere, a correlation should be seen between ^{36}Cl and stable Cl concentrations. Thus a discrepancy appears to be present.

To investigate this discrepancy further, a comparison of the ^{36}Cl concentrations with major-element concentrations was carried out. Table 6.3 shows the correlation coefficients between ^{36}Cl and major elements described in Chapter 5. Of note is that ^{36}Cl does not show a high correlation with Cl, but instead shows a strong affinity with NO_3 and to a lesser extent SO_4 and K. A multivariate analysis of the variations displayed by the major elements, ^{36}Cl and rainfall (Figure 6.21) sees ^{36}Cl grouping with NO_3, SO_4, K and inversely with rainfall amount. The correlation between ^{36}Cl and NO_3 concentration has implications about the phase (gaseous or aerosol) of ^{36}Cl

before its incorporation into rainfall. This is expanded in the Discussion (Section 6.8).

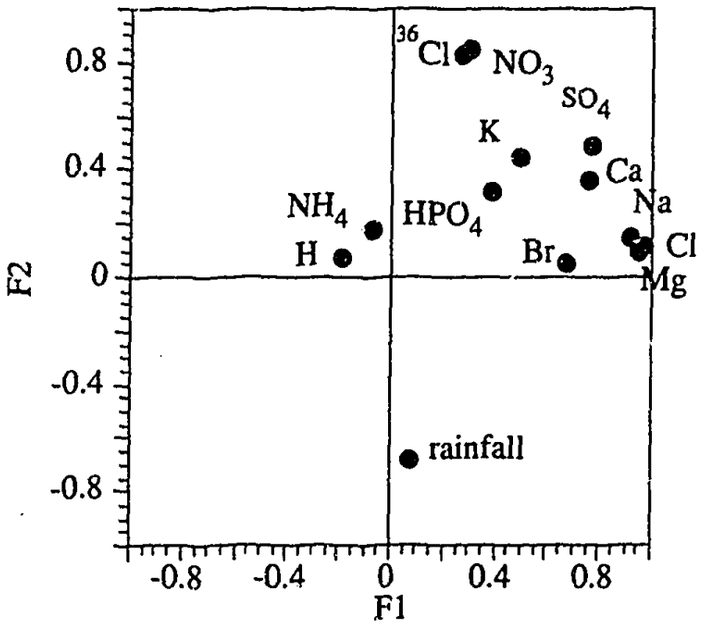

FIGURE 6.21 Factor loading plot for major element and ^{36}Cl concentrations (atoms/L). ^{36}Cl plots close to NO_3, near the F2 axis, not with stable Cl, near the F1 axis.

TABLE 6.3 Correlation coefficients between major element ions, ^{36}Cl fallout and rainfall amount. Bold values highlight coefficients of greater than 0.6. Note that ^{36}Cl has a high correlation with NO_3 and not with Cl or Na.

	H	Cl	SO_4	NO_3	HPO_4	Na	K	NH_4	Ca	Mg	^{36}Cl	rain
H	1.00	.02	-.031	.013	-.12	.08	-.07	-.12	-.06	.03	-.13	-.04
Cl		1.00	**.83**	.14	.55	**.97**	**.73**	.45	**.81**	**.98**	.27	-.06
SO_4			1.00	.57	**.65**	**.90**	**.81**	.58	**.79**	**.86**	**.69**	-.18
NO_3				1.00	.37	.23	.42	.30	.35	.22	**.84**	-.21
HPO_4					1.00	.52	**.88**	**.93**	.58	.59	.50	-.13
BR						.41	.22	.12	.26	.30	.25	-.02
Na						1.00	**.69**	.41	**.81**	**.97**	.31	-.07
K							1.00	**.82**	**.73**	**.78**	**.62**	-.18
NH_4								1.00	.48	.48	.47	-.12
Ca									1.00	**.85**	.45	-.15
Mg										1.00	.34	-.09
^{36}Cl											1.00	-.27
rain												1.00

Dry Deposition

The measurement of $^{36}Cl/Cl$ ratios in samples that showed nil rainfall are an opportunity to investigate the extent of dry deposition of ^{36}Cl to particular sites along each array. Table 6.4 lists the fallout for dry samples compared with the total fallout at the site of dry deposition over the entire sampling period (excluding summer monsoonal fallout, which has been shown to be anomalously high). As the number of measurements differs between sites, the total ^{36}Cl fallout for each site is averaged. Table 6.4 shows that dry deposition contributes less than 50% of the total wet and dry fallout per sample collection period for each of the northern sites of the SN array which typically experience nil rainfall during the winter seasons.

TABLE 6.4 Percentage of ^{36}Cl fallout attributable to dry deposition at sites that experienced nil rainfall during any part of the sampling program.

site	^{36}Cl (atoms/m^2/s) wet + dry	^{36}Cl (atoms/m^2/s) dry	% of ^{36}Cl in dry deposition
30 Tennant Creek	14.77 n=4	0.45 n=2	3±0.5
31 Dunmarra	5.39 n=5	0.84n=3	16±1.9
32 Katherine	4.06 n=4	1.87 n=2	46±10.8
33 Kapalga	5.38 n=3	1.94 n=2	36±6.0

The estimates of dry deposition for the present investigation are comparable with those of Hainsworth (1994) for a site in North America (latitude 38°N). There, dry deposition was seen to range from 19% to 40%. While it is interesting to compare the results of the present study with the results of Hainsworth, the methods used to compare wet and dry deposition in these two studies differ. Hainsworth compared a wet-only with a bulk-deposition collector over three collection periods. In that study uncertainties were introduced by missing wet-only precipitation values arising from equipment malfunction. The present investigation provides an unambiguous assessment of dry deposition, by comparing the ^{36}Cl composition of samples containing precipitation (and therefore representing both wet and dry deposition) with samples of nil rainfall, representing dry deposition only.

It is unfortunate that the only measurements of dry deposition occur along the northern section of the SN array. This section of the SN array experiences different rainfall regimes and climates to the southern section of the SN array and the WE array. Thus, caution should be used when applying the results of dry deposition from the northern section of the SN array to other sample sites. However, assuming

that dry deposition of ^{36}Cl is more important during periods of low precipitation rates, the results from the present investigation may be considered as the maximum amount of dry deposition, since they are associated with nil rainfall.

Table 6.5 compares $^{36}Cl/Cl$ ratios with Ca/Na ratios for the dry samples collected from the northern section of the SN array. Simpson and Herczeg (1994) suggested that Ca/Na ratios of greater than 1 denoted input of resuspended soil material to precipitation. The discussions in Chapter 5 noted that Ca/Na ratios of greater than 1 were only observed in samples from the SN array, during periods of nil precipitation. Sites 32 (Katherine) and 33 (Kapalga) appear to be affected by resuspended soil material during winter seasons. The high Ca/Na and $^{36}Cl/Cl$ ratios observed during winter 1993 at site 33 may suggest a recycled soil source with high $^{36}Cl/Cl$ ratio.

The estimates of dry deposition from Table 6.4 represent upper limits. Thus wet deposition is more significant to the fallout of ^{36}Cl to the northern section of the NS array even when the summer monsoonal periods are not considered. This, and the positive relationship between rainfall amount and ^{36}Cl fallout suggests that wet deposition is the most significant mechanism by which ^{36}Cl is removed from the atmosphere.

TABLE 6.5 $^{36}Cl/Cl$ ratios, stable Cl concentrations and Ca/Na ratios dry deposition samples compared to mean $^{36}Cl/Cl$ ratios and stable Cl concentrations.

site	mean $^{36}Cl/Cl$ $*10^{-15}$	season	$^{36}Cl/Cl$ $x10^{-15}$	Ca/Na
30 Tennant Creek	260±27	winter 92	133	0.30
30		autumn 93	278	0.57
31 Dunmarra	378±25	winter 92	734	0.24
31		winter 93	446	0.16
31		autumn 94	181	0.41
32 Katherine	232±22	winter 92	201	1.58
32		autumn 92	152	0.56
33 Kapalga	179±11	winter 92	155	0.48
33		winter 93	367	1.23

6.6 DISCUSSIONS

Comparison of Measured Fallouts with Predicted Fallouts

As discussed in Section 6.3, the range of latitudes sampled in this project enables us to test the predictions of latitude dependence of ^{36}Cl fallout (Lal and Peters 1967, Andrews and Fontes 1992). The data from this investigation fit the general shape of the predicted curve, but the curve underestimates the amount of fallout. Instead the best fit to the data is obtained by scaling the predicted curve by a factor of 1.4 (the three anomalous points from the northern section of the SN array are removed for this fit) as shown in Figure 6.22. Thus, a revised mean fallout of 15.4 atoms/m^2/s is suggested from this investigation.

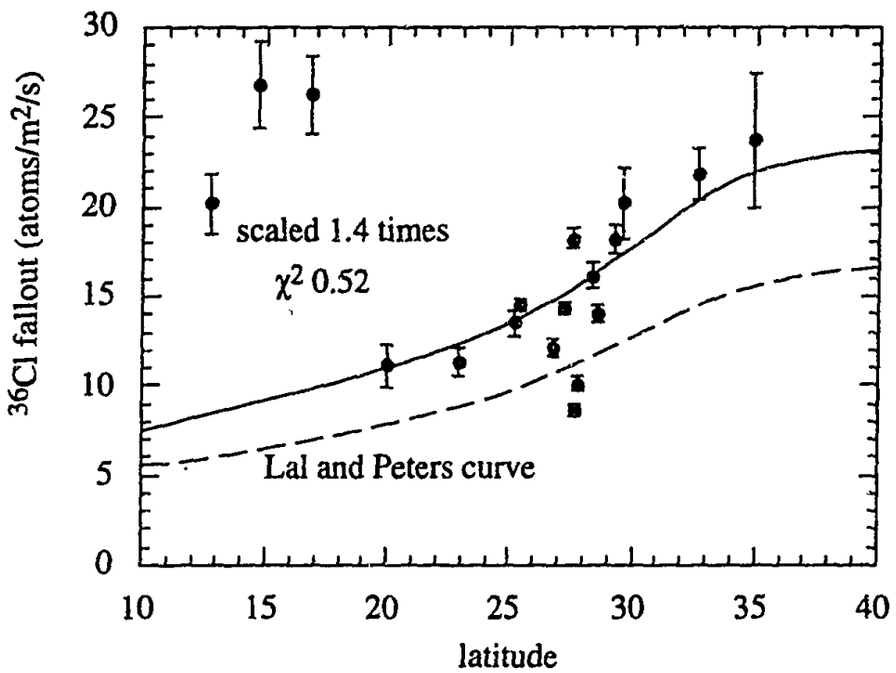

FIGURE 6.22 Mean ^{36}Cl fallout as a function of latitude and the predicted curve of Lal and Peters (1967) scaled by 1.4 times. The scaled curve is the solid line, the unscaled curve is the dashed line. The $\chi 2$ represents the degree of fit each curve shows to the data. The χ^2 for the data to the unscaled Lal and Peters curve is 2.

Solar Activity Effects

Lal and Peters (1967) discussed the dependence of the flux of cosmic rays to the Earth's surface upon solar activity and how the predicted curve needs to be adjusted depending on the 11-year sunspot cycle. At polar regions, cosmic ray fluxes decrease by 30% from a sunspot minimum to maximum. Middle latitudes see a decrease of 25% from sunspot minima to maxima, while the equator sees a decrease of 7%. The curve of Lal and Peters (1967) was calculated for 1948-1949, which represents a sunspot minimum (Figure 6.2). Thus this curve represents maximum

fallout during the 11-year sunspot cycle. The present investigation encompassed a sunspot maximum in 1991 and a reduction in sunspot activity through to 1994. The change in solar activity cannot be used to explain the higher fallouts observed during the present study, since a reduction in fallout is expected with the maxima in sunspot activity.

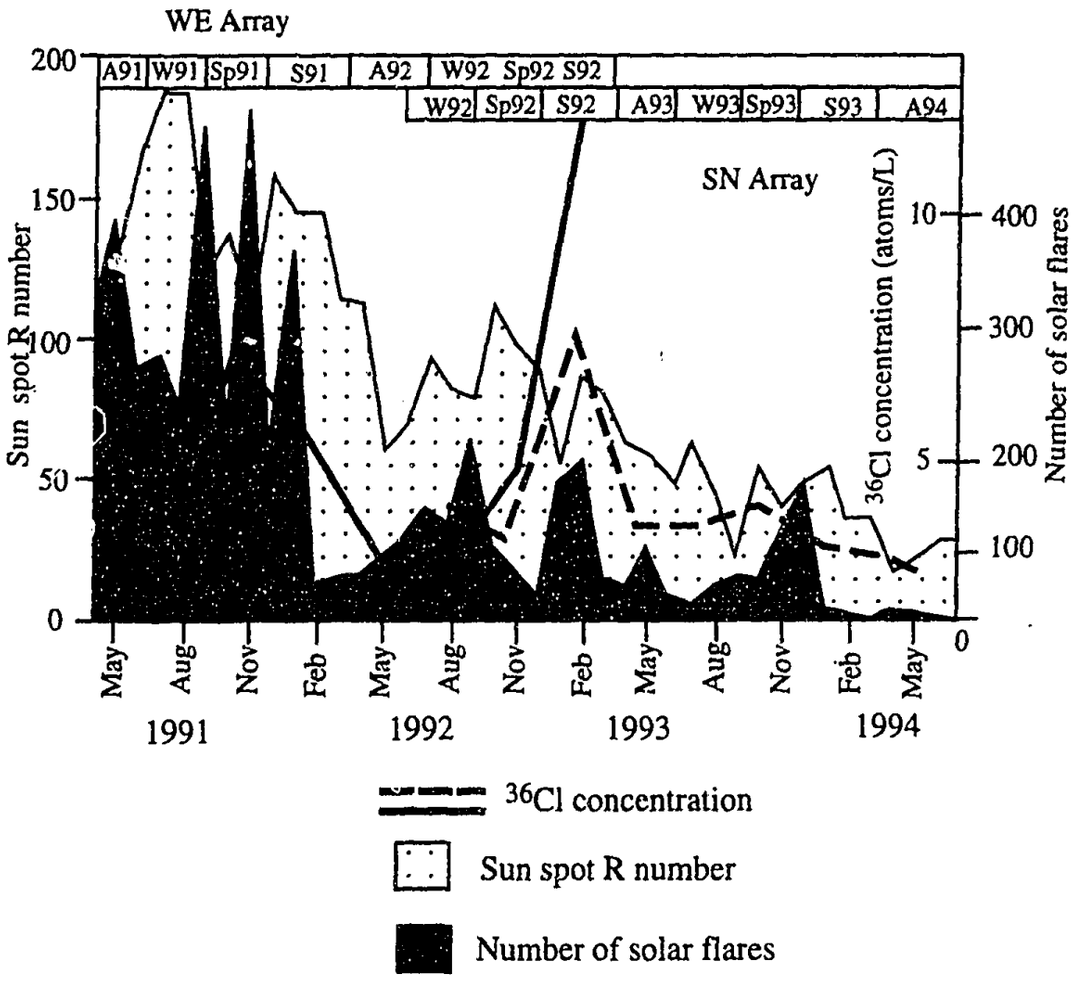

FIGURE 6.23 Sun spot R numbers and the number of solar flares recorded during the sampling program, compared with the ^{36}Cl concentration of precipitation collected at latitude 12.8°S (site 18 of WE array and site 28 of SN array). R numbers = (# of sun spot groups) - # of sun spots) measured by the National Solar Observatory, Sacramento Peak, New Mexico. Solar flare numbers recorded by BATSE (Burst and Transient Source Experiment) from the Gamma Ray Astronomy Group, NASA.

The relationship between solar activity and ^{36}Cl fallout for the present sampling program is shown in Figure 6.23. Sunspot R numbers and the number of solar flares are compared with ^{36}Cl concentration measured in rainfall at latitude 13°S (i.e. site 18 on the WE array and site 28 on the SN array). Sunspot R numbers were measured by the U.S. National Solar Observatory, Sacramento Peak and the number of solar flares was measured by BATSE, NASA. An overall trend of decreasing

sunspot R number and solar flare number is seen as the collection program progresses. However ^{36}Cl concentration of rainfall remains constant (excepting a peak on both arrays during summer 1993). An inverse relationship between solar activity and cosmic ray flux has been demonstrated by ^{10}Be in ice-cores from Greenland and Antarctica (Beer et al 1991). These ice cores have been compared with ^{14}C from tree-ring records to extend the record of solar activity back in time to 2,500 years BP. However it can be seen in Figure 6.23 that the inverse relationship does not appear to be recorded by ^{36}Cl in rainfall from the present investigation. This suggests that transport and depositional processes control the fallout of ^{36}Cl to the Earth's surface on the time scales used in this investigation (i.e. 3 months), rather than changes in solar activity. This is consistent with results from the Camp-Century ice core (Elmore et al 1987) where a correlation between sunspot activity and ^{36}Cl concentration could only be seen after the data had been mathematically smoothed.

Atmospheric Implications

Global Fallouts

The mean fallout of ^{36}Cl to the Earth's surface in the latitudes investigated in this research agree with the general form of the fallout curve predicted by Lal and Peters (1967), but are a factor of 1.4 greater. The mean global fallout calculated from this research is 15.4 atoms/m^2/s. While higher than the predicted mean global fallout of Lal and Peters (11 atoms/m^2/s) this is much lower than the fallouts measured from northern hemisphere investigations, eg. Greenland ice-core data measures a pre-bomb mean global fallout of 30-60 atoms/m^2/s i.e. 3 to 5 times greater than predicted (Suter et al 1987). Hainsworth (1994) and Knies (1994) measured fallouts at 40°N of 40-50 atoms/m^2/s (4 times greater than predicted). However, the fallout measured in this project is similar to that deduced from the only published measurements of ^{36}Cl concentrations in modern precipitation from the southern hemisphere. From Antarctic ice (Table 6.1) a fallout of between 10-14 atoms/m^2/s can be deduced.

This work suggests that the fallout of ^{36}Cl to the Earth's surface in the southern hemisphere is lower (by approximately 3 times) than in the northern hemisphere. Some possible reasons for this are:

a) the production of ^{36}Cl in the northern hemisphere stratosphere is greater than in the southern hemisphere stratosphere.

Such a situation would require a greater flux of cosmic rays to the northern hemisphere and/or a greater concentration of target ^{40}Ar. This is not possible or observed. Cosmic ray fluxes are affected by the Earth's geomagnetic field, but the geomagnetic field is symmetric about the geomagnetic equator. The main components of the atmosphere i.e. N_2, O_2, Ar and CO_2 are mixed in constant proportions up to the mesopause (Warneck 1988).

b) there is an additional supply of ^{36}Cl in the northern hemisphere that does not exist in the southern hemisphere.

This supply may include output from nuclear reactor and processing activities, or recycled ^{36}Cl, remnant from the bomb testing of the 1950s. The density of nuclear installations in North America and Europe is higher than in the southern hemisphere. An investigation of the release of ^{36}Cl to the atmosphere at the Chalk River Laboratories in Ontario (Milton et al 1993), found that only small quantities of ^{36}Cl were released during reactor operations. The dispersion of ^{36}Cl (as measured in rainfall and snow) was dependent on wind direction, with most of the estimated release being deposited locally. Background levels of ^{36}Cl were measured at 140 km from the reactor site. Beasley et al (1992) however, reported that nuclear fuel reprocessing activities at the US Department of Energy's Savannah River Site increased the flux of ^{36}Cl from natural levels of 20-25 atoms/m^2/s by factors of 10 to 20 within 200 km of the site. Measurement of soil cores and groundwaters confirmed the presence of site-derived ^{36}Cl at a similar facility in Idaho (Beasley et al 1990, reported in Beasley et al 1992). The information regarding the atmospheric release of ^{36}Cl from nuclear processing activities appears inconsistent. This inconsistency may simply arise from differences in the magnitude of the operations at the different facilities. A nuclear activity source of ^{36}Cl does not explain the high pre-bomb fallout levels measured in the Greenland ice-cores. The pre-bomb fallouts were measured for 1945 to 1950 (Suter et al 1987), a period before extensive development of nuclear facilities in the northern hemisphere. Thus, while nuclear reactor and processing activities may be important on a local scale, they are not considered to be the main cause of the large difference seen between northern and southern hemisphere fallouts.

Cornett et al (1994) suggest that high fallouts of ^{36}Cl measured in environmental samples from Canada is due to recycling of bomb ^{36}Cl. Phillips et al (1988) compared ^{36}Cl in soil profiles under laboratory and field conditions. They found the movement of ^{36}Cl through the soil profile is dependent upon many conditions

including water content, time, temperature etc. The rate of movement of ^{36}Cl through the soils profile from arid New Mexico was considerably slower than simulated in laboratory experiments. The 1950s bomb spike was retained near the soil surface. Fifield et al (1987) measured the ^{36}Cl in soils from a semi-arid region in South Australia and recorded the bomb spike between 1-1.5 m into the soil.

In order for recycling of bomb-produced ^{36}Cl to influence measurements of ^{36}Cl in precipitation, the ^{36}Cl must reside in the soil surface. While this appears to be the case for New Mexico, experimental studies (Phillips et al 1988) and other investigations (eg. Fifield et al 1987) suggest that the movement of ^{36}Cl through the soil profile is geographically variable. The influence of recycled bomb-produced Cl on the high fallouts of ^{36}Cl measured from the northern hemisphere cannot be discounted. However, a great deal more information regarding the behaviour of ^{36}Cl and soil and the release of ^{36}Cl from soils is required before this possibility can be discussed further.

c) there is greater transfer of ^{36}Cl from the stratosphere to the troposphere in the northern hemisphere.

The review of transfer between atmospheric domains (Section 6.1) showed an asymmetry in the stratosphere-troposphere transfer of ^{90}Sr (Lal 1962), ozone (Fabian and Pruchniewicz 1973) and aerosols (Hitchman et al 1994) between the two hemispheres. Modelling of climate data revealed transfer to be up to 50% greater in the northern hemisphere (Holton 1990). Transfer from the stratosphere to the troposphere occurs at middle-latitudes in association with tropopause gaps (or folding events). Danielsen (1968) suggested baroclinic waves associated with the jet stream enhanced movement of material through the gap region. A global circulation model that incorporates stratospheric-tropospheric transfer (Mote et al 1994) supported this. The asymmetry of transfer between the two hemispheres has been attributed to enhanced lower stratospheric wave driving in the northern hemisphere (particularly during the northern hemisphere winter).

The higher ^{36}Cl fallouts measured in the northern hemisphere are most likely explained in terms of the enhanced transfer of ^{36}Cl from the stratosphere to the troposphere. This occurs in response to the more dynamically active nature of the lower stratosphere in the northern hemisphere, which arises from the difference in orographic and thermal forcing between the two hemispheres.

Revised Estimate of Global Fallout

A mean global ^{36}Cl fallout of 25 to 35 atoms/m^2/s can be calculated. This value incorporates the results from the present investigation (15.4 atoms/m^2/s), estimates from Antarctic ice (10 to 14 atoms/m^2/s, Nishiizumi et al 1979, Finkel et al 1980 and Nishiizumi et al 1983), the higher fallout calculated from measurements of ^{36}Cl in northern hemisphere precipitation (40-50 atoms/m^2/s, Hainsworth 1994 and Knies 1994) and Greenland Ice Core data (30-60 atoms/m^2/s eg. Suter et al 1987). This mean global value is 2-3 times greater than predicted by Lal and Peters (1967). The calculation of production rates is dependent on information pertaining to nuclear reaction cross sections, which for ^{36}Cl production were estimated by Lal and Peters (1967) based upon similar reactions at lower energies than those actually required for the production of ^{36}Cl. It is realised that the estimation of cross-section energies may introduce a variation factor in the production rate calculation of up to two (eg. see Hainsworth 1994).

Phase of ^{36}Cl in the Atmosphere

The behaviour of ^{36}Cl and stable Cl in the atmosphere have been discussed throughout this work. The two species arrive in the atmosphere by very different processes. Chlorine-36 is produced in the stratosphere by cosmic ray spallation of ^{40}Ar, where it exists predominantly as HCl gas. Seawater is the main source of stable Cl to the lower atmosphere. Stable Cl is introduced as an aerosol by breaking waves at the ocean's surface (Erickson and Duce 1988). The bulk of Cl remains associated with large aerosol particles. However, 3-20% is released as gaseous inorganic Cl (Cicerone 1991). The mechanisms of release are not well understood. Numerous workers (including Ericksson 1959, Duce 1969 and Martens et al 1973 to name a few) suggest that Cl release from the aerosol may occur by direct volatilisation of seasalt aerosol that is acidified to low pH by the incorporation of HNO_3 and H_2SO_4. Mechanisms of release of gaseous Cl involving reactions of various N gases with the seasalt aerosol have also been demonstrated (Finlayson-Pitts 1983 and Finlayson-Pitts et al 1989). Keene et al (1990) proposed a photochemical mechanism involving the reaction of O_3 at NaCl surfaces to explain release of Cl in the marine atmosphere. This process produces HCl that can be efficiently rescavenged by the aerosol.

The lack of correlation between ^{36}Cl and seasalt aerosol species such as Na and Cl, and the good correlation between ^{36}Cl and NO_3 concentrations allows us to

speculate about the behaviour of ^{36}Cl from its production in the stratosphere to its deposition at the Earth's surface. In the stratosphere, ^{36}Cl exists predominantly as $H^{36}Cl$ (Wahlen et al 1991). It moves through the tropopause, into the troposphere as a gas. The possible courses of action that may follow are:

a) in the troposphere $H^{36}Cl$ it is scavenged by NaCl aerosol and deposited.

This does not fit our observations as a correlation is not observed between ^{36}Cl, Na and Cl concentrations.

b) in the troposphere, $H^{36}Cl$ remains as a gas and mixes with HCl released by volatilisation of NaCl.

As described above, the volatilisation process only releases less than 30% of Cl contained in NaCl aerosols. The mixed $H^{36}Cl$, HCl and other atmospheric gases such as HNO_3 and H_2SO_4 are then deposited at the Earth's surface. Chapter 2 describes the incorporation of gases and aerosols into cloud drops and raindrops both in and below-clouds. At pH of 4.5 (the typical pH of cloudwater) strong acids (such as HCl and HNO_3) are directly scavenged from the gas phase (Warneck 1988). The correlation observed between ^{36}Cl and NO_3 tends to suggest that ^{36}Cl is directly scavenged from the gas phase before deposition.

Hydrological Implications

The results of this study suggest that on a short timescale (i.e. seasonal), fallout of ^{36}Cl is dependent upon rainfall amount. However, the long-term averages measured in this project are only slightly greater than predicted values. Hydrological investigations generally require estimates of long-term fallouts. Thus this investigation supports the use of scaled predicted ^{36}Cl fallout levels as estimates of inputs of ^{36}Cl to groundwater systems. The Cl concentrations of rainfall from the present investigation display exponential decreases with increasing distance from the coast, as has been shown world-wide. However, it is not possible to characterise the exponential decrease by using regression equations derived from earlier investigations. Thus, this project clearly shows the caution that is required when trying to use a particular regression equation to predict the Cl concentration of rainfall at a given distance from the coast. It is important to recognise that Cl concentration of rainfall is geographically variable. The most effective method of overcoming uncertainties due to Cl concentration of rainfall when estimating $^{36}Cl/Cl$

input to groundwater systems is to undertake a reconnaissance survey of rainfall Cl concentrations.

6.7 SUMMARY

The fallout of ^{36}Cl to the Earth's surface at the latitudes sampled in this project agree with the general form of Lal and Peters (1967) but are 1.4 times greater. The mean fallout of ^{36}Cl calculated for west, north and south Australia is 15.4 atoms/m^2/s, comparable to that calculated for samples of Antarctic ice, but 3 times lower than measured in the northern hemisphere. The lower southern hemisphere fallout rates reflect the lower rates of transfer of stratospheric air to the troposphere in the southern hemisphere. A mean global fallout that incorporates the high fallouts measured in northern hemisphere precipitation of 25-35 atoms/m2/s can be calculated. This value is 2-3 times greater than predicted by Lal and Peters (1967), suggesting that the cross-section for the cosmic-ray production of ^{36}Cl may be underestimated in their paper.

The spatial pattern of stable Cl deposition to the Australian continent is for decreasing deposition from south to north, reflecting the importance of the southern marine airmasses in the supply of Cl. The northern tropical airmasses play a less significant part in this process. The relationship between Cl deposition and distance from the coast can be explained in terms of a double exponential decay, suggesting that two processes control this relationship. These processes may reflect the enhanced mixing of airmasses moving inland and/or differences in the rate of removal of Cl aerosol and Cl gas from marine and continental airmasses.

The $^{36}Cl/Cl$ ratio of precipitation increases exponentially with increasing distance from the coast. The opposite trend displayed by stable Cl concentrations of precipitation reflects the decreasing influence of stable Cl of marine origin on the $^{36}Cl/Cl$ ratios at inland sites.

Low $^{36}Cl/Cl$ ratios are observed at coastal localities and at inland sites when synoptic conditions favour the transport of seawater aerosols great distances inland (eg. during cold frontal activity). Low $^{36}Cl/Cl$ ratios at inland sites on the WE array reflect the diluting effect of stable recycled Cl from local salt lakes which have low ^{36}Cl contents.

Seasonal variations in ^{36}Cl fallouts and $^{36}Cl/Cl$ show high ratios and fallouts during spring, and at some localities, during summer (i.e. the north of the SN array). These

increased spring ^{36}Cl fallouts are attributed to increased transfer of stratospheric ^{36}Cl to the troposphere that occurs as the tropopause height increases during the warmer months. High fallouts during summer in the north of the SN array may be attributed to the direct entrainment of stratospheric air into cumulus clouds during the monsoonal convection.

Wet deposition appears to be the major process of removal of ^{36}Cl from the atmosphere. Chlorine-36 fallout and rainfall amount can be correlated, particularly along the SN array where extremes in rainfall regimes are experienced. Dry deposition accounts for less than 50% of fallout in the north of the SN array.

Chlorine-36 exists in the stratosphere predominantly as HCl gas (Wahlen et al 1991). The correlation between ^{36}Cl and NO_3 and the lack of any relationship between ^{36}Cl, stable Cl and Na concentrations, suggest that ^{36}Cl is scavenged from the atmosphere as a gas rather than aerosol phase.

Long-term average predictions of ^{36}Cl fallout rates used to predict the input ratios of $^{36}Cl/Cl$ in hydrological investigations should be increased by a factor of 1.4 for the southern hemisphere. A simple correlation between stable Cl concentrations and distance from the coast is not the rule however. While stable Cl concentrations in precipitation display a general exponential decrease with distance, the nature of this relationship is geographically variable, and should be investigated for each study by local direct measurements, a process that is simple and inexpensive.

CHAPTER 7 SUMMARY AND CONCLUSIONS

The major-element and ^{36}Cl chemistry of bulk precipitation collected from 18 sites in remote areas of Australia, over two years at three-monthly intervals, has been assessed. Samples were collected from two arrays: the WE array extended in an west-east direction from the coast of Western Australia south of Geraldton, inland to Warburton in Central Australia, and the SN array, extended in a south-north direction from Port Lincoln in South Australia to Kakadu in the Northern Territory. The work can be divided into two related sections: major elements and ^{36}Cl.

7.1 MAJOR ELEMENTS

The aims of investigating the major-element chemistry of precipitation in this project were to assess the sources of ionic constituents to precipitation, assess the seasonal variations in the supply of these sources and to asses the accession rate of ionic constituents to the Australian landmass. This work also adds to the Australian data base of precipitation chemistry, and provides the background on which interpretation of ^{36}Cl data can be based.

A synoptic classification system described in Chapter 2, was used as a simplified proxy for airmass trajectory analysis, to trace the movement of airmasses associated with rainfall during each collection period. In most cases, rainfall events were associated with synoptic processes involving airmasses of marine origin, in particular cold fronts that sourced airmasses travelling from south of the Australian landmass and tropical events that sourced airmasses from north of Australia. Cold fronts were most active during winter with coastal cold front activity occurring all year round. During winter 1991, cold fronts were seen to penetrate as far inland as 2000 km from the west coast of Western Australia. Tropical events mainly affected the northern half of Australia during summer months, and were seen to extend 1000 km southwards from the north coast. Therefore, it was anticipated that precipitation chemistry across Western Australia in winter and northern Australia in summer would exhibit a strong marine signature.

Data quality checks were performed on the WE and SN data sets to remove samples that were not representative of bulk precipitation deposited over the collection area for the collection time. These checks removed 9% of data from the WE array and 16% of data from the SN array. Large ion imbalances in the SN data set were

attributed to the presence of organic acids, which were unmeasured in this analytical program.

All the ionic species displayed an approximately log-normal distribution of depositional rates. The relative magnitude of species in precipitation was Cl > Na > SO_4 >Ca > NO_3 > Mg > H > NH_4 > HPO_4 > Br, with NH_4 showing locally high concentrations at sites from the north of the SN array. An inverse correlation between ionic species concentrations and rainfall amount was attributed to a "washout" effect during the initial stages of a rain event, the initially concentrated rainfall being diluted as the rain event continued.

All ionic species displayed a decrease in deposition with increasing distance from the coast, with generally lower deposition rates at the north coast compared to the south and west. Hingston and Gailitis (1973) found a similar trend for the south and north of Western Australia. Sites along the WE array and southern section of the SN array experienced maximum deposition of all ionic species during winter and minimum deposition during summer. Sites along the northern section of the SN array showed the opposite relationship with maximum deposition occurring during summer. These differences can be correlated with seasonal differences in rainfall amount.

Three main sources/processes were found to control the chemistry of precipitation collected in the sampling vessels: a mixed seawater/continental source represented by simultaneous variances between Cl, Mg, Na, SO_4, Ca and K; acid-base balances in which some or all of H, NO_3, SO_4 and K showed similar variances; and biodegradation. The mixed seawater/continental source was responsible for most variance (usually about 75%) of the WE data set and the southern section of the SN data set. Isolating the two end-members of this source was only possible when the data sets were divided into coastal and non-coastal subsets. Most of the variance in the SN data set was caused by the mixed continental/seawater source and biodegradation. Dividing the data set into wet and dry subsets isolated the seawater source in a factor responsible for only 10% of variance in the wet data set, suggesting that the tropical monsoon activity may provide only a limited supply of ionic species to precipitation in the north of Australia. The components of the acid-base balance factor were suggested to be derived from natural sources such as biogenic emissions, biomass burning and lightning flash production. The nature of the collection program (i.e. sampling vessels were open to the atmosphere for three

months without preservatives) means that biodegradation was also a consequence of sampling procedures.

Seasonal variations of ionic species to Na (acting as a seawater tracer) and Ca (acting as a continental tracer) were used to ascertain periods dominated by a seasalt source. Seasalt was found to dominate precipitation chemistry at southern and western coastal localities throughout the sampling program, and during winter, extend up to 1800 km inland from the west coast. This was associated with cold front activity. A marine signature was also found for the coastal northern site, and was associated with monsoonal activity. However, this marine signature did not extend to 200 km from the northern coast, suggesting that the tropical marine airmass is rapidly modified as it moves southwards over the Australian landmass.

7.2 CHLORINE-36

One of the aims of investigating ^{36}Cl in precipitation was to test the latitudinal-dependent predicted fallout curve of ^{36}Cl to the Earth's surface (Lal and Peters 1967), commonly used to calculate $^{36}Cl/Cl$ ratios in recharge for hydrological investigations. The results of the present investigation agree with the general shape of the predicted curve, but suggest the curve underestimates the true rate of fallout. A revised southern hemisphere fallout of 15.4 ^{36}Cl atoms/m^2/s is suggested. Long-term average predictions of ^{36}Cl fallout rates used to predict the input ratios of $^{36}Cl/Cl$ in hydrological investigations should thus be increased by a factor of 1.4 for the southern hemisphere. The common assumption of a simple correlation between stable Cl concentrations and distance from the coast was not uniformly observed. While stable Cl concentrations in precipitation displayed a general exponential decrease with distance from the coast, the nature of this relationship was shown to be geographically variable, and for theoretical $^{36}Cl/Cl$ estimates, should be investigated for each study by local direct measurements, a process that is simple and inexpensive.

Wet deposition appeared to be the major process of removal of ^{36}Cl from the atmosphere. Chlorine-36 fallout and rainfall could be correlated, particularly along the SN array where extremes in rainfall regimes are experienced. Dry deposition is shown to account for less than 50% of fallout in the north of the SN array.

The spatial pattern of stable Cl deposition to the Australian continent is for decreasing deposition from south to north, reflecting the importance of the southern marine airmasses in the supply of Cl. The northern tropical airmasses play a less

significant part in this process. The relationship between Cl deposition and distance from the coast can be explained in terms of a double exponential decay, suggesting that two processes control this relationship. These processes may reflect the enhanced mixing of airmasses moving inland and/or differences in the rate of removal of Cl aerosol and Cl gas from marine and continental airmasses.

As expected, the $^{36}Cl/Cl$ ratio of precipitation increases exponentially with increasing distance from the coast, due to the opposing trend displayed by stable Cl concentrations in precipitation, reflecting the decreasing influence of stable Cl of marine origin at inland sites. The $^{36}Cl/Cl$ ratio was often perturbed however, by the supply of a source of stable Cl with insignificant or low ^{36}Cl content. For example, low $^{36}Cl/Cl$ ratios were observed at inland sites when synoptic conditions favoured the transport of seawater aerosols great distances inland (eg. during cold frontal activity). Also, low $^{36}Cl/Cl$ ratios at inland sites on the WE array reflect the diluting effect of stable, recycled Cl from local salt lakes with low ^{36}Cl contents.

This work supports the use of ^{36}Cl as a tracer of atmospheric processes. Its production primarily in the stratosphere suggests that it may trace stratosphere-troposphere exchange. Chlorine-36 fallouts and $^{36}Cl/Cl$ ratios were high during spring, and for the north of the SN array, during summer. The increased spring ^{36}Cl fallouts may be attributed to increased transfer of stratospheric ^{36}Cl to the troposphere occurring as the tropopause increases height during the warmer months. High ^{36}Cl fallouts during summer in the north of the SN array may be attributed to the direct entrainment of stratospheric air into cumulus clouds during the monsoonal convection.

The mean fallout calculated from this work, while higher than the theoretical estimate, is three times lower than has been measured for precipitation in the northern hemisphere. Several possible explanations are suggested for this observation: i) an additional supply of ^{36}Cl that is not present in the southern hemisphere. Output from nuclear reactors, which are concentrated in the northern hemisphere is suggested. However, releases of ^{36}Cl to the environment from nuclear reactor operations are too localised and thus cannot be considered to be the cause of the total fallout discrepancy between the northern and southern hemisphere. ii) recycling of bomb-produced ^{36}Cl is also suggested as an explanation, although this does not explain the high fallouts measured in pre-bomb Greenland ice. Further investigations into the behaviour of ^{36}Cl in soil profiles may allow more comment on the role of bomb-produced ^{36}Cl in enhancing fallout of ^{36}Cl in the northern

hemisphere. iii) It is suggested here that enhanced ^{36}Cl fallout in the northern hemisphere actually reflects the lower rates of transfer of stratospheric air to the troposphere in the southern hemisphere, a consequence of the less dynamic nature of the lower southern hemisphere stratosphere as compared to the northern hemisphere.

A mean global ^{36}Cl fallout of 25 to 35 atoms/m^2/s can be calculated. This value incorporates the results from the present investigation, estimates from Antarctic ice and the higher fallout calculated from measurements of ^{36}Cl in northern hemisphere precipitation. This value is 2-3 times greater than predicted by Lal and Peters (1967), suggesting that the cross-section for the cosmic-ray production of ^{36}Cl may be underestimated in their paper.

Another implication from this work for atmospheric investigations arises from the ^{36}Cl relationship to major elements measured in precipitation. A correlation between ^{36}Cl and NO_3 and the lack of any relationship between ^{36}Cl, stable Cl and Na concentrations, suggests that ^{36}Cl is scavenged from the atmosphere as a gas rather than aerosol phase. This is a very preliminary suggestion, and further investigations into the phase of ^{36}Cl through cross-sections of the atmosphere may provide more information required to develop this hypothesis.

REFERENCES

Andreae, M. O. (1984). The emission of sulfur to the remote atmosphere: background paper, in Galloway, J., N.,, Charlson, R. J., Andreae, M. O. and Rodhe, H., eds., *The Biogeochemical Cycling of Sulfur and Nitrogen in the Remote Atmosphere*, NATO ASIO Series, v. Dordrecht, D. Reidel Publishing Company, p. 5-21.

Andrews, D. G. (1989). Some comparisons between the middle atmosphere dynamics of the southern and northern hemispheres: *Pure and Applied Geophysics,* v. 130, p. 213-232.

Andrews, J. N. and Fontes, J. C. (1992). Importance of in-situ production of chorine-36, argon-36 and carbon-14 in Hydrology and hydrochemistry, in IAEA, eds., *Isotope Techniques in Water Resources Development, Vienna*, p. 245-269.

Avery, R. (1984). A preliminary study of rainwater acidity around Newcastle, N.S.W: *Clean Air (Australia)*, v. 18, p. 94-101.

Ayers, G. P. and Gillett, R. W. (1982). Acidity of summer rainfall in Sydney, in Carras, J. N. and Johnson, G. M., eds., *The Urban Atmosphere-Sydney, a case study*, Melbourne, CSIRO, p. 421-432.

Ayers, G. P. and Gillett, R. W. (1988a). Acidification in Australia, in Rodhe, H. and Herrera, R., eds., Acidification in Tropical Countries, SCOPE 36, Chichester, John Wiley and Sons, p. 347-402.

Ayers, G. P. and Gillett, R. W. (1988b). First observations of cloudwater acidity in tropical Australia: *Clean Air (Australia)*, v. 22, p. 53-57.

Ayers, G. P. and Ivey, J. P. (1988). Precipitation composition at Cape Grim, 1977-1985: *Tellus*, v. 40B, p. 297-307.

Ayers, G. P. and Manton, M. J. (1991). Rainwater compositions at two BAPMoN regional stations in SE Australia: *Tellus,* v. 43B, p. 379-389.

Barry, R. G. and Chorley, R. J. (1976). Atmosphere, Weather and Climate. Suffolk, Methuen and Co Ltd, 432.

Beasley, T. M., Elmore, D. E., Kubik, P. W. and Sharma, P. (1992). Chlorine-36 release from the Savannah River site nuclear fuel reprocessing plants: *Groundwater*, v 30 p2539-548.

Beasley, T., Cecil, L., Mann, L., Kubik, P., Sharma, P., Fehn, U. and Gove, H. (1990). Chlorine-36 in the Snake River Plain Aqcuifer. *Fourteenth Annual Radiocarbon Conference*, 20-24 May, 1990., Tucson, Arizona.

Beer, J., Raisbeck, G. M. and Yiou, F. (1991). Time variations of ^{10}Be and solar activity, in Sonett, C. P., Giampapa, M. S. and Matthews, M. P., eds., The Sun in Time, Space Science Series, Arizona, The University of Arizona Press, p. 343-359.

Bentley, H. W., Phillips, F. M. and Davies, S. N. (1986a). Chlorine-36 in the terrestrial environment, in Fritz, P. and Fontes, J. C., eds., Handbook of Environmental Isotope Geochemistry, v. 2. Amsterdam, Elsevier, p. 427-475.

Bentley, H. W., Phillips, F. M., Davis, S. N., Gifford, S., Elmore, D., Tubbs, L. E. and Gove, H. E. (1982). Thermonuclear ^{36}Cl pulse in natural water: *Nature*, v. 300, p. 737-740.

Bentley, H. W., Phillips, F. M., Davis, S. N., Habermehl, M. A., Airey, P. L., Calf, G. E., Elmore, D., Gove, H. E. and Torgersen, T. (1986b). Chlorine-36 dating of very old groundwater 1. The Great Artesian Basin, Australia: *Water Resources Research*, v. 22, p. 1991-2001.

Bird, J. R., Calf, G. E., Davie, R. F., Fifield, L. K., Ophel, T., R., Evans, W. R., Kellett, J. R. and Habermehl, M. A. (1989). The role of ^{36}Cl and ^{14}C measurements in Australian groundwater studies: *Radiocarbon*, v. 31, p. 877-883.

Bird, J. R., Davie, R. F., Chivas, A. R., Fifield, L. K. and Ophel, T. R. (1991). Chlorine-36 production and distribution in Australia: *Palaeogeography, Palaeoclimatology, Palaeoecology*, v. 84, p. 299-307.

Blackburn, G. and McLeod, S. (1983). Salinity of atmospheric precipitationin the Murray-Darling Drainage Division, Australia: *Australian Journal of Soil Research*, v. 21, p. 411-434.

Blanchard, D. C. and Woodcock, A. H. (1957). Bubble formation and modification in the sea and its meteorological significance: Tellus, v. 9, p. 145-158.

Bridgeman, H. A. (1990). Acid rain studies in Australia and New Zealand: *Archives of Environmental Contamination and Toxicology*, v. 18, p. 137-146.

Bridgeman, H. A., Rothwell, R., Pang Way, C., Peng Hing Tio, Carras, J. N. and Smith, M. Y. (1988a). Rainwater acidity and composition in the Hunter Region, New South Wales: *Clean Air (Australia)*, v. 22, p. 45-52.

Bridgeman, H. A., Rothwell, R., Peng-Hing Tio and Pang Way, C. (1988b). The Hunter Region (Australia) acid rain project: *Bulletin of the Meteorological Society of America*, v. 69, p. 266-271.

Brimblecomb, P. (1986). Air Composition and Chemistry. Cambridge Environmental Series, Cambridge, Cambridge University Press, 217.

Brimblecomb, P. and Dawson, G. A. (1984). Wet removal of highly soluble gases: *Journal of Atmospheric Chemistry*, v. 2, p. 95-107.

Browne, E. and Firestone, R. B. (1986). Table of radioactive isotopes. Brisbane, John Wiley and Sons.

Bulletin of Volcanic Eruptions. (1994). Annual report of world volcanic eruptions in 1991: *Bulletin of Volcanic Eruptions, v. 31 for 1991, Supplement to Bulletin of Volcanology 56*, p. 56-58.

Bureau of Meteorology 1991a, Monthly Weather Review, Western Australia (April). Government Printer, Australia.

Bureau of Meteorology 1991b, Monthly Weather Review, Western Australia (December). Government Printer, Australia.

Bureau of Meteorology 1991c, Monthly Weather Review, South Australia (May). Government Printer, Australia.

Bureau of Meteorology 1991d, Monthly Weather Review, Western Australia (July). Government Printer, Australia.

Bureau of Meteorology 1992a, Monthly Weather Review, Western Australia (January to December). Government Printer, Australia.

Bureau of Meteorology 1992b, Monthly Weather Review, South Australia (October). Government Printer, Australia.

Bureau of Meteorology 1993a, Monthly Weather Review, Northern Territory (January to December). Government Printer, Australia.

Bureau of Meteorology 1993b, Monthly Weather Review, South Australia (January to December). Government Printer, Australia.

Cautenet, S. and Lefeivre, B. (1994). Contrasting behaviour of gas and aerosol scavenging in convective rain: a numerical and experimental study in the African equatorial forest: *Journal of Geophysical Research*, v. 99, p. 13013-13024.

Chameides, W. L., Stedman, D. H., Dickenson, R. R., Rusch, D. W. and Cicerone, R. J. (1977). NOx production in lightning: *Journal of Atmospheric Science*, v. 34, p. 143-149.

Chivas, A. R., Kiss, E., Keywood, M. D., Fifield, L. K. and Allan, G. L. (1994). Chlorine-36 in Australian rainfall and playas and the residence time of chlorine in the Australian landscape. *Eight International Conference on Geochronology, Cosmochronology and Isotope Geology* . Berkeley, CA, p. 58.

Cicerone, R. J. (1981). Halogens in the atmosphere: *Reviews in Geophysics and Space Physics*, v. 19, p. 123-139.

Cornett, R., Milton, J., Andrews, H. R., Chant, L. A., Greiner, B. F., Imahori, Y., Kowlosky, V. T., Kramer, S. J. and Milton, J. C. D. (1994). Chlorine-36 deposition: reconciling models and measurements. *Abstract of the Geological Society of Canada Waterloo Meeting*, May 1994.

Crawley, J. and Sievering, H. (1986). Factor analysis of the MAP3S/RAINE Precipitation Chemistry Network: 1976-1980: *Atmospheric Environment*, v. 20, p. 1001-1013.

Danielsen, E. F. (1968). Stratospheric-tropospheric exchange based on radioactivity, ozone and potential vorticity: *Journal of Atmospheric Science*, v. 25, p. 502-518.

Davie, R. F., Kellet, J. R., Fifield, L. K., Evans, W. R., Calf, G. E., Bird, J. R., Topham, S. and Ophel, T. R. (1989). Chlorine-36 measurements in the Murray Basin: preliminary results from the Victorian and South Australian Mallee region: *BMR Journal of Geology and Geophysics*, v. 11, p. 261-272.

Davis, J. C. (1986). Statistics and Data Analysis in Geology. New York, John Wiley and Sons, 646.

Denmead, O. T., Freney, J. R. and Simpson, J. R. (1976). A closed ammonia cycle within a plant canopy: *Soil Biology and Biochemistry*, v. 8, p. 161-164.

Duce, R. A. (1969). On the source of gaseous chlorine in the marine atmosphere: *Journal of Geophysical Research*, v. 74, p. 4597-4599.

Elmore, D., Conrad, N., M., Kubik, P. W., Gove, H. E., Wahlen, M., Beer, J. and Suter, M. (1987). ^{36}Cl and ^{10}Be profiles in Greenland ice: dating and production rate variations: *Nuclear Instruments and Methods in Physics Research*, v. B29, p. 207-210.

Elmore, D., Fulton, B. R., Clover, M. R., Marsden, J. R., Gove, H. E., Naylor, H., Purser, K. H., Kilius, L. R., Beukens, R. P. and Litherland, A. E. (1979). Analysis of ^{36}Cl in environmental water samples using an electrostatic accelerator.: *Nature*, v. 277, p. 22-25.

Elmore, D., Tubbs, L. E., Newman, D., Ma, X. Z., Finkel, R., Nishiizumi, K., Beer, J., Oeschger, H. and Andree, M. (1982). ^{36}Cl bomb pulse measured in a shallow ice core from Dye 3, Greenland.: *Nature*, v. 300, p. 735-740.

Erickson, D. J. and Duce, R. A. (1988). On the global flux of atmospheric seasalt: *Journal of Geophysical Research*, v. 74, p. 14079-14088.

Ericksson, E. (1959). The yearly circulation of chlorine and sulfur in nature: Meteorological, geochemical and pedological implications 1: Tellus, v. 11, p. 375-403.

Erisman, J. W., Beier, C., Draaijers, G. and Lindberg, S. (1994). Review of deposition monitoring methods: Tellus, v. 46B, p. 79-93.

Fabian, P. and Pruchniewicz, P. G. (1977). Meridional distribution of ozone in the troposphere and its seasonal variations: *Journal of Geophysical Research*, v. 82, p. 2063-2073.

Farrington, P. and Bartle, G. A. (1988). Accession of chloride from rainfall on the Gnangara Groundwater Mound, Western Australia, Technical Memorandum, Division of Water Resources, CSIRO, 88/1, 10 pp.

Farrington, P., Salama, R. B., Bartle, G. A. and Watson, G. D. (1993). Accession of major ions in rainfall in the southwestern region of Western Australia, Division of Water Resources, 93/1, 11 pp.

Fifield, L. K., Ophel, T. R., Bird, J. R., Calf, G. E., Allison, G., B., and Chivas, A. R. (1987). The chlorine-36 measurement program at the Australian National University: *Nuclear Instruments and Methods in Physics Research*, v. B29, p. 114-119.

Finkel, R. C., Nishiizumi, K., Elmore, D., Ferraro, R. D. and Gove, H. E. (1980). ^{36}Cl in polar ice, rainwater and seawater: Geophysical Research *Letters*, v. 7, p. 983-986.

Finlayson-Pitts, B. J. (1983). Reaction of NO_2 with NaCl and atmospheric implications of NOCl formation: *Nature*, v. 306, p. 676-677.

Finlayson-Pitts, B. J., Ezell, M. J. and N., P. J. J. (1989). Formation of chemically active chlorine compounds by reaction of atmospheric NaCl particles with gaseous N_2O_5 and $ClONO_2$: *Nature*, v. 337, p. 241-244.

Follows, M. J. (1992). On the cross-tropopause exchange of air: *Journal of Atmospheric Science*, v. 49, p. 879-882.

Galbally, I. E. (1984). The emission of nitrogen to the remote atmosphere: background paper, in Galloway, J. N., Charlson, R. J., Andreae, M. O. and Rodhe, H., eds., Biogeochemical Cycling of Sulfur and Nitrogen in the Remote Atmosphere, NATO ASI Series, v. Dordrecht, D. Reidel Publishing Company, p. 27-54.

Galbally, I. E., Freney, J. R., Denmead, O. T. and Roy, C. R. (1980). Processes controlling the nitrogen cycle in the atmosphere over Australia, in Trudinger, P. A., Walter, M. R. and Ralph, B. J., eds., Biogeochemistry of Ancient and Modern Environments, v. Canberra, Australian Academy of Science, p. 319-326.

Galloway, J. N., Likens, G. E., Keene, W. C. and Miller, J. M. (1982). The composition of precipitation in remote areas of the world: *Journal of Geophysical Research*, v. 87, p. 8771-8786.

Gatz, D. F. and Dingle, A. N. (1971). Trace substances in rainwater: concentration variations during convective rains and their interpretation: Tellus, v. 23, p. 14-27.

Genstat 5 Committee. (1989). Genstat 5 Reference Manual. Oxford, Clarendon Press, 749.

Gentilli, J. (1971). Australian climatic factors: Climates of Australia and New Zealand. World Survey of Climatology, 13, Amsterdam, Elsevier, (J. Gentilli, ed), 35-52.

Gill, A. E. (1982). Atmosphere-Ocean Dynamic. International Geophysics Series, 30, California, Academic Press, 662.

Gillett, R. W. and Ayers, G. P. (1991). The use of thymol as a biocide in rainwater samples: *Atmospheric Environment*, v. 25A, p. 2677-2681.

Gillett, R. W. and Ayers, G. P., Noller, B. N. (1990). Rainwater acidity at Jabiru, Australia, in the wet season of 1983/84: Science of the Total Environment, v. 92, p. 129-144.

Gossard, E. E. and Hooke, W. H. (1975). Waves in the Atmosphere. Developments in Atmospheric Science, 2, Amsterdam, Elsevier, 456.

Hainsworth, L. J. (1994). Spatial and Temporal Variations in Chlorine-36 Deposition in the Northern United States, The University of Maryland, PhD Thesis.

Hainsworth, L. J., Mignerey, A. C., Helz, G. R., Sharma, P. and Kubik, P. W. (1994). Modern chlorine-36 deposition in Southern Maryland, U.S.A. : *Nuclear Instruments and Methods in Physics Research*, v. B29, p. 345-349.

Henry, R. (1987). Current factor analysis receptor models are ill-posed: *Atmospheric Environment*, v. 21, p. 1815-1820.

Herlihy, L. J., Galloway, J. N. and Mills, A. L. (1987). Bacterial utilization of formic and acetic acid in rainwater: *Atmospheric Environment*, v. 21, p. 2397-2402.

Herut, B., Starinsky, A., Katz, A., Paul, M., Boaretto, E. and Berkovits, D. (1992). ^{36}Cl in chloride-rich rainwater, Israel: *Earth and Planetary Science Letters*, v. 109, p. 179-183.

Hingston, F. J. and Gailitis, V. (1976). The geographic variation of salt precipitated over Western Australia: Australian Journal of Soil Research, v. 14, p. 319-335.

Hirsch, R. M. and Gilroy, E. J. (1984). Methods of fitting a straight line to data: Examples in water resources: *Water Resources Bulletin*, v. 20, p. 705-711.

Hitchman, M. H., McKay, M. and Trepte, C. R. (1994). A climatology of stratospheric aerosol: *Journal of Geophysical Research*, v. 99, p. 20689-20700.

Holton, J. R. (1990). On the global exchange of mass between the stratosphere and troposphere: *Journal of Atmospheric Science*, v. 47, p. 392-395.

Hurst, D. F., Griffith, D. W. T. and Cook, G. D. (1994). Trace gas emissions from biomass burning in tropical Australian savannas: *Journal of Geophysical Research*, v. 99, p. 16441-16456.

Hutton, J. T. (1968). The redistribution of the more soluble chemical elements associated with soils as indicated by analysis in rainwater, soils and plants. 9th International Congress of Soil Science, Adelaide, p. 313-328.

Hutton, J. T. (1976). Chloride in rainwater in relation to distance from the ocean: *Search*, v. 7, p. 207-208.

Hutton, J. T. (1983). Soluble ions in rainwater collected near Alice Springs, N.T., and their relation to locally derived atmospheric dust: *Transactions of the Royal Society of South Australia*, v. 107, p. 138.

Hutton, J. T. and Leslie, T. I. (1958). Accession of non-nitrogenous ions dissolved in rainwater to soils in Victoria: *Australian Journal of Agricultural Research*, v. 9, p. 492-507.

Iribarne, J. V. and Cho, H. R. (1980). Atmospheric Physics. Boston, Reidel Publishing Co., 212.

Isbell, R. F., Reeve, R. and Hutton, J. T. (1983). Salt and sodicity in "Soils: an Australian Viewpoint" Division of Soils (CSIRO, pp. 107-118. Melbourne, Academic Press: London .

Janssen, L. H. J. M., Visser, H. and Romer, F. G. (1989). Analysis of large scale sulphate, nitrate, chloride and ammonium concentrations in the Netherlands using an aerosol measuring network: *Atmospheric Environment*, v. 23, p. 2783-2796.

Jiang, S. S., Hemmick, T. K., Kubik, P. K., Elmore, D., Gove, H. E., Tullai-Fitzpatrick, S. and Hossain, T. Z. (1990). Measurement of the $^{36}Ar(n,p)^{36}Cl$ cross section at thermal energies using the AMS technique: *Nuclear Instruments and Methods in Physics Research*, v. B52, p. 608-611.

Junge, C. E. (1963). Air Chemistry and Radioactivity. International Geophysics Series, New York, Academic Press, 382.

Keene, W. C., Pszenny, A. A. P., Jacob, D. J., Duce, R. A., Galloway, J. N., Schultz-Tokos, J. J., Sievering, H. and Boatman, J. (1990). The geochemical cycling of reactive chlorine through the marine troposphere: *Global Biogeochemical Cycles*, v. 4, p. 407-430.

Keene, W. C., Pszenny, A. P., Galloway, J. N. and Hawley, M. E. (1986). Sea-salt corrections and interpretation of constituent ratios in marine precipitation: *Journal of Geophysical Research*, v. 91, p. 6647-6666.

Kessler, C. J., Porter, T. H., Firth, D., Sager, T. W. and Hemphill, M. W. (1992). Factor analysis of trends in Texas acid deposition: *Atmospheric Environment*, v. 26A, p. 1137-1146.

Knies, D. (1994). Cosmogenic Radionuclides in Precipitation, Purdue University, PhD Thesis.

Knies, D. L., Elmore, D., Sharma, P., Vogt, S., Li, R., Lipschutz, M. E., Petty, G., Farrell, J., Monaghan, M. C., Fritz, S. and Agee, E. (1994). ^{7}Be, ^{10}Be and ^{36}Cl in precipitation: *Nuclear Instruments and Methods in Physics Research*, v. B29, p. 350-356.

Lacaux, J. P., Delmas, R., Kouadio, G., Cros, B. and Andreae, M. O. (1992). Precipitation chemistry in the Mayombe forest of Equatorial Africa: *Journal of Geophysical Research*, v. 97, p. 6195-6206.

Lal, D. and Peters B. (1962). Cosmic ray produced isotopes and their application to problems in geophysics: *Progress in Cosmic Ray Physics and Elementary Particle Physics*, v. 6. Amsterdam, North Holland Publishing Co., p. 3-74.

Lal, D. and Peters, B. (1967). Cosmic ray produced radioactivity on the Earth: *Handbuch Der Physik*, v. 46, p. 551-612.

Likens, G. E., Bormann, F. H., Pierce, R. S., Eaton, J. S. and Munn, R. E. (1984). Long-term trends in precipitation at Hubbard Brook, New Hampshire: *Atmospheric Environment*, v. 18, p. 2641.

Likens, G. E., Keene, W. C., Miller, J. M. and Galloway, J. N. (1987). Chemistry of precipitation from a remote, terrestrial site in Australia: *Journal of Geophysical Research*, v. 92, p. 13,299-13,314.

Lilly, D. K., Waco, D. E. and Adelfang, S. I. (1974). Stratospheric mixing estimated from high-altitude turbulence measurements: *Journal of Applied Meteorology*, v. 13, p. 488-493.

Linacre, E. and Hobbs, J. (1982). The Australian Climatic Environment. Brisbane, John Wiley and Sons, 354

Lindberg, S. E. (1982). Factors influencing trace metals, sulfate and hydrogen ion concentrations in rain: *Atmospheric Environment*, v. 16, p. 1707-1709.

Ling Xing and Chameides, W. L. (1990). Model simulations of rainout and washout from a warm stratiform cloud: *Journal of Atmospheric Chemistry*, v. 10, p. 1-26.

Magaritz, M., Kaufman, A., Paul, M. and Boaretto, E. (1990). A new method to determine regional evapotranspiration: *Water Resources Research*, v. 26, p. 1759-1762.

Manabe, S. and Terpstra, T. B. (1974). The effects of mountains on the general circulation of the atmosphere as identified by numerical experiments: *Journal of Atmospheric Science*, v. 27, p. 871-883.

Martens, C. S., Wesolowski, J. J., Harriss, R. C. and Kaifer, R. (1973). Chlorine loss from Puerto Rican and San Francisco Bay area marine aerosols: *Journal of Geophysical Research*, v. 78, p. 8778-8792.

Millero, F. T. (1974). Physical chemistry of seawater: Annual Reviews in *Earth and Planetary Science*, v. 2, p. 101-150.

Milton, G. M., Andrews, H. R., Causey, S. E., Chant, L. A., Cornett, R. J., Davies, W. G., Greiner, B. F., Kowolsky, V. T., Imahori, Y., Kramer, S. J., McKay, J. W. and Milton, J. C. D. (1993). Chlorine-36 dispersion in the Chalk River area: *Nuclear Instruments and Methods in Physics Research*, v. B92, p. 376-379.

Monaghan, M. C., Krishnaswami, S. and Turekian, K. K. (1985/1986). The global-average production of ^{10}Be: *Earth and Planetary Science Letters*, v. 76, p. 279-287.

Moore, A. W., Isbell, R. F. and Northcote, K. H. (1983). Classification and mapping of Australian soils, 'Soils: an Australian Viewpoint', p. 253-266, (Division of Soils, CSIRO). Melbourne, Academic Press, London.

Mote, P. W., Holton, J. R. and Boville, B. A. (1994). Characteristics of stratosphere-troposphere exchange in a general circulation model: *Journal of Geophysical Research*, v. 99, p. 16815-16829.

Neiburger, M., Edinger, J. G. and Bonner, W. D. (1982). Understanding Our *Atmospheric Environment*. San Francisco, W. H. Freeman and Company. 453.

Nishiizumi, K., Arnold, J. R., Elmore, D. E., Ma, X., Newman, D. and Gove, H. E. (1983). 36Cl and 53Mn in Antarctic meteorites and 10Be-36Cl dating of Antarctic ice: *Earth and Planetary Science Letters*, v. 62, p. 407-417.

Nishiizumi, K., Arnold, J. R., Elmore, D., Ferraro, R. D., Gove, H. E., Finkel, R. C., Beukens, R. P., Chang, K. H. and Kilius, L. R. (1979). Measurements of ^{36}Cl in Antarctic meteorites and Antarctic ice using a Van De Graaff Accelerator: *Earth and Planetary Science Letters*, v. 45, p. 285-292.

Noller, B. N., Currey, N. A., Ayers, G. P. and Gillett, R. W. (1986). Naturally acidic rainwater at a site in Northern Australia. *Proceedings of the Seventh World Clean Air Congress, Sydney, Australia*, J. G. Holmes Pty. Ltd., p. 189-190.

Noller, B. N., Currey, N. A., Ayers, G. P. and Gillett, R. W. (1990). Chemical composition and acidity of rainfall in the Alligator Rivers region, Northern Territory, Australia: *Science of the Total Environment*, v 91. p 23-48.

Noller, B. N., Currey, N. A., Cusbert, P. J., Tuor, M., Bradley, P. and Harrison, A. (1985). Temporal variability in atmospheric nutrient flux to the Magela, Nourlangie Creek system, Northern Territory, in Ridpath, M. G. and Corbett, L. K., eds., Ecology of the Wet-Dry Tropics, *Proceedings of the Ecological Society of Australia*, v. 13. Darwin, Darwin Institute of Technology, p. 21-31.

Onufriev, V. G. (1968). Formation of chlorine-36 in nature: *Yad. Geofiz. Geokhim, Izot. Metody. Geol*, v. 1968, p. 364-369.

Peck, A. J., Thomas, J. F. and Williamson, D. R. (1983). Salinity Issues: Effects of Man on Salinity in Australia. *Water 2000: Consultants Report*, No. 8, Canberra, Australian Government Publishing Service, 78.

Phillips, F. M., Mattick, J. L., Duval, T. A., Elmore, D. and Kubik, P. W. (1988). Chlorine-36 and tritium from nuclear weapons fallout as tracers for long-term liquid and vapour movement of desert soils: *Water Resources*, v. 24, p. 1877-1891.

Plumb, R. A. (1989). On the seasonal cycle of stratospheric planetary waves: *Pure and Applied Geophysics*, v. 130, p. 233-242.

Pruchniewicz, P. G. (1973). The average tropospheric ozone content and its variation with season and latitude as a result of global ozone circulation: P*ure and Applied Geophysics*, v. 106-108, p. 1058-1073.

Pruppacher, H. R. and Klett, J. D. (1978). Microphysics of Clouds and Precipitation. Dordrecht, Holland, D. Reidel and Co., 714.

Qin, Y. and Chameides, W. L. (1986). The removal of soluble species by warm stratiform clouds: *Tellus*, v. 35B, p. 285-299.

Raisbeck, G. M., Yiou, F., Fruneau, M., Loiseaux, J. M. and Lieuvin, M. (1978). Measurements of ^{10}Be in 1000- and 5000-year old Antarctic Ice: *Nature*, v. 275, p. 731-732.

Raisbeck, G. M., Yiou, F., Fruneau, M., Loiseaux, J. M., Lieuvin, M. and Ravel, J. C. (1979). Deposition rate and seasonal variations in precipitation of cosmogenic ^{10}Be: *Nature*, v. 282, p. 279-280.

Reiter, E. R. (1975). Stratospheric-tropospheric exchange processes: *Reviews in Geophysics and Space Physics*, v. 13, p. 1-35.

Robinson, E. and Robbins, R. C. (1972). Emission concentrations and the fate of gaseous atmospheric pollutants, in Strauss, W., eds., Air Pollution Control Part 2, v. New York, John Wiley and Sons, p. 1-93.

Robinson, G. D. (1980). The transport of minor atmospheric constituents between the troposphere and stratosphere: *Quarterly Journal of the Royal Meteorology Society*, v. 106, p. 227-253.

Ryaboshapko, A. G. (1983). The atmospheric sulphur cycle, in Ivanov, M. V. and Freney, J. R., eds., The Global Biogeochemical Sulphur Cycle, SCOPE 19, v. Chichester, John Wiley and Sons, p. 203-275.

Saylor, R. D., Butt, K. M. and Peters, L. K. (1992). Chemical characterisation of precipitation from monitoring network in the Lower Ohio River Valley: *Atmospheric Environment*, v. 26A, p. 1147-1156.

Schaeffer, O. A., Thompson, S. O. and Lark, N. L. (1960). Chlorine-36 radioactivity in rain: *Journal of Geophysical Research*, v. 65, p. 4013-4016.

Shaw, G. E. (1991a). Aerosol chemical components in Alaska air masses 1. Aged Pollution: *Journal of Geophysical Research*, v. 96, p. 22357-22368.

Shaw, G. E. (1991b). Aerosol chemical components in Alaska air masses 2. Sea salt and marine product: *Journal of Geophysical Research*, v. 96, p. 22369-22372.

Simpson, H. J. and Herczeg, A. L. (1994). Delivery of marine chloride in precipitation and removal by rivers in the Murray-Darling Basin, Australia: *Journal of Hydrology*, v. 154, p. 323-350.

Smeyers-Verbeke, J., Den-Hartog, J. C., Dekker, W. H., Coomans, D., Buydens, L. and Massart, D. L. (1984). The use of principal component analysis for the investigation of an organic air pollutants data set: *Atmospheric Environment*, v. 18, p. 2471-2478.

Smith, R. B. (1979). The influence of mountains on the atmosphere: *Advances in Geophysics*, v. 21, p. 87-230.

Smith, R. B. and Davies (1977). A note on some numerical experiments with model mountain barriers: *Tellus*, v. 29, p. 97-106.

Smithsonian Institute. (1993). Institute Global Volcanism Network, Summary of recent Volcanic eruptions: *Bulletin of Volcanology*, v. 56, p. 148.

SPSS (1990). Base Systems User's Guide. Chicago, SPSS Inc,

Staley, D. O. (1962). On the mechanism of mass and radioactive transport from stratosphere to troposphere: *Journal of Atmospheric Science*, v. 19, p. 450-467.

Suter, M., Beer, J., Bonani, G., Hoffman, H. J., Michel, D., Oeschger, H., Synal, H. A. and Wolfi, W. (1987). ^{36}Cl studies at the ETH/SIN AMS facility: *Nuclear Instruments and Methods in Physics Research*, v. B29, p. 211-215.

Synal, H. A., Beer, J., Bonani, G., Suter, M. and Wolfi, W. (1990). Atmospheric transport of bomb produced ^{36}Cl: *Nuclear Instruments and Methods in Physics Research*, v. B52, p. 483-488.

Tapper, N., Hurry, L. (1994). Australia's Weather Patterns. Victoria, Dellasta Pty Ltd, 130.

Teakle, L. J. H. (1937). The salt (sodium chloride) content of rainwater: *Journal of Agriculture, Western Australia*, v. 14, p. 115-123.

Turekian, K., Nozaki, Y. and Benninger, L. K. (1977). Geochemistry of atmospheric radon and radon products: *Annual Reviews in Earth and Planetary Science*, v. 5, p. 227-255.

Vesely, J. (1990). Stability of the pH and contents of ammonium and nitrate in precipitation samples: *Atmospheric Environment*, v. 24A, p. 3085-3089.

Vet, R. J. (1991). Wet deposition: Measurement techniques, in Hutzinger, O., eds., Environmental Chemistry: Reactions and Processes, v. 2 part F. Berlin, Springer-Verlag,

Wahlen, M., Deck, B., Weyer, H., Kubik, P. K., Sharma, P. and Gove, H. (1991). ^{36}Cl in the stratosphere: *Radiocarbon*, v. 33, p. 257-258.

Warneck, P. (1988). Chemistry of the Natural Atmosphere. International Geophysics Series, 41, San Diego, Academic Press. 757.

Wedland, W. M. and McDonald, N. S. (1985). Mean airstreams of Australia: *Australian Geographical Studies*, v. 23, p. 28-37.

Wetselaar, R. and Hutton, J. T. (1962). The ionic composition of rainwater at Katherine, N.T., and its part in the cycling of plant nutrients: *Australian Journal of Agricultural Research*, v. 14, p. 319-329.

Willsmore, N. T. M. and Wood, W. (1929). Salinity of rain in Western Australia: *Royal Society of Western Australia*, v. 25, p. xxii-xxx.

Yulaeva, E., Holton, J. R. and Wallace, J. M. (1994). On the cause of the annual cycle in tropical lower stratospheric temperatures: *Journal of Atmospheric Science*, v. 51, p. 169-174.

Zeng, Y. and Hopke, P. K. (1989). A study of the sources of acid precipitation in Ontario, Canada: *Atmospheric Environment*, v. 23, p. 1499-1509.

Danielsen, E. F. (1982). Statistics of cold cumulonimbus anvils based on enhanced infrared photographs: Geophysical Research Letters, v 9, p601-604.

Kley, D., Schmeletkopf, A. L., Kelly, K., Winkler, R. H., Thompson, T. L. and McFarland, M. (1982). Transport of water through the tropical tropopause: Geophysical Research Letters, v9, p617-620.

Newel, R. E. and Gould-Stewart, S. (1981). A stratospheric fountain: Journal of Atmospheric Sciences, v38, p.2789-2796.

APPENDIX A RAIN-PR ODUCING SYNOPTIC CLASSIFICATION

Proportion of rainfall during each collection period at each Met station attributed to synoptic processes as defined in Chapter 2.

A91=Autumn 91, W91=Winter 91, Sp91=Spring 9, S91=Summer 91 etc. CF=cold front, TE=tropical event, WCT=West Coast Trough, T=trough, CoL=cut-off low, MLCB=middle-level cloud band, MLD=middle-level depression, TF=tropical flow, TD=tropical depression, MT=monsoonal trough, GL=gulf lines, TC=tropcial cyclone

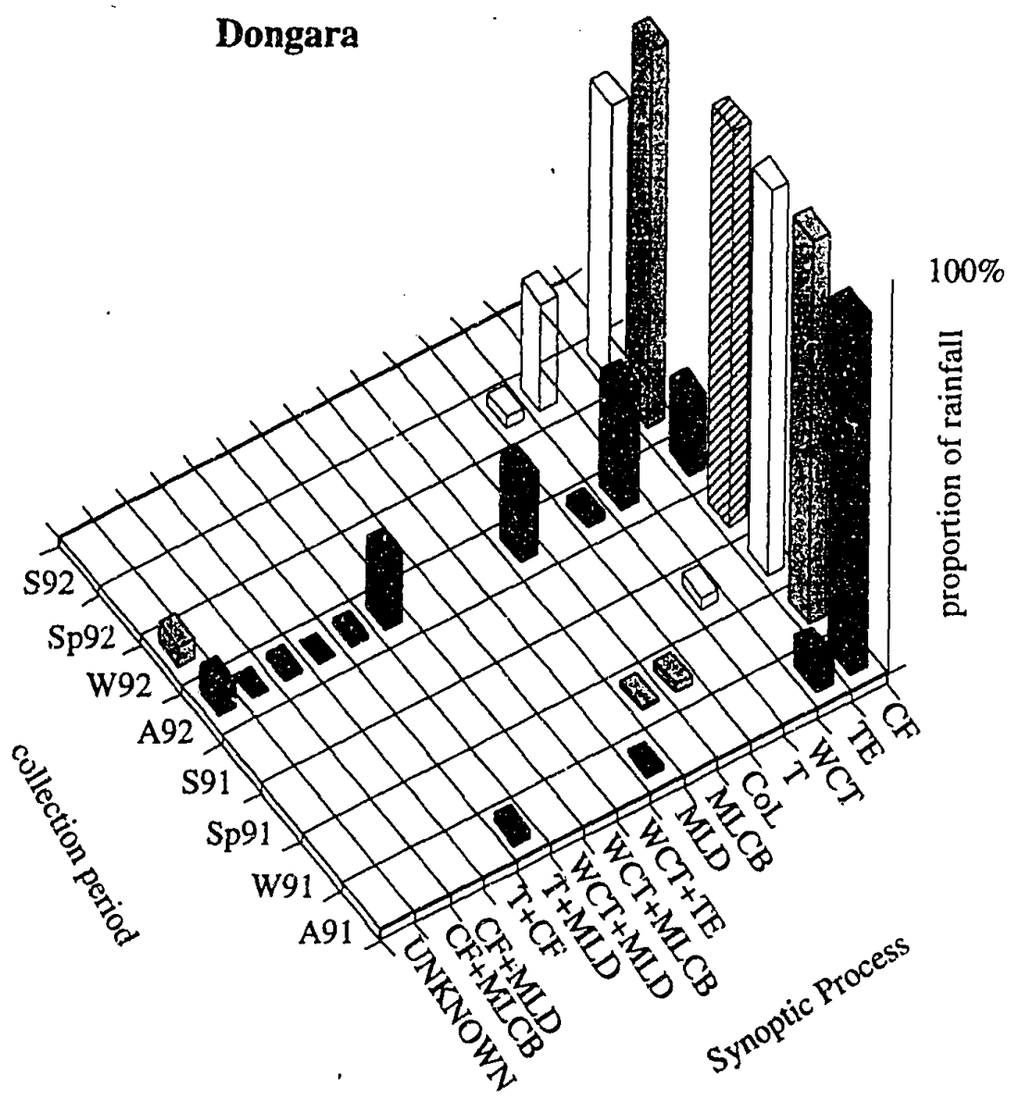

Mount Magnet

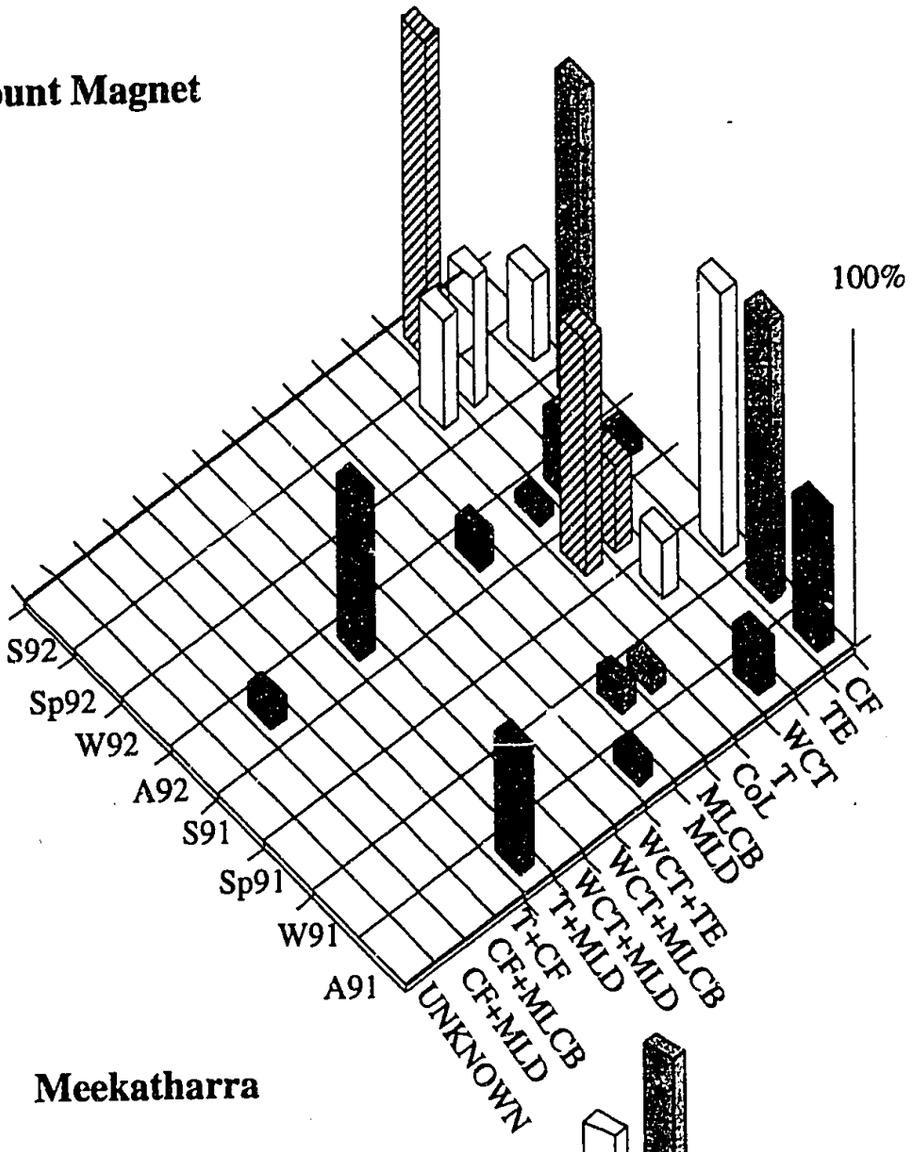

Meekatharra

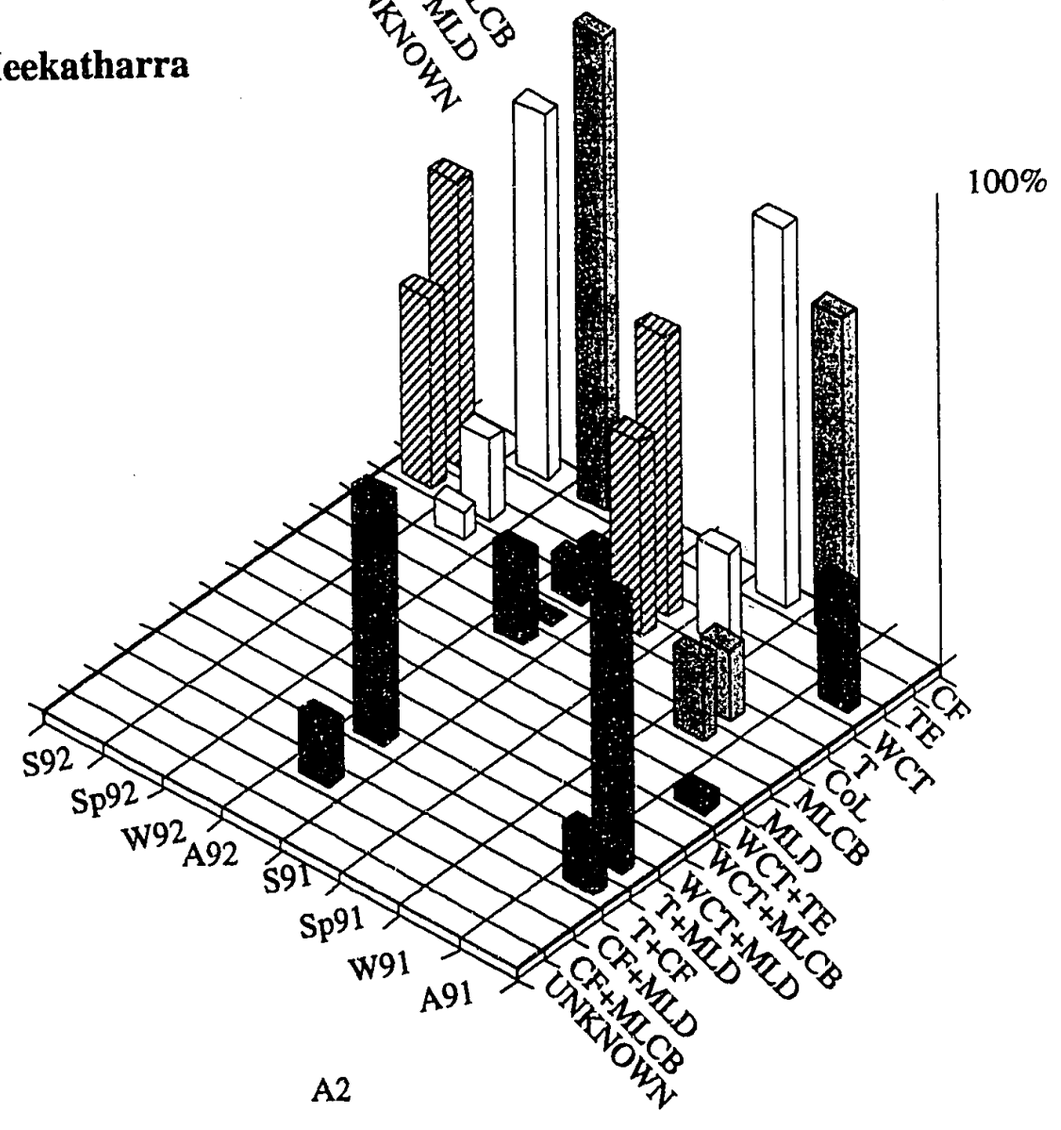

Yeelirrie

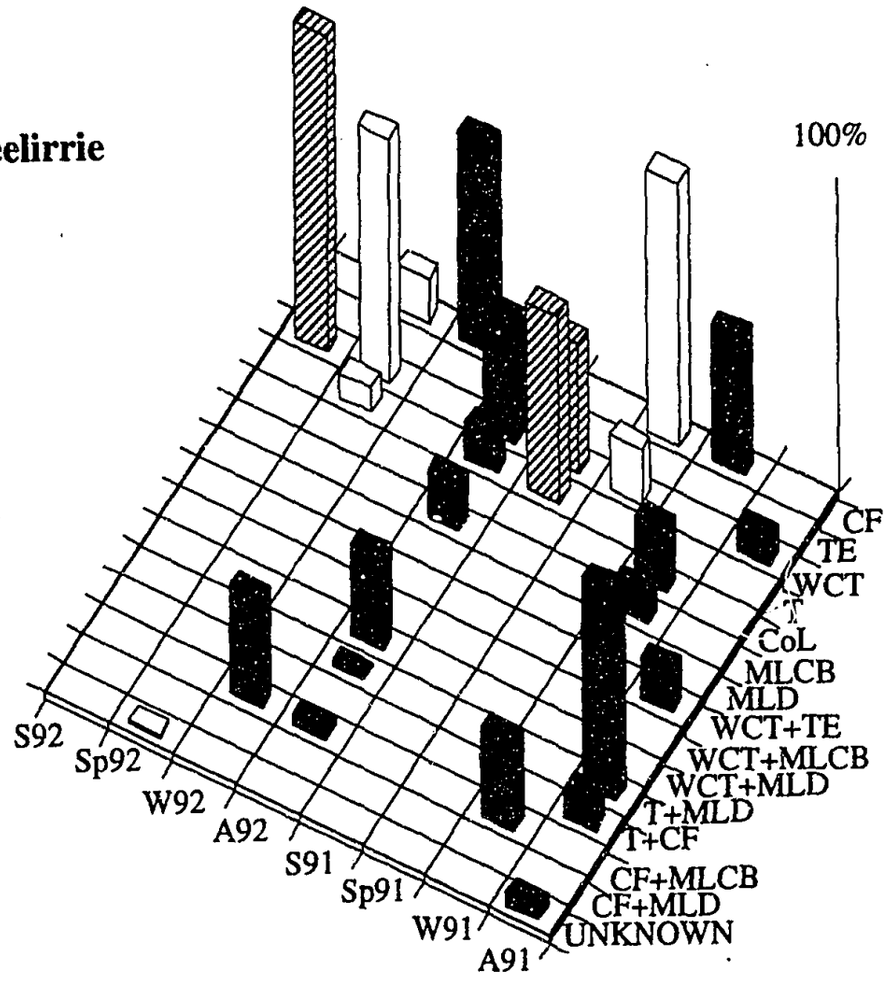

Carnegie

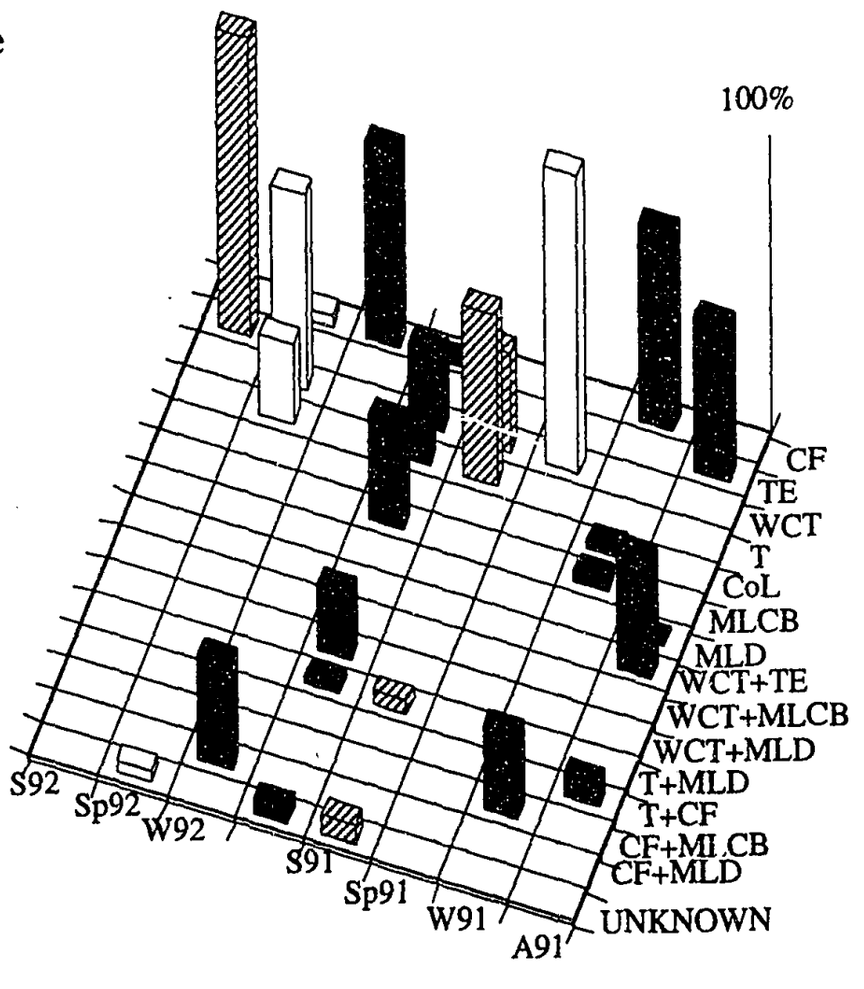

Wiluna

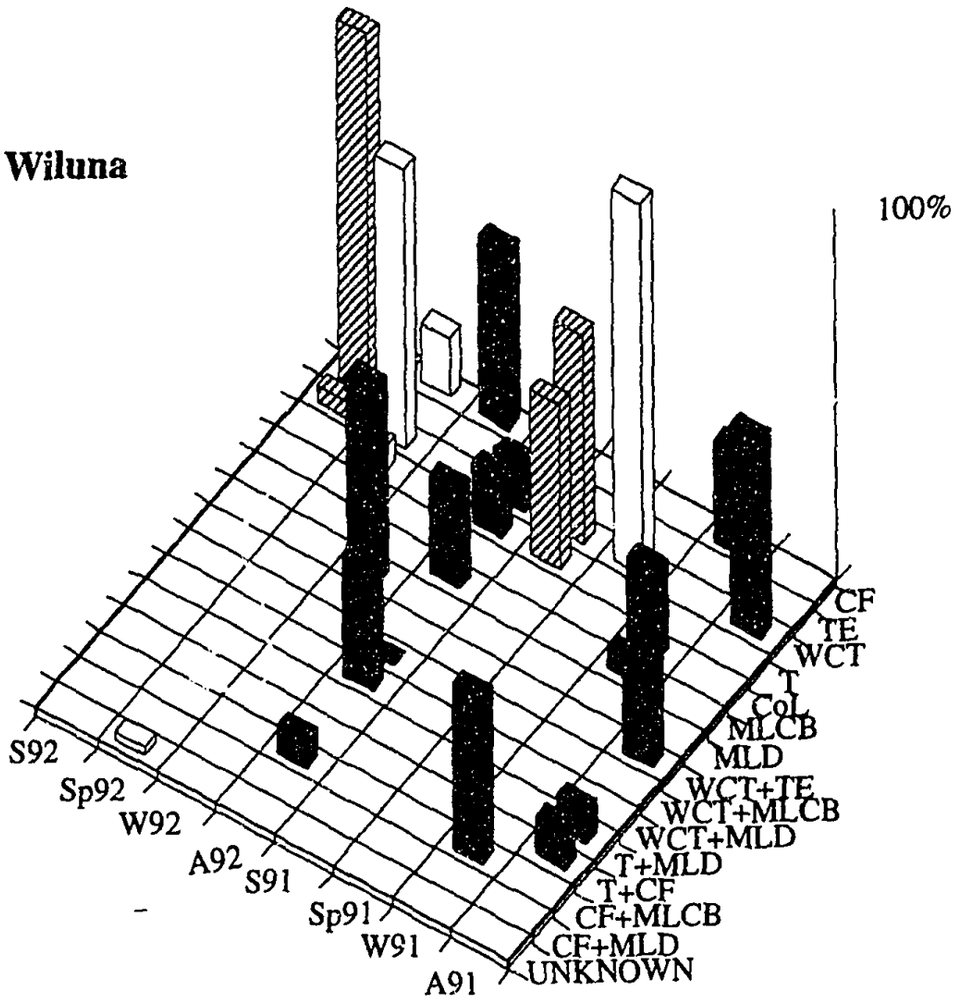

Giles

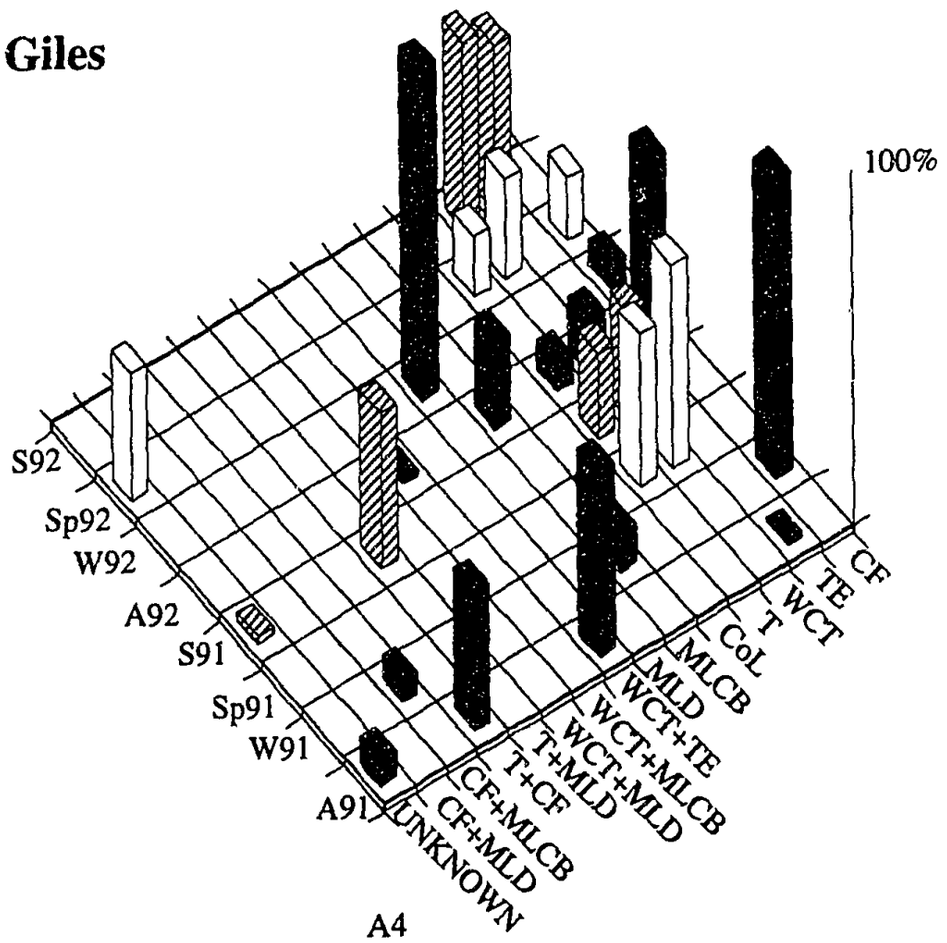

Port Lincoln

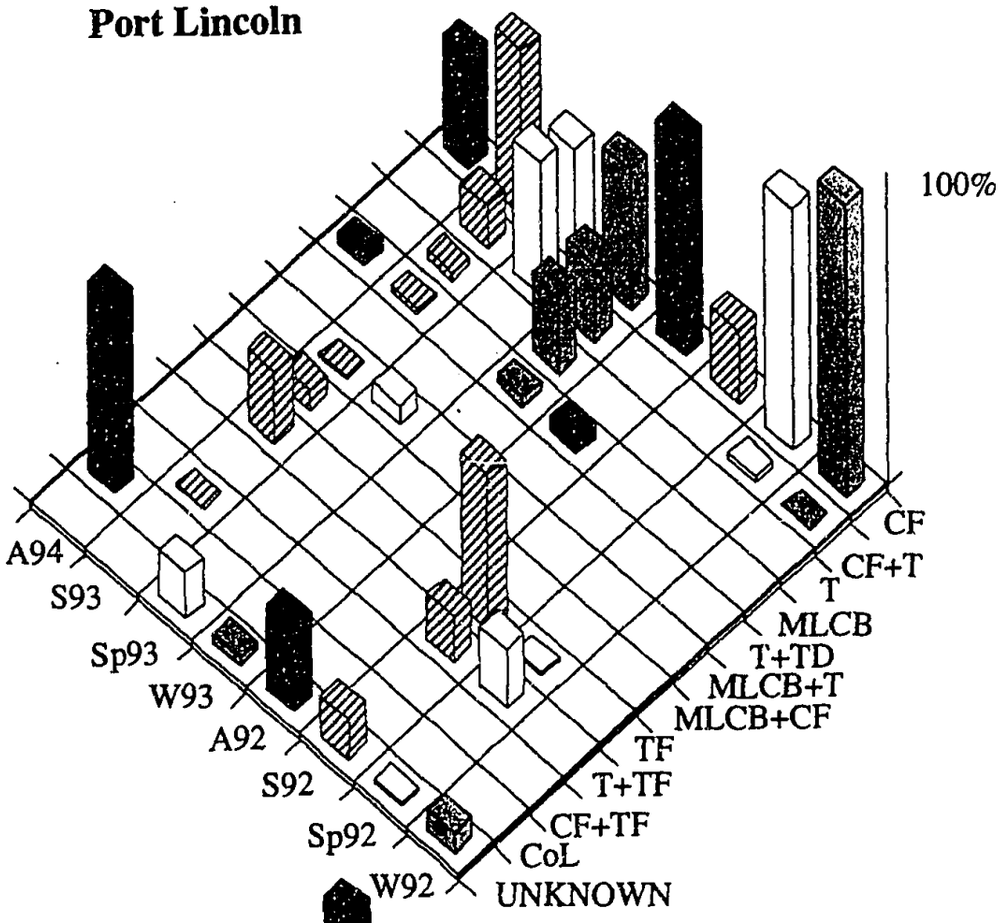

Kyancutta

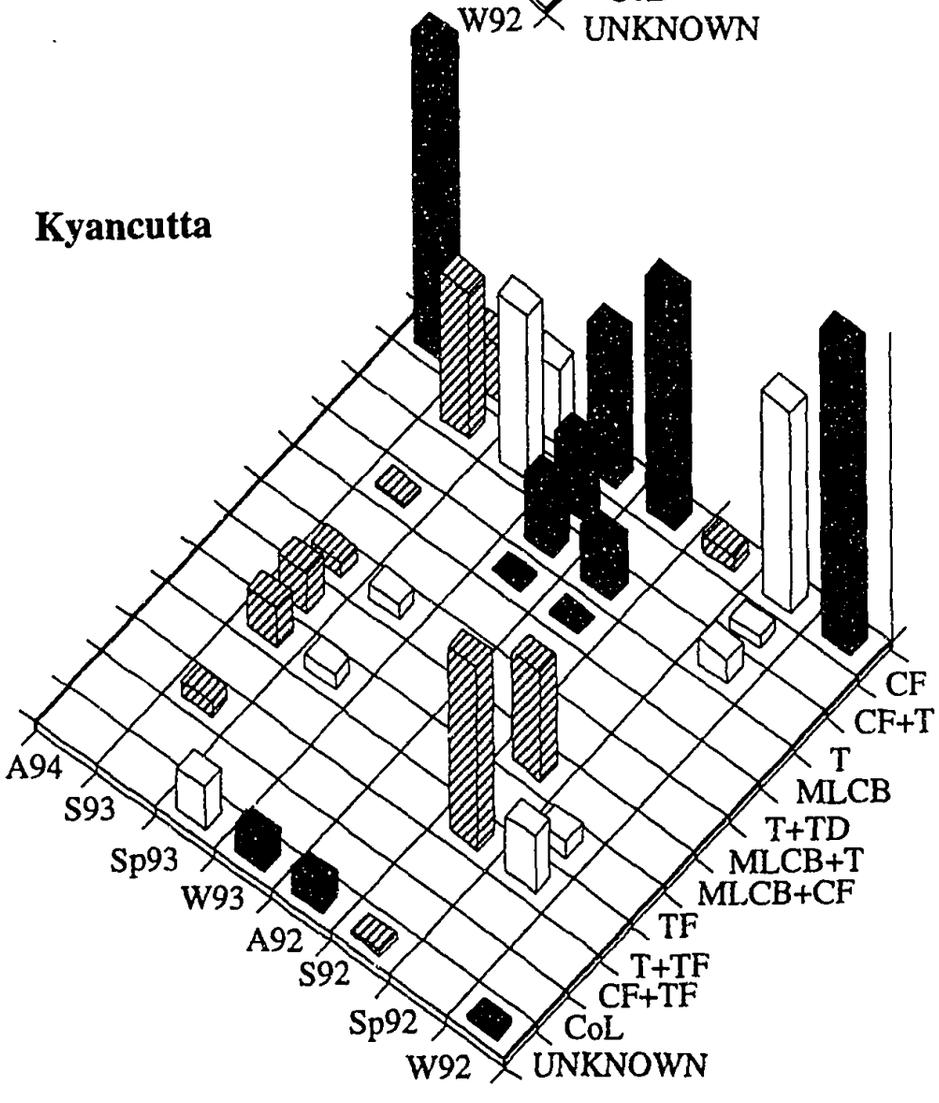

Tarcoola

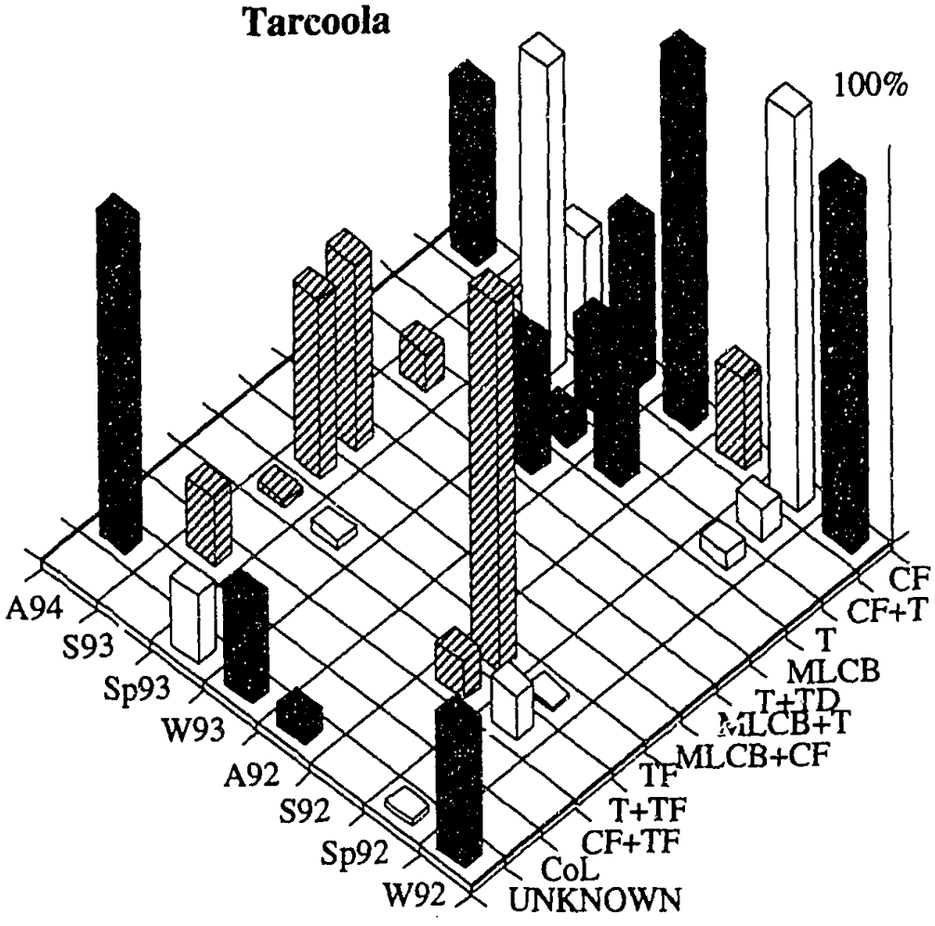

Oonandatta

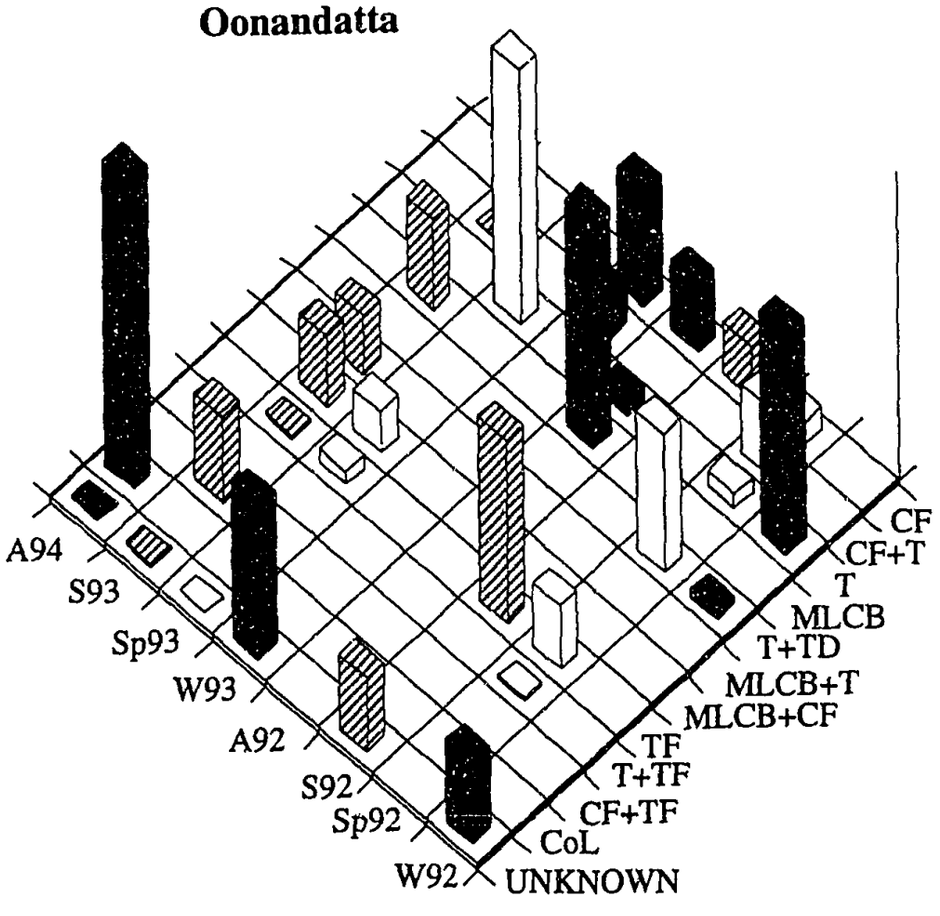

Coober Pedy

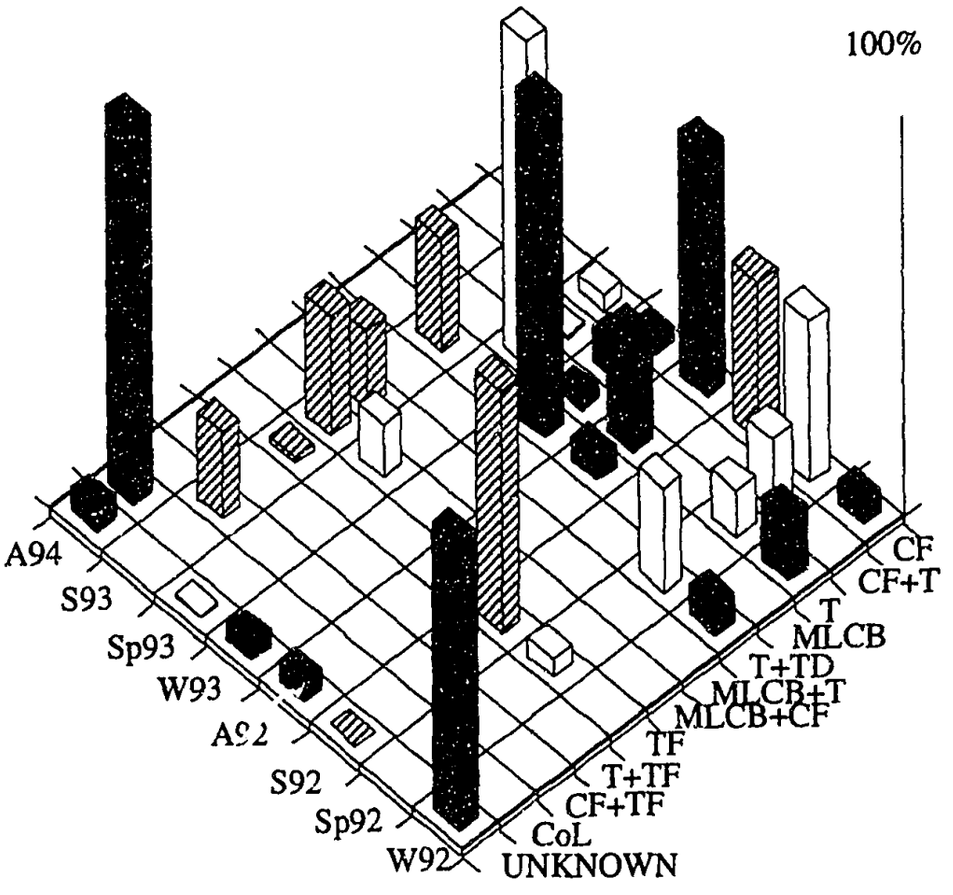

Alice Springs

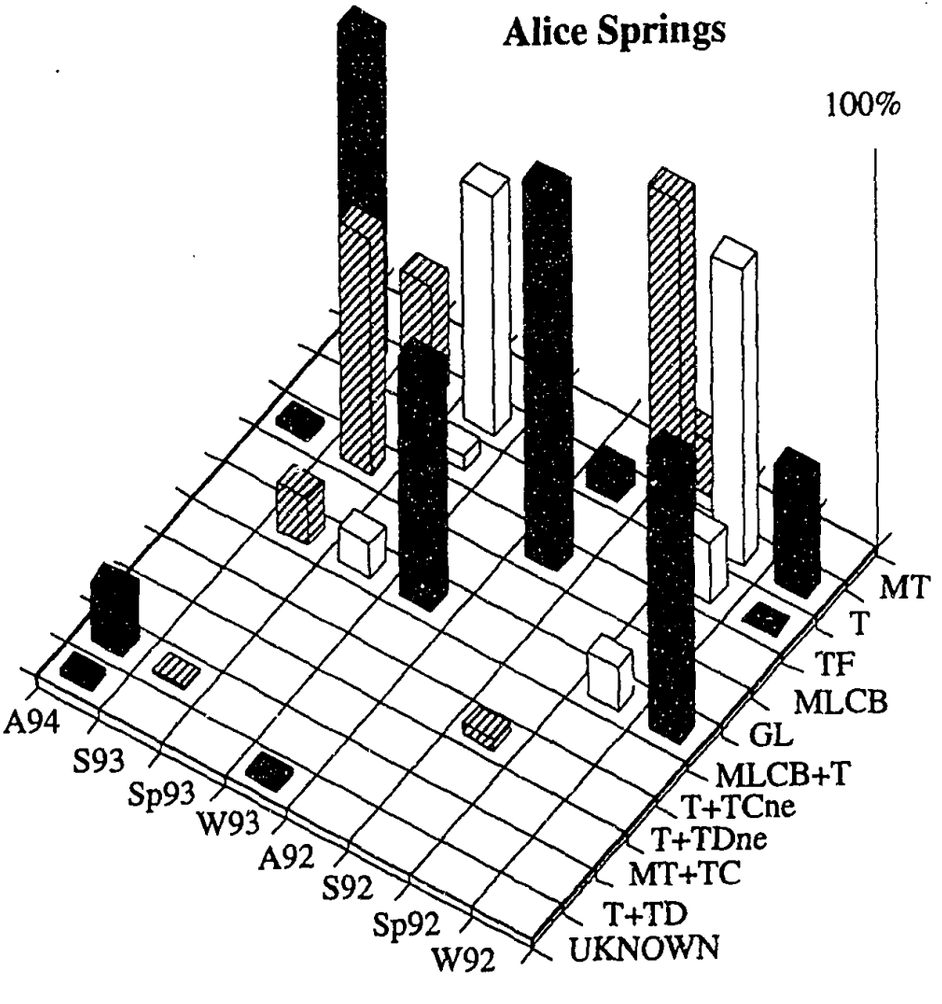

Tennant Creek

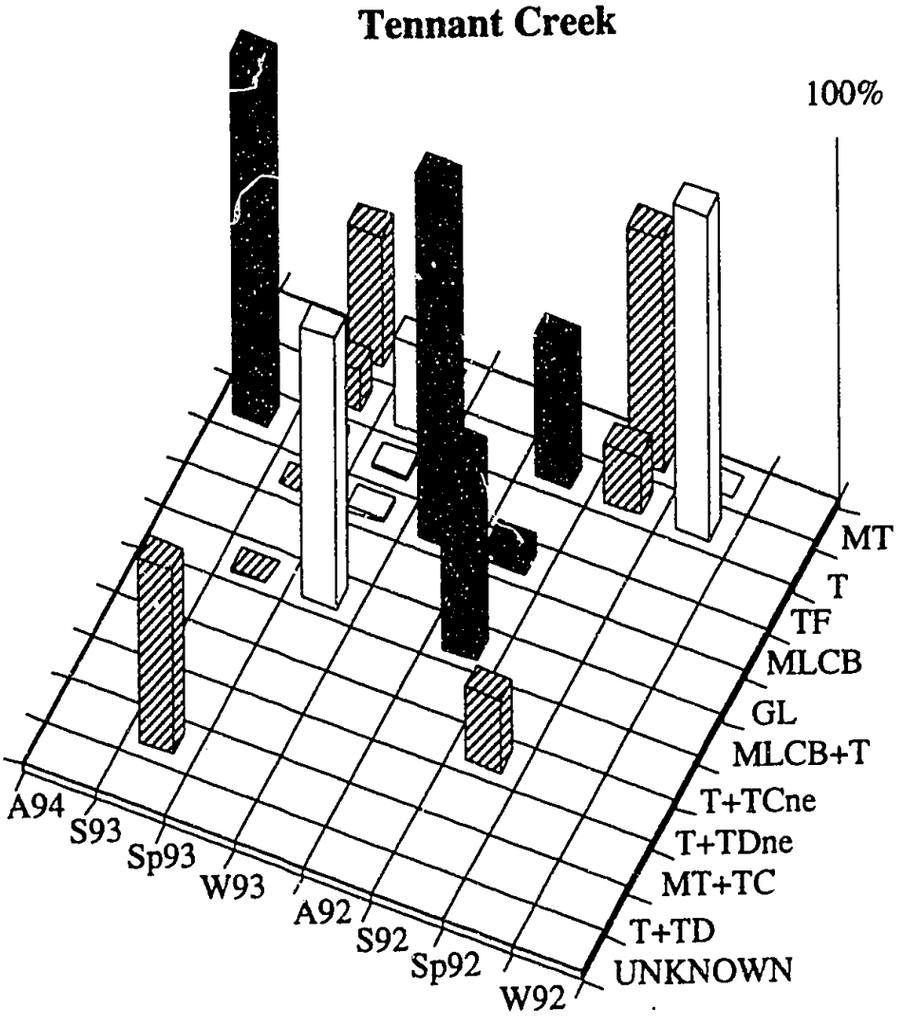

Elliott

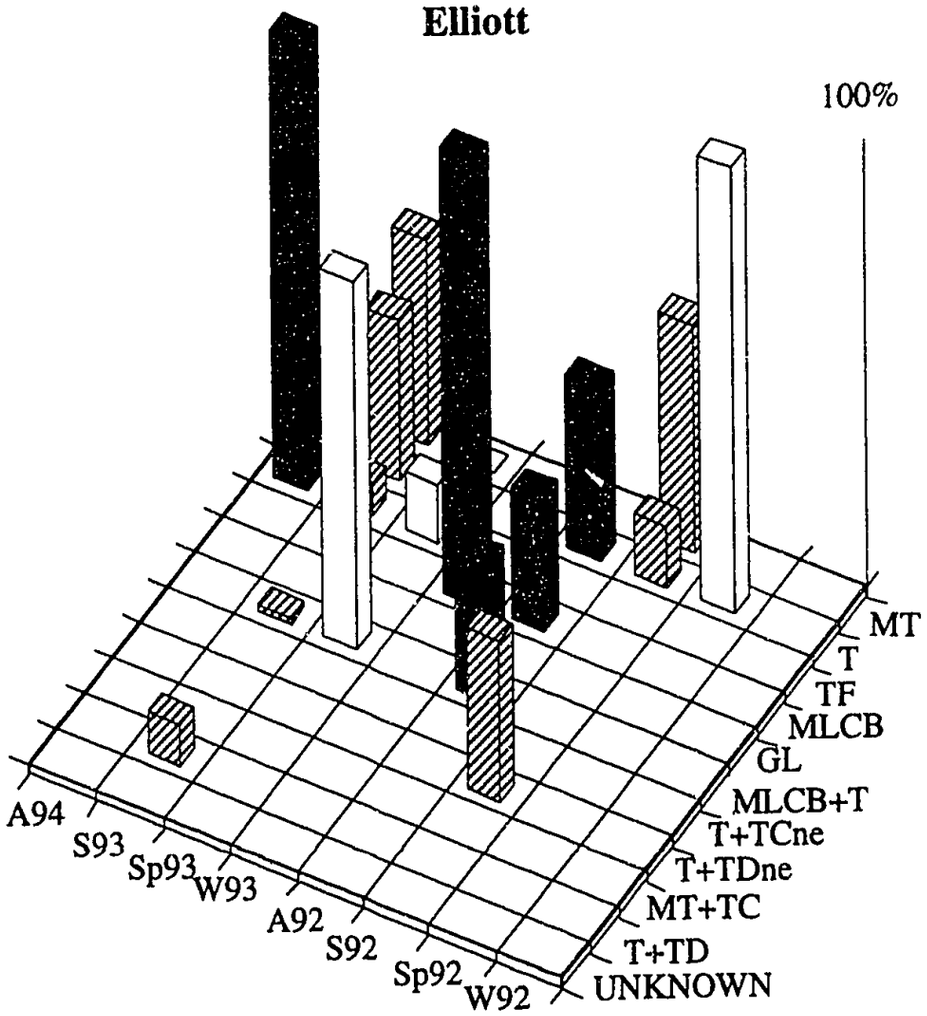

Katherine

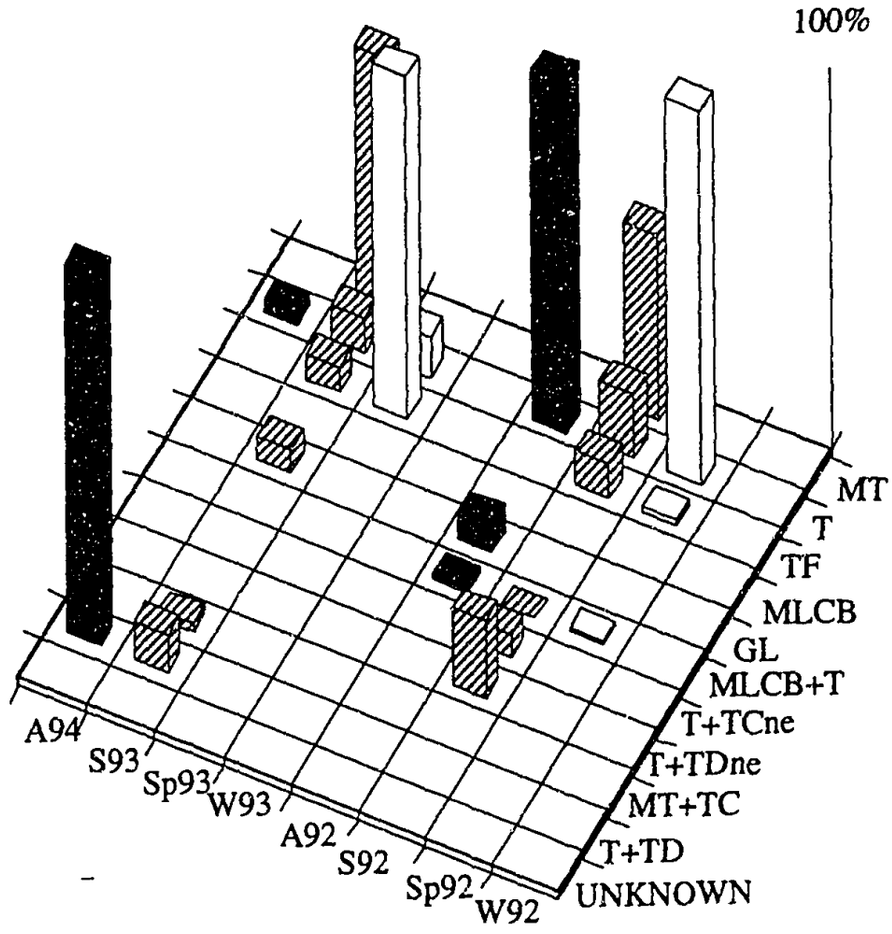

Darwin

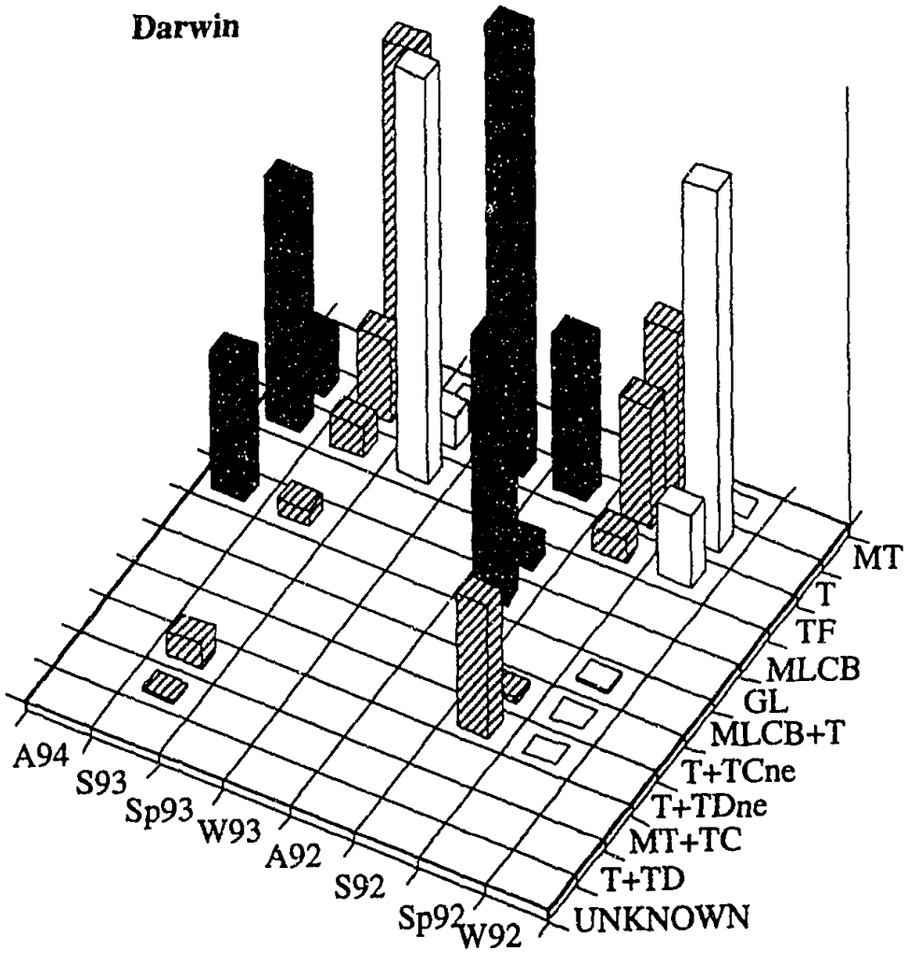

APPENDIX B DESCRIPTION OF RAIN COLLECTOR LOCALITIES

Site: 16
Name: Cliff Head
Location: 29°33'55" S, 114°38'55" E
Elevation: 10m
Physiographic Description: limestone dune ridge covered by aeolian sand; Quaternary
Vegetation: dune type and spinifex
Annual Rainfall: 441 mm (Dongara 2 years of record); 470 mm (Geraldton 48 years of record)
Rainfall Regime: winter rainfall
Climate: temperate coastal, influenced by IsTm
Land Use: recreation

Site: 17
Name: Morawa
Elevation: 409m
Location: 29°12'18" S, 115°50'05" E
Physiographic Description: dissected plateau and hills; minor laterite capping; Archaean granite
Annual Rainfall: 441 mm (Dongara 2 years of record); 470 mm (Geraldton 48 years of record)
Rainfall Regime: winter rainfall
Climate: temperate, may be influenced by IsTm , influenced by sTc all year round.
Vegetation: herbland
Land Use: cattle and sheep grazing

Site: 18
Name: Badja Homestead
Location: 28°34'05" S, 116°43'56" E
Elevation: 350m
Physiographic Description: plains dissected by ridges of the Archaean plateau; Archaean basic volcanics, banded chert and iron formations
Annual Rainfall: 246 mm (Yalgoo 30 years of record)
Rainfall Regime: arid, winter/non season rain
Climate: subtropical to warm temperate, influenced by sTc in both summer and winter months

Vegetation: open shrubland; hummocky grass understorey
Land Use: sheep grazing

Site: 19
Name: Iowna Homestead
Location: 28°30'39" S, 118°04'25" E
Elevation: 300m
Physiographic Description: granitic hills, sandplains, lateritic breakaways, small salt lakes; Archaean granite
Vegetation: open shrubland; spinifex
Annual Rainfall: 234 mm (Mt Magnet 91 years of record)
Rainfall Regime: arid (winter/non season rain)
Climate: subtropical to warm temperate, influenced by sTc both summer and winter months
Land Use: sheep grazing

Site: 20
Name: Barrambie Homestead
Location: 27°32'59" S, 119°13'53" E
Elevation: 550m
Physiographic Description: granitic hills, sandplains, lateritic breakaways, small salt lakes; Archaean granite
Vegetation: open shrubland; hummocky grass understorey
Annual Rainfall: 234 mm (Sandstone 62 years of record)
Rainfall Regime: arid (winter/non season rain)
Climate: subtropical to warm temperate, influenced by sTc in both summer and winter months
Land Use: cattle and sheep grazing

Site: 21
Name: Yeelirrie
Location: 27°11'18" S, 120°03'07" E
Elevation: 500m
Physiographic Description: granitic hills, sandplains, lateritic breakaways, small salt lakes; Archaean granite
Vegetation: open shrubland; hummocky grass understorey
Annual Rainfall: 343 mm (1991-1993)
Rainfall Regime: arid (mainly summer rain)

Climate: subtropical, influenced by sTc in both summer and winter months
Land Use: cattle and sheep grazing

Site: 22
Name: Lake Violet
Location: 26°37'08" S, 121°10'51" E
Elevation: 300m
Physiographic Description: granitic hills, sandplains, lateritic breakaways, small salt lakes; Archaean granite
Vegetation: open shrubland
Annual Rainfall: 234 mm (Wiluna 30 years of record)
Rainfall Regime: arid (mainly summer rain)
Climate: subtropical, influenced by sTc in both summer and winter months
Land Use: cattle and sheep grazing

Site: 23
Name: Carnegie Station
Location: 25°46'55" S, 122°53'38" E
Elevation: 300m
Physiographic Description: sandstone tablelands, stony plains, salt lakes; Permian Officer Basin sediments
Vegetation: open shrubland
Annual Rainfall: 292 mm (Wiluna, 1991-1993)
Rainfall Regime: arid (mainly summer rain)
Climate: subtropical, influenced by sTc in both summer and winter months
Land Use: cattle and sheep grazing

Site: 24
Name: Gunbarrel Highway
Location: 25°25'13" S, 124°00'50" E
Elevation: 300m
Physiographic Description: sandy or lateritic plains of the Gibson Desert; Cretaceous sediments of the Officer Basin
Vegetation: open shrubland
Annual Rainfall: 292 mm (Wiluna, 1991-1993), 256 mm (Giles 34 years of record)
Rainfall Regime: arid (mainly summer rain)
Climate: subtropical, influenced by sTc in both summer and winter months
Land Use: none

Site: 25
Name: Everard Junction
Location: 25°25'13" S, 124°58'26" E
Elevation: 300m
sandy or lateritic plains of the Gibson Desert; Cretaceous sediments of the Officer Basin
Vegetation: open shrubland
Rainfall Regime: arid (mainly summer rain)
Annual Rainfall: 256 mm (Giles 34 years of record)
Climate: subtropical, influenced by sTc in both summer and winter months
Land Use: none

Site: 26
Name: Port Lincoln
Location: 34°52'34" S, 135°41'21" E
Elevation: 50m
Physiographic Description: low rounded hills, partially dune covered; Quaternary
Vegetation: herbland
Annual Rainfall: 491 mm (Port Lincoln 125 years of record)
Rainfall Regime: winter rainfall
Climate: temperate, may be influenced by sPm air masses during winter months, influenced by sTc all year round
Land Use: cattle and sheep grazing

Site: 27
Name: Gawler Ranges
Location: 32°41'22" S, 135°36'53" E
Elevation: 200m
Physiographic Description: rounded hills; Mid to lower Proterozoic acid volcanics of Gawler Block
Vegetation: herbland
Annual Rainfall: 318 mm (Kyancutta 61 years of record)
Rainfall Regime: winter rainfall
Climate: temperate, may be influenced by sPm air masses during winter months, influenced by sTc all year round
Land Use: cattle and sheep grazing

Site: 28
Name: Wintinna Station
Location: 27°47'49" S, 133°57'59" E
Elevation: 300m
Physiographic Description: low tablelands, siliceous and ferruginous duricrust; Cretaceous sediments
Vegetation: shrubland
Annual Rainfall: 172 mm (Tarcoola 84 years of record), 157 mm (Coober Pedy 60 years of record)
Rainfall Regime: arid (winter/non season rain),
Climate: subtropical to warm temperate, influenced by sTc in both summer and winter months
Land Use: cattle grazing

Site: 29
Name: Alice Springs
Location: 22°53'03" S, 134°03'45" E
Elevation: 650m
Physiographic Description: granitic plains with lateritic rises overlain by alluvium, sand silt and gravel; Arunta Block metamorphosed granite and gabbro
Vegetation: shrubland with hummocky grass understorey
Annual Rainfall: 282 mm (Alice Springs 49 years of record)
Rainfall Regime: arid (mainly summer rain)
Climate: subtropical, influenced by sTc in both summer and winter months
Land Use: cattle grazing

Site: 30
Name: Tennant Creek
Location: 19°54'30" S, 134°21'50" E
Elevation: 400m
Physiographic Description: conglomerate, chert, sandstones and dolomites of the Tennant Creek Block
Vegetation: shrubland with hummocky grass and small eucalypt and acacia
Annual Rainfall: 427 mm (Tennant Creek 21 years of record)
Rainfall Regime: arid (mainly summer rain)
Climate: subtropical, influenced by sTc in both summer and winter months
Land Use: ANU Seismic Research Station

Site: 31
Name: Dunmarra
Location: 16°47'38" S, 133°27'20" E
Elevation: 250m
Physiographic Description: black clay plains, sandy rises of laterized sandstone; Cretaceous sediment.
Vegetation: open woodlands
Annual Rainfall: 574 mm (Daly Waters 78 years of record)
Rainfall Regime: summer rainfall,
Climate: tropical monsoon, influenced Tc during winter months and Tm (Pacific) and Tc air masses during summer months
Land Use: cattle grazing

Site: 32
Name: Katherine
Location: 14°37'47" S, 132°27'16" E
Elevation: 200m
Physiographic Description: shallowly dissected plateau of laterized sandstone and alluviated valleys; sediments of Daly River Basin (~500 my)
Annual Rainfall: 973 mm (Katherine 114 years of record)
Rainfall Regime: summer rainfall
Climate: tropical monsoon, influenced Tc during winter months and Tm (north of Australia) and Tc air masses during summer months
Vegetation: tropical savannah with scattered small eucalyptus
Land Use: cropping and pastoral

Site: 33
Name: Kapalga
Location: 12°40'54" S, 132°25'11" E
Elevation: 0-10m
Physiographic Description: dissected lateritic lowlands, coastal estuarine and alluvial plains; sediments in Pine Creek Geosyncline (~500 my)
Vegetation: open tropical forest with eucalyptus
Annual Rainfall: 1480 mm (Jabiru 18 years of record), 1668 (Darwin Airport 50 years of record)
Rainfall Regime: summer rainfall
Climate: tropical monsoon, influenced Tc during winter months and Tm (north of Australia) and Tc air masses during summer months

Land Use: Research Station for Division of Wildlife and Ecology, C.S.I.R.O. The main research activity is an investigation into the effects of fire on the tropical ecosystem at Kapalga. The research station is divided into compartments separated by fire breaks. Each of these compartments is subjected to a particular burning regime, early, progressive, late and natural. The rain collector was located in a compartment of natural burning (i.e. in which no man-made fires were lit). However, the collector was affected by ash fallout associated with burning elsewhere in the research station and Kakadu. Burning of vegetation is a common practise in the northern parts of the Northern Territory. By locating the rain collector in the C.S.I.R.O research station, it was felt that at least this burning was monitored.

Physiographic Description based upon Jennings and Mabbutt, in "Australia: a Geography", D.N. Jeans editor, Sydney University Press, Sydney 1977 and Geological Map of Australia 1976

Vegetation description based upon "Australia: a Geography", D.N. Jeans editor, Sydney University Press, Sydney 1977

Annual Rainfall from Bureau of Meteorology; *Rainfall Regime* from Bureau of Meteorology, "Climate of Australia", AGPS, Canberra 1979

Climate from Gentilli, "World Survey of Climatology, Australia and New Zealand", Eleseiver, Amsterdam 1977; Linarce and Hobbs, The Australian Climatic Environment, John Wiley and Sons, Brisbane 1982; Tapper and Hurry, "Australia's Weather Patterns", Dellasta, Victoria 1994.

APPENDIX C THE CHEMICAL COMPOSITION OF SOIL/DUST AT EACH SITE

The chemical composition of solutions produced after leaching soil/dust collected at each rain collector site in Milli-Q® water for 2 months. Concentration units are µeq/L. b.d is below detection.

site	Cl	error	SO_4	error	NO_3	error	HPO_4	error
Cliff Head 16	2.7	0.2	11.9	0.02	87.3	0.15	2.86	0.01
Morawa 17	0.5	0.017	3.2	0.3	96.3	0.1	b.d	b.d
Badja 18	1.6	0	0.66	0.171	27.9	0.06	b.d	b.d
Iowna 19	0.23	0.02	1.2	0.48	11.7	0.11	b.d	b.d
Barrambie 20	0.28	0.011	2.2	0	4.1	0.03	b.d	b.d
Yeelirrie 21	9.2	0.07	3.5	0.2	38.5	0.2	b.d	b.d
Lake Violet 22	5.6	0.17	43.4	0.91	83.6	0.66	b.d	b.d
Carnegie 23	2.3	0.11	1.5	0.18	22.1	0.07	b.d	b.d
Gunbarrel 24	0.28	0	0.21	0	1.3	0.05	b.d	b.d
Everard Junction 25	0.26	0.037	1	0	4.6	0.09	b.d	b.d
Gawler Ranges 27	0.03	0.002	0.24	0.004	11.5	0.08	b.d	b.d
Wintinna 28	0.28	0	0.42	0.092	13.2	0.14	b.d	b.d
Alice Springs 29	0.28	0	1.3	0.05	19.8	0.3	7.34	0.22
Tennant Creek 30	0.09	0.026	0	0	2.3	0.11	b.d	b.d
Dunmarra 31	0.28	0	0.56	0.057	7.4	0.58	b.d	b.d
Katherine 32	0.28	0	1.2	0.09	1.3	0.01	2.63	0
Kapalga 33	0.28	0	0	0	0.62	0	0	b.d

site	Na	error	K	error	Ca	error	Mg	error
Cliff Head 16	17.4	0.19	6.8	0.01	1396	22	161	2
Morawa 17	6	0.19	7.2	0.01	67	4.55	30.7	2.05
Badja 18	10.1	0.15	20.7	0.04	9.3	1.13	6.9	0.49
Iowna 19	2.9	0.13	2.7	0.01	14.1	1.59	4.5	0.28
Barrambie 20	1.4	0.01	1.2	0.02	3.8	0.64	1.8	0.23
Yeelirrie 21	12.8	0.3	9.1	0.01	12.4	1.14	13.6	0.69
Lake Violet 22	15.1	0.25	12.2	0.04	100	3	29.1	1.27
Carnegie 23	33.9	0.41	46.8	0.09	3.8	0.77	9.2	0.27
Gunbarrel 24	1.5	0.01	3.1	0.02	1.8	0.58	1.4	0.33
Everard Junction 25	1.4	0.02	3.1	0.34	2.7	0.76	2.1	0.22
Gawler Ranges 27	8	0.67	17.9	0.05	26.6	1.49	22	0.36
Wintinna 28	3.9	0.34	15.4	0.66	17.3	1.82	13.6	0.61
Alice Springs 29	1.6	0.19	37.3	0.21	10.4	0.95	20.3	0.74
Tennant Creek 30	1.4	0.11	5.7	0.46	2.4	0.64	2.3	0.37
Dunmarra 31	1.3	0.03	3.7	0.1	3.2	0.68	2.1	0.31
Katherine 32	1.5	0.09	47.1	2.74	24.2	1.96	40.5	3.58
Kapalga 33	1.4	0.02	5.3	0.07	2.6	0.63	4.4	0.53

APPENDIX D WE AND SN MAJOR-ELEMENT DATA SETS

H, Cl, SO_4, NO_3, HPO_4, Br, Na, K, NH_4, Ca and Mg in depositional units $\mu eq/m^2/day$, na is not measured, rainfall volume in brackets is mm of Milli-Q® used to leach dry bottle

WE Data Set

site	season	rainfall mm	error	time days	evaporation %	error	H	error
16	A91	36	2	80	6	5	na	na
16	W91	343	10	107	25	4	na	na
16	Sp91	87	5	69	5	5	na	na
16	S91	57	4	79	0	5	0.19	0.014
16	A92	154	6	136	16	4	0.63	0.025
16	W92	220	7	102	8	4	0.99	0.032
16	Sp92	54	4	56	0	5	0.17	0.013
16	S92	5	3	102	83	2	na	na
17	A91	45	2	80	21	4	na	na
17	W91	168	7	107	19	4	na	na
17	Sp91	63	3	70	4	5	na	na
17	S91	35	2	78	0	5	0.59	0.034
17	A92	236	10	137	42	4	0.83	0.035
17	W92	215	9	101	2	5	9.32	0.393
17	Sp92	71	3	56	4	5	2.85	0.123
17	S92	17	1	102	96	1	na	na
18	A91	36	2	81	27	4	na	na
18	W91	94	4	107	17	4	na	na
18	Sp91	33	1	70	31	4	na	na
18	S91	31	1	79	7	5	10.8	0.36
18	A92	236	10	137	5	4	1.33	0.057
18	W92	124	5	90	4	5	2.89	0.118
18	Sp92	32	1	66	0	5	0.92	0.030
18	S92	2.61	1	102	0	0	na	na
19	A91	31	1	83	14	4	na	na
19	W91	134	5	107	22	4	na	na
19	Sp91	22	1	71	0	4	na	na
19	A92	262	6	142	1	4	3.64	0.086
19	W92	128	5	87	6	4	8.53	0.342
19	Sp92	75	3	65	14	4	11.1	0.47
19	S92	22	1	103	71	2	na	na
20	A91	33	1	83	16	4	na	na
20	W91	70	3	107	9	4	na	na
20	Sp91	4	1	71	44	0	na	na
20	S91	59	2	77	0	5	2.60	0.090
20	W92	120	5	87	34	3	0.46	0.019
20	Sp92	37	1	67	0	5	6.79	0.313
20	S92	40	2	102	7	5	8.75	0.440
21	A91	35	2	82	14	4	na	na
21	W91	63	3	107	45	3	na	na
21	Sp91	1	1	71	0	173	na	na

site	season	rainfall mm	error	time days	evaporation %	error	H	error
21	S91	35	2	77	9	4	0.77	0.044
21	A92	245	10	139	20	4	7.57	0.374
21	W92	38	2	87	8	4	1.46	0.077
21	Sp92	45	2	67	22	3	3.16	0.174
21	S92	44	2	104	26	6	0.12	0.006
22	A91	16	1	81	28	4	na	na
22	W91	60	3	107	0	5	na	na
22	Sp91	2	1	72	54	15	na	na
22	S91	48	2	76	22	4	2.71	0.114
22	A92	255	10	140	20	1	3.50	0.194
22	W92	13	1	87	32	4	0.31	0.024
22	Sp92	55	2	68	37	3	2.74	0.130
22	S92	13	1	106	60	2	0.01	0.001
23	A91	16	1	82	44	3	na	na
23	W91	153	6	107	53	2	na	na
23	Sp91	1.25	1	71	0	0	na	na
23	S91	55	2	77	34	3	2.36	0.089
23	A92	194	4	139	0	5	4.73	0.166
23	W92	31	1	86	1	5	0.68	0.022
23	Sp92	20	0	68	4	4	1.48	0.014
23	S92	33	2	107	0	3	0.29	0.018
24	A91	36	2	83	13	4	na	na
24	W91	118	5	107	60	2	na	na
24	Sp91	14	1	72	6		na	na
24	A92	265	11	141	50	0	6.21	0.368
24	W92	31	1	84	0	0	3.69	0.142
24	S92	79	3	108	25	3	0.31	0.012
25	A91	11	1	83	72	2	na	na
25	W91	118	5	107	45	2	na	na
25	Sp91	50	2	72	11	4	na	na
25	A92	191	8	140	1	1	11.23	0.64
25	W92	22	1	83	0	1	2.84	0.145

SN Data Set

site	season	rainfall mm	error	time days	evaporation %	error	H	error
26	W92	199	8	90	10	4	21	0.880
26	Sp92	334	14	101	23	4	1.53	0.063
26	S92	70	3	104	4	5	0.29	0.012
26	W93	227	9	90	38	3	7.61	0.314
26	Sp93	93	4	72	7	4	6.48	0.271
26	S93	41	2	105	36	3	7.09	0.309
26	A93	103	4	107	7	4	1.21	0.050
27	W92	70	3	90	0	0	0.98	0.041
27	Sp92	299	12	100	18	4	2.97	0.122
27	S92	144	6	104	39	3	0.38	0.016
27	A93	40	2	83	1	5	0.18	0.008

site	season	rainfall mm	error	time days	evaporation %	error	H	error
27	W93	97	4	88	6	4	0.32	0.013
27	W93	97	4	88	6	4	0.29	0.012
27	Sp93	83	3	71	26	4	1.11	0.047
27	Sp93	83	3	71	29	3	0.48	0.020
27	S93	60	3	105	10	4	5.03	0.213
27	S93	60	3	105	10	4	0.73	0.031
27	A93	37	2	106	17	4	0.02	0.001
27	A93	37	2	106	13	4	0.02	0.001
28	W92	27	1	90	0	5	0.93	0.044
28	sp92	134	6	104	45	2	2.54	0.109
28	S92	31	1	105	49	2	0.05	0.002
28	A93	31	1	82	0	0	0.11	0.005
28	W93	49	2	89	6	4	0.18	0.008
28	Sp93	66	3	72	52	2	2.04	0.087
28	S93	74	7	106	37	6	0.26	0.023
28	A94	43	2	104	11	4	0.53	0.023
29	W92	10	1	84	0	0	0.15	0.011
29	Sp92	69	3	105	34	3	2.18	0.095
29	A93	149	6	82	0	0	10.43	0.571
29	W93	14	1	89	13	5	0.12	0.007
29	Sp93	62	3	70	26	3	3.76	0.161
29	S93	85	7	105	60	3	0.56	0.045
29	A94	2	0	106	0	0	0.00	0.000
30	W92	0 (2)	0	85	0	0	0.00	0.000
30	Sp92	57	2	103	35	3	5.98	0.277
30	W93	5	1	90	66	4	0.01	0.001
30	Sp93	59	6	70	13	10	0.97	0.105
30	S93	56	2	105	0	0	0.03	0.001
30	A94	0 (3)	0	106	0	0	0.37	0.012
31	W92	0 (2)	0	86	0	0	0.00	0.000
31	Sp92	57	2	103	13	4	1.89	0.081
31	W93	0 (1)	0	89	0	0	0.00	0.000
31	Sp93	94	4	70	0	0	28.58	2.088
31	S93	768	54	105	0	0	3.19	0.226
31	A94	0 (5)	0	106	0	0	0.13	0.001
32	W92	0 (4)	0	86	0	0	0.00	0.000
32	Sp92	209	9	104	16	4	0.95	0.039
32	A93	0 (3)	0	79	0	0	0.01	0.000
32	W93	0 (3)	0	89	0	0	0.00	0.000
32	S93	854	64	108	0	0	26.81	2.040
32	A94	11	0	106	0	0	0.01	0.000
33	W92	0 (3)	0	80	0	0	0.00	0.000
33	Sp92	290	12	102	0	5	9.84	0.914
33	A93	59	2	80	0	0	1.04	0.044
33	W93	0 (3)	0	89	0	0	0.00	0.000
33	S93	866	40	104	0	0	7.09	0.329

WE Data Set

site	season	Cl	error	SO_4	error	NO_3	error	HPO_4	error	Br	error
16	A91	154	9.7	25.2	1.41	25.4	1.42	1.41	0.267	0.15	0.018
16	W91	1151	41.1	127	3.8	4.65	0.143	0.50	0.015	1.20	0.036
16	Sp91	701	42.9	83.8	4.87	5.99	0.352	0.25	0.014	0.79	0.048
16	S91	122	9.0	26.4	1.89	18.0	1.32	1.65	0.193	0.05	0.003
16	A92	207	8.9	26.5	1.36	5.22	0.266	0.02	0.001	0.06	0.002
16	W92	701	26.0	108	4.3	7.04	0.478	38.0	2.03	0.12	0.004
16	Sp92	477	41.0	69.6	5.82	6.72	0.647	1.81	0.196	0.54	0.064
16	S92	33.4	20.08	6.23	3.746	0.11	0.066	1.01	0.610	0.00	0.001
17	A91	45.9	2.29	12.2	0.55	11.4	0.51	0.83	0.047	0.07	0.017
17	W91	229	10.5	28.8	1.21	3.08	0.153	0.26	0.011	0.24	0.033
17	Sp91	121	6.2	22.5	1.15	7.66	0.376	2.52	0.123	0.12	0.022
17	S91	22.0	1.36	14.3	0.86	12.4	0.76	0.01	0.001	0.03	0.002
17	A92	58.9	3.02	11.9	0.64	7.09	0.435	0.02	0.001	0.06	0.003
17	W92	170	8.0	31.3	1.51	4.37	0.304	0.04	0.002	0.13	0.006
17	Sp92	113	6.8	28.2	1.62	4.55	0.254	1.14	0.075	0.11	0.013
17	S92	4.29	0.32	2.43	0.168	2.57	0.188	0.62	0.047	0.01	0.001
18	A91	12.9	0.74	7.22	0.41	6.70	0.374	0.88	0.073	0.02	0.001
18	W91	68.7	3.27	10.3	0.46	3.18	0.159	0.15	0.007	0.05	0.002
18	Sp91	38.4	1.40	17.9	0.57	11.8	0.37	0.47	0.069	0.08	0.005
18	S91	13.0	0.44	13.4	0.47	13.0	0.50	0.76	0.155	0.02	0.001
18	A92	31.9	1.82	11.2	0.69	7.39	0.497	0.03	0.001	0.10	0.004
18	W92	83.6	4.07	17.1	0.84	2.99	0.296	0.03	0.001	0.08	0.003
18	Sp92	19.8	1.04	11.5	0.57	5.06	0.242	0.54	0.028	0.04	0.004
18	S92	5.41	2.088	5.57	2.143	3.27	1.261	0.00	0.000	0.00	0.001
19	A91	9.06	0.348	6.82	0.224	5.60	0.191	0.33	0.011	0.29	0.010
19	W91	51.5	2.38	10.8	0.44	4.88	0.214	0.20	0.008	0.06	0.002
19	Sp91	29.0	1.51	22.1	1.02	10.6	0.85	0.06	0.003	0.05	0.002
19	A92	29.9	1.29	12.2	0.61	9.43	0.510	0.04	0.001	0.11	0.003
19	W92	44.1	2.56	14.1	0.67	3.57	0.242	0.03	0.001	0.09	0.003
19	Sp92	10.7	0.61	15.7	0.87	6.56	0.353	0.02	0.001	0.06	0.003
19	S92	12.8	0.84	20.1	1.18	10.9	0.69	3.44	0.304	0.04	0.004
20	A91	9.14	0.339	7.72	0.243	6.79	0.210	0.42	0.025	0.02	0.001
20	W91	14.6	0.71	5.08	0.220	2.98	0.130	0.12	0.005	0.04	0.002
20	Sp91	9.5	2.390	13.5	3.37	4.34	1.084	1.45	0.362	0.02	0.005
20	S91	15.3	0.57	14.5	0.53	20.5	0.95	0.02	0.001	0.05	0.002
20	W92	25.2	1.51	11.7	0.57	3.38	0.26	0.02	0.001	0.06	0.002
20	Sp92	5.30	0.345	10.9	0.51	6.46	0.289	0.53	0.048	0.03	0.003
20	S92	8.86	0.612	14.1	0.87	8.04	0.532	0.01	0.000	0.02	0.001
21	A91	8.91	0.552	6.49	0.378	5.15	0.299	0.08	0.004	0.02	0.001
21	W91	6.49	0.323	3.30	0.158	1.98	0.095	0.07	0.003	0.02	0.001
21	Sp91	4.12	4.124	7.77	7.768	3.26	3.265	0.00	0.003	0.00	0.003
21	S91	14.1	0.84	16.0	0.94	13.3	0.81	0.01	0.000	0.05	0.003
21	A92	8.35	0.525	8.80	0.546	9.10	0.555	0.03	0.001	0.09	0.004
21	W92	12.4	0.84	5.60	0.327	2.20	0.172	1.76	0.125	0.03	0.001
21	Sp92	3.38	0.225	8.37	0.491	5.71	0.329	0.37	0.025	0.03	0.001
21	S92	5.03	0.328	6.11	0.361	6.27	0.395	1.55	0.101	0.02	0.001

site	season	Cl	error	SO_4	error	NO_3	error	HPO_4	error	Br	error
22	A91	5.46	0.363	4.80	0.302	5.16	0.324	0.03	0.002	0.01	0.005
22	W91	6.80	0.355	3.73	0.209	4.07	0.208	0.12	0.006	0.04	0.002
22	Sp91	2.79	1.396	3.87	1.937	1.63	0.815	0.00	0.001	0.00	0.002
22	S91	11.1	0.50	12.3	0.54	17.6	0.81	0.51	0.057	0.03	0.001
22	A92	6.17	0.484	6.97	0.467	6.58	0.359	0.03	0.001	0.09	0.004
22	W92	6.82	0.554	4.19	0.337	1.34	0.129	0.00	0.000	0.01	0.000
22	Sp92	3.84	0.206	6.94	0.366	5.04	0.258	1.05	0.137	0.06	0.006
22	S92	4.40	0.395	5.04	0.428	5.19	0.459	1.17	0.106	0.00	0.000
23	A91	4.81	0.316	5.12	0.322	4.04	0.254	0.18	0.011	0.01	0.002
23	W91	5.12	0.277	4.76	0.212	3.36	0.133	0.14	0.006	0.04	0.002
23	Sp91	5.27	4.220	10.3	8.22	3.79	3.031	0.14	0.112	0.01	0.005
23	S91	10.5	0.47	9.81	0.392	16.2	0.68	0.01	0.000	0.03	0.001
23	A92	5.51	0.420	10.5	0.43	9.9	0.427	0.03	0.001	0.09	0.002
23	W92	4.73	0.274	5.57	0.224	2.42	0.160	0.01	0.000	0.02	0.001
23	Sp92	5.73	0.559	10.3	0.39	7.02	0.252	0.71	0.030	0.04	0.004
23	S92	1.10	0.110	1.84	0.130	1.52	0.113	0.33	0.077	0.02	0.001
24	A91	7.24	0.457	7.54	0.422	4.75	0.265	0.08	0.004	0.02	0.001
24	W91	3.36	0.156	2.57	0.191	2.63	0.112	0.09	0.004	0.03	0.001
24	Sp91	5.57	0.413	7.80	0.574	4.92	0.355	0.11	0.011	0.02	0.003
24	A92	3.98	0.313	7.04	0.422	7.73	0.441	0.02	0.001	0.06	0.002
24	W92	6.25	0.395	8.06	0.330	3.45	0.224	0.01	0.000	0.02	0.001
24	S92	2.14	0.189	3.25	0.172	2.75	0.159	1.09	0.065	0.03	0.001
25	A91	4.15	0.395	6.96	0.634	4.28	0.390	0.13	0.012	0.00	0.000
25	W91	2.74	0.207	3.53	0.151	2.35	0.102	0.13	0.005	0.04	0.002
25	Sp91	7.85	0.472	11.4	1.09	8.17	0.336	0.13	0.005	0.02	0.001
25	A92	4.57	0.786	10.7	0.59	11.5	0.69	0.03	0.001	0.08	0.004
25	W92	4.34	0.311	5.74	0.294	2.69	0.194	0.01	0.000	0.02	0.001

NS Data Set

site	season	Cl	error	SO_4	error	NO_3	error	HPO_4	error	Br	error
26	W92	910	58.2	106	5.0	7.09	0.505	0.41	0.017	1.17	0.158
26	Sp92	539	50.6	118	7.9	9.6	0.903	0.53	0.022	0.76	0.121
26	S92	376	22.4	51.9	2.92	10.2	0.61	4.01	0.234	0.33	0.057
26	W93	792	34.1	96.8	5.39	5.06	0.401	0.32	0.013	1.17	0.194
26	Sp93	424	40.4	54.5	6.08	9.5	0.832	9.5	0.853	0.23	0.024
26	S93	271	12.4	48.0	2.21	24.6	1.12	1.52	0.180	0.20	0.018
26	A93	478	21.3	110	7.9	18.4	1	42.7	2.36	0.22	0.016
27	W92	123	7.8	18.4	0.88	3.27	0.215	0.16	0.007	0.10	0.004
27	Sp92	72.8	7.05	34.0	2.35	11.1	1.03	0.51	0.021	0.31	0.013
27	S92	55.4	3.05	15.7	1.16	12.2	0.69	0.18	0.007	0.11	0.004
27	A93	33.4	1.87	11.2	0.58	6.33	0.450	0.10	0.004	0.06	0.003
27	W93	151	6.7	22.9	1.23	4.82	0.322	0.22	0.009	0.13	0.005
27	W93	158	7.8	24.1	1.27	5.26	0.500	0.22	0.009	0.13	0.005
27	Sp93	73.5	7.03	12.7	1.27	4.37	0.307	0.18	0.008	0.11	0.005
27	Sp93	61.3	5.44	14.2	1.32	10.5	0.80	0.17	0.007	0.10	0.004

site	season	Cl	error	SO_4	error	NO_3	error	HPO_4	error	Br	error
27	S93	50.9	2.26	14.3	0.66	29.5	1.28	2.96	0.248	0.41	0.112
27	S93	55.7	2.48	14.1	0.67	24.8	1.13	1.20	0.074	0.40	0.032
27	A93	77.5	4.00	11.8	0.91	2.09	0.150	0.85	0.039	0.04	0.002
27	A93	75.3	3.43	11.9	0.93	2.74	0.214	0.90	0.055	0.04	0.002
28	W92	8.36	0.598	6.11	0.335	4.34	0.300	0.06	0.003	0.04	0.002
28	sp92	6.63	0.693	11.0	0.87	9.9	0.869	0.15	0.006	0.09	0.004
28	S92	9.09	0.526	10.0	0.62	10.6	0.64	0.72	0.053	0.02	0.002
28	A93	4.34	0.244	9.6	0.844	8.18	0.626	1.13	0.075	0.05	0.002
28	W93	10.6	1.18	6.71	0.351	4.25	0.255	0.11	0.005	0.07	0.003
28	Sp93	7.70	0.809	8.15	0.762	8.60	0.637	0.09	0.004	0.06	0.002
28	S93	6.29	0.582	8.15	0.823	9.12	0.850	1.22	0.123	0.05	0.005
28	A94	5.60	0.253	5.39	0.375	1.58	0.109	2.20	0.296	0.05	0.002
29	W92	2.31	0.226	4.37	0.343	2.17	0.178	0.60	0.194	0.01	0.001
29	Sp92	4.59	0.520	10.5	0.760	9.34	0.825	0.09	0.004	0.05	0.002
29	A93	2.22	0.194	11.6	0.673	10.7	1.13	0.38	0.016	0.23	0.009
29	W93	5.34	0.540	5.07	0.338	3.35	0.234	1.06	0.077	0.02	0.001
29	Sp93	11.3	1.05	15.51	1.45	16.4	1.27	2.68	0.320	0.08	0.003
29	S93	3.23	0.288	7.51	0.655	6.64	0.557	0.86	0.194	0.04	0.003
29	A94	1.55	0.021	2.64	0.135	1.75	0.096	0.13	0.013	0.00	0.000
30	W92	0.16	0.009	0.04	0.003	0.10	0.005	0.00	0.000	0.00	0.000
30	Sp92	6.67	0.747	12.2	0.82	10.9	0.94	0.08	0.003	0.05	0.002
30	W93	0.71	0.094	1.48	0.176	0.08	0.016	0.01	0.002	0.00	0.000
30	Sp93	11.4	1.60	18.1	2.47	19.9	2.74	3.00	0.491	0.09	0.010
30	S93	22.7	1.04	32.9	1.50	8.54	0.392	61.7	3.82	0.14	0.110
30	A94	0.40	0.005	0.04	0.004	0.10	0.009	0.01	0.000	0.00	0.000
31	W92	0.10	0.008	0.06	0.005	0.10	0.005	0.00	0.000	0.00	0.000
31	Sp92	8.05	0.757	12.8	0.96	11.6	0.99	0.10	0.004	0.06	0.003
31	W93	0.27	0.01	0.11	0.007	0.12	0.005	0.17	0.005	0.00	0.000
31	Sp93	9.20	3.045	15.6	1.46	26.2	1.71	0.28	0.012	0.17	0.007
31	S93	25.2	1.87	41.1	3.58	23.2	1.74	25.6	2.19	0.92	0.065
31	A94	1.64	0.058	2.57	0.174	0.18	0.018	0.33	0.007	0.01	0.000
32	W92	0.21	0.014	0.01	0.000	0.22	0.011	0.01	0.000	0.01	0.000
32	Sp92	9.69	1.081	14.4	0.95	13.5	1.26	0.35	0.015	0.21	0.009
32	A93	3.25	0.148	1.15	0.036	0.63	0.023	2.09	0.092	0.00	0.000
32	W93	0.37	0.006	0.09	0.005	0.17	0.011	0.30	0.022	0.00	0.000
32	S93	29.5	2.36	22.3	1.78	22	2	1.65	0.123	0.99	0.074
32	A94	11.50	0.65	7.53	0.497	0.93	0.052	11.6	0.23	0.01	0.000
33	W92	1.46	0.000	0.40	0.000	0.14	0.000	0.17	0.000	0.00	0.000
33	Sp92	5.84	0.693	12.8	1.019	9.9	1	0.59	0.024	0.36	0.015
33	A93	19.0	1.09	5.50	0.307	3.87	0.218	0.15	0.007	0.09	0.004
33	W93	0.90	0.000	0.28	0.000	0.14	0.000	0.66	0.000	0.00	0.000
33	S93	64.6	3.51	31.9	1.60	24.7	1.45	1.73	0.081	1.04	0.048

WE Data Set

site	season	Na	error	K	error	NH_4	error	Ca	error	Mg	error
16	A91	122	6.8	5.63	0.31	0.12	0.007	46.8	2.61	32.5	1.82
16	W91	931	27.5	17.5	0.52	0.67	0.020	181	5.4	219	6.5
16	Sp91	614	35.6	8.00	0.463	0.33	0.019	28.9	1.67	130	7.5
16	S91	117	12.4	7.38	1.079	0.20	0.014	52.8	3.72	78.5	5.55
16	A92	184	8.4	5.28	0.225	7.24	0.500	25.0	1.11	53.7	2.13
16	W92	627	25.8	38.0	1.41	191.4	16.8	71.4	4.69	157	6.4
16	Sp92	417	33.8	10.2	1.05	28.1	4.91	66.8	5.01	100	7.6
16	S92	20.9	12.52	2.00	1.198	3.25	1.958	5.52	3.309	8.48	5.087
17	A91	39.2	1.76	1.84	0.083	1.56	0.070	7.00	0.314	9.40	0.422
17	W91	179	7.48	3.68	0.154	0.35	0.015	4.44	0.186	38.7	1.62
17	Sp91	95.9	4.62	2.65	0.128	0.24	0.012	4.57	0.220	22.3	1.07
17	S91	26.7	2.64	2.41	0.339	6.23	0.656	4.32	0.266	11.7	0.69
17	A92	56.4	2.83	3.17	0.303	21.1	1.50	8.07	0.403	17.8	0.76
17	W92	155	7.19	7.11	0.363	13.9	1.46	7.12	0.591	37.7	1.96
17	Sp92	115	6.16	5.17	0.438	11.8	1.94	9.51	0.741	26.1	1.34
17	S92	3.93	0.242	0.97	0.063	1.39	0.111	1.89	0.111	1.68	0.099
18	A91	12.5	0.70	0.80	0.045	6.80	0.380	3.84	0.214	3.08	0.172
18	W91	54.6	2.34	1.38	0.059	0.20	0.009	9.09	0.389	16.8	0.72
18	Sp91	31.7	0.99	1.76	0.055	0.09	0.003	4.59	0.143	9.14	0.285
18	S91	16.8	1.41	2.80	0.373	13.0	1.152	3.38	0.118	5.34	0.181
18	A92	30.8	1.50	2.93	0.136	36.9	2.62	8.12	0.350	13.6	0.586
18	W92	74.9	3.41	3.69	0.273	10.4	0.99	5.90	0.245	19.9	0.816
18	Sp92	22.7	1.09	1.95	0.153	10.5	1.70	3.63	0.221	5.15	0.267
18	S92	8.61	3.303	0.52	0.201	0.97	0.374	3.55	1.360	2.83	1.086
19	A91	7.13	0.234	0.11	0.004	1.27	0.042	3.30	0.108	1.81	0.059
19	W91	38.8	1.46	0.12	0.005	2.06	0.078	9.74	0.366	8.56	0.322
19	Sp91	30.5	1.40	0.04	0.002	0.09	0.004	5.33	0.245	8.96	0.412
19	A92	28.4	0.98	3.55	0.094	19.9	1.22	3.01	0.267	8.91	0.206
19	W92	42.2	1.85	2.23	0.104	4.23	0.455	3.41	0.279	11.7	0.46
19	Sp92	13.3	0.69	1.42	0.128	8.38	1.366	7.44	0.445	3.61	0.169
19	S92	15.3	0.75	4.19	0.205	16.7	1.19	3.03	0.143	2.06	0.095
20	A91	7.38	0.228	0.61	0.019	4.95	0.15	2.75	0.085	2.43	0.075
20	W91	11.3	0.49	0.30	0.013	0.17	0.007	0.59	0.026	2.51	0.108
20	Sp91	14.2	3.56	1.86	0.465	0.01	0.002	3.39	0.848	4.09	1.022
20	S91	15.0	1.27	1.96	0.260	12.3	1.10	3.94	0.146	4.02	0.146
20	W92	19.2	0.89	17.1	0.786	69.0	7.29	5.68	0.239	11.0	0.47
20	Sp92	8.00	0.360	3.22	0.255	12.4	2.02	4.77	0.157	2.48	0.095
20	S92	6.68	0.725	1.20	0.083	3.25	0.535	5.11	0.268	3.06	0.155
21	A91	6.18	0.355	0.23	0.013	1.57	0.090	3.11	0.179	1.64	0.094
21	W91	5.39	0.258	0.27	0.013	0.09	0.004	0.39	0.019	1.07	0.051
21	Sp91	8.50	8.497	0.50	0.498	0.00	0.004	2.38	2.377	2.48	2.479
21	S91	16.2	1.56	1.48	0.215	5.52	0.553	2.37	0.148	1.93	0.114
21	A92	9.32	0.488	1.62	0.069	13.4	1.15	1.93	0.094	3.26	0.212
21	W92	10.4	0.59	1.11	0.067	4.76	0.466	2.11	0.113	3.35	0.184
21	Sp92	5.72	0.323	1.42	0.121	10.4	1.71	3.03	0.190	2.11	0.114
21	S92	6.65	0.348	2.12	0.162	18.3	1.32	6.36	0.329	3.13	0.143

site	season	Na	error	K	error	NH_4	error	Ca	error	Mg	error
22	A91	5.91	0.371	0.49	0.031	1.26	0.079	3.13	0.196	1.65	0.103
22	W91	5.05	0.254	0.43	0.022	0.16	0.008	0.78	0.039	1.16	0.058
22	Sp91	3.64	1.822	0.31	0.157	0.00	0.002	1.27	0.637	1.14	0.572
22	S91	15.0	1.32	2.90	0.396	8.48	0.783	3.54	0.149	2.44	0.103
22	A92	4.56	0.218	1.01	0.046	17.0	1.20	1.02	0.209	1.75	0.109
22	W92	5.09	0.405	3.52	0.279	1.16	0.130	3.85	0.309	1.93	0.154
22	Sp92	4.72	0.233	2.46	0.199	6.91	1.120	3.62	0.207	2.01	0.099
22	S92	5.72	0.452	2.01	0.160	6.00	0.564	4.89	0.382	2.49	0.193
23	A91	4.73	0.297	0.76	0.048	2.31	0.145	2.66	0.167	1.59	0.100
23	W91	3.92	0.155	0.48	0.019	0.19	0.007	0.74	0.029	0.83	0.033
23	Sp91	8.63	6.946	1.81	1.447	0.17	0.139	4.76	3.807	3.09	2.470
23	S91	12.7	1.11	1.57	0.241	6.81	0.627	6.22	0.235	4.75	0.184
23	A92	4.55	0.145	2.18	0.119	18.3	1.106	2.65	0.205	2.94	0.102
23	W92	3.77	0.146	1.36	0.056	7.08	0.625	3.35	0.167	1.92	0.075
23	Sp92	6.87	0.224	1.93	0.139	10.0	1.579	3.94	0.175	2.83	0.023
23	S92	2.40	0.162	0.99	0.096	4.27	0.376	2.07	0.126	1.31	0.082
24	A91	4.27	0.238	0.63	0.035	0.10	0.006	2.58	0.144	1.34	0.075
24	W91	2.00	0.085	0.38	0.016	0.12	0.005	0.42	0.018	0.47	0.020
24	Sp91	5.48	0.393	1.47	0.106	0.05	0.004	2.42	0.174	2.61	0.188
24	A92	3.31	0.188	1.03	0.161	9.08	0.718	1.62	0.075	1.75	0.091
24	W92	4.83	0.194	1.22	0.072	4.22	0.424	3.55	0.119	2.24	0.098
24	S92	3.99	0.205	1.99	0.319	10.6	0.74	3.47	0.154	1.93	0.080
25	A91	5.27	0.480	0.63	0.057	0.01	0.001	2.04	0.185	1.41	0.128
25	W91	2.01	0.085	0.25	0.011	0.17	0.007	0.36	0.015	0.50	0.021
25	Sp91	7.50	0.305	0.95	0.039	0.17	0.007	1.76	0.071	4.14	0.168
25	A92	5.93	0.375	1.76	0.079	12.1	1.17	3.33	0.148	2.46	0.189
25	W92	3.54	0.176	0.81	0.039	0.80	0.069	1.89	0.127	1.62	0.086

NS Data Set

site	season	Na	error	K	error	NH_4	error	Ca	error	Mg	error
26	W92	786	36.0	16.7	0.80	5.97	0.656	50.6	4.65	192	18.8
26	Sp92	831	44.2	19.1	1.12	25.7	1.86	89.0	5.41	247	21.7
26	S92	322	14.8	10.1	0.65	7.65	0.494	38.0	2.28	98.1	8.74
26	W93	699	29.5	14.4	0.82	7.43	0.809	59.2	4.54	208	21.7
26	Sp93	359	18.8	11.3	0.48	45.3	2.75	46.8	2.77	117	9.0
26	S93	316	25.5	8.44	0.556	1.86	0.177	41.6	3.47	82.7	5.71
26	A93	475	45.2	10.5	0.75	0.99	0.041	153	10.2	110	7.5
27	W92	110	5.5	2.72	0.197	6.30	0.546	14.8	1.44	30.9	3.20
27	Sp92	112	6.2	4.80	0.480	29.5	2.36	36.5	2.79	40.8	3.76
27	S92	47.5	2.25	2.04	0.298	12.0	1.014	33.7	2.03	17.6	1.78
27	A93	30.4	1.48	1.58	0.243	3.99	0.450	28.3	2.22	12.5	1.24
27	W93	130	5.6	2.78	0.120	8.33	0.850	50.9	3.54	39.6	3.89
27	W93	137	5.9	2.84	0.132	7.04	0.403	50.8	3.85	41.5	2.06
27	Sp93	58.5	3.36	3.09	0.226	24.9	1.66	17.0	1.29	20.1	1.75
27	Sp93	55.1	2.88	2.88	0.215	18.9	1.08	18.0	1.49	20.0	1.91

site	season	Na	error	K	error	NH_4	error	Ca	error	Mg	error
27	S93	45.4	4.01	4.09	0.239	2.73	0.229	36.9	2.06	14.0	0.96
27	S93	48.2	3.97	3.16	0.272	0.97	0.073	39.8	1.97	14.2	1.15
27	A93	71.3	7.10	3.35	0.496	8.06	0.359	131	9.1	23.0	1.67
27	A93	67.3	6.58	2.43	0.178	6.73	0.570	125	11.1	22.0	1.75
28	W92	7.93	0.413	0.79	0.039	2.93	0.168	2.16	0.182	2.51	0.273
28	sp92	10.2	0.63	1.91	0.121	11.9	0.96	9.72	0.721	5.36	0.574
28	S92	10.5	0.55	1.41	0.135	14.1	0.98	7.24	0.475	3.89	0.350
28	A93	6.05	0.296	1.58	0.223	24.4	1.46	6.98	0.583	3.34	0.476
28	W93	8.97	0.482	0.28	0.084	2.87	0.171	3.35	0.237	3.19	0.415
28	Sp93	7.49	1.529	1.47	0.114	10.8	0.62	7.69	0.442	3.62	0.276
28	S93	8.39	0.986	2.18	0.246	14.3	1.73	8.46	0.819	3.18	0.447
28	A94	5.59	0.704	7.49	0.950	7.13	0.761	6.35	0.511	2.79	0.569
29	W92	2.08	0.158	1.51	0.116	3.14	0.282	2.54	0.287	1.57	0.214
29	Sp92	7.07	0.487	2.09	0.127	10.5	0.84	7.55	0.436	4.60	0.442
29	A93	8.99	0.587	3.71	0.154	4.33	1.152	5.06	0.373	3.97	0.639
29	W93	5.51	0.333	1.80	0.110	4.52	0.364	3.27	0.278	2.50	0.258
29	Sp93	10.7	0.66	3.54	0.177	22.3	1.27	8.93	0.664	5.82	0.608
29	S93	4.08	0.453	1.47	0.169	8.44	1.044	5.99	0.527	2.61	0.339
29	A94	2.10	0.174	0.62	0.038	1.50	0.088	2.55	0.129	1.09	0.077
30	W92	0.07	0.004	0.05	0.003	0.45	0.016	0.04	0.003	0.04	0.004
30	Sp92	10.3	0.70	1.79	0.123	7.45	0.576	6.56	0.398	5.54	0.479
30	W93	0.65	0.076	0.77	0.090	0.50	0.090	0.50	0.071	0.34	0.054
30	Sp93	10.6	1.23	4.93	0.558	32.4	3.89	15.9	1.81	8.15	1.135
30	S93	23.2	1.97	30.8	1.88	224	19.0	23.0	1.15	15.6	1.18
30	A94	0.10	0.008	0.63	0.062	0.17	0.010	0.11	0.011	0.13	0.036
31	W92	0.15	0.007	0.29	0.006	0.34	0.015	0.07	0.005	0.09	0.013
31	Sp92	12.4	0.67	2.59	0.176	11.7	0.94	9.5	0.562	8.36	0.740
31	W93	0.17	0.005	0.50	0.007	0.96	0.039	0.05	0.003	0.08	0.010
31	Sp93	8.20	0.42	4.92	0.207	14.0	0.94	7.83	0.672	11.5	1.01
31	S93	31.5	4.59	24.7	1.98	239	24.8	29.9	2.40	20.6	4.33
31	A94	2.04	0.179	2.24	0.125	1.16	0.042	1.66	0.115	1.26	0.128
32	W92	0.23	0.006	0.17	0.012	0.71	0.020	0.72	0.086	0.30	0.031
32	Sp92	14.9	1.00	15.3	0.99	26.6	2.24	33.4	1.98	29.9	2.83
32	A93	2.28	0.059	3.67	0.104	2.86	0.103	2.56	0.105	2.02	0.155
32	W93	0.35	0.026	0.67	0.015	0.89	0.038	1.40	0.084	0.77	0.077
32	S93	30.3	3.52	7.89	1.251	8.79	0.854	23.7	1.87	18.3	2.10
32	A94	9.8	0.829	15.6	0.93	44.4	0.96	8.43	2.343	7.21	0.786
33	W92	1.29	0.000	1.30	0.000	0.43	0.000	1.25	0.000	1.52	0.000
33	Sp92	9.01	0.660	3.70	0.264	24.7	2.05	5.66	0.308	8.44	1.03
33	A93	17.6	0.85	3.34	0.268	1.19	0.287	4.72	0.262	9.6	0.91
33	W93	1.02	0.000	1.31	0.000	0.69	0.000	2.49	0.000	3.19	0.000
33	S93	63.0	7.01	16.0	1.10	187	16.0	22.8	2.63	29.6	5.14

APPENDIX E MEAN, MINIMUM AND MAXIMUM DEPOSITION OF IONIC SPECIES AND RAINFALL AMOUNT AT EACH SAMPLE SITE ON THE WE AND NS ARRAYS

H, Cl, SO_4, NO_3, HPO_4, Br, Na, K, NH_4, Ca and Mg in units of $\mu eq/m^2/day$

site		rainfall (mm)	error	H	error	Cl	error	SO_4	error
site 16	mean	120	5	0.40	0.007	443	10.1	59.1	1.32
Cliff Head	min	5		0.01		33.4		6.23	
n=7	max	343		0.99		1151		127	
site 17	mean	89	4	2.72	0.055	95.4	2.13	19.0	0.38
Morawa	min	3		0.00		4.29		2.43	
n=8	max	236		10.8		229		31.3	
site 18	mean	87	3	3.19	0.071	34.2	0.95	11.8	0.38
Badja	min	22		0.04		9.14		5.08	
n=8	max	262		11.1		44.1		22.1	
site 19	mean	51	2	5.84	0.090	26.7	0.56	14.6	0.29
Iowna	min	1		0.04		4.12		3.30	
n=7	max	120		8.75		25.2		14.5	
site 20	mean	69	3	4.65	0.091	12.6	0.43	11.1	0.52
Barrambie	min	16		0.12		3.38		3.73	
n=7	max	245		3.16		14.1		16.0	
site 21	mean	43	2	2.62	0.055	7.84	0.546	7.81	0.986
Yeelirrie	min	2		0.01		2.79		3.87	
n=8	max	153		4.16		11.1		12.3	
site 22	mean	61	2	1.85	0.034	5.92	0.225	5.98	0.275
Lake Violet	min	1		0.29		1.10		1.84	
n=8	max	194		5.05		10.5		10.5	
site 23	mean	90	4	1.91	0.036	5.35	0.617	7.27	1.181
Carnegie	min	11		0.31		2.14		3.25	
n=8	max	265		10.4		7.85		11.4	
site 24	mean	30	2	3.40	0.078	4.75	0.128	6.04	0.155
Gunbarrel	min	22		0.05		4.34		4.27	
n=6	max	38		0.84		7.38		7.20	
site 25	mean	92	4	7.04	0.141	4.73	0.114	7.67	0.239
Everard Junction	min	23		0.03		2.30		3.19	
n=5	max	268		0.05		20.6		25.2	
site 26	mean	153	2	6.50	0.128	541	12.4	83.5	1.9
Port Lincoln	min	41		0.29		271		48.0	
n=8	max	334		21.3		910		118	
site 27	mean	92	1	1.04	0.021	82.3	1.55	17.1	0.34
Gawler Ranges	min	37		0.02		33.4		11.2	
n=12	max	299		5.03		158		34.0	
site 28	mean	57	1	0.83	0.019	7.33	0.238	8.15	0.234
Wintinna	min	27		0.05		4.34		5.39	
n=8	max	134		2.54		10.6		11.0	

site		rainfall (mm)	error	H	error	Cl	error	SO_4	error
site 29	mean	56	2	2.46	0.086	4.36	0.194	8.17	0.279
Alice Springs	min	2		0.00		1.55		2.64	
n=7	max	149		10.4		11.3		15.5	
site 30	mean	30	1	1.23	0.049	7.01	0.341	10.8	0.50
Tennant Creek	min	0		0.00		0.00		0.00	
n=6	max	59		5.98		22.7		32.9	
site 31	mean	155	9	5.63	0.350	7.40	0.608	12.0	0.66
Dunmarra	min	0		0.00		0.00		0.00	
n=6	max	768		28.6		25.2		41.1	
site 32	mean	225	29	5.72	0.362	17.3	1.278	10.9	0.63
Katherine	min	0		0.00		0.00		0.00	
n=6	max	854		26.8		66.9		30.5	
site 33	mean	289	11	9.84	0.162	103	1.0	33.6	0.46
Kapalga	min	3		0.00		0.90		0.28	
n=5	max	866		9.84		32.4		14.1	

site		NO_3	error	HPO_4	error	Br	error	Na	error
site 16	mean	9.15	0.269	5.59	0.270	0.37	0.011	379	8.15
Cliff Head	min	0.11		0.02		0.00		20.9	
n=7	max	25.4		38.0		1.20		931	
site 17	mean	6.65	0.147	0.68	0.020	0.09	0.006	83.8	1.70
Morawa	min	2.57		0.00		0.00		3.93	
n=8	max	13.0		2.52		0.29		179	
site 18	mean	6.67	0.227	0.36	0.027	0.05	0.001	31.6	0.84
Badja	min	2.98		0.02		0.02		7.38	
n=8	max	10.9		3.44		0.11		42.2	
site 19	mean	7.37	0.188	0.59	0.044	0.10	0.002	25.1	0.44
Iowna	min	1.98		0.00		0.00		5.39	
n=7	max	20.5		0.53		0.06		19.2	
site 20	mean	7.50	0.229	0.37	0.052	0.03	0.001	11.7	0.57
Barrambie	min	2.20		0.01		0.01		5.05	
n=7	max	13.3		1.76		0.09		16.2	
site 21	mean	5.87	0.433	0.48	0.020	0.03	0.001	8.55	1.087
Yeelirrie	min	1.34		0.00		0.00		3.64	
n=8	max	17.6		1.17		0.06		15.0	
site 22	mean	5.83	0.172	0.37	0.023	0.03	0.001	6.21	0.300
Lake Violet	min	1.52		0.01		0.01		2.00	
n=8	max	16.2		0.71		0.09		12.7	
site 23	mean	6.03	0.452	0.19	0.020	0.03	0.001	5.95	1.007
Carnegie	min	2.35		0.02		0.00		2.01	
n=8	max	8.17		1.09		0.06		7.50	
site 24	mean	4.37	0.115	0.23	0.011	0.03	0.001	3.98	0.096
Gunbarrel	min	0.02		0.01		0.02		3.54	
n=6	max	9.00		7.14		0.02		60.1	

site		NO_3	error	HPO_4	error	Br	error	Na	error
site 25	mean	5.81	0.148	0.08	0.002	0.03	0.001	4.85	0.118
Everard Junction	min	0.03		0.04		0.02		3.41	
n=5	max	11.8		29.7		0.11		21.6	
site 26	mean	12.1	0.28	8.42	0.316	0.58	0.036	541	10.7
Port Lincoln	min	5.06		0.32		0.20		316	
n=8	max	24.6		42.7		1.17		831	
site 27	mean	9.75	0.202	0.64	0.022	0.16	0.010	76.1	1.41
Gawler Ranges	min	2.09		0.10		0.04		30.4	
n=12	max	29.5		2.96		0.41		137	
site 28	mean	7.07	0.211	0.71	0.042	0.05	0.001	8.14	0.279
Wintinna	min	1.58		0.06		0.02		5.59	
n=8	max	10.6		2.20		0.09		10.5	
site 29	mean	7.20	0.285	0.83	0.061	0.06	0.002	5.79	0.169
Alice Springs	min	1.75		0.09		0.00		2.08	
n=7	max	16.4		2.68		0.23		10.7	
site 30	mean	6.60	0.487	10.8	0.64	0.05	0.018	7.48	0.404
Tennant Creek	min	0.00		0.00		0.00		0.00	
n=6	max	19.9		61.7		0.14		23.2	
site 31	mean	10.2	0.438	4.41	0.364	0.19	0.011	9.08	0.776
Dunmarra	min	0.00		0.00		0.00		0.00	
n=6	max	26.2		25.6		0.92		31.5	
site 32	mean	8.34	3.072	2.42	0.043	0.26	0.015	18.5	1.39
Katherine	min	0.00		0.00		0.00		0.00	
n=6	max	22.5		11.6		0.99		71.6	
site 33	mean	24.7	0.336	13.9	0.240	1.04	0.009	103	1.3
Kapalga	min	0.14		0.15		0.00		1.02	
n=5	max	8.72		2.87		0.35		32.6	

site		K	error	NH_4	error	Ca	error	Mg	error
site 16	mean	12	0.31	28.9	2.20	59.8	1.32	97.3	2.02
Cliff Head	min	2.00		0.12		5.52		8.48	
n=7	max	38		191		181		219	
site 17	mean	3.37	0.095	7.08	0.366	5.86	0.144	20.7	0.41
Morawa	min	0.11		0.09		1.89		1.68	
n=8	max	7.11		36.9		9.7		39	
site 18	mean	1.98	0.079	9.9	0.502	5.26	0.217	9.48	0.244
Badja	min	0.04		0.09		0.59		2.06	
n=8	max	4.19		19.9		7.44		11.7	
site 19	mean	1.67	0.040	7.51	0.319	5.04	0.108	51	0.108
Iowna	min	0.23		0.00		0.39		1.07	
n=7	max	17		69.0		5.68		11.0	
site 20	mean	3.75	0.141	14.6	1.095	3.75	0.136	4.22	0.165
Barrambie	min	0.43		0.16		0.78		1.16	
n=7	max	2.12		18.3		6.36		3.35	

site		K	error	NH_4	error	Ca	error	Mg	error
site 21	mean	1.09	0.073	6.75	0.320	2.71	0.303	2.37	0.313
Yeelirrie	min	0.31		0.00		0.74		0.83	
n=8	max	3.52		8.48		4.89		2.49	
site 22	mean	1.64	0.072	5.12	0.239	2.76	0.112	1.82	0.082
Lake Violet	min	0.38		0.10		0.42		0.47	
n=8	max	2.18		18.3		6.22		4.75	
site 23	mean	1.38	0.212	6.14	0.309	3.30	0.548	2.41	0.355
Carnegie	min	0.25		0.01		0.36		0.50	
n=8	max	1.99		10.6		3.47		4.14	
site 24	mean	1.12	0.064	4.03	0.186	2.34	0.051	1.72	0.043
Gunbarrel	min	0.81		0.80		1.19		1.62	
n=6	max	10		74.4		8.14		11.5	
site 25	mean	0.88	0.019	2.65	0.195	1.88	0.046	2.02	0.049
Everard Junction	min	2.37		29.7		3.28		2.49	
n=5	max	37		244		19.4		23.9	
site 26	mean	12.9	0.25	13.6	0.44	68.3	1.77	151	4.9
Port Lincoln	min	8.44		0.99		38.0		82.7	
n=8	max	19.1		45.3		153		247	
site 27	mean	2.98	0.081	10.8	0.29	48.6	1.35	24.7	0.66
Gawler Ranges	min	1.58		0.97		14.8		12.5	
n=12	max	4.80		29.5		131		41.5	
site 28	mean	2.14	0.12	11.0	0.35	6.49	0.190	3.49	0.154
Wintinna	min	0.28		2.87		2.16		2.51	
n=8	max	7.49		24.4		9.72		5.36	
site 29	mean	2.10	0.051	7.82	0.318	5.13	0.158	3.17	0.157
Alice Springs	min	0.62		1.50		2.54		1.09	
n=7	max	3.71		22.3		8.93		5.82	
site 30	mean	6.50	0.329	44.2	3.24	7.69	0.364	4.96	0.284
Tennant Creek	min	0.00		0.00		0.00		0.00	
n=6	max	30.8		224		23.0		15.6	
site 31	mean	5.87	0.333	44.5	4.14	8.18	0.426	6.98	0.751
Dunmarra	min	0.00		0.00		0.00		0.00	
n=6	max	24.7		239		29.9		20.6	
site 32	mean	7.78	0.389	17.4	1.07	20.0	1.48	14.3	1.037
Katherine	min	0.00		0.00		0.00		0.00	
n=6	max	15.6		44.4		70.0		41.5	
site 33	mean	20.9	0.23	187	4.1	29.2	0.54	56.1	1.18
Kapalga	min	1.30		0.43		1.25		1.52	
n=5	max	7.75		66.5		11.0		18.1	

APPENDIX F DETAILS OF FACTOR ANALYSES PERFORMED ON SUBSETS OF THE WE AND SN DATA SETS AS DESCRIBED IN CHAPTER 5

Factor loadings for the coastal subset (n=24) of the WE data set

Loadings	Factor 1	Factor 2	Factor 3
% variance	59.1%	13.3%	10.3%
eigen value	6.4991	1.4606	1.1329
H	.07959	**.86501**	.25986
Cl	**.96785**	.14013	.00819
SO_4	**.93572**	.26229	.06506
NO_3	.07130	**.77087**	-.27935
HPO_4	**.45361**	-.04509	-.05780
Br	**.75746**	**.54200**	-.05442
Na	**.96420**	.18174	.03570
K	**.93029**	.09335	.23900
NH_4	.01785	-.02301	**.96090**
Ca	**.90601**	-.03262	-.08901
Mg	**.97067**	.12202	.01246

Factor loadings for the non-coastal data subset (n=49) of the WE data set

Loadings	Factor 1	Factor 2	Factor 3
% variance	42.1%	16.3%	14.3%
eigen value	4.628	1.790	1.575
H	.04092	.00569	**.92769**
Cl	**.88638**	-.11856	.22293
SO_4	**.84034**	.23231	.20643
NO_3	**.51934**	**.41632**	**.41688**
HPO_4	-.05854	.28065	-.27390
Na	**.95915**	-.00064	.00822
K	.10688	**.80364**	-.18094
NH_4	.16136	**.84883**	.23461
Ca	**.64232**	**.46642**	-.29773
Mg	**.89925**	.19965	-.05541

Factor loadings for the northern data subset, wet data subset and dry data subsets of the NS data set

	all seasons (n=25)		wet samples (n=14)		dry samples (n=11)	
factor	factor 1	factor 2	factor 1	factor 2	factor 1	factor 2
eigen value	8.479	1.168	8.085	1.168	7.69	0.8
percentage var	81.8	11.7	80.8	11.7	77.0	8.0
H	.11701	**.97178**	.04181	**.97366**	-.19498	**-.95129**
Cl	**.93720**	.28184	**.76690**	**.54809**	**.91972**	.29688
SO_4	**.92057**	.25436	**.82524**	**.52829**	**.80597**	.39634
NO_3	**.83001**	**.49515**	**.56149**	**.77499**	**.65938**	**.43028**
HPO_4	**.92071**	-.24488	**.94368**	.03656	**.77643**	**.54426**
Na	**.94048**	.30126	**.75898**	**.58606**	**.95589**	.25826
K	**.97056**	.05432	**.93724**	.26479	**.85558**	.30428
NH_4	**.91924**	.17185	**.91545**	.25690	**.69921**	**.48964**
Ca	**.93380**	.24174	**.78618**	**.55473**	**.90443**	.20231
Mg	**.93950**	.26410	**.74441**	**.62817**	**.92706**	.20525

Factor loadings for southern subset (n=32) of the NS data set

	factor 1	factor 2	factor 3
eigen value	6.709	1.369	1.114
% variation	61.0	12.4	10.1
H	.23014	**.88266**	-.18040
Cl	**.96415**	.13812	.01778
SO_4	**.87664**	**.41408**	.01322
NO_3	.13116	**.82305**	.23283
HPO_4	.32317	.25682	**.66145**
Br	**.68493**	**.64124**	-.07399
Na	**.96575**	.20102	.00446
K	**.77934**	**.40717**	.07778
NH_4	.13875	.13301	**-.75461**
Ca	**.91057**	.03745	.14910
Mg	**.96788**	.21780	-.03139

Factor loadings southern coastal subset (n=19) of the NS data set

	factor 1	factor 2	factor 3
eigen value	6.225	1.805	1.709
% variance	56.6	16.4	15.5
H	**.51802**	**.80141**	-.00244
Cl	**.97211**	.02786	.04578
SO_4	**.95652**	.17055	.13940
NO_3	.01922	**.71708**	**.60728**
HPO_4	.38209	-.04140	**.76950**
Br	**.68349**	**.60452**	.10013
Na	**.98752**	.04423	.04781
K	**.94501**	.19468	.15426
NH_4	.16897	-.07885	**-.79167**
Ca	**.43585**	**-.64148**	**.51731**
Mg	**.99185**	.03989	-.01564

Factor loadings for southern inland subset (n=15) of the NS data set

	factor 1	factor 2	factor 3
eigen value	5.981	1.7807	.9508
% variance	59.8	17.8	9.5
H	.26437	**.90911**	.03321
Cl	**.88141**	-.06643	-.06266
SO_4	**.71186**	**.60889**	.25540
NO_3	**.71936**	**.50814**	.13097
HPO_4	.02604	-.16500	**.91425**
Na	**.84980**	.39032	-.01680
K	-.09850	**.51234**	**.78398**
NH_4	**.66622**	.22248	**.63138**
Ca	**.58344**	.38748	**.56340**
Mg	**.76917**	**.58222**	.19537

APPENDIX G CHLORINE-36 DATA SET

site	season	Volume (Litres)	error	time ±0.5 days	Cl (mg/L)	error	$^{36}Cl/Cl$ ($*10^{-15}$)	error
16	A91	3.02	0.001	80	12.9	0.32	13	2
16	W91	23.12	0.021	107	17.0	0.34	4	1
16	Sp91	7.41	0.006	69	20.7	0.41	5	2
16	S91	5.22	0.001	79	5.99	0.13	21	3
16	A92	11.60	0.012	136	7.72	0.14	4	2
16	W92	18.30	0.018	102	12.5	0.23	8	2
16	Sp92	5.33	0.001	56	17.5	0.75	8	1
16	S92	0.26	0.001	102	142	6.64	6	2
17	A91	3.23	0.001	80	3.66	0.08	35	5
17	W91	12.26	0.013	107	6.37	0.12	6	2
17	Sp91	5.49	0.001	70	4.96	0.09	53	4
17	S91	3.17	0.001	78	1.74	0.04	134	5
17	A92	12.34	0.013	137	2.09	0.06	28	3
17	W92	18.99	0.018	101	2.89	0.06	18	3
17	Sp92	6.06	0.001	56	3.28	0.14	20	2
17	S92	0.22	0.001	102	22.8	1.06	98	8
18	A91	2.30	0.001	81	1.41	0.02	121	8
18	W91	7.04	0.005	107	3.34	0.07	19	3
18	Sp91	2.06	0.001	70	4.18	0.08	81	5
18	S91	2.57	0.001	79	1.26	0.02	198	9
18	A92	20.21	0.019	137	0.69	0.02	64	6
18	W92	10.77	0.011	90	2.24	0.06	31	3
18	Sp92	3.25	0.001	66	1.45	0.06	109	7
18	S92	0.235	0.001	102	7.50	0.35	110	10
19	A91	2.37	0.001	83	1.00	0.02	246	11
19	W91	9.34	0.009	107	1.87	0.05	30	3
19	A92	23.62	0.021	140	0.58	0.02	91	6
19	W92	10.39	0.011	87	1.13	0.06	43	9
19	S92	5.79	0.001	65	0.38	0.02	254	19
19	S92	0.58	0.001	104	7.35	0.34	189	15
20	A91	2.48	0.001	83	0.97	0.02	268	13
20	W91	5.68	0.001	107	0.87	0.02	88	7
20	S91	5.67	0.001	77	0.71	0.01	241	8
20	W92	7.15	0.005	87	0.98	0.04	144	9

site	season	Volume (Litres)	error	time ±0.5 days	Cl (mg/L)	error	$^{36}Cl/Cl$ ($*10^{-15}$)	error
20	Sp92	3.60	0.001	67	0.34	0.02	459	25
20	S92	3.34	0.001	104	0.86	0.04	225	11
21	A91	4.89	0.001	82	0.86	0.02	244	14
21	W91	5.49	0.001	107	0.71	0.01	390	16
21	S91	5.09	0.001	77	1.21	0.02	198	9
21	A92	32.49	0.026	139	0.21	0.01	309	15
21	W92	5.54	0.005	87	1.09	0.05	99	10
21	Sp92	5.60	0.001	67	0.23	0.01	561	22
21	S92	5.15	0.001	105	0.57	0.03	270	11
22	A91	1.86	0.001	81	1.36	0.03	214	11
22	W91	5.42	0.000	107	0.43	0.01	238	12
22	Sp91	0.14	0.001	72	7.74	0.15	151	10
22	A92	26.81	0.023	140	0.15	0.01	119	8
22	W92	1.46	0.001	87	2.38	0.06	375	27
22	Sp92	5.59	0.001	68	0.27	0.01	471	20
22	S92	0.86	0.001	106	3.18	0.15	253	13
23	A91	1.42	0.001	82	1.56	0.03	261	13
23	W91	11.52	0.012	107	0.27	0.01	285	12
23	S91	5.80	0.001	77	0.79	0.02	236	16
23	A92	32.37	0.026	139	0.14	0.01	535	16
23	W92	4.85	0.001	86	0.47	0.02	263	17
23	Sp92	3.06	0.001	68	0.72	0.07	367	16
23	S92	5.20	0.001	107	0.13	0.01	239	17
24	A91	5.01	0.001	83	0.68	0.02	353	14
24	W91	7.62	0.006	107	0.27	0.01	660	25
24	Sp91	2.03	0.001	72	1.08	0.02	483	11
24	A92	32.21	0.026	141	0.15	0.01	621	18
24	W92	5.12	0.001	84	0.60	0.03	298	16
24	S92	5.40	0.001	108	0.14	0.01	406	19
25	A91	0.48	0.001	83	3.96	0.11	277	11
25	W91	10.32	0.010	107	0.16	0.01	527	22
25	Sp91	7.16	0.005	72	0.45	0.02	335	14
25	A92	30.48	0.025	140	0.12	0.02	647	27
25	W92	3.85	0.001	83	0.58	0.03	170	15
26	W92	16.11	0.016	90	16.2	0.79	5	2
26	S92	6.11	0.001	104	20.4	0.86	12	2

site	season	Volume (Litres)	error	time ±0.5 days	Cl (mg/L)	error	$^{36}Cl/Cl$ ($*10^{-15}$)	error
26	W93	12.59	0.013	90	18.1	0.22	5	3
26	Sp93	7.82	0.007	72	12.4	1.07	13	2
26	S93	2.38	0.001	105	38.1	0.54	6	1
26	A94	8.6148	0.01	107	19.0	0.312	4.3	3.2
27	W92	6.36	0.003	90	5.60	0.03	20	2
27	Sp92	22.21	0.020	100	1.05	0.09	86	7
27	S92	7.96	0.007	104	2.31	0.08	79	6
27	A93	3.60	0.001	83	2.46	0.09	56	6
27	S93	4.86	0.001	105	3.50	0.05	52	5
27	S93	4.87	0.001	105	3.83	0.05	49	5
27	A94	5.694	0.001	106	7.59	0.253	11	4
28	W92	4.44	0.001	90	0.99	0.05	149	15
28	Sp92	11.92	0.012	104	0.33	0.03	290	16
28	S92	2.58	0.001	104	2.10	0.08	175	15
28	A93	5.31	0.001	82	0.40	0.01	301	11
28	W93	7.43	0.007	89	0.72	0.07	165	15
28	Sp83	5.13	0.007	72	0.61	0.06	236	12
28	S93	7.42	0.007	106	0.51	0.01	174	13
28	A94	6.0487	0.005	104	0.55	0.007	134	8.4
29	W92	1.50	0.001	86	0.70	0.05	340	42
29	SP92	7.30	0.012	105	0.37	0.04	354	22
29	A92	23.60	0.324	82	0.21	0.02	408	14
29	W93	1.90	0.007	89	1.42	0.12	190	16
29	Sp93	7.31	0.007	70	0.61	0.05	222	11
29	S93	5.41	0.007	105	0.36	0.14	295	11
29	A94	0.323	0.001	106	2.91	0.037	520	48
30	W92	0.2411	0.001	85	0.31	0.017	133	110
30	Sp92	5.94	0.001	103	0.66	0.07	184	9
30	Sp93	8.24	0.007	70	0.55	0.05	625	49
30	S93	0.61	0.001	105	1.51	0.03	84	19
30	A94	0.4213	0.001	106	0.56	0.007	276	56
31	W92	0.3152	0.001	86	0.16	0.013	734	123
31	SP92	8.00	0.007	103	0.59	0.01	129	7
31	W93	0.23	0.001	89	0.58	0.02	446	73
31	SP93	15.46	0.017	70	0.24	0.08	260	16
31	S93	7.68	0.007	105	0.12	0.00	519	26

site	season	Volume (Litres)	error	time ±0.5 days	Cl (mg/L)	error	$^{36}Cl/Cl$ ($*10^{-15}$)	error
31	A94	0.4447	0.001	106	1.25	0.044	181	26
32	W92	0.34	0.001	86	0.17	0.01	201	71.0
32	SP92	15.85	0.016	104	0.20	0.02	140	11
32	A92	0.28	0.001	79	2.90	0.13	152	32
32	S93	8.54	0.007	108	0.13	0.00	459	29
32	A93	0.3197	0.001	106	3.93	0.222	208	21
33	W92	0.24	0.001	80	1.55	0.08	155	22.0
33	A93	5.32	0.247	80	0.92	0.02	92	5
33	W93	0.25	0.001	89	1.04	0.01	367	38
33	S93	8.660	0.007	104	0.28	0.01	103	8

site	season	^{36}Cl (atom/m^2/s)	error	^{36}Cl ($*10^6$ atoms /L)	error
16	A91	14	2.4	2.92	0.49
16	W91	32	8.1	1.15	0.29
16	Sp91	23	8.8	1.66	0.64
16	S9i	19	2.9	2.18	0.34
16	A92	5	3.0	0.47	0.28
16	W92	37	8.4	1.60	0.36
16	Sp92	27	4.6	2.23	0.37
16	S92	5	1.6	14.95	4.87
17	A91	11	1.7	2.18	0.31
17	W91	10	2.4	0.65	0.16
17	Sp91	45	3.7	4.47	0.35
17	S91	21	1.0	3.96	0.17
17	A92	11	1.3	0.98	0.11
17	W92	21	3.6	0.88	0.15
17	Sp92	16	1.7	1.11	0.12
17	S92	10	1.0	38.00	3.57
18	A91	11	0.7	2.89	0.19
18	W91	9	1.3	1.10	0.15
18	Sp91	22	1.5	5.75	0.37
18	S91	18	1.0	4.24	0.20
18	A92	14	1.5	0.74	0.08
18	W92	18	1.9	1.18	0.12
18	Sp92	17	1.4	2.69	0.21
18	S92	4	0.4	14.02	1.43

site	season	^{36}Cl (atom/m^2/s)	error	^{36}Cl (*10^6 atoms /L)	error
19	A91	15	0.9	4.18	0.21
19	W91	11	1.3	0.95	0.11
19	A92	19	1.5	0.90	0.07
19	W92	13	2.8	0.82	0.18
19	S92	19	1.8	1.64	0.15
19	S92	17	1.6	23.60	2.17
20	A91	17	1.0	4.41	0.23
20	W91	9	0.8	1.30	0.11
20	S91	28	1.2	2.91	0.10
20	W92	25	2.0	2.40	0.18
20	Sp92	18	1.5	2.65	0.21
20	S92	14	1.0	3.29	0.22
21	A91	15	1.0	3.57	0.22
21	W91	17	0.9	4.70	0.22
21	S91	19	1.0	4.07	0.20
21	A92	19	1.3	1.10	0.08
21	W92	8	0.9	1.83	0.20
21	Sp92	13	0.8	2.19	0.13
21	S92	9	0.6	2.61	0.16
22	A91	8	1.0	4.95	0.27
22	W91	6	1.0	1.74	0.10
22	Sp91	3	1.0	19.86	1.34
22	A92	4	1.0	0.30	0.02
22	W92	18	1.5	15.16	1.17
22	Sp92	13	0.8	2.16	0.12
22	S92	8	0.6	13.67	0.94
23	A91	9	0.5	6.90	0.37
23	W91	10	0.6	1.31	0.08
23	S91	17	1.3	3.17	0.23
23	A92	21	1.7	1.27	0.10
23	W92	9	0.7	2.10	0.16
23	Sp92	15	1.6	4.49	0.48
23	S92	2	0.2	0.53	0.05
24	A91	18	0.9	4.07	0.18
24	W91	16	0.8	3.03	0.15
24	Sp91	18	0.6	8.86	0.26
24	A92	26	1.2	1.58	0.07

site	season	^{36}Cl (atom/m^2/s)	error	^{36}Cl (*10^6 atoms /L)	error
24	W92	13	1.0	3.03	0.23
24	S92	3	0.3	0.97	0.09
25	A91	8	0.4	18.63	0.88
25	W91	10	0.8	1.43	0.11
25	Sp91	18	1.2	2.56	0.16
25	A92	21	3.9	1.32	0.25
25	W92	6	0.6	1.68	0.17
26	W92	32	13	1.38	0.56
26	S92	32	6	4.24	0.82
26	W93	29	18	1.60	1.01
26	Sp93	38	8	2.68	0.54
26	S93	6	2	3.76	0.91
26	A94	8	6	1.38	1.03
27	W92	17	2	1.90	0.19
27	Sp92	44	5	1.53	0.18
27	S92	31	3	3.10	0.26
27	A93	13	2	2.34	0.26
27	S93	10	1	3.09	0.30
27	S93	11	1	3.19	0.33
27	A94	5	2	1.42	0.52
28	W92	9	1	2.49	0.28
28	Sp92	13	2	1.62	0.18
28	S92	11	1	6.24	0.58
28	A93	10	1	2.05	0.10
28	W93	12	2	2.03	0.28
28	Sp83	13	1	2.46	0.27
28	S93	8	1	1.51	0.12
28	A94	5	0	1.24	0.08
29	W92	5	1	4.06	0.57
29	SP92	11	1	2.25	0.27
29	A92	31	3	1.47	0.13
29	W93	7	1	4.57	0.54
29	SP93	17	2	2.31	0.22
29	S93	7	3	1.78	0.70
29	A94	6	1	25.68	2.39
30	W92	0.15	0	0.71	0.59
30	SP92	9	1	2.05	0.24

site	season	^{36}Cl (atom/m^2/s)	error	^{36}Cl (*10^6 atoms /L)	error
30	SP93	50	6	5.83	0.69
30	S93	14	3	2.16	0.49
30	A94	0.76	0	2.64	0.54
31	W92	0.52	0	1.97	0.37
31	SP92	7	0	1.29	0.07
31	W93	0.83	0.14	4.42	0.73
31	SP93	17	6	1.08	0.36
31	S93	91	8	1.08	0.06
31	A94	1.2	0	3.83	0.57
32	W92	0.29	0	0.57	0.21
32	SP92	9	1	0.48	0.06
32	A92	3	1	7.48	1.61
32	S93	94	9	1.03	0.07
32	A93	3	0	13.89	1.61
33	W92	2	0	4.08	0.62
33	A93	12	1	1.43	0.09
33	W93	2	0	6.50	0.68
33	S93	46	5	0.48	0.04

APPENDIX H MEAN SEASONAL SURFACE WIND DIRECTIONS FOR INLAND SITES ALONG THE WE ARRAY

Mean seasonal wind directions are plotted on wind roses, and the wind roses plotted on a map of salt lakes along the inland section (sites 19 to 25) of the WE array. The wind roses are plotted on Met station sites closest to the sample site (Table 1). The wind roses are drawn from mean daily wind directions during each day of the sampling period. The mean daily wind directions were calculated from three-hourly surface wind direction data purchased from the Bureau of Meteorology. The size of the wedge on the wind rose represents the number of days of a particular wind direction, eg. when the wind direction is predominantly from the southeast, a large wedge will feature in the southeast section of the wind rose.

Table 1 Sample sites and corresponding Met Stations

Sample Site	Met Station
Iowna (19)	Mt Magnet
Barrambie (20)	Meekatharra
Yeelirrie (21)	Yeelirrie
Lake Violet (22)	Wiluna
Carnegie (23)	Carnegie
Gunbarrel (24)	Giles
Everard Junction (25)	

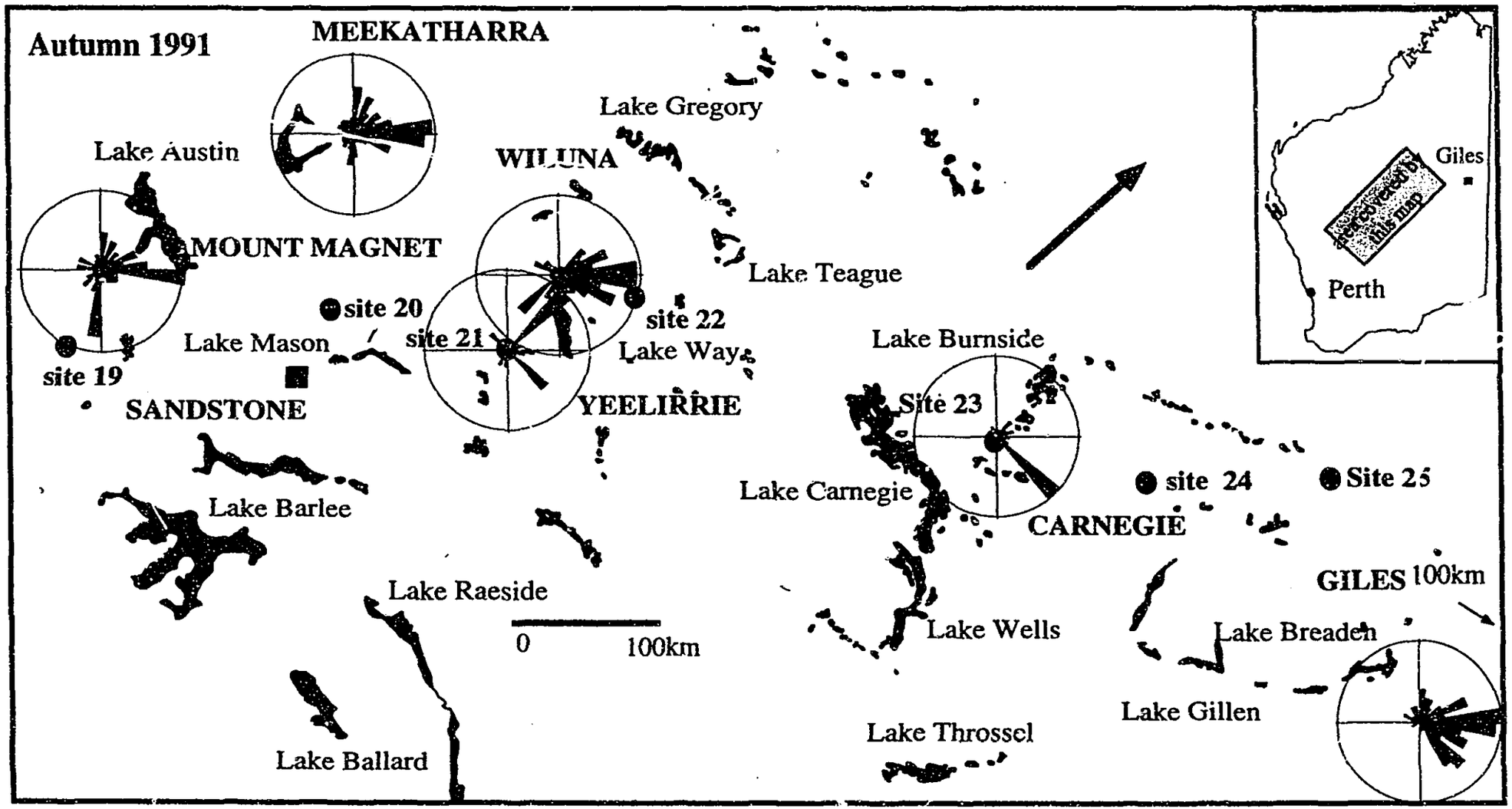

Appendix H Mean Wind Directions During Each Sampling Season for Inland Sites on the WE Array

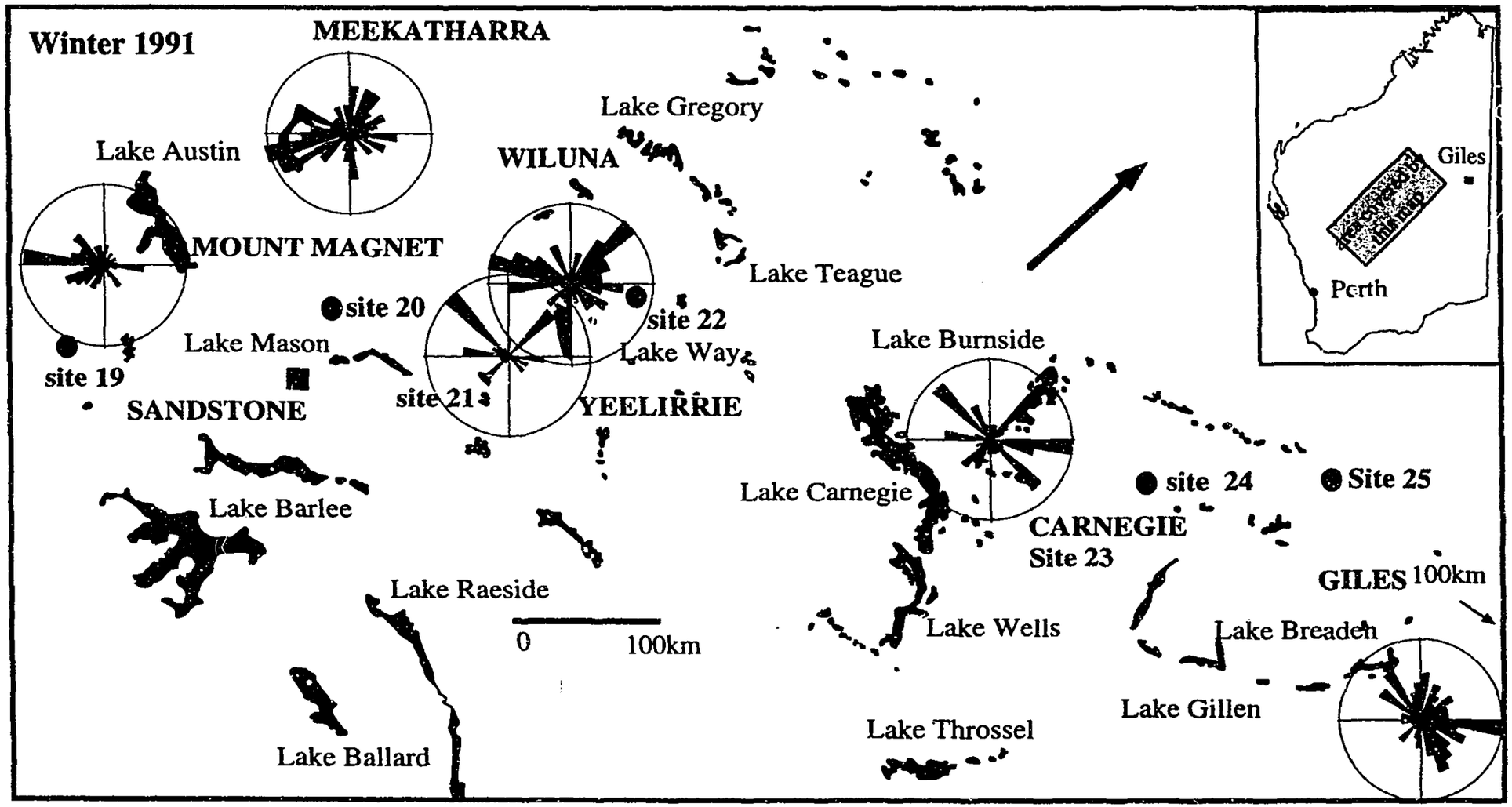
Winter 1991
MEEKATHARRA
Lake Austin
WILUNA
Lake Gregory
MOUNT MAGNET
Lake Teague
site 20
site 22
Lake Mason
Lake Way
site 19
site 21
YEELIRRIE
SANDSTONE
Lake Burnside
Lake Barlee
Lake Carnegie
site 24
Site 25
CARNEGIE
Site 23
GILES
100km
Lake Raeside
0
100km
Lake Wells
Lake Breaden
Lake Gillen
Lake Throssel
Lake Ballard
Giles
Perth

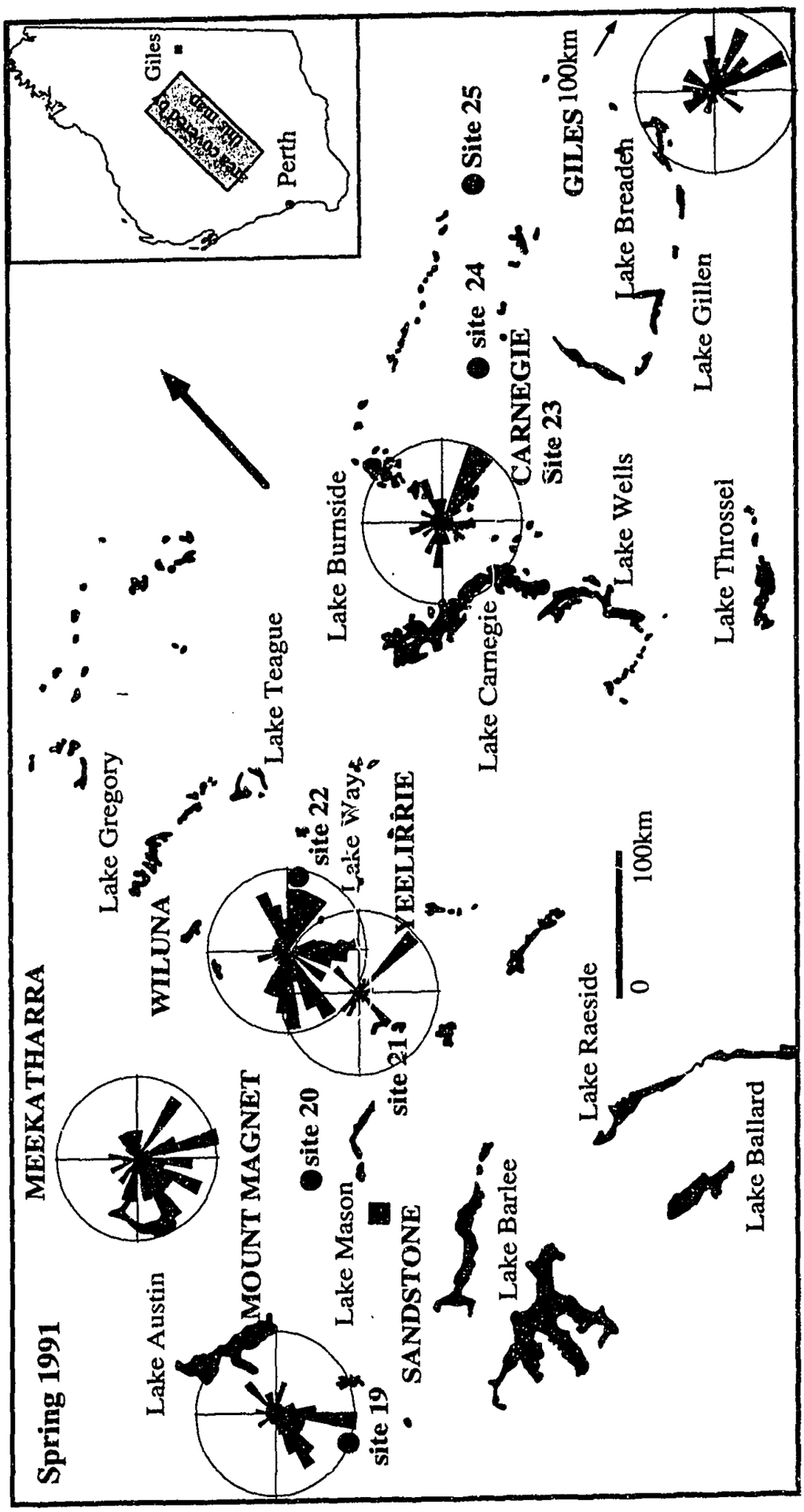
Spring 1991
MEEKATHARRA
MOUNT MAGNET
SANDSTONE
WILUNA
YEELIRRIE
GILES
CARNEGIE
Site 23
Site 25
site 24
site 22
site 21
site 20
site 19
Lake Austin
Lake Mason
Lake Barlee
Lake Gregory
Lake Teague
Lake Way
Lake Raeside
Lake Ballard
Lake Burnside
Lake Carnegie
Lake Wells
Lake Throssel
Lake Breaden
Lake Gillen
0
100km
100km
Giles
Perth

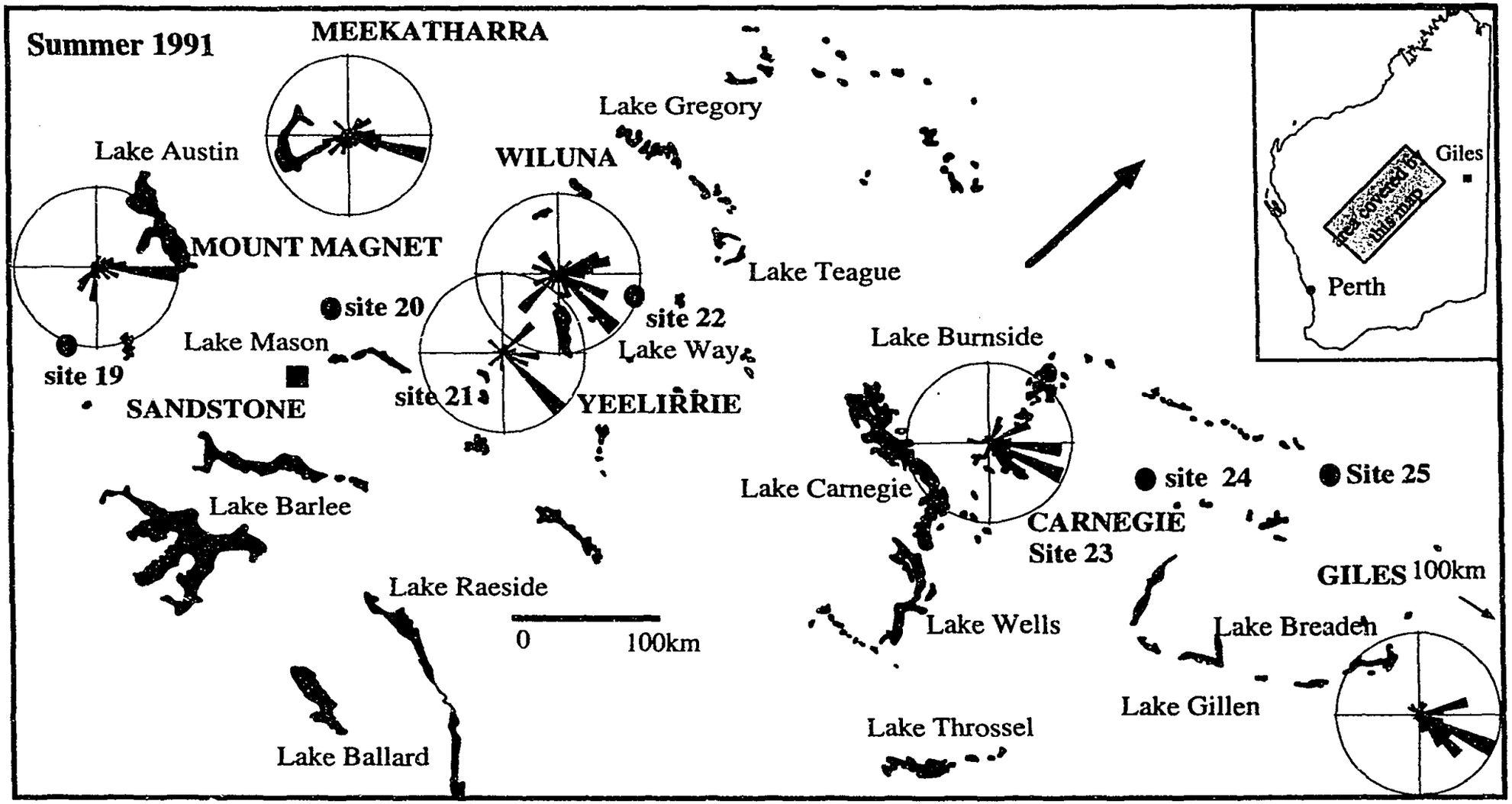

Appendix H Mean Wind Directions During Each Sampling Season for Inland Sites on the WE Array

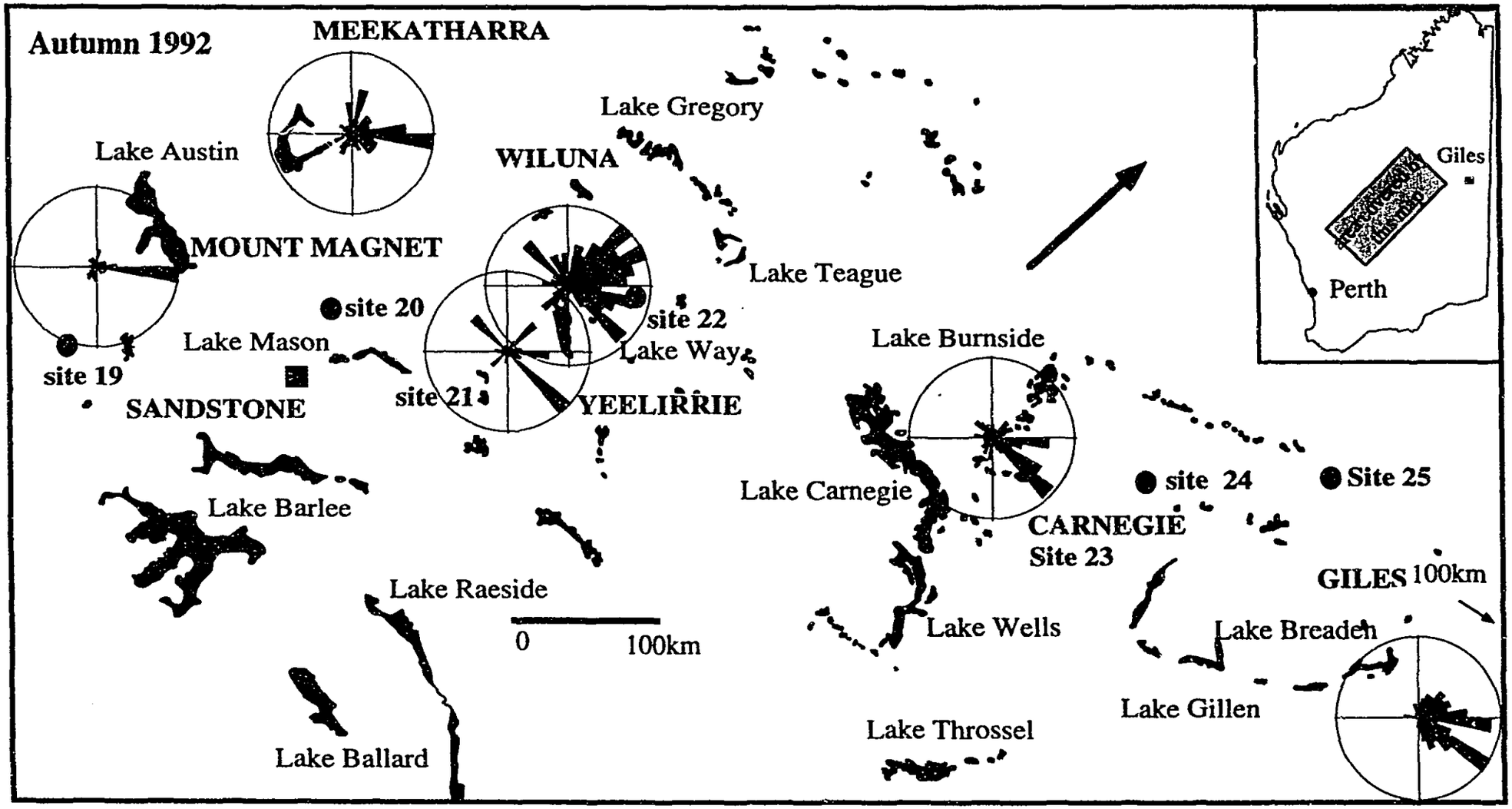

Appendix H Mean Wind Directions During Each Sampling Season for Inland Sites on the WE Array

Appendix H Mean Wind Directions During Each Sampling Season for Inland Sites on the WE Array

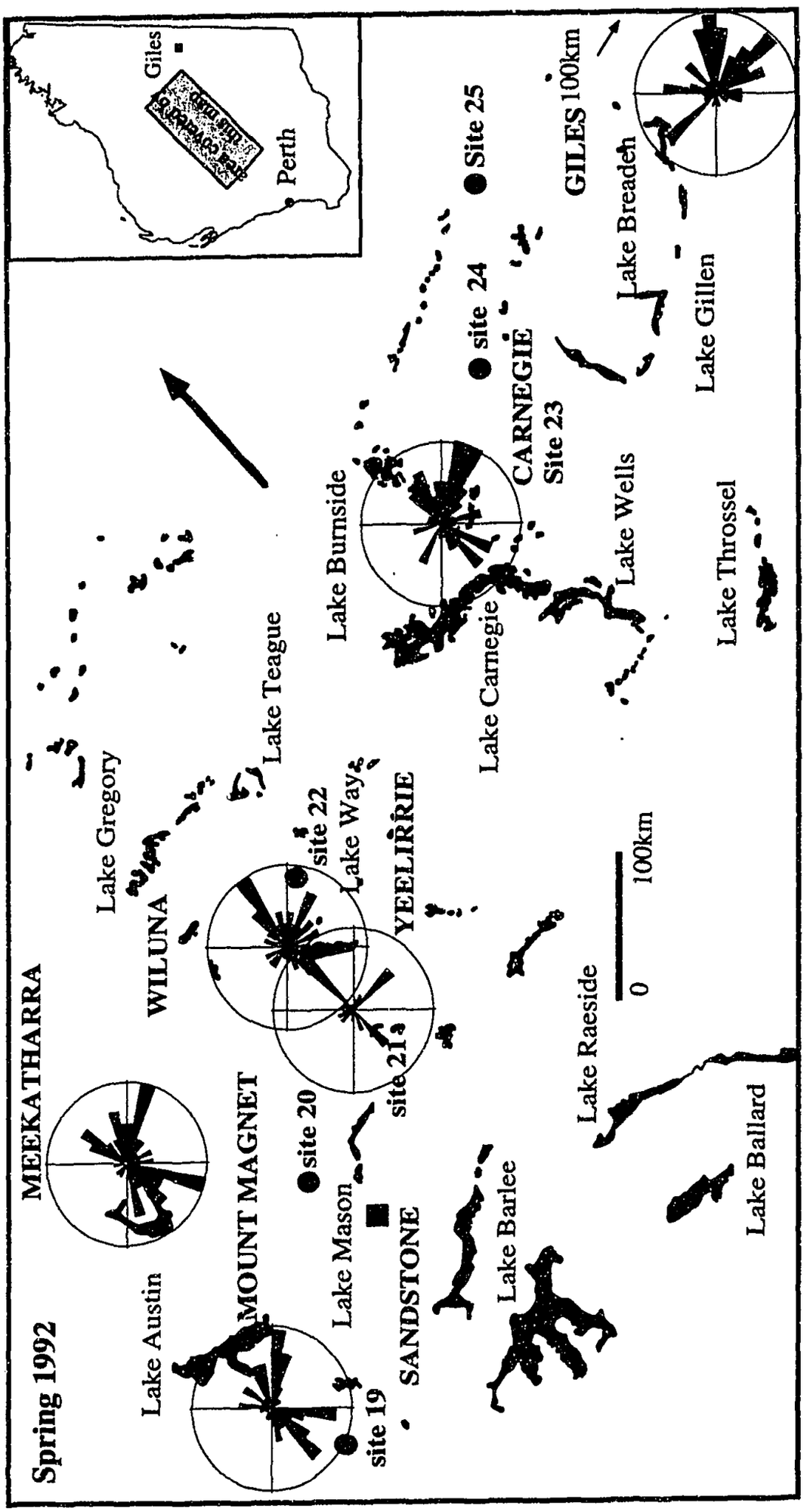
Spring 1992
MEEKATHARRA
Lake Austin
MOUNT MAGNET
site 19
Lake Mason
SANDSTONE
site 20
Lake Gregory
WILUNA
Lake Teague
site 22
Lake Way
YEELIRRIE
site 21
Lake Barlee
Lake Raeside
Lake Ballard
Lake Burnside
Lake Carnegie
site 24
Site 25
CARNEGIE
Site 23
Lake Wells
Lake Throssel
GILES 100km
Lake Breaden
Lake Gillen
0
100km
Giles
Perth

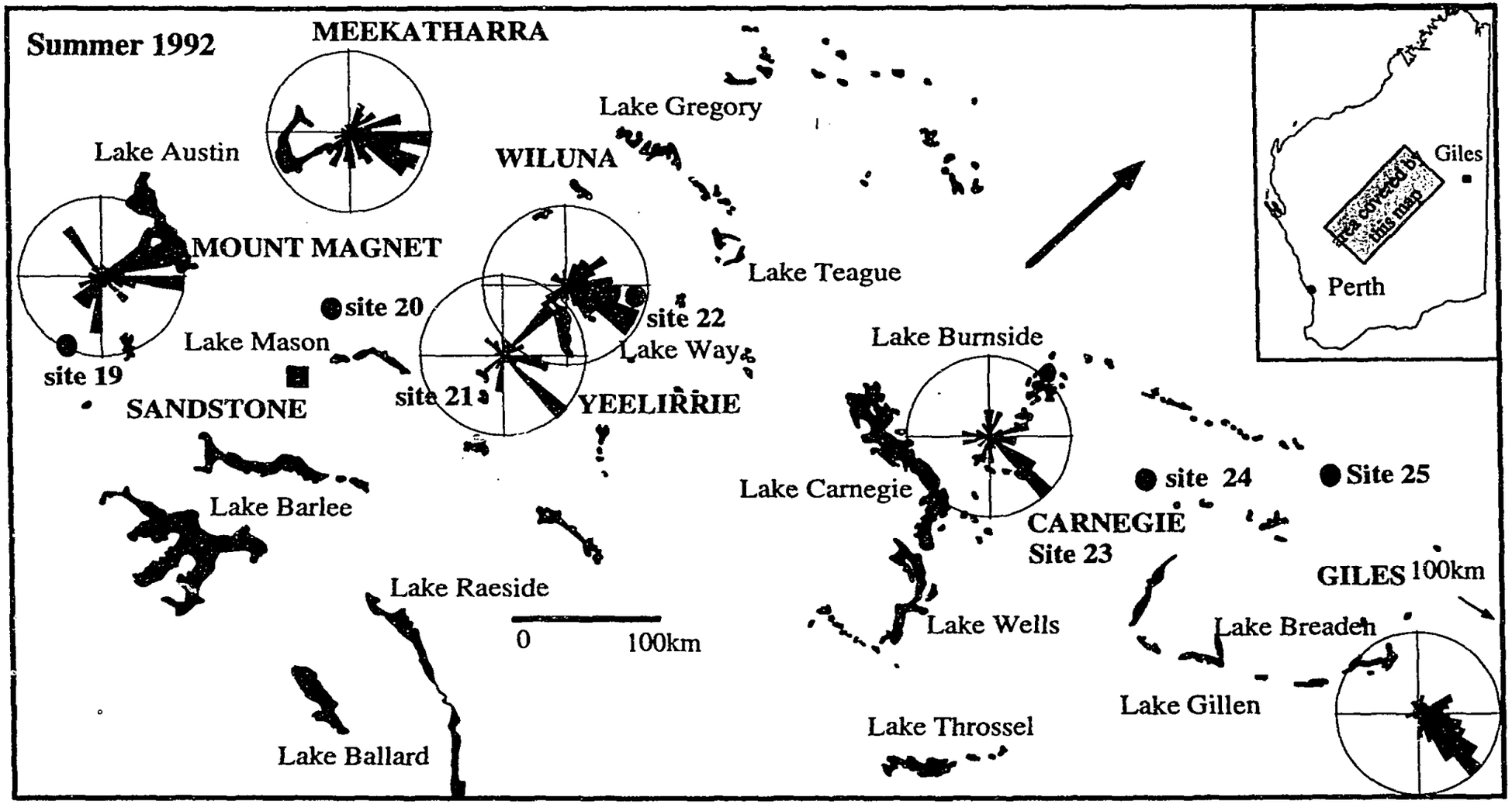

Appendix H Mean Wind Directions During Each Sampling Season for Inland Sites on the WE Array

Examiner 1

The examiner states "p 191, last paragraph- given some variations in ^{36}Cl measurements spatially from different studies, extending the results of this study to represent the entire Southern Hemisphere is questionable. What happens if the seasons in question becomes unusually wet?"

> Response: The fallout values in atoms/m^2/s take into account factors such as rainfall volume etc. I recognise that it is premature to state these fallouts are representative of the southern hemisphere. The main point here is that we cannot take fallouts measured in the northern hemisphere as representative of global fallouts, and as these are the only measurements made for the southern hemisphere, for now, they provide us with an idea of the hemispheric differences in fallout.

The examiner states "...choose an accessible representative site for major-element evaluation on a more detailed temporal scale for one or more seasons. If this was done on an event (or even weekly scale), a much better evaluation of the relationship with meteorology would have been possible, which might have been extended to the rest of the array."

> Response: I agree, and I did consider undertaking a similar activity during the monsoon period at one of the northern sites of the SN array, but time and financial constraints made this impossible.

the examiner states "p98 and elsewhere- if Br is below the detection limit almost all of the time, why not remove it from the data set"

> Response: Br was present in the coastal samples (site 16 and 26) and represents the input of seawater to rainfall at these sites. Thus data from sites 16 and 26 were used in the factor analysis, Br data was kept in the data set in the hope that it would indicate the seawater source.

The examiner states "p 102-103- individual site analysis. Some spatial distributions of the PC variances mapped on the site location maps would have been useful to enhance interpretation. Also the tabular FA results for the individual sites for both arrays should be included in an appendix."

> Response: FA was not performed on data from individual sites because the FA procedure could not be carried out on data sets with few number of cases than variables. This is outlined in Chapter 3.

The examiner states " p126 top paragraph- the speculations regarding sources of acidity are disappointing. The author cannot formally justify biodegradation as a source of acidity from the data (see FA results)."

> Response: I did not mean this discussion to suggest that biodegradation is a source of acidity. Rather that the acidity of the sample is something that has been altered after deposition, rather than a true representation of the atmospheric acidity. Thus biodegradation is used here more as a term to explain the post-depositional degradation.

The examiner states "p2 last two lines- salinisation in the landscape is mainly caused by salt from ancient seas rising to the surface after land clearing and over irrigation. It is not clear whether the author is implying a major role for rainfall chemistry, which is unlikely".

Response: this is not what I am implying. Instead I am stating that in order to remedy salinisation problems we need information such as how much salt is naturally accessed in order make mass balance calculations.

The examiner states "p39 I would have liked a better discussion of the potential problems that the use of glass bottles could have on rainwater chemistry, especially over a three-month exposure period."

Response : Borosilicate glass bottles were chosen for this sampling program to cater for the ^{36}Cl measurements. Fresenius et al (1988) state that "glass bottles are particularly necessary for sampling if a substance to be determined could be secondarily changed by plastics or if changes in concentration of substances contained in water can occur by adsorption onto plastic". Plastic containers use Cl as a binding agent, and although polyethylene bottles have been found to be inert (Fresenius et al 1988), as we were measuring such trace levels of ^{36}Cl in rainwater, we decided it was unnecessary to risk interference from the collection container. Major-elements were sampled from the borosilicate glass bottles so that the Cl concentration used in the ^{36}Cl calculations was analysed from the same sampling vessel.

Disadvantages of glass collection vessels for the collection and measurement of major-elements have been noted. In particular, glass containers are unsuitable for the collection of water with low concentrations of Na and K (Rump and Kirst 1988) since the ion exchange properties of the glass are greater than those of plastic. A review of the properties of collection vessel material (Krajca 1989), however reveals that borosilicate glass is able to withstand heat and weakly acid solutions for long periods of time, making this type of glass particularly suitable in the present investigation where temperatures at central Australian sites can reach over 40oC and where the rainfall is weakly acidic.

As discussed in Chapter 3, the effect of the collection vessel material on the sample chemistry under simulated field sampling conditions was tested and found to be negligible.

Fresenius, W., Quentin, K. E. and Schneider, W. (1988). Water Analysis. Springer Verlag, Berlin 804 pp.

Krajca, J. M. (1989). Water Sampling. Ellis and Horwood Ltd, England 212pp.

Rump, H. H. and Krist, H. (1988). Laboratory Manual for the Examination of Water, Waste Water and Soil. VCH Publishers, Germany 190pp.

Examiner 2
No response required

Examiner 3

The examiner states " Chapter 3- Since no acid is added prior to volume reduction, heating may permit additional biodegradation, and possibly formation of volatiles and/or organic complexes containing Cl which will not be recovered later. I would suggest measurement of stable Cl both before and after volume reduction. Acid is usually added to promote exchange between sample Cl and dead carrier Cl when required."

> Response: The stable Cl concentration of the concentrate was not measured because of low sample amounts. However, the waste material from the concentrating process was analysed for stable Cl on a number of occasions and was found to be below detection. Carrier was added on a very few occasions which is why we did not add acid which may have provided a source of impurities.

The examiner states "Chapter 4- Acid-base balance- little is said about the pH of these samples, but unless this parameter is measured soon after precipitation falls it is unlikely to be accurate. However H appears in all listings of cations. Is this measurement significant in samples that have been sitting for several months?"

> Response: I acknowledge that H concentrations (measured as pH) do not represent the pH of the atmosphere but the processes of sample degradation between deposition and retrieval from the field. This is reflected in the discussions, where H, NO_3, NH_4 and HPO_4 are suggested to indicate biodegradation in the multivariate analysis.